APPLICATION OF PLANT BIODIVERSITY FOR IMPROVING NUTRIENT CYCLING

EDITED BY: Katja Witzel, Christoph Martin Geilfus and Christian Roger Marc Hermans

PUBLISHED IN: Frontiers in Plant Science

frontiers Research Topics

frontiers

ISSN 1664-8714
ISBN 978-2-88974-414-5
DOI 10.3389/978-2-88974-414-5

About Frontiers

Frontiers is more than just an open-access publisher of scholarly articles: it is a pioneering approach to the world of academia, radically improving the way scholarly research is managed. The grand vision of Frontiers is a world where all people have an equal opportunity to seek, share and generate knowledge. Frontiers provides immediate and permanent online open access to all its publications, but this alone is not enough to realize our grand goals.

Frontiers Journal Series

The Frontiers Journal Series is a multi-tier and interdisciplinary set of open-access, online journals, promising a paradigm shift from the current review, selection and dissemination processes in academic publishing. All Frontiers journals are driven by researchers for researchers; therefore, they constitute a service to the scholarly community. At the same time, the Frontiers Journal Series operates on a revolutionary invention, the tiered publishing system, initially addressing specific communities of scholars, and gradually climbing up to broader public understanding, thus serving the interests of the lay society, too.

Dedication to Quality

Each Frontiers article is a landmark of the highest quality, thanks to genuinely collaborative interactions between authors and review editors, who include some of the world's best academicians. Research must be certified by peers before entering a stream of knowledge that may eventually reach the public - and shape society; therefore, Frontiers only applies the most rigorous and unbiased reviews.
Frontiers revolutionizes research publishing by freely delivering the most outstanding research, evaluated with no bias from both the academic and social point of view. By applying the most advanced information technologies, Frontiers is catapulting scholarly publishing into a new generation.

What are Frontiers Research Topics?

Frontiers Research Topics are very popular trademarks of the Frontiers Journals Series: they are collections of at least ten articles, all centered on a particular subject. With their unique mix of varied contributions from Original Research to Review Articles, Frontiers Research Topics unify the most influential researchers, the latest key findings and historical advances in a hot research area! Find out more on how to host your own Frontiers Research Topic or contribute to one as an author by contacting the Frontiers Editorial Office: frontiersin.org/about/contact

APPLICATION OF PLANT BIODIVERSITY FOR IMPROVING NUTRIENT CYCLING

Topic Editors:
Katja Witzel, Leibniz Institute of Vegetable and Ornamental Crops, Germany
Christoph Martin Geilfus, Humboldt University of Berlin, Germany
Christian Roger Marc Hermans, Université libre de Bruxelles, Belgium

Citation: Witzel, K., Geilfus, C. M., Hermans, C. R. M., eds. (2022). Application of Plant Biodiversity for Improving Nutrient Cycling. Lausanne: Frontiers Media SA. doi: 10.3389/978-2-88974-414-5

Table of Contents

frontiers in Plant Science

ORIGINAL RESEARCH
published: 26 June 2020
doi: 10.3389/fpls.2020.00966

The Interaction of Arbuscular Mycorrhizal Fungi and Phosphorus Inputs on Selenium Uptake by Alfalfa (*Medicago sativa* L.) and Selenium Fraction Transformation in Soil

Qi Peng[1,2,3], *Miaomiao Wu*[1,4], *Zekun Zhang*[1,4], *Rui Su*[1,4], *Honghua He*[1,2,4*] *and Xingchang Zhang*[1,2,4*]

[1] State Key Laboratory of Soil Erosion and Dryland Farming on the Loess Plateau, Northwest A&F University, Yangling, China, [2] Institute of Soil and Water Conservation, Chinese Academy of Sciences and Ministry of Water Resources, Yangling, China, [3] University of Chinese Academy of Sciences, Beijing, China, [4] College of Natural Resources and Environment, Northwest A&F University, Yangling, China

OPEN ACCESS

Edited by:
Christian Roger Marc Hermans, Université libre de Bruxelles, Belgium

Reviewed by:
Nieves Goicoechea, University of Navarra, Spain
Christoph Martin Geilfus, Humboldt University of Berlin, Germany

***Correspondence:**
Honghua He
honghuahe@ms.iswc.ac.cn
Xingchang Zhang
zhangxc@ms.iswc.ac.cn

Specialty section:
This article was submitted to Plant Nutrition, a section of the journal Frontiers in Plant Science

Received: 12 February 2020
Accepted: 12 June 2020
Published: 26 June 2020

Citation:
Peng Q, Wu M, Zhang Z, Su R, He H and Zhang X (2020) The Interaction of Arbuscular Mycorrhizal Fungi and Phosphorus Inputs on Selenium Uptake by Alfalfa (Medicago sativa L.) and Selenium Fraction Transformation in Soil. Front. Plant Sci. 11:966. doi: 10.3389/fpls.2020.00966

Selenium (Se) is a beneficial element to plants and an essential element to humans. Colonization by arbuscular mycorrhizal fungi (AMF) and supply of phosphorus (P) fertilizer may affect the bioavailability of Se in soils and the absorption of Se by plants. To investigate the interaction between AMF and P fertilizer on the transformation of soil Se fractions and the availability of Se in the rhizosphere of alfalfa, we conducted a pot experiment to grow alfalfa in a loessial soil with three P levels (0, 5, and 20 mg kg^{-1}) and two mycorrhizal inoculation treatments (without mycorrhizal inoculation [–AMF] and with mycorrhizal inoculation [+AMF]), and the interaction between the two factors was estimated with two-way ANOVA. The soil in all pots was supplied with Se (Na_2SeO_3) at 1 mg kg^{-1}. In our results, shoot Se concentration decreased, but plant Se content increased significantly as P level increased and had a significant positive correlation with AMF colonization rate. The amount of total carboxylates in the rhizosphere was strongly affected by AMF. The amounts of rhizosphere carboxylates and alkaline phosphatase activity in the +AMF and 0P treatments were significantly higher than those in other treatments. The concentration of exchangeable-Se in rhizosphere soil had a positive correlation with carboxylates. We speculated that rhizosphere carboxylates promoted the transformation of stable Se (iron oxide-bound Se) into available Se forms, i.e. exchangeable Se and soluble Se. Colonization by AMF and low P availability stimulated alfalfa roots to release more carboxylates and alkaline phosphatase. AMF and P fertilizer affected the transformation of soil Se fractions in the rhizosphere of alfalfa.

Keywords: alkaline phosphatase activity, *Glomus mosseae*, legume, phosphorus, rhizosphere carboxylates, selenium fraction

HIGHLIGHTS

1. AM inoculation and P input enhanced alfalfa P and Se accumulation and availability
2. Carboxylates and alkaline phosphatase affected Se translocation in soil-alfalfa systems
3. AM inoculation and P input increased Se availability through increasing EX-Se
4. Fe-Se and EX-Se could reflect Se availability in loessial soil

INTRODUCTION

Selenium (Se) is a naturally occurring metalloid element which is essential at low concentrations to humans and animals, but toxic at high concentrations (Sors et al., 2005). Se concentrations in staple foods should not be lower than the critical standard of 100 μg kg^{-1}, below which a human's basic needs cannot be met (Combs, 2001). Low intakes of Se by humans can cause health disorders and increase the risk of cancers (Liu et al., 2004; Whanger, 2004; He et al., 2017a). Se in soil can enter food chain *via* plant uptake, and humans mainly acquire dietary Se from plant-based foods through the food chain (Rayman, 2000; Yu et al., 2011). Besides, low concentrations of Se in soil can upregulate the production of higher plant enzymes (e.g., peroxidases and reductases) and protect plants from abiotic stresses (Wang et al., 2019), and have beneficial effects on plant growth and yield (Wang, Q. et al., 2016; White, 2018). Therefore, in agricultural production, the application of Se fertilizers is one of the effective ways to increase plant Se uptake, thus meeting the requirements of human health (Zhang et al., 2014).

The bioavailability of Se in soils is not only affected by soil properties such as pH, redox conditions, organic matter content, and synergy or antagonism of coexisting elements (Eich-Greatorex et al., 2010; Wang, Q. et al., 2016), but is also related to soil Se content and fraction (Wang et al., 2012). Activating stable Se in soil is a key process to increase the content of available Se and promote Se uptake by plants. According to the differences in water solubility and binding strength with various soil components, soil Se can be divided into different fractions, including soluble Se, exchangeable Se, iron oxide-bound Se, organic-matter-bound Se, and residual Se. These fractions are widely used to study the chemical Se forms (Wang, Q. et al., 2016; Zhang et al., 2017). Soluble Se and exchangeable Se are easily taken up by plants, and considered as plant-available fractions (Zhang et al., 2017). Iron oxide-bound Se is firmly fixed on the mineral surface, so it's not readily absorbed by plants (Qin et al., 2012). Organic-matter-bound Se is a potential source of available Se, and it can be released into soil solution and absorbed by plant through mineralization (Kulp and Pratt, 2004; Wang et al., 2018). Some reports have indicated that low molecular weight organic acids (LMWOAs) play a key role in mobilizing Se, thus greatly increasing bioavailable Se (Qin et al., 2004). The mobilization process with LMWOAs, through competitive adsorption or desorption, can release Se from the solid phase in soil into soluble Se and exchangeable Se (Dinh et al., 2017). Li et al. (2017b) reported that organic acids can activate stable Se and increase Se availability in low pH soils.

Phosphorus (P) plays an important role in plant growth, and P deficiency limits crop production in many regions of the world (He et al., 2017b). Mainly due to the poor solubility and slow diffusion of P salts, and tight adsorption of P by iron-oxides, aluminum-oxides/hydroxides or calcium compounds in soil, P availability in soils is often very low (Turrión et al., 2018). To increase the availability of soil P, P fertilizers are commonly added to the soil to maintain crop P demand and achieve yield targets (Wang et al., 2015). The reliance on high rates of P fertilizers not only consumes the limited rock phosphate reserves, but also causes environmental pollution (Pang et al., 2018). Therefore, increasing the availability of P in soils and the amount of available P for plant uptake is very important to overcome P deficiencies in agricultural ecosystems. On the other hand, due to the strong competition between phosphate and selenite by sorption sites, it is expected to raise selenite availability to plants by the use of phosphate fertilizers (Barrow et al., 2005; Mora et al., 2008). Ngigi et al. (2019) observed that addition of P fertilizers positively affects the impact of Se fertilization with low soil P, and Li et al. (2018) got a similar conclusion in rice (*Oryza sativa*). However, some studies have conflicting results that P fertilizer has a negative effect on the uptake of Se by plants (Liu et al., 2004; Zhang et al., 2014). As yet, the effects of P fertilizers on Se uptake by plants are controversial.

Arbuscular mycorrhizal fungi (AMF) are an important component of the soil microbial community living in the rhizosphere and are present around more than 80% of terrestrial plant roots (Nanjareddy et al., 2014; He et al., 2017b). AMF are mandatory symbionts, which colonize most terrestrial plants and help in plant growth, nutrition, and tolerance for diseases (He et al., 2017c). They provide a direct link between plant roots and soil, and explore soil beyond the rhizosphere by increasing the absorptive root surface through hyphae, thus helping host plant acquire water and essential nutrients, especially P (Smith and Read, 1997; Langer et al., 2010). Due to higher phosphatase activity of the internal hyphae of mycorrhizal fungi, which can hydrolyze more organic P, mycorrhizal association benefited yield in barley by improving phosphatase activity for P uptake (Goicoechea et al., 2004). Smith and Read (2008) indicated that the inoculation of AMF can improve P uptake by increasing the volume of soil explored by roots. When roots were colonized by AMF, the mycorrhizal pathway of uptake was the dominant pathway for P acquisition (Smith et al., 2003; Watts-Williams et al., 2015). Seymour et al. (2019) also found that AMF markedly increased P content of the linseed (*Linum usitatissimum* L.). Meanwhile, there are some studies about the effects of AMF on the uptake and accumulation of Se by plants, which are controversial. In the study of Durán et al. (2016), there was no significant difference in Se concentrations between mycorrhizal and non-mycorrhizal plants. Munier-Lamy et al. (2007) reported that AMF reduced

Se uptake by 30% in ryegrass. Goicoechea et al. (2015) got a similar conclusion in leaves of lettuces. Researches by Yu et al. (2011) showed that mycorrhizal inoculation increased plant uptake of P, but inhibited selenite uptake by plant roots. In contrary, Luo et al. (2019) indicated that AMF significantly enhanced Se accumulation in winter wheat in selenite-spiked soils. Nevertheless, the mechanisms related to the interaction of AMF and P input on Se uptake by alfalfa and fractions transformation in the soil systems are still not clear.

Alfalfa (*Medicago sativa* L.) is a perennial forage legume grown widely, it is sensitive to changes in soil P supply, and it is also able to accumulate Se (He et al., 2020; Peng et al., 2020). In Se-deficient areas, the production of Se-enriched alfalfa is one of the most important ways to supply Se to humans and livestock (He et al., 2019). Previous studies have reported the effects of AMF or P fertilizers on the uptake and accumulation of Se by plants, but little is known about soil available Se levels and the transformation of soil Se fractions under P and AMF interaction. The objective of this study was to investigate how AMF treatments affect the transformation of soil Se fractions in a plant-soil system with three levels of P fertilizer treatments. We hypothesized that: 1) colonization by AMF and low P availability would stimulate alfalfa roots to release more carboxylates and alkaline phosphatase; 2) AMF and P fertilizer would affect the transformation of soil Se fractions in the rhizosphere of alfalfa; 3) variations in carboxylates exudation and alkaline phosphatase activity in the rhizosphere are important for P and Se acquisition.

MATERIALS AND METHODS

Substrate Preparation

The loessial soil was collected from the top plow layer (0–20 cm) of the Ansai County in the middle of the Loess Plateau in China (approximately 108°5'E, 36°30'N). The soil was air-dried and passed through a 2-mm sieve for the pot experiment. The texture of the soil was 45% sand, 41.6% silt, and 13.4% clay. The soil had a pH of 8.7, it had 0.1 mg kg^{-1} total Se, 0.1 g kg^{-1} total nitrogen (N), 0.5 g kg^{-1} total P, 3.3 μg g^{-1} plant-available P, 16.4 mg kg^{-1} total potassium (K), 2.8 g kg^{-1} organic matter, and 41.1 mg g^{-1} total calcium (Ca), 4.2 mg g^{-1} total magnesium (Mg), 12.4 mg g^{-1} total iron (Fe), 257 μg g^{-1} total manganese (Mn), 9.7 μg g^{-1} total copper (Cu), 37.9 μg g^{-1} total zinc (Zn). The substrates in all pots were amended with 1 mg Se kg^{-1} (supplied as sodium selenite [Na_2SeO_3] [Analytically pure, Xiya Reagent, China]).

The experiment included three P-application levels (0 [0P], 5 [5P], and 20 [20P] mg kg^{-1}) and two mycorrhizal inoculation treatments, i.e. without mycorrhizal inoculation (−AMF) and with mycorrhizal inoculation (+AMF). The AMF inoculum specie was vesicular-arbuscular mycorrhiza *Glomus mosseae* BGC YN02 (511C0001BGCAM0022, National Infrastructure of Microbial Resources, China), supplied by the Bank of Glomeromycota in China. We cultivated each fungal isolate using capsicum (*Capsicum annuum* L) as the host species in pot cultures in a greenhouse in the Institute of Plant Nutrition and Resources, Beijing Academy of Agriculture and Forestry Sciences. The substrate of these cultures was collected after 4 months, air-dried, and controlled for the presence of viable AM fungal spores of the correct morphotype. The inoculum consisted of a mixture of soil, hyphae, spores, and infected root fragments. Non-transparent PVC tubes of 15-cm diameter and 25-cm height with a sealed bottom were used as pots for the experiment. Each pot was first filled with 4 kg of the loessial soil. The soils used for this experiment were sterilized once by autoclaving at 120°C for 2 h. The +AMF treatments contained 20 g of the mycorrhizal inoculum. For the -AMF treatments, 20 g of the same inoculum was filtered using distilled water through 11 μm filter papers (Whatman, UK) to obtain 20 ml filtrate to supply the soil with microbes without AMF communities, then the same amount of mycorrhizal inoculum was autoclaved and added to the soil in each pot.

One hundred milligrams N kg^{-1} as ammonium nitrate (NH_4NO_3) was used for all treatments, and 5 and 20 mg P kg^{-1} as monopotassium phosphate (KH_2PO_4) were used in the 5P and 20P treatment groups, respectively. In all groups, KCl was added to each pot to obtain the dose of K supply at 50 mg K kg^{-1} soil. The experiment was set as a completely randomized block design, with four replicates for each treatment. The soil in all pots was incubated for 8 weeks by watering with deionized (DI) water at about 60% field capacity in a greenhouse before growing plants.

Plant Cultivation and Harvest

Medicago sativa L. cv Golden Empress, an introduced cultivar of alfalfa, was used in this study. Seeds were first sterilized in a 30% (v:v) hydrogen peroxide (H_2O_2) solution, rinsed with DI water repeatedly. Twenty seeds were sown in each pot and thinned to 10 plants per pot 4 weeks after sowing. DI water was added to maintain the soil moisture content at about 60% field capacity by regular weighing. Plant fresh weight (about 30 g per pot at harvest) was small compared with the water content (about 792 g per pot), therefore, it was ignored when the amount of water that should be replenished was calculated. The experiment was carried out from May 2018 to September 2018 for a total of 120 d in a greenhouse in the Institute of Soil and Water Conservation, Yangling, Shaanxi, China.

At harvest, shoots were carefully cut from the pots. The root systems were gently shaken to remove excess soil, the soil remaining attached to the roots was defined as rhizosphere soil (Pang et al., 2018). The rhizosphere soil was divided into two parts, one air-dried for analysis of Se fractions and soil P, and another stored at −20°C for the determination of alkaline phosphatase activity and microbial P immobilization.

Collection and Determination of Rhizosphere Carboxylates

Carboxylates in the rhizosphere were extracted according to Pang et al. (2018) and He et al. (2017b). For each pot with plants, about 1.0 g fresh roots with rhizosphere soil was transferred to a beaker containing 20 ml of 0.2 mM $CaCl_2$ to ensure cell integrity and gently shaken to remove the rhizosphere soil. The pH of the rhizosphere extract was measured using a pH meter. A 1 ml subsample of the rhizosphere extract was filtered

through a 0.22-μm syringe filter into a 1-ml HPLC vial, then acidified with one drop of concentrated phosphoric acid, and frozen at −20°C until HPLC analysis. HPLC analysis of the elution liquid was performed using a Waters 1525 HPLC equipped with Waters 2489 detector and Alltima C-18 reverse phase column (250 × 4.6 mm, 5 μm) (Waters, Milford MA, USA). Working standards of malic acid, oxalic acid, citric acid, acetic acid, malonic acid, and tartaric acid were used to identify carboxylates at 210 nm (Cawthray, 2003). The root in the beaker after the extraction of carboxylates was cleaned, oven-dried at 60°C for 72 h, and RDM recorded. Amount of rhizosphere carboxylates were calculated as μmol g root^{-1} dry mass.

Determination of Root Colonization by AMF

After the extraction of carboxylates, all roots in each pot were picked out and placed in individual plastic bag. These roots were washed carefully with DI water and then kept at 4°C. Fresh root subsamples were randomly taken to evaluate root AMF colonization. Roots were maintained in 10% (w/v) KOH solution in a 90°C water bath for 40 min, rinsed with water, acidified with 2% (v/v) HCl, and then stained with 0.05% (w/v) Trypan blue (Wen et al., 2019). For each root sample, 15 pieces of 1-cm segment were randomly selected and mounted on three slides for observation with a light microscope. The percentages of AM colonization were calculated under a microscope using the gridline intersect method (Giovannetti and Mosse, 1980).

Determination of Plant Phosphorus and Selenium Concentrations

Shoots and roots were oven-dried at 60°C for 72 h, and weighed separately to obtain the dry mass. The oven-dried samples were then finely ground for analysis of P and Se concentrations. For each plant sample, about 0.5 g subsample was digested using a mixture of nitric and perchloric acid (v/v, 4:1). Plant P concentration was determined using the molybdenum blue method after digestion (Lu, 2000). For plant Se analysis, the digested solution was treated with 6 M HCl and heated for 20 min at 93–95°C to reduce all species of Se to selenite. Se concentration was determined using an atomic fluorescence spectrophotometer (AFS-230E, Beijing Haiguang Instruments Company, China) (Wang et al., 2012).

Analysis of Soil Phosphorus and Alkaline Phosphatase Activity

Bulk soil samples were taken from each pot after being mixed thoroughly at harvest. The bulk soil was divided into two parts, one air-dried for analysis of Se fractions and soil P, and another stored at −20°C for the determination of alkaline phosphatase activity and microbial P immobilization.

Soil available phosphorus (Olsen-P) was extracted with 0.5 M $NaHCO_3$, and its concentration was determined by the molybdenum blue method (Lu, 2000). Soil microbial biomass phosphorus (MBP) were determined using the method of chloroform fumigation-extraction (Brookes et al., 1985; Vance et al., 1987). Alkaline phosphatase (EC 3.1.3.1) activity was measured based on the absorption of released phenol (Guan et al., 1986).

Determination of Soil Selenium Fractions

Soil Se fractions were determined using the sequential extraction procedure described by Wang et al. (2012). In brief, soil samples (about 1.000 g) were placed into 50 ml centrifuge tubes and extracted using different solutions (solid/liquid = 1:10) for each step. The solutions for extracting the soluble fraction (SOL-Se), exchangeable fraction (EX-Se), iron oxide-bound fraction (Fe-Se), and organic-matter-bound fraction (OR-Se) are 0.25 M KCl, 0.1 M KH_2PO_4-0.1 M K_2HPO_4, 2.5 M HCl, and 0.1 M $K_2S_2O_8$, respectively. All solutions obtained were heated at 93–95°C for 20 min in 6 M HCl solution to transform selenate into selenite. Se concentration in the solution was determined using an atomic fluorescence spectrophotometer (AFS-230E, Beijing Haiguang Instruments Company, China) (Wang et al., 2012).

Statistical Analysis

The data were statistically analyzed using analysis of variance (ANOVA) and Pearson correlation analysis procedures with the SPSS 20.0 statistical software. Linear regression analysis was conducted in Origin 9.0. The effect of AMF treatment (+AMF and −AMF), P fertilizer (0P, 5P, and 20P), and the interaction between the two factors were estimated with two-way ANOVA. One-way ANOVA and Tukey test were performed individually for each P fertilizer level (0P, 5P, and 20P) and AMF treatments (+AMF and −AMF). Significance level was set at 0.05. Partial least squares path modeling (PLS-PM) was used to identify the major pathways of the influences of predictor variables on plant Se uptake using the "innerplot" function of the plspm package in R 3.6.0.

RESULTS

AMF Root Colonization and Plant Growth

In the +AMF treatments, the mean values of AMF root colonization rate in 0P, 5P, and 20P treatments was 54, 45, and 69% (**Figure S1**). Shoot dry mass (SDM) and root dry mass (RDM) significantly increased in 5P and 20P treatments compared to 0P treatment ($P < 0.01$), and increased in +AMF treatments compared to −AMF treatments at the same P level. The two-way ANOVA revealed that P level had a stronger effect on SDM and RDM compared to inoculation (**Table S1**). Root to shoot ratio was higher in +AMF treatments than in −AMF treatments within the 0P and 20P treatments. Inoculation and P level had a significant interaction on the root to shoot ratio ($P < 0.01$) (**Figure 1**).

Phosphorus and Selenium Concentrations in Plants

Shoot and root P concentrations increased in 5P and 20P treatments compared to 0P treatment (**Figure 1**). Only P level had a significant effect on shoot and root P concentration, yet there was a significant interaction between P level and

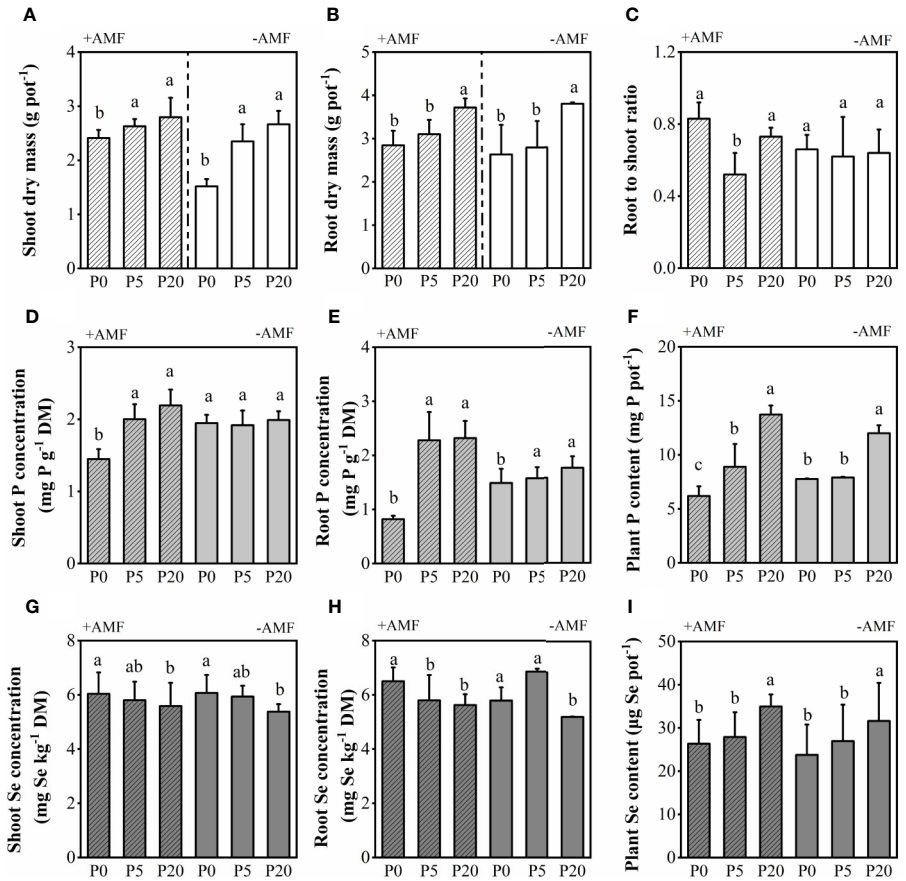

FIGURE 1 | Shoot dry mass **(A)**, root dry mass **(B)**, root to shoot ratio **(C)**, P and Se concentrations **(D, E, G, H)**, total P and Se contents in plants per pot **(F, I)** for all treatments. Data are presented as means ± S.E. (n = 4). One-way ANOVA and Tukey's test were performed for each AMF treatment (+AMF or −AMF). Significant differences ($P < 0.05$) between treatments are indicated with different letters above the bars.

inoculation on shoot and root P concentrations (both $P < 0.01$). Plant P content was higher in +AMF treatment than in −AMF treatment within the 5P and 20P treatments, and it significantly increased in 5P and 20P treatments compared to 0P treatment ($P < 0.001$) (**Table S1**).

Shoot Se concentration decreased when soil P level increased, being significantly lower in 20P treatment than in 0P treatment ($P < 0.05$). Root Se concentration significantly decreased in 20P treatment compared to 0P treatment ($P < 0.05$). Only soil P level had a significant effect on shoot and root Se concentrations. Plant Se content significantly increased when soil P level increased ($P < 0.001$). At the same P level, +AMF treatment significantly increased Se content compared to −AMF treatment. (**Figure 1**; **Table S1**).

Soil Microbial Biomass Phosphorus and Plant-Available Phosphorus

Soil MBP decreased when soil P level increased in both the rhizosphere soil and bulk soil (**Figure 2**). In all treatments, rhizosphere soil MBP was significantly higher than bulk soil MBP within the same P and inoculation treatments ($P < 0.001$). Soil Olsen-P in both the rhizosphere soil and bulk soil significantly increased with increasing P level (both $P < 0.05$). In +AMF treatment, Olsen-P was higher in bulk soil than in rhizosphere soil within the 5P and 20P treatments. On the contrary, in the −AMF treatment, Olsen-P was lower in bulk soil than rhizosphere soil within the 5P and 20P treatments. Inoculation did not have a significant effect on MBP and Olsen-P (**Table S1**).

Soil pH, Rhizosphere Soil Alkaline Phosphatase Activity, and Carboxylates

Rhizosphere pH was significantly lower than bulk soil pH ($P < 0.05$) and significantly declined as P level increased ($P < 0.05$) (**Figure S2**). Rhizosphere pH was 7.90–8.09 in the −AMF treatments, and 7.72–8.06 in the +AMF treatments. Alkaline phosphatase activity in the rhizosphere soil is presented in **Figure 3**. In the +AMF and −AMF treatments, alkaline phosphatase activity significantly decreased, i.e. by 16–38% ($P < 0.001$) and 14–32% ($P < 0.001$) respectively, as P level increased. Alkaline phosphatase activity was significantly higher in +AMF treatment than in −AMF treatment within the same P treatments

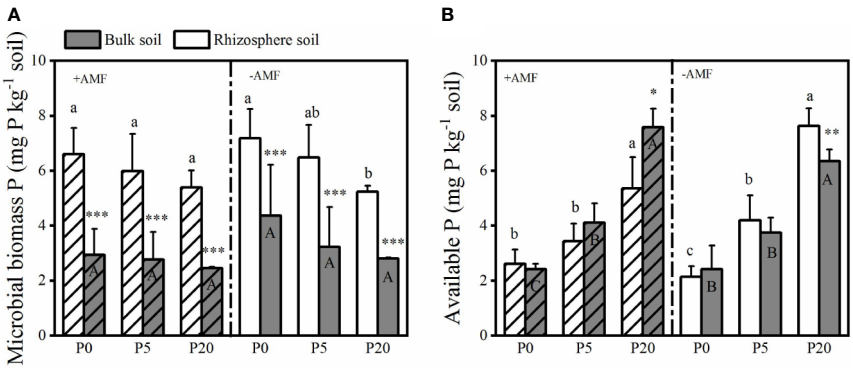

FIGURE 2 | Microbial-biomass P **(A)** and available P **(B)** in the rhizosphere soil and bulk soil. Data are presented as means ± S.E. (n = 4). One-way ANOVA and Tukey's test were performed in the +AMF and –AMF treatments separately for the bulk soil and rhizosphere soil. Lower-case letters indicate significant differences between the rhizosphere soil, and upper-case letters indicate significant differences between the bulk soil. One-way ANOVA significance ($P < 0.05$) to test for significant differences between the bulk soil and rhizosphere soil for each treatment is indicated by *. *$P < 0.05$; **$P < 0.01$; ***$P < 0.001$.

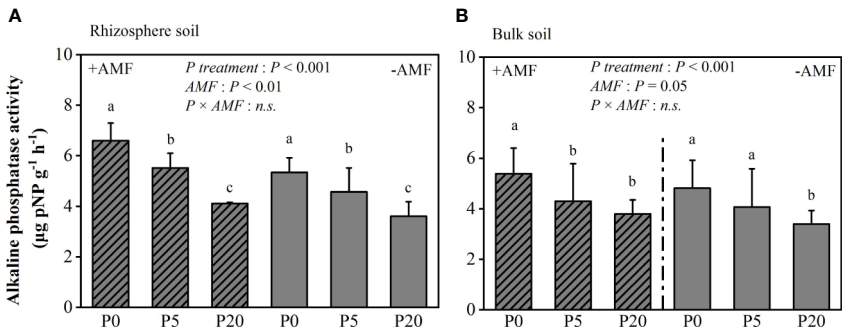

FIGURE 3 | Alkaline phosphatase activity in the rhizosphere **(A)** and bulk soil **(B)**. Data are presented as means ± S.E. (n = 4). Two-way ANOVA and Tukey's test were performed for each AMF treatment (+AMF and –AMF) and P treatment (P0, P5, and P20). ANOVA P-values are indicated in the graphs. Significant differences ($P < 0.05$) between treatments are indicated with different letters above the bars.

($P < 0.001$). According to the two-way ANOVA, AMF and P treatments did not have a significant interaction on rhizosphere alkaline phosphatase activity, and P treatment had a stronger effect compared to AMF treatment (**Table S1**). Alkaline phosphatase activity in rhizosphere soil was significantly higher than that in bulk soil ($P < 0.05$).

The amounts of carboxylates in the rhizosphere are presented in **Figure 4**. In +AMF treatment, the amount of oxalate, tartrate, malate, malonate, acetate, citrate, and the total amount of rhizosphere carboxylates measured relative to RDM was 35–69, 191–378, 278–311, 189–263, 337–369, 122–152, and 1,196–1,457 μmol g^{-1}, respectively. In –AMF treatment, the amount of oxalate, tartrate, malate, malonate, acetate, citrate, and the total amount of rhizosphere carboxylates measured relative to RDM was 31–45, 47–121, 209–248, 100–163, 120–203, 65–111, and 674–863 μmol g^{-1}, respectively. In both +AMF and –AMF treatments, the amounts of carboxylates decreased when soil P level increased, and it was significantly higher in +AMF treatment than in –AMF treatment within the same P treatments ($P < 0.001$) (**Table S1**).

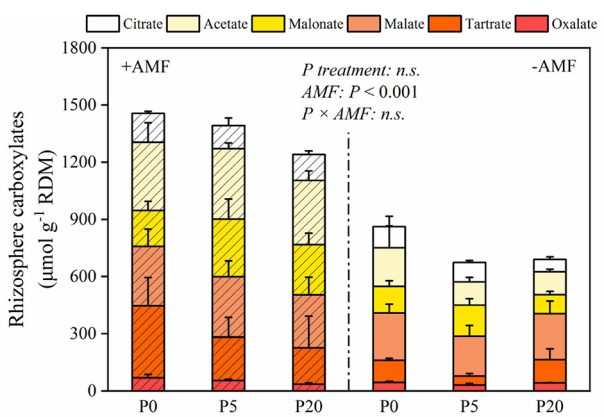

FIGURE 4 | The amount of carboxylates relative to root dry mass. Data are presented as means ± S.E. (n = 4). Two-way ANOVA and Tukey's test were performed for each AMF treatment (+AMF and –AMF) and P treatments (P0, P5, and P20). ANOVA P-values are indicated on the graph.

Soil Selenium Fractions

Se fractions in bulk soil and rhizosphere soil Se in the soil was fractionated into four fractions. The average proportions of Se in different fractions followed the order of EX-Se > SOL-Se > Fe-Se > OR-Se (**Figure S3**). In the rhizosphere soil, SOL-Se decreased in the +AMF treatment, but increased significantly in the −AMF treatment as the P level increased, while EX-Se concentration did not change significantly in the +AMF or −AMF treatment (**Figure 5**). Compared to bulk soil, SOL-Se and EX-Se concentrations in rhizosphere soil increased by 2–36 and 17–50% in the +AMF treatment, and decreased by 2–49 and 2–18% in the −AMF treatment, respectively. In the rhizosphere soil, Fe-Se concentration was higher in 20P treatment compared to 0P and 5P treatments in +AMF and −AMF treatments. In the +AMF treatment, Fe-Se concentration increased by 7–29% in rhizosphere soil compared to bulk soil, and decreased by 4–26% in the −AMF treatment. In bulk soil, OR-Se concentration increased significantly as the P level increased in +AMF treatment ($P < 0.05$), but decreased significantly in −AMF treatment ($P < 0.05$). In the rhizosphere soil, OR-Se concentration was higher in 20P treatment than in 0P and 5P treatments. In the +AMF treatment, OR-Se concentration increased by 13–39% in rhizosphere soil compared to bulk soil. No significant difference among three P levels in the bulk soil was observed in SOL-Se, EX-Se, and Fe-Se concentrations in +AMF or −AMF treatment.

Correlations and Partial Least Squares Path Modeling

Plant Se content showed a significant correlation with plant P content ($r = 0.729$, $P < 0.01$), dry mass ($r = 0.599$, $P < 0.01$), alkaline phosphatase activity ($r = -0.391$, $P < 0.05$), MBP ($r = -0.620$, $P < 0.001$), rhizosphere pH ($r = -0.518$, $P < 0.01$), Olsen-P ($r = -0.514$, $P < 0.05$), and carboxylates ($r = -0.452$, $P < 0.05$) (**Table 1**). Root Se concentration had a significant positive correlation with total carboxylates ($r = 0.453$, $P < 0.05$) and citrate ($r = 0.485$, $P < 0.01$) (**Figure 6**), but no significant correlation with oxalate ($r = 0.045$, $P > 0.05$), tartrate ($r = 0.163$, $P > 0.05$), malate ($r = 0.014$, $P > 0.05$), malonate ($r = 0.140$, $P > 0.05$), or acetate ($r = 0.055$, $P > 0.05$).

The PLS-PM identified direct and indirect effects of the colonization by AMF colonization rate, P supply rate, rhizosphere carboxylates amount, soil properties (rhizosphere

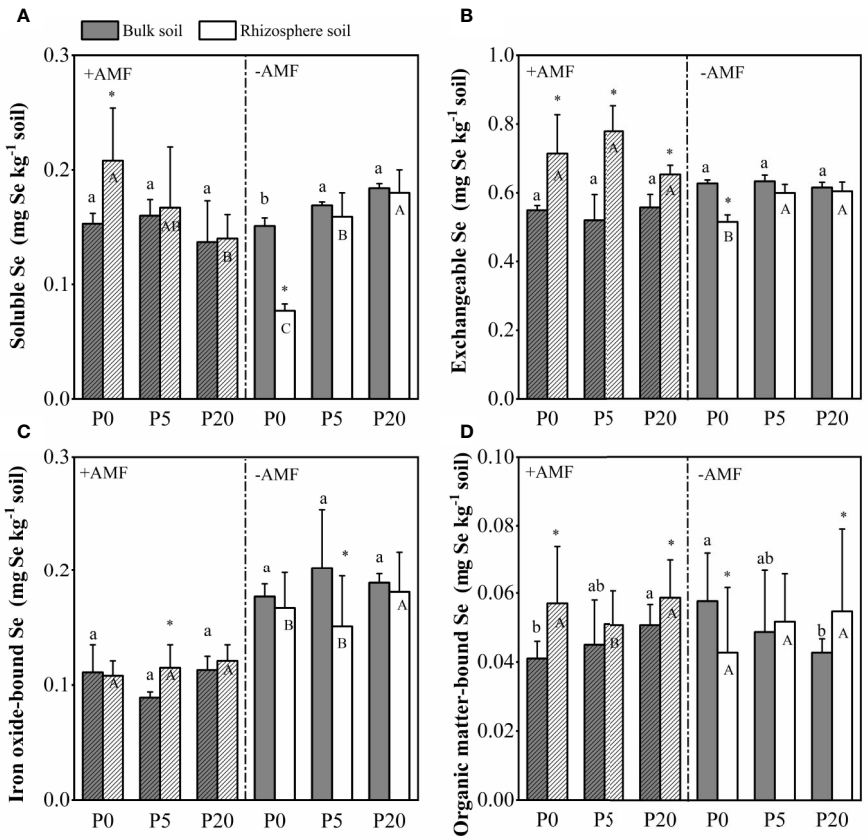

FIGURE 5 | Sequential extraction results of selenium fractions in the bulk soil and rhizosphere soil. **(A)** Soluble Se; **(B)** Exchangeable Se; **(C)** Iron oxide-bound Se; **(D)** Organic matter-bound Se. Data are presented as means ± S.E. ($n = 4$). One-way ANOVA and Tukey's test were performed for each Se fraction in the +AMF and −AMF treatments separately for the bulk soil and rhizosphere soil. Lower-case letters indicate significant differences between the bulk soil, and upper-case letters indicate significant differences between the rhizosphere soil. One-way ANOVA significance ($P < 0.05$) to test for significant differences between the bulk soil and rhizosphere soil for each treatment is indicated by *.

TABLE 1 | Pearson's correlation matrix for plant traits and soil properties.

	Plant P content	Plant Se content	Dry mass	Root to shoot ratio	Apase	MBP	pH	Olsen-P	Carboxylates
Plant Se content	**0.729****								
Dry mass	**0.588****	**0.599****							
Root to shoot ratio	−0.092	0.172	**0.441***						
Apase	**−0.751****	**−0.391***	**−0.432***	0.257					
MBP	**−0.556****	**−0.620****	**−0.638****	−0.229	0.391				
pH	**−0.538****	**−0.518****	−0.389	0.027	0.383	**0.717****			
Olsen-P	**0.736****	**−0.514***	**0.608****	−0.074	**−0.707****	**−0.540****	**−0.479***		
Carboxylates	0.001	**−0.452***	−0.028	0.070	**0.467***	0.046	−0.049	−0.360	
AMF colonization	0.242	0.384	0.199	0.383	0.233	−0.243	−0.300	0.097	**0.750****

*Apase, rhizosphere alkaline phosphatase activity; MBP, microbial-biomass P; Olsen-P, available P; pH, rhizosphere pH; carboxylates, the amount of total carboxylates in the rhizosphere. *P < 0.05. **P < 0.01; ***P < 0.001.*

Correlation coefficients with P < 0.05 were shown in bolded.

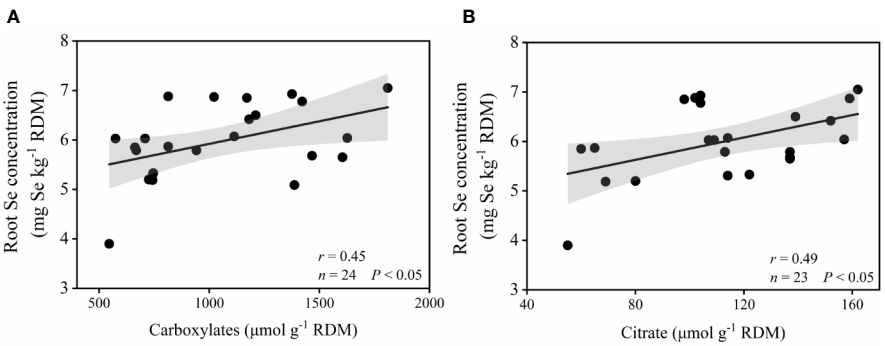

FIGURE 6 | Correlation between root Se concentration and total carboxylates **(A)**, and citrate **(B)** in the rhizosphere. ANOVA *P*-values are indicated in the graphs. Gray areas are the 95% confidence intervals of the models.

pH, MBP, and Olsen-P), rhizosphere soil alkaline phosphatase activity, plant biomass, and plant P content on plant Se content (**Figure 7**). The soil properties (−0.098), rhizosphere carboxylates (−0.400), and alkaline phosphatase activity (−0.455) had negative total-effects on plant Se content, while the colonization by AMF (0.234), P supply (0.523), plant biomass (0.564), and plant P content (0.597) showed positive total-effects on it.

DISCUSSION

Our results show that alfalfa dry mass and shoot and root P concentrations were significantly increased by the interaction of AMF and P treatments. Patharajan and Raaman (2012) reported that alfalfa dry mass in mycorrhizal plants were significantly higher than that in non-mycorrhizal plants. Mycorrhizal symbiosis can play an important role in improving plant viability (Patharajan and Raaman, 2012; Ju et al., 2019). In the 5P and 20P treatments, inoculation of AMF increased plant P content, possibly due to the higher plant growth and greater mobilization of soil P by external hyphae (Asghari et al., 2005; Parihar et al., 2019). Some previous reports also indicated that mycorrhizal colonization can improve the P status of plants (Chen et al., 2010; Goicoechea et al., 2014; He et al., 2017c). The result that mycorrhizal colonization rate was the highest in P20 treatment in the present study did not agree with the conclusions of some studies, which have shown a negative correlation between AMF colonization rate and soil available P (Asghari et al., 2005; Kowalska and Konieczny, 2019). It might be due to the relatively low levels of available P in the soil in all treatments (<10 mg available P kg^{-1} soil). Fornara et al. (2019) reported that when soil available P concentration reached 50 mg kg^{-1} and beyond, AMF colonization rate decreased significantly. On the other hand, AM fungi may be parasitic to their host plants if the net cost of AM symbiosis exceeds the net benefit (Johnson et al., 1997). AM symbiosis could be altered by the level of soil available P, and mutualism likely occur in P-deficient soils (Johnson et al., 2015). In the results of Liu et al. (2020), AMF colonization rate was the highest in P30 treatment compared with the control and P100 treatments. In the present study, both AMF colonization rate and P content were the highest in P20 treatment, likely indicating the best benefit of AM symbiosis (Sawers et al., 2017).

In our results, shoot Se concentration decreased from 6.0 to 5.5 μg kg^{-1}, but plant Se content per pot increased from 26 to 35 μg as the P level increased in the +AMF treatments. It can be explained by the dilution effect that the increased biomass diluted the Se concentration in plants (Mora et al., 2008; Lee et al., 2011). Carter et al. (1972) found that P-fertilizer

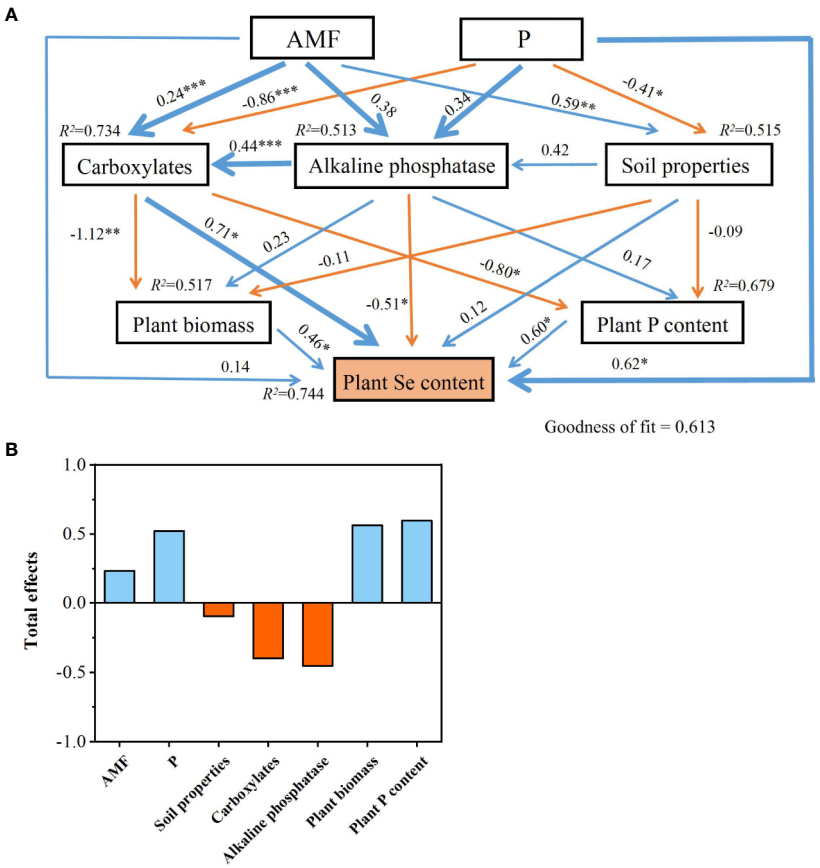

FIGURE 7 | Cascading relationships of plant Se content with plant traits and soil properties. Partial least squares path modelling disentangles the major pathways of the influences of plant traits and soil properties on plant Se content **(A, B)**. Blue and red arrows indicate positive and negative flows of causality, respectively. $^{*}P < 0.05$; $^{**}P < 0.01$; $^{***}P < 0.001$. Numbers on the arrow indicate significant standardized path coefficients. R^2 indicates the variance of dependent variable explained by the model.

application increased Se content in alfalfa grown in alkaline soils, and speculated that the addition of P replaced soil-adsorbed Se, since P had a higher adsorption capacity than Se. The presence of P in soil decreased Se adsorption on soil surfaces, and increased Se concentration in soil solution, thereby increasing Se uptake by plants (Nakamaru and KenjiSekine, 2008; Lee et al., 2011). The effects of AMF on plant Se uptake are still not clear. In the study of Yu et al. (2011), mycorrhizal inoculation inhibited Se uptake by plant roots, due to enhanced binding of Se on hyphae and root surface, which inhibited further movement of Se to roots. However, Luo et al. (2019) reported that mycorrhizal inoculation significantly increased uptake of selenate and selenite by increasing the valid absorption area of roots in winter wheat (*Triticum aestivum* L.). Golubkina et al. (2019) reported that colonization by AMF increased yield and Se content of shallot bulbs (*Allium cepa* L.) by increasing the antioxidant activity of ascorbic acid when compared with the non-inoculated control. Most of previous studies have been focused on the effects of only P input or mycorrhiza colonization on plant Se uptake. Our study demonstrated for the first time that the synergistic effect of colonization by AMF and low P input promoted Se uptake by alfalfa, and the release of carboxylates, especial citrate, and alkaline phosphatase in the rhizosphere was the key factor driving increased Se uptake. In the present results, the AMF had a positive effect on plant Se content, which was increased by 5–10% with AMF. Our hypothesis that carboxylates are important for Se acquisition was supported by the observation of a significant positive correlation between root Se concentration and total carboxylates ($r = 0.45$, $P < 0.05$), especially citrate ($r = 0.49$, $P < 0.01$). There are studies showing that root exudates can compete with Se for sorption sites and reduce the retention of Se in soil, thus promoting the release of Se and facilitating plant Se uptake (Kaiser and Guggenberger, 2003; Adeleke et al., 2017; Dinh et al., 2017). Furthermore, the results of PLS-PM also supported that the colonization by AMF directly determined the carboxylates in the rhizosphere, and indirectly caused the increase of plant Se content.

Inoculation by AMF can affect plant rooting patterns as well as the supply of available nutrients to hosts, thereby changing the composition and quantity of root exudates, which may modify

fungal and microbial activity (Barea et al., 2005). Lower P availability and +AMF stimulated plant roots to release more carboxylates to the soil, and AMF had a stronger effect than P treatments on the carboxylates content (**Table S1**). The amount of total carboxylates had a positive correlation with root to shoot ratio, alkaline phosphatase activity, and MBP (**Table 1**). Given the high alkaline phosphatase activity close to the roots, alfalfa roots apparently released substantial amounts of carboxylates. Roots inoculated by AMF can improve the acquisition of the mobilized P (Gerke, 2015). The release of carboxylates, especially oxalate and citrate, was considered the most effective way of P mobilization (Gerke, 2015). Compared to −AMF treatment, oxalate and citrate concentrations significantly increased in +AMF treatment within the same P levels. The increase in microbial activity and the change in microbial community structure could have affected the oxalate and citrate secretion (Dessaux et al., 2016; Bornø et al., 2018).

Soil phosphatases affect soil P cycling and can be affected by many factors, including rhizosphere processes and growth periods (Ye et al., 2018; Duan et al., 2019). Some reports have indicated that the high activities of the rhizosphere enzymes are due to their release by roots or fungi (Asmar et al., 1995; Kandeler et al., 2002; Wang, Y. L. et al., 2016). Our results showed that alkaline phosphatase activity was significantly affected by the P and AMF treatments. Within the same AMF and P treatments, alkaline phosphatase activity was significantly higher in rhizosphere soil than in bulk soil. We also found that alkaline phosphatase activity had a positive correlation with root to shoot ratio (**Table 1**). Therefore, the increase in alkaline phosphatase activity in rhizosphere soil might be due to release greater amounts of alkaline phosphatase from the roots. Wang, Y. L. et al. (2016) got similar results in canola (*B. napus* cv. MARIE). Kandeler et al. (2002) also revealed that alkaline phosphatase activity was affected by the presence of maize roots. Furthermore, inoculation by AMF can influence soil microbial community, which determined the potential for enzyme synthesis (Kandeler et al., 2002). In our study, alkaline phosphatase activity in the rhizosphere was higher in +AMF treatment compared with −AMF treatment, and had a significant positive correlation with carboxylates and MBP. The differences between +AMF and −AMF treatments in alkaline phosphatase activity can be explained by the increased microbial biomass (Li et al., 2017a) and the shift in microbial community structure (Ventura et al., 2014).

Se availability depends not only on the content of Se but also on its fractions in the environment (Dinh et al., 2017). Some reports indicated that SOL-Se and EX-Se are available for plant uptake because they are free in soil solution or weakly adsorbed on the surface of soil particles (Kulp and Pratt, 2004; Wang, Q. et al., 2016). In this study, the main Se fraction in the soil was EX-Se. EX-Se concentration was significantly higher in +AMF treatment than that in −AMF treatment, and higher in the rhizosphere soil than that in bulk soil. EX-Se had a positive correlation with the amount of carboxylates (**Table S2**). Previous reports indicated that organic acids significantly reduced the number of sorption sites by affecting soil surface characteristics (Kaiser and Guggenberger, 2003; Zhu et al., 2016). Kaiser and Guggenberger (2003) indicated that after equilibration for 24 h, surface sorption sites were reduced by 33.8% by oxalate. Therefore, carboxylates compete with Se for adsorption sites, thereby reducing the retention of Se in soil and promoting the release of soil Se, promoting plant Se uptake (Adeleke et al., 2017; Dinh et al., 2017). On the other hand, EX-Se and SOL-Se concentrations significantly increased as P supply increased. It also can explain the increased plant Se content by the increasing available Se concentrations. Meanwhile, compared to −AMF treatments, Fe-Se concentrations were decreased by 23–35%, and the total amount of carboxylates were increased by 41–53% in +AMF treatments. Fe-Se is firmly fixed by mineral surfaces and thus not readily absorbed by plants. This process is controlled by the quantity and quality of organic acids (Qin et al., 2012). Our results indicated that the increased amounts of organic acids caused the transformation of stable Se into available Se forms that are relatively available to plants.

CONCLUSION

The present study provides an integrated perspective of how AMF and P fertilizer enhance the Se acquisition by alfalfa *via* altering the rhizosphere. Colonization by AMF and low P availability stimulated alfalfa roots to release more carboxylates and alkaline phosphatase, which are important in P and Se acquisition. Rhizosphere carboxylates, especially citrate, increased when roots were colonized by AMF and under low P input, indicating that the response of alfalfa to AMF and P fertilizer can alter the composition and amounts of root exudates. The presence of P in soil reduced Se adsorption on soil surfaces, and increased Se concentration in soil solution, thereby increasing Se uptake by alfalfa. Furthermore, the increased amounts of carboxylates likely reduced the retention of Se in soil, caused the transformation of stable Se into available Se forms and consequently promoted the absorption of Se by alfalfa. Therefore, the variations in carboxylates exudation and alkaline phosphatase activity in the rhizosphere might play a major role in promoting P and Se acquisition by alfalfa. The results in this study are valuable for understanding Se and P uptake by alfalfa and the transformation of Se fractions in soil under the interaction between AMF and P fertilizers.

DATA AVAILABILITY STATEMENT

The datasets generated for this study are available on request to the corresponding authors.

AUTHOR CONTRIBUTIONS

HH conceived and designed the experiments. All authors performed the experiments. QP was responsible for preparing the first draft of the manuscript, and HH and XZ revised the

manuscript. All authors contributed to the article and approved the submitted version.

FUNDING

This work was financially supported by The National Key Research and Development Plan of China (2017YFC0504504), The National Natural Science Foundation of China (41301570), The Light of West China Program of Chinese Academy of Sciences, and Fundamental Research Funds for Central Universities in China.

SUPPLEMENTARY MATERIAL

The Supplementary Material for this article can be found online at: https://www.frontiersin.org/articles/10.3389/fpls.2020.00966/full#supplementary-material

REFERENCES

Adeleke, R., Nwangburuka, C., and Oboirien, B. (2017). Origins, roles and fate of organic acids in soils: a review. *South Afr. J. Bot.* 108, 393–406. doi: 10.1016/j.sajb.2016.09.002

Asghari, H. R., Chittleborough, D. J., Smith, F. A., and Smith, S. E. (2005). Influence of arbuscular mycorrhizal (AM) symbiosis on phosphorus leaching through soil cores. *Plant Soil* 275, 181–193. doi: 10.1007/s11104-005-1328-2

Asmar, F., Gahoonia, T. S., and Nielsen, N. E. (1995). Barley genotypes differ in activity of soluble extracellular phosphatase and depletion of organic phosphorus in the rhizosphere. *Plant Soil* 172, 117–122. doi: 10.1007/BF00020865

Barea, J. M., Pozo, M. J., Azcón, R., and Azcón-Aguilar, C. (2005). Microbial co-operation in the rhizosphere. *J. Exp. Bot.* 417, 1761–1778. doi: 10.1093/jxb/eri197

Barrow, N. J., Cares, P., and Mora, M. L. (2005). Modifications to the Freundlich equation to describe anion sorption over a large range and to describe competition between pairs of ions. *Eur. J. Soil Sci.* 56, 601–606. doi: 10.1111/j.1365-2389.2005.00700.x

Bornø, M. L., Eduah, J. O., Müller-Stöver, D. S., and Liu, F. (2018). Effect of different biochars on phosphorus (P) dynamics in the rhizosphere of *Zea mays* L.(maize). *Plant Soil* 431 (1–2), 257–272. doi: 10.1007/s11104-018-3762-y

Brookes, P., Landman, A., Pruden, G., and Jenkinson, D. (1985). Chloroform fumigation and the release of soil nitrogen: a rapid direct extraction method to measure microbial biomass nitrogen in soil. *Soil Biol. Biochem.* 17, 837–842. doi: 10.1016/0038-0717(85)90144-0

Carter, D. L., Robbins, C. W., and Brown, M. J. (1972). Effect of phosphorus fertilization on the selenium concentration in alfalfa (*Medicago sativa*). *Soil Sci. Soc Am. J.* 36, 75–80. doi: 10.2136/sssaj1972.03615995003600040035x

Cawthray, G. R. (2003). An improved reversed-phase liquid chromatographic method for the analysis of low-molecular mass organic acids in plant root exudates. *J. Chromatogr. A.* 1011, 233–240. doi: 10.1016/S0021-9673(03)01129-4

Chen, M. M., Yin, H. B., O'Connor, P., Wang, Y. S., and Zhu, Y. G. (2010). C:N:P stoichiometry and specific growth rate of clover colonized by arbuscular mycorrhizal fungi. *Plant Soil* 326 (1–2), 21–29. doi: 10.1007/s11104-009-9982-4

Combs, G. F. (2001). Selenium in global food systems. *Brit. J. Nutr.* 85, 517–547. doi: 10.1079/BJN2000280

Dessaux, Y., Grandclément, C., and Faure, D. (2016). Engineering the Rhizosphere. *Trends Plant Sci.* 21, 266–278. doi: 10.1016/j.tplants.2016.01.002

Dinh, Q. T., Li, Z., Tran, T. A. T., Wang, D., and Liang, D. L. (2017). Role of organic acids on the bioavailability of selenium in soil, a review. *Chemosphere* 184, 618–635. doi: 10.1016/j.chemosphere.2017.06.034

Duan, C. J., Razavi, B. S., Shen, G. T., Cui, Y. X., Ju, W. L., Li, S. Q., et al. (2019). Deciphering the rhizobium inoculation effect on spatial distribution of phosphatase activity in the rhizosphere of alfalfa under copper stress. *Soil Biol. Biochem.* 137. doi: 10.1016/j.soilbio.2019.107574

Durán, P., Acuña, J., Armada, E., López-Castillo, O., Cornejo, P., Mora, M., et al. (2016). Inoculation with selenobacteria and arbuscular mycorrhizal fungi to enhance selenium content in lettuce plants and improve tolerance against drought stress. *J. Soil Sci. Plant Nutri.* 16, 201–225. doi: 10.4067/S0718-95162016005000017

Eich-Greatorex, S., Krogstad, T., and Sogn, T. (2010). Effect of phosphorus status of the soil on selenium availability. *J. Plant Nutr. Soil Sci.* 173, 337–344. doi: 10.1002/jpln.200900004

Fornara, D., Flynn, D., and Caruso, T. (2019). Improving phosphorus sustainability in intensively managed grasslands: The potential role of arbuscular mycorrhizal fungi. *Sci. Total Environ.* 706. doi: 10.1016/j.scitotenv.2019.135744

Gerke, J. (2015). The acquisition of phosphate by higher plants: Effect of carboxylate release by the roots. A critical review. *J. Plant Nutr. Soil Sci.* 178, 351–364. doi: 10.1002/jpln.201400590

Giovannetti, M., and Mosse, B. (1980). An evaluation of techniques for measuring vesicular arbuscular mycorrhizal infection in roots. *New Phytol.* 84, 489–500. doi: 10.1111/j.1469-8137.1980.tb04556.x

Goicoechea, N., Sánchez-Díaz, M., Sáez, R., and Irañeta, J. (2004). The association of barley with AM fungi can result in similar yield and grain quality as a long term application of P or P-K fertilizers by enhancing root phosphatase activity and sugars in leaves at tillering. *Biol. Agric. Hortic.* 22, 69–80. doi: 10.1080/01448765.2004.9754989

Goicoechea, N., Baslam, M., Erice, G., and Irigoyen, J. J. (2014). Increased photosynthetic acclimation in alfalfa associated with arbuscular mycorrhizal fungi (AMF) and cultivated in greenhouse under elevated CO_2. *J. Plant Physiol.* 171 (18), 1774–1781. doi: 10.1016/j.jplph.2014.07.027

Goicoechea, N., Garmendia, I., Fabbrin, E., Bettoni, M., Palop, J., and Sanmartín, C. (2015). Selenium fertilization and mycorrhizal technology may interfere in enhancing bioactive compounds in edible tissues of lettuces. *Sci. Hortic.* 195, 163–172. doi: 10.1016/j.scienta.2015.09.007

Golubkina, N., Zamana, S., Seredin, T., Poluboyarinov, P., Sokolov, S., Baranova, H., et al. (2019). Effect of selenium biofortification and beneficial microorganism inoculation on yield, quality and antioxidant properties of shallot bulbs. *Plants* 8, 102. doi: 10.3390/plants8040102

Guan, S. Y., Zhang, D., and Zhang, Z. (1986). *Soil Enzyme and its Research Methods* (Beijing: China Agriculture Press), 274–320.

He, H. H., Dong, Z. G., Peng, Q., Wang, X., Fan, C. B., and Zhang, X. C. (2017a). Impacts of coal fly ash on plant growth and accumulation of essential nutrients and trace elements by alfalfa (*Medicago sativa*) grown in a loessial soil. *J. Environ. Manage.* 197, 428–439. doi: 10.1016/j.jenvman.2017.04.028

He, H. H., Peng, Q., Wang, X., Fan, C. B., Pang, J. Y., Lambers, H., et al. (2017b). Growth, morphological and physiological responses of alfalfa (*Medicago sativa*) to phosphorus supply in two alkaline soils. *Plant Soil* 416, 565–584. doi: 10.1007/s11104-017-3242-9

He, S. B., Long, M. X., He, X. Q., Guo, L. X., Yang, J. Y., Yang, P. Z., et al. (2017c). Arbuscular mycorrhizal fungi and water availability affect biomass and C:N:P ecological stoichiometry in alfalfa (*Medicago sativa* L.) during regrow. *Acta Physiol. Plant* 39 (9), 199. doi: 10.1007/s11738-017-2493-7

He, H. H., Pang, J. Y., Wu, G. L., and Lambers, H. (2019). The application potential of coal fly ash for selenium biofortification. *Adv. Agron.* 157, 1–54. doi: 10.1016/bs.agron.2019.05.002

He, H. H., Wu, M. M., Guo, L., Fan, C. B., Zhang, Z. K., Sui, R., et al. (2020). Release of tartrate as a major carboxylate by alfalfa (*Medicago sativa* L.) under phosphorus deficiency and the effect of soil nitrogen supply. *Plant Soil.* 449, 169–178. doi: 10.1007/s11104-020-04481-9

Johnson, N. C., Graham, J. H., and Smith, F. A. (1997). Functioning of mycorrhizal associations along the mutualism-parasitism continuum. *New Phytol.* 135, 575–585. doi: 10.2307/2558989

Johnson, N. C., Wilson, G. W. T., Wilson, J. A., Miller, R. M., and Bowker, M. A. (2015). Mycorrhizal phenotypes and the law of the minimum. *New Phytol.* 205, 1473–1484. doi: 10.1111/nph.13172

Ju, W. L., Liu, L., Fang, L. C., Cui, Y. X., Duan, C. J., and Wu, H. (2019). Impact of co-inoculation with plant-growth-promoting rhizobacteria and rhizobium on the biochemical responses of alfalfa-soil system in copper contaminated soil. *Ecotoxicol. Environ. Saf.* 167, 218–226. doi: 10.1016/j.ecoenv.2018.10.016

Kaiser, K., and Guggenberger, G. (2003). Mineral surfaces and soil organic matter. *Eur. J. Soil Sci.* 54, 219–236. doi: 10.1046/j.1365-2389.2003.00544.x

Kandeler, E., Marschner, P., Tscherko, D., Gahoonia, T. S., and Nielsen, N. E. (2002). Microbial community composition and functional diversity in the rhizosphere of maize. *Plant Soil* 238, 301–312. doi: 10.1023/a:1014479220689

Kowalska, I., and Konieczny, A. (2019). Effect of mycorrhiza on yield and quality of lettuce grown on medium with different levels of phosphorus and selenium. *Agr. Food Sci.* 28, 84–92. doi: 10.23986/afsci.78169

Kulp, T. R., and Pratt, L. M. (2004). Speciation and weathering of selenium in Upper Cretaceous chalk and shale from South Dakota and Wyoming, USA. *Geochem. Cosmochim. Acta* 68, 3687–3701. doi: 10.1016/j.gca.2004.03.008

Langer, I., Syafruddin, S., Steinkellner, S., Puschenreiter, M., and Wenzel, W. W. (2010). Plant growth and root morphology of *Phaseolus vulgaris* L. grown in a split-root system is affected by heterogeneity of crude oil pollution and mycorrhizal colonization. *Plant Soil* 332, 339–355. doi: 10.1007/s11104-010-0300-y

Lee, S., Doolittle, J. J., and Woodard, H. J. (2011). Selenite adsorption and desorption in selected south Dakota Soils as a function of pH and other oxyanions. *Soil Sci.* 176, 73–79. doi: 10.1097/ss.0b013e31820a0ff6

Li, S., Liang, C., and Shangguan, Z. (2017a). Effects of apple branch biochar on soil C mineralization and nutrient cycling under two levels of N. *Sci. Total Environ.*, 607, 109–119. doi: 10.1016/j.scitotenv.2017.06.275

Li, Z., Liang, D., Peng, Q., Cui, Z., Huang, J., and Lin, Z. (2017b). Interaction between selenium and soil organic matter and its impact on soil selenium bioavailability: a review. *Geoderma* 295, 69–79. doi: 10.1016/j.geoderma.2017.02.019

Li, Y. Y., Yu, S. H., and Zhou, X. B. (2018). Effects of phosphorus on absorption and transport of selenium in rice seedlings. *Environ. Sci. Pollut. R.* 26 (13), 755–761. doi: 10.1007/s11356-018-2690-y

Liu, Q., Wang, D. J., Jiang, X. J., and Cao, Z. H. (2004). Effects of the interactions between selenium and phosphorus on the growth and selenium accumulation in rice (*Oryza sativa*). *Environ. Geochem. Hlth.* 26, 325–330. doi: 10.1023/b:egah.0000039597.75201.57

Liu, M., Zhao, Z., Chen, L., Chen, L., Wang, L., Ji, L., et al. (2020). Influences of arbuscular mycorrhizae, phosphorus fertiliser and biochar on alfalfa growth, nutrient status and cadmium uptake. *Ecotox. Environ. Safe* 196, 110537. doi: 10.1016/j.ecoenv.2020.110537

Lu, R. (2000). *Analytical methods of soil agricultural chemistry* (Beijing: China Agriculture Press).

Luo, W., Li, J., Ma, X., Niu, H., Hou, S. W., and Wu, F. Y. (2019). Effect of arbuscular mycorrhizal fungi on uptake of selenate, selenite, and selenomethionine by roots of winter wheat. *Plant Soil* 438, 71–83. doi: 10.1007/s11104-019-04001-4

Mora, M. D., Pinilla, L., and Analí, R. (2008). Selenium uptake and its influence on the antioxidative system of white clover as affected by lime and phosphorus fertilization. *Plant Soil* 303, 139–149. doi: 10.1007/s11104-007-9494-z

Munier-Lamy, C., Deneux-Mustin, S., Mustin, C., Merlet, D., Berthelin, J., and Leyval, C. (2007). Selenium bioavailability and uptake as affected by four different plants in a loamy clay soil with particular attention to mycorrhizae inoculated ryegrass. *J. Environ. Radioact.* 97, 148–158. doi: 10.1016/j.jenvrad.2007.04.001

Nakamaru, Y., and KenjiSekine, (2008). Sorption behavior of selenium and antimony in soils as a function of phosphate ion concentration. *Soil Sci. Plant Nutr.* 54, 10. doi: 10.1111/j.1747-0765.2008.00247.x

Nanjareddy, K., Blanco, L., Arthikala, M. K., Affantrange, X. A., Sánchez, F., and Lara, M. (2014). Nitrate regulates rhizobial and mycorrhizal symbiosis in common bean (*Phaseolus vulgaris* L.). *J. Integr. Plant Biol.* 56 (3), 281–298. doi: 10.1111/jipb.12156

Ngigi, P. B., Lachat, C., Masinde, P. W., and Laing, G. D. (2019). Agronomic biofortification of maize and beans in Kenya through selenium fertilization. *Eviron. Geochem. Health* 19, 309–312. doi: 10.1007/s10653-019-00309-3

Pang, J. Y., Bansal, R., Zhao, H. X., Bohuon, E., Lambers, H., Ryan, M. H., et al. (2018). The corboxylate-releasing phosphorus-mobilizing strategy can be proxied by foliar manganese concentration in a large set of chickpea germplasm under low phosphorus supply. *New Phytol.* 219, 518–529. doi: 10.1111/nph.15200

Parihar, M., Meena, V. S., Mishra, P. K., Rakshit, A., Choudhary, M., Yadav, P. R., et al. (2019). Arbuscular mycorrhiza: a viable strategy for soil nutrient loss reduction. *Arch. Microbiol.* 201, 723–735. doi: 10.1007/s00203-019-01653-9

Patharajan, S., and Raaman, N. (2012). Influence of arbuscular mycorrhizal fungi on growth and selenium uptake by garlic plants. *Arch. Phytopathol. Plant Prot.* 45 (2), 1–14. doi: 10.1080/03235408.2010.501166

Peng, Q., He, H. H., Fan, C. B., Wu, M. M., Guo, L., Wang, X., et al. (2020). The interaction of phosphate and selenite in alkaline soil and accumulation by alfalfa (*Medicago sativa* L.). *Arch. Agron. Soil Sci.* doi: 10.1080/03650340.2020.1718112

Qin, F., Shan, X. Q., and Wei, B. (2004). Effects of low-melecular-weight organic acids and residence time on desorption of Cu, Cd, and Pb from soils. *Chemosphere* 57, 253–263. doi: 10.1016/j.chemosphere.2004.06.010

Qin, H. B., Zhu, J. M., and Su, H. (2012). Selenium fractions in organic matter from Se-rich soils and weathered stone coal in selenosis areas of China. *Chemosphere* 86, 626–633. doi: 10.1016/j.chemosphere.2011.10.055

Rayman, M. P. (2000). The importance of selenium to human health. *Lancet* 356, 233–241. doi: 10.1016/S0140-6736(00)02490-9

Sawers, R. J. H., Svane, S. F., Quan, C., Grønlund, M., Wozniak, B., Gebreselassie, M. N., et al. (2017). Phosphorus acquisition efficiency in arbuscular mycorrhizal maize is correlated with the abundance of root-external hyphae and the accumulation of transcripts encoding PHT1 phosphate transporters. *New Phytol.* 214, 632–643. doi: 10.1111/nph.14403

Seymour, N. P., Edwards, D. G., and Thompson, J. P. (2019). A dual rescaled Mitscherlich model of the simultaneous savings in phosphorus and zinc fertiliser from arbuscular mycorrhizal fungal colonisation of linseed (*Linum usitatissimum* L.). *Plant Soil* 440, 97–118. doi: 10.1007/s11104-019-04065-2

Smith, S. E., and Read, D. J. (1997). *Mycorrhizal symbiosis* (London: Academic Press).

Smith, S. E., and Read, D. J. (2008). *Mycorrhizal symbiosis, 3rd edn* (San Diego: Academic Press).

Smith, S. E., Smith, F. A., and Jakobsen, I. (2003). Mycorrhizal fungi can dominate phosphate supply to plants irrespective of growth responses. *Plant Physiol.* 133, 16–20. doi: 10.1104/pp.103.024380

Sors, T. G., Ellis, D. R., and Salt, D. E. (2005). Selenium uptake, translocation, assimilation and metabolic fate in plants. *Photosyn. Res.* 86, 373–389. doi: 10.1007/s11120-005-5222-9

Turrión, M. B., Bueis, T., Lafuente, F., Lopez, O., San, J. E., Eleftheriadis, A., et al. (2018). Effects on soil phosphorus dynamics of municipal solid waste compost addition to a burnt and unburnt forest soil. *Sci. Total Environ.* 642, 374–382. doi: 10.1016/j.scitotenv.2018.06.051

Vance, E. D., Brookes, P. C., and Jenkinson, D. S. (1987). An extraction method for measuring soil microbial biomass C. *Soil Biol. Biochem.* 19, 703–707. doi: 10.1016/0038-0717(87)90052-6

Ventura, M., Zhang, C., Baldi, E., Fornasier, F., Sorrenti, G., Panzacchi, P., et al. (2014). Effect of biochar addition on soil respiration partitioning and root dynamics in an apple orchard. *Eur. J. Soil Sci.* 65, 186–195. doi: 10.1111/ejss.12095

Wang, S., Liang, D., Wang, D., Wei, W., Fu, D., and Liu, Z. (2012). Selenium fractionation and speciation in agriculture soils and accumulation in corn (*Zea mays* L.) under field conditions in Shaanxi Province, China. *Sci. Total Environ.*, 427, 159–164. doi: 10.1016/j.scitotenv.2012.03.091

Wang, Y. Z., Chen, X., Whalen, J. K., Cao, Y. H., Quan, Z., Lu, C., et al. (2015). Kinetics of inorganic and organic phosphorus release influenced by low molecular weight organic acids in calcareous, neutral and acidic soils. *J. Plant Nutr. Soil Sci.* 178, 556–566. doi: 10.1002/jpln.201500047

Wang, Q., Zhang, J., Zhao, B., Xin, X., Deng, X., and Zhang, H. (2016). Influence of long-term fertilization on selenium accumulation in soil and uptake by crops. *Pedosphere* 26, 120–129. doi: 10.1016/S1002-0160(15)60028-5

Wang, Y. L., Krogstad, T., Clarke, J. L., Halama, M., Øgaard, A. F., Eich-Greatorex, S., et al. (2016). Rhizosphere organic anions play a minor role in improving crop species' ability to take up residual phosphorus (P) in agricultural soils low in P availability. *Front. Plant Sci.* 7, 1664. doi: 10.3389/fpls.2016.01664

Wang, D., Dinh, Q. T., Anh, T. T. T., Zhou, F., Yang, W. X., Wang, M. K., et al. (2018). Effect of selenium-enriched organic material amendment on selenium

fraction transformation and bioavailability in soil. *Chemosphere* 199, 417–426. doi: 10.1016/j.chemosphere.2018.02.007

Wang, M., Yang, W., Zhou, F., Du, Z. K., Xue, M. Y., Chen, T., et al. (2019). Effect of phosphate and silicate on selenite uptake and phloem-mediated transport in tomato (*Solanum lycopersicum* L.). *Environ. Sci. Pollut. R.* 26, 475–484. doi: 10.1007/s11356-019-04717-x

Watts-Williams, S. J., Smith, F. A., McLaughlin, M. J., Patti, A. F., and Cavagnaro, T. R. (2015). How important is the mycorrhizal pathway for plant Zn uptake? *Plant Soil* 390, 157–166. doi: 10.1007/s11104-014-2374-4

Wen, Z., Li, H., Shen, Q., Tang, X., Xiong, C., Li, H., et al. (2019). Tradeoffs among root morphology, exudation and mycorrhizal symbioses for phosphorus-acquisition strategies of 16 crop species. *New Phytol.* 223, 882–895. doi: 10.1111/nph.15833

Whanger, P. D. (2004). Selenium and its relationship to cancer: an update. *Brit. J. Nutr.* 91, 11–28. doi: 10.1079/BJN20031015

White, P. J. (2018). Selenium metabolism in plants. *BBA-Gen. Subj.* 11, 2333–2342. doi: 10.1007/978-3-642-10613-2_10

Ye, D. H., Liu, D., Li, T. X., Zhang, X. Z., and Zheng, Z. C. (2018). Phosphorus accumulation characteristics in *Polygonum hydropiper* and rhizosphere properties affected by poultry manure application. *Appl. Soil Ecol.* 131, 12–21. doi: 10.1016/j.apsoil.2018.07.005

Yu, Y., Luo, L., Yang, K., and Zhang, S. Z. (2011). Influence of mycorrhizal inoculation on the accumulation and speciation of selenium in maize growing in selenite and selenate spiked soils. *Pedobiologia* 54 (5–6), 267–272. doi: 10.1016/j.pedobi.2011.04.002

Zhang, L., Hu, B., Li, W., Che, R., Deng, K., and Chu, C. (2014). *OsPT2*, a phosphate transporter, is involved in the active uptake of selenite in rice. *New Phytol.* 201, 1183–1191. doi: 10.1111/nph.12596

Zhang, D., Dong, T., and Ye, J. (2017). Selenium accumulation in wheat (*Triticum aestivum* L.) as affected by coapplication of either selenite or selenate with phosphorus. *Soil Sci. Plant Nutr.* 63, 8. doi: 10.1080/00380768.2017.1280377

Zhu, X. J., He, J. T., Su, S. H., Zhang, X. L., and Wang, F. (2016). Concept model of the formation process of humic acid-kaolin complexes deduced by trichloroethylene sorption experiments and various characterizations. *Chemosphere* 151, 116–123. doi: 10.1016/j.chemosphere.2016.02.068

Conflict of Interest: The authors declare that the research was conducted in the absence of any commercial or financial relationships that could be construed as a potential conflict of interest.

frontiers in Plant Science

ORIGINAL RESEARCH
published: 26 June 2020
doi: 10.3389/fpls.2020.00755

Multivariate Analysis Models Based on Full Spectra Range and Effective Wavelengths Using Different Transformation Techniques for Rapid Estimation of Leaf Nitrogen Concentration in Winter Wheat

*Lantao Li[1], Di Lin[2], Jin Wang[3], Liu Yang[2] and Yilun Wang[1]**

[1] College of Resources and Environment, Henan Agricultural University, Zhengzhou, China, [2] College of Forestry, Henan Agricultural University, Zhengzhou, China, [3] Soil and Fertilizer Station of Jiaozuo City, Jiaozuo, China

OPEN ACCESS

Edited by:
Katja Witzel, Leibniz Institute of Vegetable and Ornamental Crops, Germany

Reviewed by:
Salah Elsayed Mohamed Elsayed, University of Sadat City, Egypt
Shawn Carlisle Kefauver, University of Barcelona, Spain
Werner B. Herppich, Leibniz Institute for Agricultural Engineering and Bioeconomy (ATB), Germany

***Correspondence:**
Yilun Wang
wangyilunrl@163.com;
wangyilunhenau@126.com

Specialty section:
This article was submitted to Plant Nutrition, a section of the journal Frontiers in Plant Science

Received: *25 March 2020*
Accepted: *12 May 2020*
Published: *26 June 2020*

Citation:
Li L, Lin D, Wang J, Yang L and Wang Y (2020) Multivariate Analysis Models Based on Full Spectra Range and Effective Wavelengths Using Different Transformation Techniques for Rapid Estimation of Leaf Nitrogen Concentration in Winter Wheat. Front. Plant Sci. 11:755. doi: 10.3389/fpls.2020.00755

To develop a stable estimation model and identify effective wavelengths that could explain the variations in leaf nitrogen (N) concentration with different N supplies, growing seasons, ecological locations, growth stages, and wheat cultivars. Four field experiments were performed during two consecutive years (2017–2019) at three sites (Yuanyang, Hebi, and Wenxian) in Henan, China. *In situ* canopy spectral reflectance data under the aforementioned N supply conditions were obtained over a range of 400–950 nm (visible and near-infrared region). On the basis of the canopy raw spectral reflectance data and their subsequent transformation by two different techniques, first-derivative reflectance (FDR) and continuum removal (CR), four multivariate regression methods were comparatively analyzed and used to develop predictive models for estimating leaf N concentration: multiple linear regression (MLR), principal component regression (PCR), partial least square (PLS), and support vector machine (SVM). Results showed that leaf N concentration and canopy reflectance significantly varied with the levels of N fertilization, and a good correlation was observed for all the spectral techniques. Seven wavelengths with relatively higher *r* values than the bands of the raw spectra centered at 508, 525, 572, 709, 780, 876, and 925 nm were specified using the FDR technique. Based on the full wavelengths, the FDR-SVM model exhibited a good performance for leaf N concentration estimation, with coefficients of determination (r^2_{val}) for the validation datasets and corresponding relative percent deviations (RPD_{val}) values of 0.842 and 2.383, respectively. However, the FDR-PLS yielded a more accurate assessment of the leaf N concentration than did the other methods, with r^2_{val} and RPD_{val} values of 0.857 and 2.535, respectively. The variable importance in projection (VIP) scores from the FDR-PLS with the all canopy spectral region were used to screen the effective wavelengths of the spectral data. Therefore, six effective wavelengths centered at 525, 573, 710, 780, 875, and 924 nm were identified for leaf N concentration estimation. The SVM regression method with the effective wavelengths

showed excellent performance for leaf N concentration estimation with r^2_{val} = 0.823 and RPD_{val} = 2.280. These results demonstrated that the *in situ* canopy spectral technique is promising for the estimation of leaf N concentration in winter wheat based on the FDR-PLS regression model and the effective wavelengths identified.

Keywords: precision nitrogen management, spectral analysis, estimation model, first derivative reflectance, partial least square regression

INTRODUCTION

Nitrogen (N) is an essential element of pigments as well as proteins associated with crop N status, and N is important in terms of plant vigor, yield formation, and grain quality (Din et al., 2018). Precise N management and accurate estimation of crop N status are the most common problems in modern agricultural systems not only for economic reasons but also for minimizing the atmospheric, soil, and water pollution associated with excessive N supply (Zhao et al., 2016; Din et al., 2018). Currently, several techniques for the non-destructive estimation of crop N have been proposed, including leaf color charts, SPAD-502, Dualex 4, and CCM-2000 (Schächtl et al., 2005; Din et al., 2018; Zhao et al., 2018). However, all these instruments center on the local test of the leaves and are not practical for application across large fields. Moreover, the techniques actually rely on the absorption of crop chlorophyll and carotenoid instead of N. Several elements, such as leaf thickness, leaf specific mass, the leaf position, the areas from which leaves are measured (Daughtry et al., 2000; Muñoz-Huerta et al., 2013), crop growth, cultivar, and solar radiation (Tahir Ata-Ul-Karim et al., 2016; Din et al., 2018), can influence the results. To overcome these problems, canopy spectral remote sensing (CSRS) has emerged and is recommended as an alternative effective and non-destructive technique for rapidly estimating crop N status (Yao et al., 2015; Prey and Schmidhalter, 2019).

Canopy spectral remote sensing is a promising approach for the accurate and real-time estimation of crop N status and other growth variables over large areas (Ecarnot et al., 2013; Feng et al., 2015). CSRS analyses may be performed with field-based spectral radiometers such as the ASD FieldSpec Handheld 2, which can generate a high resolution (<5 nm) and continuous spectrum at each pixel that is influenced by N compounds, chlorophyll status, and crop structures; therefore, it provides an effective method for assessing leaf N concentration at whole canopy scales (Gómez-Casero et al., 2010; Yao et al., 2010; Feng et al., 2015). However, the canopy raw spectra are, however, influenced by the solar radiant flux, crop structure characteristics (e.g., biomass, leaf area index, blade incidence, and plant height), and soil background conditions (Feng et al., 2014; Mahajan et al., 2014). Thus, identifying effective wavelengths for rapidly estimating crop leaf N concentration has become an extremely important topic in canopy spectral studies. Several canopy spectral transformation techniques, such as first-derivative reflectance (FDR) (Ihuoma and Madramootoo, 2019; Wen et al., 2019) and continuum removal (CR) (Tian et al., 2017; Tan et al., 2019), have been used to improve the signal-to-noise ratio, minimize the impact of atmospheric noise, and enhance weak spectral information of remote monitoring of leaf N concentration in crops. Experimental investigations have shown that the FDR technique can resolve overlapping absorption phenomena and can minimize the influences of soil or atmospheric background noise (Hruschka, 1987; Miphokasap et al., 2012). Moreover, the CR technique can smooth the spectra, eliminate signal errors caused by the instruments themselves, and suppress the noise within spectral data (Mutanga et al., 2005; Summers et al., 2009; Tan et al., 2019).

On the basis of nearly contiguous spectral wavelengths, overfitting, redundancy, and multicollinearity problems might occur during the modeling of the canopy raw spectra and their subsequent transformation (e.g., *via* FDR or CR). Multivariable statistical regression methods such as multiple linear regression (MLR), principal component regression (PCR), and partial least square (PLS) analysis were used to reduce multicollinearity and establish a quantitative monitoring model for estimating leaf N concentration (Hansen and Schjoerring, 2003; Wang et al., 2011; Thorp et al., 2017). Rather than using individual wavelengths for the construction of vegetation indices, the aforementioned approaches incorporate all wavelength data into models for the estimation of plant physiological and biochemical properties (Thorp et al., 2017). For example, MLR is the linear combination of the full-range spectral reflectance and is also the most widely used method for rapidly estimating crop leaf N concentration using spectral measurements (Huang et al., 2004; Wang et al., 2011). The PCR is a linear regression that first decomposes the spectra into a suite of PCs that offers the maximum variation of the spectra with the aim of optimizing the estimative capacity of the model; it then regresses the PCs against the response variable (Cho et al., 2007; Foster et al., 2016). PLS is closely related to PCR. The difference between PCR and PLS is that while the former uses only the independent variables (e.g., spectral wavelengths) to construct new PCs, the PLS uses both the independent and dependent variables (e.g., leaf N concentration) that will play the role of explanatory variables to construct PCs. Moreover, the PLS method can reduce the high dimensional and collinear spectral reflectance data to a small quantity of latent variables and effectively eliminate or minimize the overfitting problem (Foster et al., 2016). However, MLR, PCR, and PLS were initially selected for laboratory spectroscopy but are now increasingly used for analyzing CSRS data of maize (Weber et al., 2012; Kawamura et al., 2018), rice (Inoue et al., 2012; Li F. et al., 2014; Li X. C. et al., 2014), and grasslands (Kawamura et al., 2010). Previous studies showed that the selection of effective wavelengths can refine the predictive ability

of the standard full spectrum by optimizing important effective wavelengths; therefore, several effective wavelength selection methods such as MLR, PCR, and PLS have been developed (Bolster et al., 1996; Yao et al., 2015; Kawamura et al., 2018). Nonetheless, only a limited number of studies made an attempt to evaluate the aforementioned effective wavelength selection methods in combination with spectral transformation techniques (CR and FDR) for a comparative and comprehensive estimation of leaf N concentration of winter wheat. Moreover, limited previous research, along with its recommended algorithms and spectral indices, has been conducted to estimate the leaf N concentration in the same ecological locations (Montes et al., 2011; Cao et al., 2017; Zhao et al., 2018; Bruning et al., 2019), neglecting the problem of unsynchronized winter wheat growth stages under different conditions. Therefore, further work is needed to systematically analyze the performance of multiple methods for predicting leaf N concentration in winter wheat under different ecological areas, unsynchronized growth stages, cultivars, and N supply.

The specific objectives of this study were to (1) study the relationship between winter wheat leaf N concentration and the *in situ* canopy raw spectra and the transformation techniques from field spectral data; (2) compare the reliability and performance of the applied multivariate regression methods based on the raw and the transformed (FDR, CR) spectra for the estimation of leaf N concentration; (3) determine the optimal method with highest robustness and accuracy and lowest complexity that can rapidly estimate the leaf N concentration of winter wheat; and (4) determine the sensitivity of the effective wavelengths by using the identified monitoring method and construction of an estimation model of wheat leaf N concentration.

MATERIALS AND METHODS

Experimental Design

Four experiments on wheat were carried out across two growing seasons, with one field located in Yuanyang County (35°6′ N, 113°56′ E), two in Hebi city (35°40′ N, 114°17′ E), and one in Wenxian County (34°57′ N, 112°59′ E) in Henan Province, North China (**Figure 1A**). The following variables were included in the study of hexaploid winter wheat: year, ecosystem, cultivar, N application rate, and sampling date. A randomized complete block design including all treatments in the field experiments was applied, with three replications (**Supplementary Table S1** and **Figures 1B,C**). For all the treatments, phosphorus (P) and potassium (K) nutrition were applied. The recommended P and K fertilizer rates were 120 kg ha^{-1} (as superphosphate, 12% P_2O_5) and 90 kg ha^{-1} K_2O (as potassium chloride, 60% K_2O). Moreover, the detailed information of N supply (as controlled-release urea, 44% N) is shown in **Supplementary Table S1**. All nutrient resources were applied as a basal fertilizer prior to sowing. Other winter wheat management practices, such as the use of herbicides and disease and pest control followed the local standard practices during the two growing seasons.

Sampling and Measurement

Spectral Measurements

In this study, all the *in situ* canopy reflectance spectra were obtained with an ASD FieldSpec Handheld 2 passive spectroradiometer (ASD Inc., Boulder, CO, United States) at nadir from a height of approximately 1.0 m above the winter wheat canopy under sunny conditions between 11:00 and 14:00 (**Figure 1D**). To reduce the influence of atmospheric and field conditions, the winter wheat canopy spectral reflectance was measured at six sites in each plot, and 60 scans served as the mean canopy spectrum for each plot. A 30 × 30-cm $BaSO_4$ calibration Spectralon® panel (Spectralon®, Labsphere, Inc., North Sutton, NH, United States) was applied to calibrate the reflectance and radiance before and after taking a measurement. Wavelengths below 400 and above 900 nm were excluded due to the low signal. Therefore, the canopy reflectance data were resampled within the range of 400–900 nm.

Leaf Nitrogen Concentration

After each measurement of *in situ* canopy spectral reflectance, four areas of 0.30 m^2 (60 cm long × 50 cm wide; the spacing interval between the two rows was 20 cm) of winter wheat plants from each plot were immediately selected to determine the leaf N concentration (%) values by the H_2SO_4-H_2O_2 method (Thomas et al., 1967). The leaf N concentration was measured *via* a flow injection auto-analyzer (AA3, Bran and Luebbe, Norderstedt, Germany).

Transformation Techniques of Winter Wheat *in situ* Canopy Spectra

To smooth the spectra, the frequently used Savitzky-Golay filter was applied, and a second-order polynomial with a window size of five spectral wavelengths was added to eliminate signal noise (Gholizadeh et al., 2015). Afterward, two spectral transformation techniques, FDR and CR, were compared to identify the best techniques for the rapid estimation of the leaf N concentration from the raw reflectance spectra (Curran et al., 2001; Sims and Gamon, 2002).

First-Derivative Reflectance

First-Derivative Reflectance spectral transformation technique was applied to reduce the impacts of multiple scattering of radiation (Ihuoma and Madramootoo, 2019). The FDR formula is as follows (Miphokasap et al., 2012):

$$\mathrm{FDR}(\lambda_{\mathrm{i}} = \frac{\left[\mathrm{R}(\lambda_{i+1}) - \mathrm{R}(\lambda_{\mathrm{i}-1})\right]}{2\Delta\lambda} \quad (1)$$

Where $\mathrm{R}(\lambda_{i+1})$ and $\mathrm{R}(\lambda_{i-1})$are the reflectance values at i + 1 and i−1, respectively; and $\Delta\lambda$ is the wavelength increment.

Continuum Removal

The CR spectral transformation technique was also used to estimate the leaf N concentration. The continuum line is a convex hull to connect the local maxima of a spectrum (**Figure 2**). The method was used to assess crop biochemicals with dried plant leaves (Curran et al., 2001), and to the best of our knowledge,

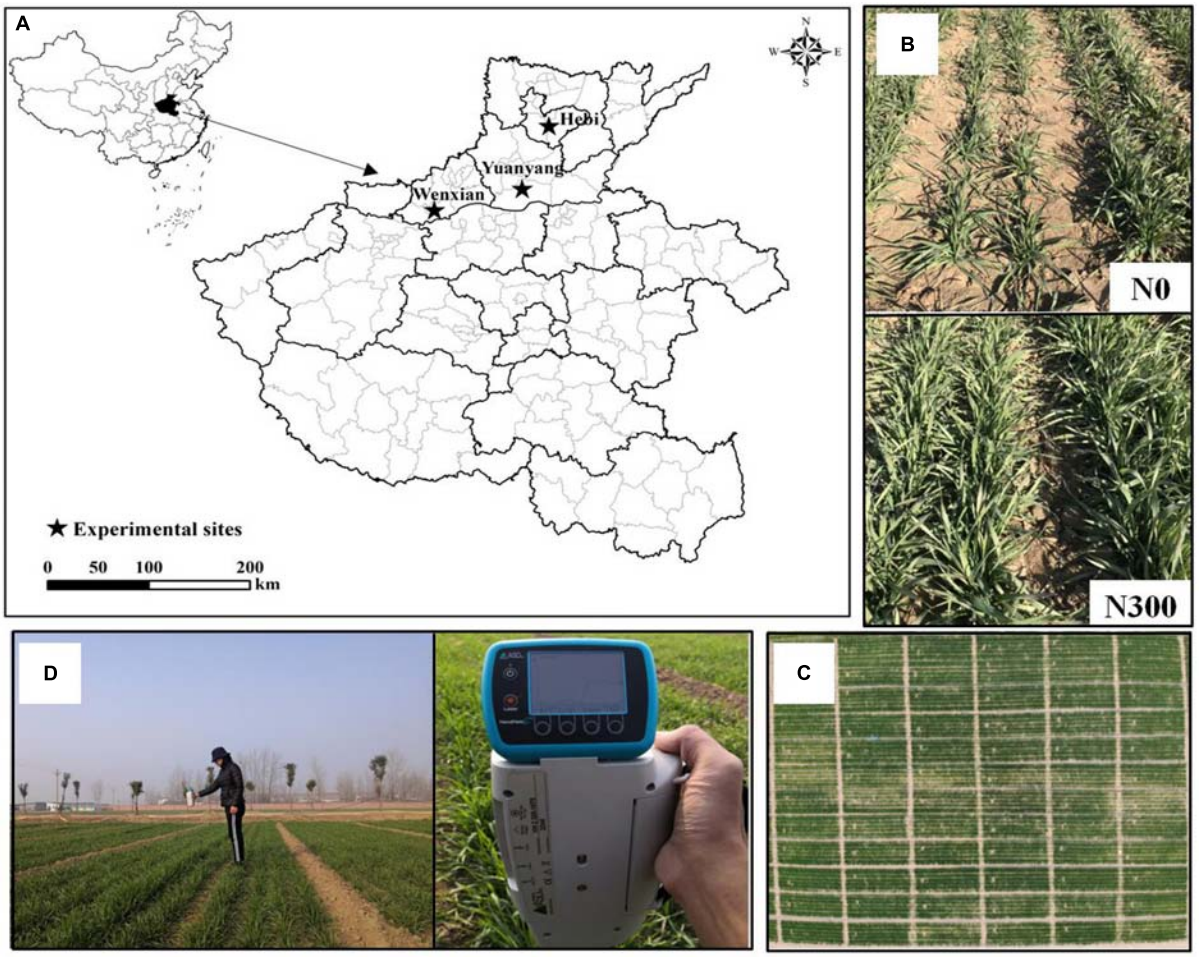

FIGURE 1 | Sites **(A)**, close-up view **(B)** of the field experiments, aerial view of the N supply plots **(C)**, and measurements of winter wheat canopy spectral reflectance **(D)**.

studies that have extended this technique to *in situ* canopy spectra under field conditions combined with the quantification of leaf N concentration in winter wheat are relatively rare (Li et al., 2019).

Data Analysis

Four different multivariate regression methods were comparatively analyzed and used to estimate the winter wheat N status at the canopy levels: MLR, PCR, PLS, and support vector machine (SVM).

Multiple Linear Regression Analysis

Multiple linear regression is a common approach used to calibrate the relationship between multiple independent variables and a dependent variable, which was successfully used for the evaluation of *in situ* canopy spectra and involved stretching the results of a simple linear regression analysis from a single dimension into multiple dimensions (Bruning et al., 2019).

Principal Component Regression Analysis

Principal component regression is based on principal component analysis and is also a widely adopted method for dimensionality reduction of spectral data. The optimal number of components to contain in the model was identified by the number of components that had the lowest root mean square error of cross-validation (RMSECV). A 20-fold leave-one-out cross-validation procedure was applied for validating the PCR models to avoid overfitting or underfitting.

Partial Least Square Analysis

Partial least square is a powerful method that can be used to reduce the *in situ* reflectance data effectively into a few latent variables with information content and thus maximize the covariance between the spectra and leaf N concentration. The optimal number of latent variables (ONLVs) of the PLS was the same as that of the PCR and was confirmed based on the lowest RMSECV using the leave-one-out method. In addition, reflectance spectra obtained in this study contained 551

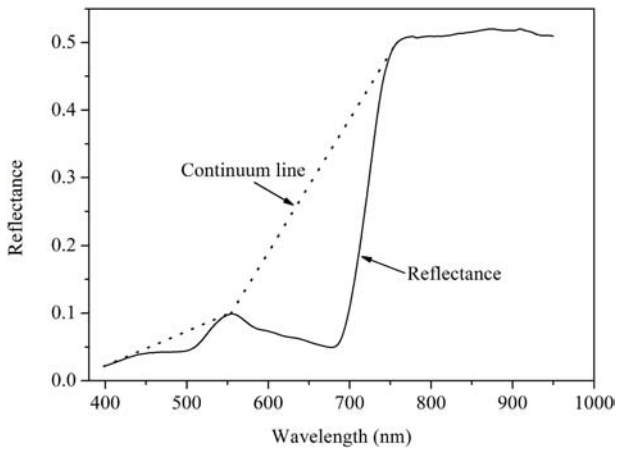

FIGURE 2 | Schematic diagram of the continuum removal technique on the winter wheat canopy.

bands in the range of 400–950 nm. The variable importance in projection (VIP) scores resulting from the PLS were applied to select the effective wavelengths for rapidly estimating the leaf N concentration. The threshold score of a VIP is 1.0; therefore, a higher VIP score indicates that the wavelength is more important to estimate the leaf N concentration, while the wavelength having a lower VIP score has less impact on the estimation (Word et al., 2001).

Support Vector Machine Analysis

In this study, the Gaussian radial basis function (RBF) kernel was used for the SVM technique, and the detailed introduction of the SVM regression model is reported by Schölkopf et al. (2000) and Bishop (2006).

Model Calibration and Validation

The data function from the four field experiments is shown in **Supplementary Table S1**. Correlation analysis between the *in situ* reflectance spectra and leaf N concentration was performed using the SAS 8.0 (SAS Institute, Cary, NC, United States). The MLR, PCR, PLS, and SVM methods were analyzed using MATLAB 2019a (MathWorks, Natick, MA, United States). The performance of all the regression models was evaluated by the coefficient of determination (r^2), root mean square error (RMSE), and relative percent deviation (RPD) in both the calibration and validation datasets. Detailed information concerning the r^2 and RPD values of the regression methods is shown in **Table 1** (Chang et al., 2001).

RESULTS

Leaf Nitrogen Concentration in Winter Wheat

Table 2 shows the results of the descriptive analyses of the leaf N concentration in the calibration, validation, and combined datasets. In the combined datasets, the treatments (N rates, ecological sites, and growing seasons and stages) generated a wide range of leaf N concentration (1.06–6.16%). Among the datasets, compared with those of validation datasets, the mean and range of the calibration datasets were greater, showing that the classification of the data is appropriate.

TABLE 1 | Classification of the performance of the regression methods in terms of r^2 and RPD values.

Standards	Model performance		
	Unacceptable	Acceptable	Excellent
r^2	<0.50	0.75–0.50	>0.75
RPD	<1.40	2.00–1.40	>2.00

RPD, relative percent deviation.

Variability of the *in situ* Spectra Obtained at Various Nitrogen Supplies

The spectral characteristics of canopy reflectance were significantly different under the different N treatments but exhibited similar patterns in both the calibration and validation datasets (**Figure 3**). In the visible spectral region (400–710 nm), the *in situ* canopy reflectance was higher at low N supply, whereas in the near-infrared spectral region (70–950 nm), the canopy reflectance tended to decrease with decreasing N rates. In addition, reflectance in the near-infrared region led to greater variability compared with that in the visible region, the radiation of which chlorophyll absorbs. The results show that radiation in the near-infrared region was responsive to the different N supply during different growth stages but tended to saturate at high N supply.

Correlation of the Leaf Nitrogen Concentration With *In situ* Canopy Spectra for the Calibration Datasets

To clarify the relationships of the canopy raw spectra and their subsequent transformation (*via* the FDR and CR techniques) with the winter wheat leaf N concentration, correlation analysis was applied to 551 spectral bands from 400 to 950 nm for the calibration datasets (**Figure 4**). First, a negative correlation was detected for the visible wavelengths, with the lowest r in the 525–570 nm range ($r < 0.60$, $n = 165$), whereas a positive correlation was found in the near-infrared region, with the greatest r value in the 720–745 nm region ($r > 0.80$, $n = 165$) for the raw spectra (**Figure 4A**). The FDR spectra showed a correlations throughout the full wavelength region (400–950 nm) that was stronger than the region of the raw spectra and exhibited more prominent valleys and peaks, for example, at 508, 525, 572, 709, 780, 876, and 925 nm, etc., (**Figure 4B**). Moreover, the leaf N concentrations exhibited a weak negative correlation with the CR spectra in the ultraviolet wavelength region (400–420 nm) and a strong positive relationship in the visible near-infrared wavelength region (420–950 nm). The average r values in the ultraviolet,

TABLE 2 | Statistics of winter wheat leaf nitrogen concentration for the calibration and validation datasets.

Datasets	Number of samples	Mean (%)	Maximum (%)	Minimum (%)	SD	CV (%)
Calibration datasets	165	3.90	6.16	1.06	1.21	31.03
Validation datasets	150	3.70	6.02	1.12	1.27	34.32
All datasets	315	3.80	6.16	1.06	1.24	32.63

SD, standard deviation; CV (%), coefficient of variation.

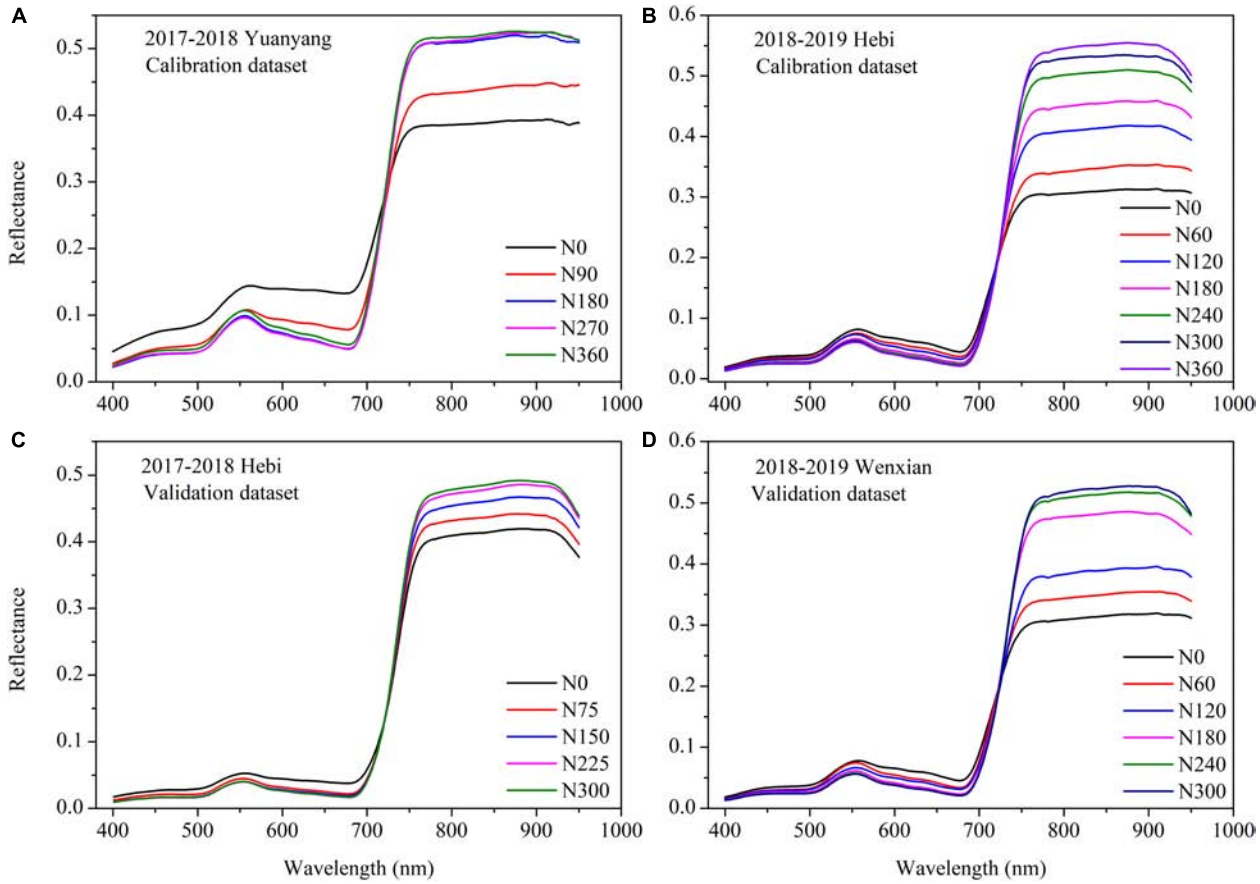

FIGURE 3 | Effect of nitrogen (N) status on the *in situ* canopy spectral reflectance of winter wheat for the calibration **(A,B)** and validation **(C,D)** datasets.

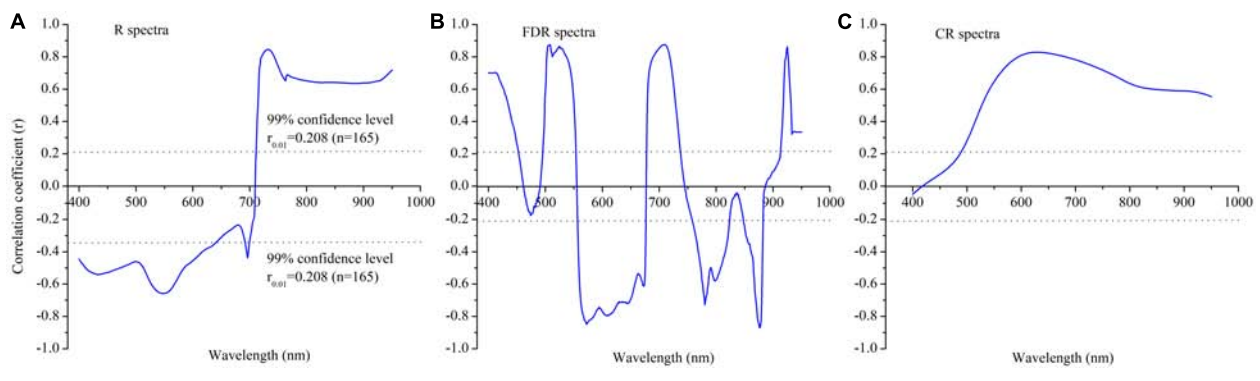

FIGURE 4 | Correlation analysis between the leaf nitrogen concentration in winter wheat and canopy hyperspectral reflectance and its transformation in the calibration dataset under various N rates: **(A)** R spectra, **(B)** FDR spectra and **(C)** CR spectra.

visible, and near-infrared regions were −0.021, 0.551, and 0.636, respectively (**Figure 4C**).

Accuracy of Leaf Nitrogen Concentration Estimation With the Multiple Linear Regression, Principal Component Regression, Partial Least Square, and Support Vector Machine

The robustness and accuracy of the four regression methods for leaf N concentration estimation using the statistical indicators $r^2_{cal/val}$, $RMSE_{cal/val}$, and $RPD_{cal/val}$ based on different spectral transformation techniques (raw, FDR and CR spectra) were evaluated and compared (**Table 3**). The FDR based on the PLS analysis generally yielded a measurement accuracy (r^2_{cal} = 0.886, RPD_{cal} = 2.973; r^2_{val} = 0.857, RPD_{val} = 2.535) that was greater than that of the other three methods and models. Moreover, the second most important technique for leaf N concentration estimation after the FDR-PLS was FDR-SVM, which yielded relatively low $r^2_{cal/val}$ (1.96 and 1.78%, respectively) and $RPD_{cal/val}$ (3.69 and 6.38%, respectively) values in the calibration and validation datasets, respectively. The poorest performance was acquired using the FDR-MLR model (**Table 3**), with an r^2_{cal} of 0.784, RPD_{cal} of 2.086, r^2_{val} of 0.746, and RPD_{val} of 1.584, respectively. The aforementioned results indicate that the FDR-PLS model estimated the leaf N concentration the best and was identified as the preferred model for use in subsequent analyses.

Effective Wavelength Identification

Number of Latent Variables and Cross-Validation

In this study, the ONLVs was first determined according to the lowest value of the RMSECV (**Figure 5A**) *via* the leave-one-out method based on the FDR-PLS model (**Figure 5B**). To identify the ONLVs, the calibration datasets were applied to investigate how well the model with a different number of latent variables fit the data. As shown in **Figure 5A**, when the number of latent variables increased, the RMSECV value of the FDR-PLS model tended to decrease. However, the presence of inadequate latent variables led to underfitting, showing the requirement of a balance between the RMSECV value and the number of latent variables. With this criterion, the ONLVs for the FDR-PLS was 7. **Figure 5B** shows the accuracy of the cross-validation based on the FDR-PLS for the leaf N concentration estimation. Compared with those from the best fit technique (FDR) for the PLS method, both the r^2 (r^2_{CV} = 0.868) and RPD (RPD_{CV} = 2.756) values in the cross-validation were relatively high, indicating that the model was acceptable and that the ONLVs was suitable.

Loading Weights of the First-Derivative Reflectance–Partial Least Square Regression Model

To first clarify the relative impact of each wavelength, the loading weight value was computed and analyzed on the basis of the FDR-PLS model output (**Figure 6**). The loading weights showed how the latent variables resulting from the FDR-PLS model were developed from scaled estimators of the *in situ* reflectance spectra (**Figures 5**, **6**). A relatively high absolute loading weight value indicates that the specific wavelength is crucial for the estimation of the leaf N concentration of winter wheat. In this study, the first four latent variables elucidated more than 81% of the canopy spectral reflectance variances and 82% of the leaf N concentration variances. The highest absolute loading weight values of each wavelength for rapidly estimating the leaf N concentration were in the visible (525 and 573 nm), red-edge (710 nm), and near-infrared wavelengths region (785, 870, and 930 nm) in the first latent variables of the FDR-PLS model (**Figure 6**). The selected wavelengths of the second loading weight were also in the visible (525 and 570 nm), red-edge (678, and 730 nm), and near-infrared wavelengths region (930 nm), while those of the third and fourth loading weights were nearly the same as those of the first and second loading weights.

TABLE 3 | MLR, PCR, PLS, and SVM for predicting leaf nitrogen concentration in winter wheat based on different spectral transformation techniques.

Methods	Spectral techniques	Calibration datasets			Validation datasets		
		r^2_{cal}	$RMSE_{cal}$	RPD_{cal}	r^2_{val}	$RMSE_{val}$	RPD_{val}
MLR	Raw Spectra	0.706	0.699	1.731	0.681	0.824	1.542
	FDR Spectra	**0.784**	**0.580**	**2.086**	**0.746**	**0.802**	**1.584**
	CR Spectra	0.753	0.631	1.918	0.731	0.792	1.604
PCR	Raw Spectra	0.764	0.585	2.068	0.755	0.631	2.013
	FDR Spectra	**0.837**	**0.501**	**2.415**	**0.811**	**0.575**	**2.209**
	CR Spectra	0.814	0.522	2.318	0.793	0.603	2.106
PLS	Raw Spectra	0.816	0.518	2.336	0.806	0.601	2.113
	FDR Spectra	**0.886**	**0.407**	**2.973**	**0.857**	**0.501**	**2.535**
	CR Spectra	0.854	0.463	2.613	0.824	0.576	2.205
SVM	R Spectra	0.804	0.573	2.112	0.789	0.624	2.035
	FDR Spectra	**0.869**	**0.422**	**2.867**	**0.842**	**0.533**	**2.383**
	CR Spectra	0.831	0.501	2.415	0.807	0.604	2.103

The FDR is highlighted to emphasize the best predictive performance of the four models for predicting leaf nitrogen concentration. MLR, multiple linear regression; PCR, principal component regression; PLS, partial least square; SVM, support vector machine.

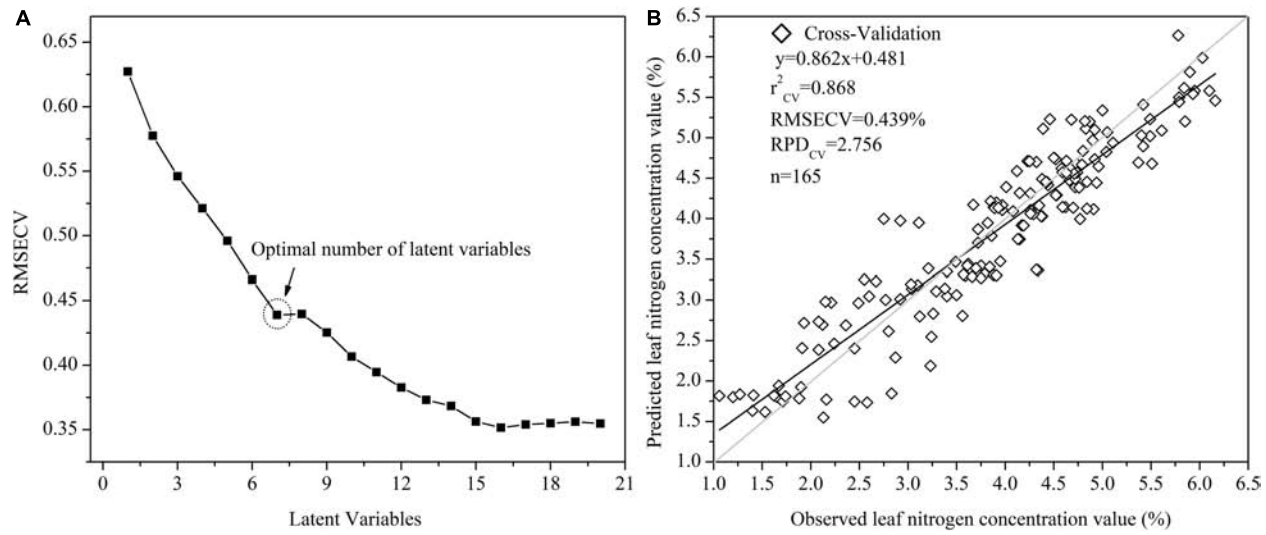

FIGURE 5 | Plots with the root mean square error of cross-validation (RMSECV) with the number of latent variables **(A)** and cross-validation between the observed and predicted leaf nitrogen concentration values **(B)**.

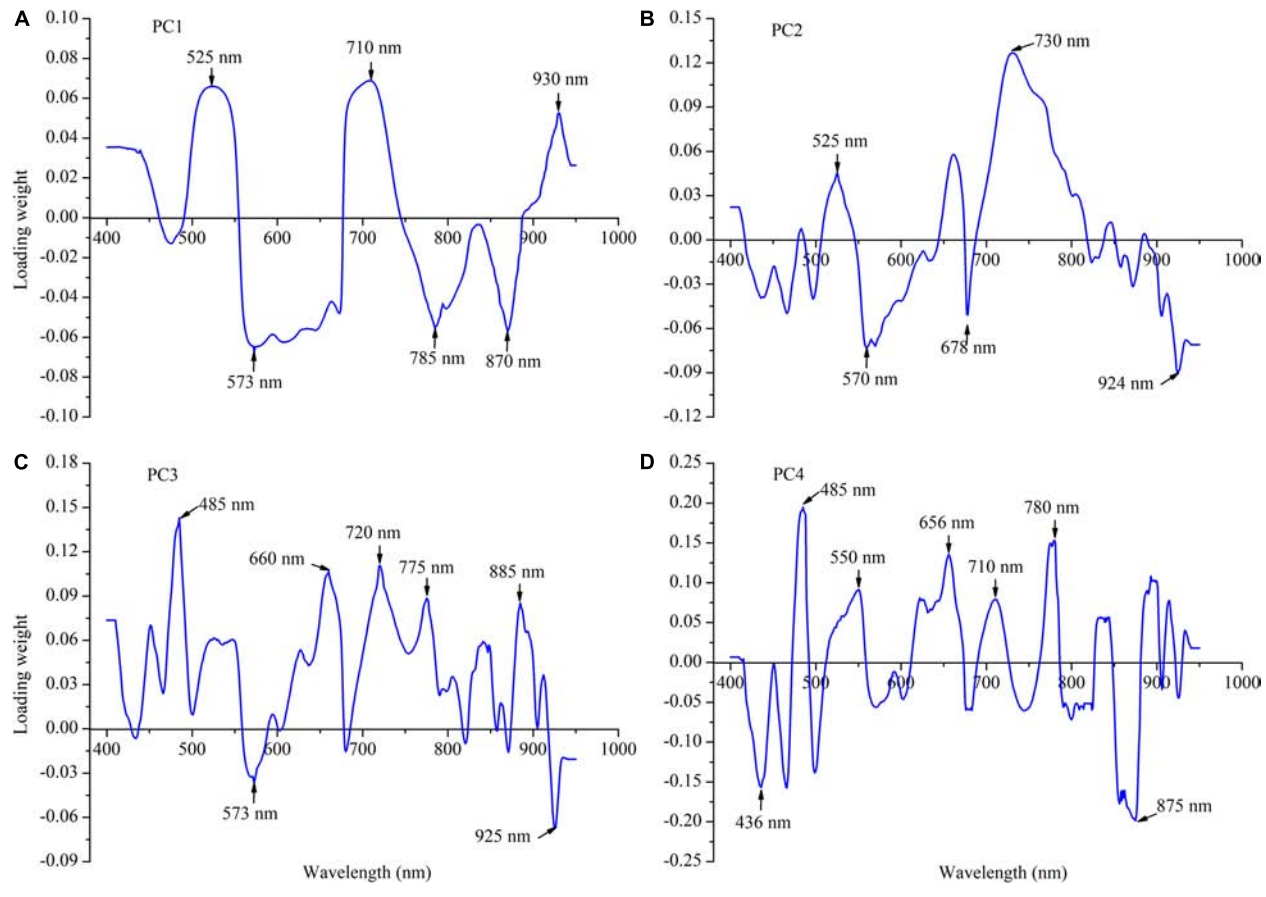

FIGURE 6 | Loading weight over the full wavelength regions for the first four latent variables (PC1–PC4) of the first-derivative reflectance (FDR)-partial least square (PLS) for leaf nitrogen concentration estimation: **(A)** PC1, **(B)** PC2, **(C)** PC3, and **(D)** PC4.

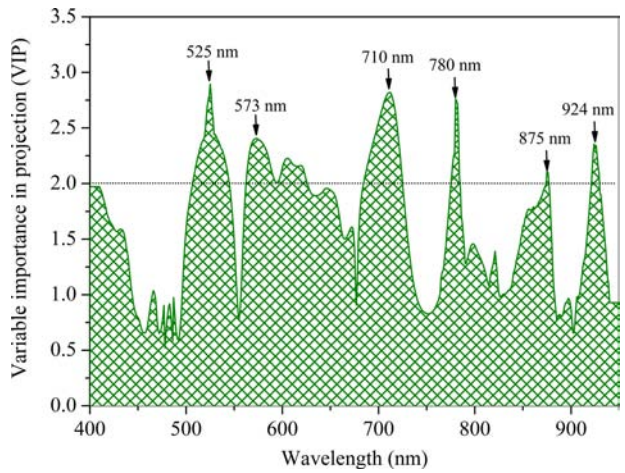

FIGURE 7 | The variable importance in projection (VIP) values over the full wavelength regions for leaf N concentration estimation.

Effective Wavelength Identification by Variable Importance in Projection Values Based on the First-Derivative Reflectance–Partial Least Square Model

Owing to the high dimensionality of canopy spectral reflectance data with redundancy between the adjacent wavelengths, it was necessary to select several effective wavelengths that have the most representative information for rapidly estimating the leaf N concentration of winter wheat. Thus, the VIP scores were applied to select the effective wavelengths for predicting the leaf N concentration from the full spectral region on the basis of the FDR-PLS model (**Figure 7**). Generally, a high VIP score shows that the specific wavelength is of vital importance (the threshold value of VIP is 1.0). As shown in **Figure 7**, given that numerous wavelengths have relatively high VIP scores (>1.0), it was difficult to identify and distinguish the effective wavelengths for rapidly estimating the leaf N concentration. Therefore, the threshold value of the VIP was set at 2.0 in this study, and six wavelengths were selected as effective, two in the visible (525 and 573 nm), one in the red-edge (710 nm), and three in the near-infrared region (780, 875, and 924 nm) (**Figure 7**). Obviously, the identified effective wavelengths based on the VIP for estimating the leaf N concentration were shown in the same region of PC1 loading weight (**Figure 6A**).

Multiple Linear Regression, Principal Component Regression, Partial Least Square, and Support Vector Machine Analysis With Effective Wavelengths

To further illuminate the potential and robustness of the identified effective wavelengths for rapidly estimating the leaf N concentration of winter wheat, MLR, PCR, PLS, and SVM analyses were developed again based on these effective wavelengths. **Figure 8** shows the optimal setting of the meta-parameters with the FDR-SVM model. In this study, the optimal combination of epsilon (0.1), g (3.16), and c (100) were calculated based on the RMSECV. Moreover, the results shown in **Table 4** indicated that the FDR-PLS model not only exhibited better performance on the calibration datasets, but also offered higher prediction accuracy on the validation datasets. Although 98.91% (551 vs. 6) of the canopy spectral reflectance variable information was eliminated for the leaf N concentration estimation, the r^2_{val} (4.6% for FDR-PLS and 2.3% for FDR-SVM) and RPD (13.5% for FDR-PLS and 4.5% for FDR-SVM) values only showed a slight reduction. The results showed that the identified effective wavelengths and selected revalidated models were promising for rapidly estimating the leaf N concentration of winter wheat with less computational effort.

DISCUSSION

Our study demonstrates that CSRS can successfully estimate winter wheat N status. Canopy reflectance decreased from visible region and increased from near-infrared region as leaf N concentration increased (**Figure 3**). Increased N rates could increase greenness, reflecting a combination of chlorophyll concentration, structural agronomic parameters, and leaf anatomical structure characteristics (Colwell, 1974; Yao et al., 2013; Barankova et al., 2016). The interpretation of the effect of canopy spectral reflectance followed the general assumption that a decrease in greenness or chlorophyll creates higher reflectance in the visible region due to decreased light absorption from a lower chlorophyll concentration (Hinzman et al., 1986; Li et al., 2018a,b). The opposite effect was found in the near-infrared region; the relative high reflectance spectra observed were due to the canopy and leaf internal scattering and the apparent structure parameters, such as leaf area index and biomass (Colwell, 1974; Hansen and Schjoerring, 2003).

In general, two major approaches have been developed for remote estimation of crop N status: (i) empirical statistical methods and (ii) physically based retrieval methods such as canopy radiative transfer models (RTMs) (Darvishzadeh et al., 2011; Li et al., 2016). These two methods are mutually complementary (Viña et al., 2011), however, the main disadvantages in using RTM is the ill-posed nature of model inversion (Combal et al., 2002; Houborg et al., 2009), meaning that the inverse solution is not always unique as various combinations of canopy parameters may yield almost similar spectra (Fang et al., 2003). Consequently, the empirical approaches are used more extensively than RTM due to their straightforward mechanisms and efficient computations and have been proposed as better predictors of crop N status (Viña et al., 2011; Delegido et al., 2013). Our study also demonstrates that CSRS can successfully estimate winter wheat N status using the multivariate statistical approaches. Results indicated that the FDR-PLS was superior to the other models in estimation accuracy (**Table 3**). These results are consistent with those of Wang et al. (2017) and Nguyen and Lee (2006), showing that the PLS method could reduce the high dimensionality and

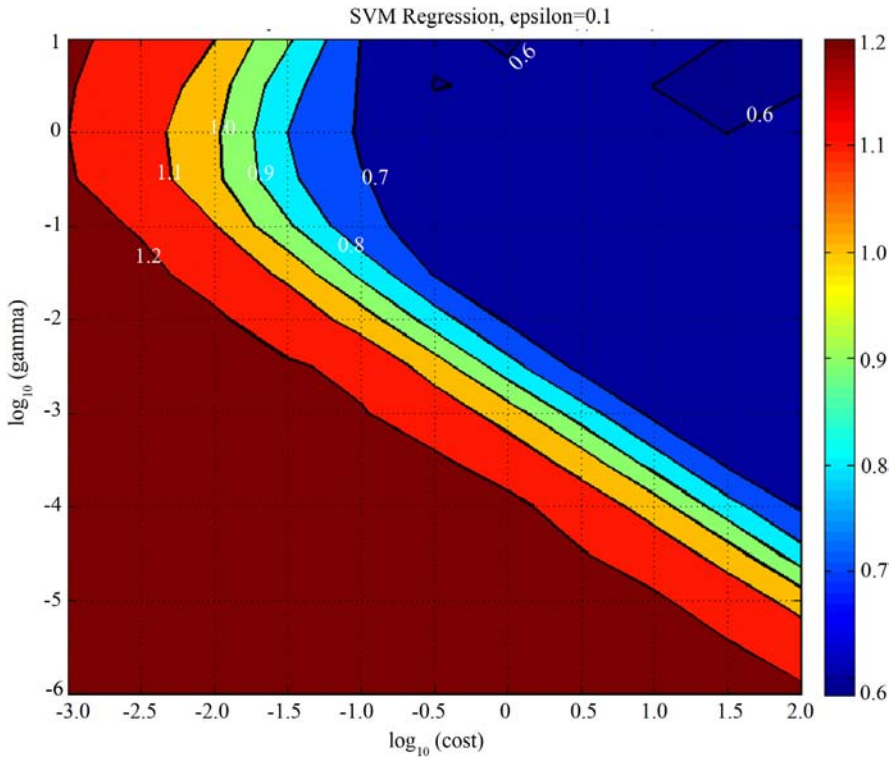

FIGURE 8 | Contour map view of *g, c*, selected by the grid-search method with the first-derivative reflectance (FDR)–support vector machine (SVM) model for leaf nitrogen concentration prediction.

multicollinearity problem of spectral data. The PCR method accounts for only the variance of the explanatory independent variables without considering the internal relationships between the wavelengths and response dependent variables, whereas the PLS accounts for both (Atzberger et al., 2010). Although MLR is the most widely used method for crop biophysical and biochemical estimation using spectral method (Curran et al., 2001; Wang et al., 2011), it might have a collinearity problem (Grossman et al., 1996).

To further rank the estimation models in their predictive power, we calculated several other statistical parameters like the slope (b), intercept (a), and coefficient of deviation (CD) of the linear regressions ($y = a + bx$) (**Supplementary Table S2**). The CD values are all higher than 1.0, indicating that the four models overestimated the predicted values compared to the measured data (Müller et al., 2008). The reason for this is presumably the higher range of the calibration datasets than the validation datasets (**Table 2**), which can be subject to the field conditions uncertainty and as a result lead to considerably overestimation error in the modeling process.

TABLE 4 | FDR-MLR, FDR-PCR, FDR-PLS, and FDR-SVM analysis for leaf nitrogen concentration prediction of winter wheat using effective wavelengths.

Models	Calibration datasets			Validation datasets		
	r^2_{cal}	RMSE $_{cal}$	RPD $_{cal}$	r^2_{val}	RMSE $_{val}$	RPD $_{val}$
FDR-MLR	0.753	0.642	1.885	0.713	0.895	1.419
FDR-PCR	0.808	0.581	2.083	0.784	0.615	2.065
FDR-PLS	0.854	0.452	2.677	0.819	0.569	2.232
FDR-SVM	0.857	0.458	2.642	0.823	0.557	2.280

In this study, we mainly discussed the effect of the visible near-infrared range of canopy reflectance on winter wheat N estimation. For a typical crop canopy, reflectance in the visible spectrum and near-infrared region is often used to estimate leaf N concentration indirectly due to the strong positive correlation with leaf chlorophyll content and pronounced sensitivity to canopy structures (Kokaly, 2001; Gitelson et al., 2005; Li et al., 2019). However, the sensitive absorption wavelength of N lies in short-wave-infrared, which is easily obscured by water-vapor absorption characteristics (Curran, 1989; Fourty et al., 1996; Feng et al., 2008). Moreover, the spectral sensing information obtained in this study was from field-based spectral radiometers; research on aerial-based hyperspectral imagery for crop N status estimation is an important tendency in precision agriculture (Nigon et al., 2015; Bruning et al., 2019). Unlike conventional field-based spectrometers that only collect spectral information for a single point, a hyperspectral imaging system can obtain images of the whole target for each wavelength recorded (Wu and Sun, 2013). Future work should evaluate these results for diverse species, under different environmental conditions, and using not only *in situ* measurements but also airborne and satellite data.

CONCLUSION

The overall results from this research showed that winter wheat leaf N concentration could be assessed with reasonable accuracy from field *in situ* canopy spectral data. We conclude that: (i) the FDR-PLS regression model was performed better than other model techniques evaluated for leaf N concentration of winter wheat; (ii) Six bands centered at 525, 573, 710, 780, 875, and 924 nm were identified as effective wavelengths for leaf N concentration estimation using the *in situ* canopy spectra; (iii) An acceptable accuracy with r^2 (r^2_{cal} = 0.857; r^2_{val} = 0.823) and RPD (RPD_{cal} = 2.642; RPD_{val} = 2.280) was acquired using the FDR-SVM based on the effective wavelengths.

DATA AVAILABILITY STATEMENT

All datasets presented in this study are included in the article/**Supplementary Material**.

AUTHOR CONTRIBUTIONS

LL designed the study and wrote the manuscript. YW conceptualized the manuscript. DL and LY conducted the field experiments. JW contributed the tables and figures. All authors contributed to the article and approved the submitted version.

FUNDING

This research work was financially supported by the National Key R&D Program of China (2017YFD0301106) and the special fund for young talents in Henan Agricultural University (30500427).

ACKNOWLEDGMENTS

We are grateful to the reviewers for their insightful comments, which greatly improved the manuscript.

SUPPLEMENTARY MATERIAL

The Supplementary Material for this article can be found online at: https://www.frontiersin.org/articles/10.3389/fpls.2020.00755/full#supplementary-material

REFERENCES

Atzberger, C., Guerif, M., Baret, F., and Werner, W. (2010). Comparative analysis of three chemometric techniques for the spectroradiometric assessment of canopy chlorophyll content in winter wheat. *Comput. Electron. Agric.* 73, 165–173. doi: 10.1016/j.compag.2010.05.006

Barankova, B., Lazar, D., and Naus, J. (2016). Analysis of the effect of chloroplast arrangement on optical properties of green tobacco leaves. *Remote Sens. Environ.* 174, 181–196. doi: 10.1016/j.rse.2015.12.011

Bishop, C. M. (2006). *Pattern Recognition And Machine Learning*. New York, NY: Springer.

Bolster, K. L., Martin, M. E., and Aber, J. D. (1996). Determination of carbon fraction and N concentration in tree foliage by near infrared reflectance: a comparison of statistical methods. *Can. J. Forest Res.* 26, 590–600.

Bruning, B., Liu, H. J., Brien, C., Berger, B., Lewis, M., and Garnett, T. (2019). The development of hyperspectral distribution maps to predict the content and distribution of nitrogen and water in wheat (*Triticum awstivum*). *Front. Plant Sci.* 10:1380. doi: 10.3389/fpls.2019.01380

Cao, Q., Miao, Y. X., Feng, G. H., Gao, X. W., Liu, B., Liu, Y. Q., et al. (2017). Improving nitrogen use efficiency with minimal environmental risks using an active canopy sensor in a wheat-maize cropping system. *Field Crops Res.* 214, 365–372.

Chang, C., Laird, D. A., Mausbach, M. J., and Hurburgh, C. R. (2001). Near infrared reflectance spectroscopy: principal components regression analysis of soil properties. *Soil Sci. Soc. Am. J.* 65, 480–490.

Cho, M. A., Skidmore, A., Corsi, F., Van Wieren, S. E., and Sobhan, I. (2007). Estimation of green grass/ herb biomass from airborne hyperspectral imagery using spectral indices and partial least squares regression. *Intern. J. Appl. Earth Observ. Geoinform.* 9, 414–424. doi: 10.1016/j.jag.2007.02.001

Colwell, J. E. (1974). Vegetation canopy reflectance. *Remote Sens. Environ.* 3, 175–183. doi: 10.1016/0034-4257(74)90003-90000

Combal, B., Baret, F., and Weiss, M. (2002). Improving canopy variables estimation from remote sensing data by exploiting ancillary information. Case study on sugar beet canopies. *Agronomie* 22, 205–215. doi: 10.1051/agro:2002008

Curran, P. J. (1989). Remote sensing of foliar chemistry. *Remote Sens. Environ.* 30, 271–278. doi: 10.1016/0034-4257(89)90069-90062

Curran, P. J., Dungan, J. L., and Peterson, D. L. (2001). Estimating the foliar biochemical concentration of leaves with reflectance spectrometry. Testing the Kokaly and Clark methodologies. *Remote Sens. Environ.* 76, 349–359. doi: 10.1016/S0034-4257(01)00182-181

Darvishzadeh, R., Atzberger, C., Skidmore, A., and Schlerf, M. (2011). Mapping grassland leaf area index with airborne hyperspectral imagery: a comparison study of statistical approaches and inversion of radiative transfer models. *ISPRS J. Photogram. Remote Sens.* 66, 894–906. doi: 10.1016/j.isprsjprs.2011.09.013

Daughtry, C. S. T., Walthall, C. L., Kim, M. S., De Colstoun, E. B., and McMurtrey, J. E. (2000). Estimating corn leaf chlorophyll concentration from leaf and canopy reflectance. *Remote Sens. Environ.* 74, 229–239. doi: 10.1016/S0034-4257(00)00113-119

Delegido, J., Verrelst, J., Meza, C. M., Rivera, J. P., Alonso, L., and Moreno, J. (2013). A red edge spectral index for remote sensing estimation of green LAI over agroecosystems. *Eur. J. Agron.* 46, 42–52. doi: 10.1016/j.eja.2012.12.001

Din, M., Ming, J., Hussain, S., Ata-Ul-Karim, S. T., Rashid, M., Tahir, M. N., et al. (2018). Estimation of dynamic canopy variables using hyperspectral derived vegetation indices under varying N rates at diverse phonological stages of rice. *Front. Plant Sci.* 9:1883. doi: 10.3389/fpls.2018.01883

Ecarnot, M., Compan, F., and Rounmet, P. (2013). Assessing leaf nitrogen content and leaf mass per unit area of wheat in the field throughout plant cycle with a portable spectrometer. *Field Crops Res.* 140, 44–50. doi: 10.1016/j.fcr.2012.10.013

Fang, H. L., Liang, S. L., and Kuusk, A. (2003). Retrieving leaf area index using a genetic algorithm with a canopy radiative transfer model. *Remote Sens. Environ.* 85, 257–270. doi: 10.1016/S0034-4257(03)00005-1

Feng, W., Guo, B. B., Wang, Z. J., He, L., Song, X., Wang, Y. H., et al. (2014). Measuring leaf nitrogen concentration in winter wheat using double-peak spectral reflection remote sensing data. *Field Crops Res.* 159, 43–52. doi: 10.1016/j.fcr.2014.01.010

Feng, W., Guo, B. B., Zhang, H. Y., He, L., Zhang, Y. S., Wang, Y. H., et al. (2015). Remote estimation of above ground nitrogen uptake during vegetative growth in winter wheat using hyperspectral red-edge ratio data. *Field Crops Res.* 180, 197–206. doi: 10.1016/j.fcr.2015.05.020

Feng, W., Yao, X., Zhu, Y., Tian, Y. C., and Cao, W. X. (2008). Monitoring leaf nitrogen status with hyperspectral reflectance in wheat. *Eur. J. Agron.* 28, 394–404. doi: 10.1016/j.eja.2007.11.005

Foster, A. J., Kakani, V. G., and Mosali, J. (2016). Estimation of bioenergy crop yield and N status by hyperspectral canopy reflectance and partial least square regression. *Precis. Agric.* 17, 1–18.

Fourty, T., Baret, F., Jacquemoud, S., Schmuck, G., and Verdebout, J. (1996). Leaf optical properties with explicit description of its biochemical composition: direct and inverse problems. *Remote Sens. Environ.* 56, 104–117. doi: 10.1016/0034-4257(95)00234-230

Gholizadeh, A., Boruvka, L., Saberioon, M. M., Kozak, J., Vasat, R., and Nemecek, K. (2015). Comparing different data preprocessing methods for monitoring soil heavy metals based on soil spectral features. *Soil Water Res.* 10, 218–227. doi: 10.17221/113/2015-SWR

Gitelson, A. A., Vina, A., Ciganda, V., Rundquist, D. C., and Arkebauer, T. J. (2005). Remote estimation of canopy chlorophyll content in crops. *Geophys. Res. Lett.* 32, 93–114.

Gómez-Casero, M. T., Castillejo-González, I. L., García-Ferrer, A., Peña-Barragán, J. M., Jurado-Expósito, M., García-Torres, L., et al. (2010). Spectral discrimination of wild oat and canary grass in wheat fields for less herbicide application. *Agron. Sustain. Dev.* 30, 689–699. doi: 10.1051/agro/2009052

Grossman, Y. L., Ustin, S. L., and Jacquemoud, J. (1996). Critique of stepwise multiple linear regression for the extraction of leaf biochemistry information from leaf reflectance data. *Remote Sens. Environ.* 56, 182–193. doi: 10.1016/0034-4257(95)00235-9

Hansen, P. M., and Schjoerring, J. K. (2003). Reflectance measurement of canopy biomass and nitrogen status in wheat crops using normalized difference vegetation indices and partial least squares regression. *Remote Sens. Environ.* 86, 542–553. doi: 10.1016/S0034-4257(03)00131-137

Hinzman, L. D., Bauer, M. E., and Daughtry, C. S. T. (1986). Effects of nitrogen fertilization on growth and reflectance characteristics of winter wheat. *Remote Sens. Environ.* 19, 47–61. doi: 10.1016/0034-4257(86)90040-90044

Houborg, R., Anderson, M., and Daughtry, C. (2009). Utility of an image-based canopy reflectance modeling tool for remote estimation of LAI and leaf chlorophyll content at the field scale. *Remote Sens. Environ.* 113, 259–274. doi: 10.1016/j.rse.2008.09.014

Hruschka, W. R. (1987). "Data analysis: wavelength selection methods," in *Near-Infrared Technology in the Agricultural and Food Industries*, eds P. Williams and K. Norris (St. Paul, MN: American Association of Cereal Chemists, Inc.), 35–53.

Huang, Z., Turner, B. J., Dury, S. J., Wallis, I. R., and Foley, W. J. (2004). Estimating foliage nitrogen concentration from HYMAP data using continuum removal analysis. *Remote Sens. Environ.* 93, 18–29. doi: 10.1016/j.rse.2004.06.008

Ihuoma, S. O., and Madramootoo, C. A. (2019). Sensitivity of spectral vegetation indices for monitoring water stress in tomato plants. *Comput. Electron. Agric.* 163:104860. doi: 10.1016/j.compag.2019.104860

Inoue, Y., Sakaiya, E., Zhu, Y., and Takahashi, W. (2012). Diagnostic mapping of canopy nitrogen content in rice based on hyperspectral measurements. *Remote Sens. Environ.* 126, 210–221. doi: 10.1016/j.rse.2012.08.026

Kawamura, K., Ikeura, H., Phongchanmaixay, S., and Khanthavong, P. (2018). Canopy hyperspectral sensing of paddy fields at the booting stage and PLS regression can assess grain yield. *Remote Sens. Environ.* 10:81249. doi: 10.3390/rs10081249

Kawamura, K., Watanabe, N., Sakanoue, S., Lee, H. J., Inoue, Y., and Odagawa, S. (2010). Testing genetic algorithm as a tool to select relevant wavebands from field hyperspectral data for estimating pasture mass and quality in a mixed sown pasture using partial least squares regression. *Grassland Sci.* 56, 205–216. doi: 10.1111/j.1744-697x.2010.00196.x

Kokaly, R. F. (2001). Investigating a physical basis for spectroscopic estimates of leaf nitrogen concentration. *Remote Sens. Environ.* 75, 153–161. doi: 10.1016/S0034-4257(00)00163-162

Li, F., Mistele, B., Hu, Y., Chen, X., and Schmidhalter, U. (2014). Reflectance estimation of canopy nitrogen content in winter wheat using optimised hyperspectral spectral indices and partial least squares regression. *Eur. J. Agron.* 52, 198–209. doi: 10.1016/j.eja.2013.09.006

Li, X. C., Zhang, Y. J., Bao, Y. S., Luo, J. H., Jin, X. L., Xu, X. G., et al. (2014). Exploring the best hyperspectral features for LAI estimation using partial leaf squares regression. *Remote Sens.* 6, 6221–6241. doi: 10.3390/rs6076221

Li, F. L., Wang, L., Liu, J., Wang, Y. N., Chang, Q. R., and Li, F. (2019). Evaluation of leaf N concentration in winter wheat based on discrete wavelet transform analysis. *Remote Sens.* 11:1331. doi: 10.3390/rs11111331

Li, L. T., Jákli, B., Lu, P. P., Ren, T., Ming, J., Liu, S. S., et al. (2018a). Assessing leaf nitrogen concentration of winter oilseed rape with canopy hyperspectral technique considering a non-uniform vertical nitrogen distribution. *Industr. Crops Products* 116, 1–14. doi: 10.1016/j.indcrop.2018.02.051

Li, L. T., Wang, S. Q., Ren, T., Wei, Q. Q., Ming, J., Li, J., et al. (2018b). Ability of models with effective wavelengths to monitor nitrogen and phosphorus status of winter oilseed rape leaves using *in situ* canopy spectroscopy. *Field Crops Res.* 215, 173–186. doi: 10.1016/j.fcr.2017.10.018

Li, L. T., Ren, T., Ma, Y., Wei, Q. Q., Wang, S. Q., Li, X. K., et al. (2016). Evaluating chlorophyll density in winter oilseed rape (*Brassica napus* L.) using canopy hyperspectral red-edge parameters. *Comput. Electron. Agric.* 126, 21–31.

Mahajan, G. R., Sahoo, R. N., Pandey, R. N., Gupta, V. K., and Kumar, D. (2014). Using hyperspectral remote sensing techniques to monitor nitrogen, phosphorus, sulphur and potassium in wheat (*Triticum aestivum* L.). *Precis. Agric.* 15, 499–522. doi: 10.1007/s11119-014-9348-9347

Miphokasap, P., Honda, K., Vaiphasa, C., Souris, M., and Nagai, M. (2012). Estimating canopy nitrogen concentration in sugarcane using field imaging spectroscopy. *Remote Sens.* 4, 1651–1670. doi: 10.3390/rs4061651

Montes, J. M., Technow, F., Dhillon, B. S., Mauch, F., and Melchinger, A. E. (2011). High-throughput non-destructive biomass determination during early plant developmentin maize under field conditions. *Field Crops Res.* 121, 268–273. doi: 10.1016/j.fcr.2010.12.017

Müller, K., Böttcher, U., Meyer-Schatz, F., and Kage, H. (2008). Analysis of vegetation indices derived from hyperspectral reflection measurements for estimating crop canopy parameters of oilseed rape (*Brassica napus* L.). *Biosyst. Eng.* 101, 172–182. doi: 10.1016/j.biosystemseng.2008.07.004

Muñoz-Huerta, R., Guevara-Gonzalez, R. G., Contreras-Medina, L. M., Torres-Pacheco, I., Prado-Olivarez, J., and Ocampo-Velazquez, R. V. (2013). A review of methods for sensing the nitrogen status in plants: advantages, disadvantages and recent advances. *Sensors* 13, 10823–10843. doi: 10.3390/s130810823

Mutanga, O., Skidmore, A. K., Kumar, L., and Ferwerda, J. (2005). Estimating tropical pasture quality at canopy level using band depth analysis with continuum removal in the visible domain. *Intern. J. Remote Sens.* 26, 1093–1108. doi: 10.1080/01431160512331326738

Nguyen, H. T., and Lee, B. W. (2006). Assessment of rice leaf growth and nitrogen status by hyperspectral canopy reflectance and partial least square regression. *Eur. J. Agron.* 24, 349–356. doi: 10.1016/j.eja.2006.01.001

Nigon, T. J., Mulla, D. J., Rosen, C. J., Cohen, Y., and Alchanatis, V. (2015). Hyperspectral aerial imagery for detecting nitrogen stress in two potato cultivars. *Comput. Electron. Agric.* 112, 36–46. doi: 10.1016/j.compag.2014.12.018

Prey, L., and Schmidhalter, U. (2019). Simulation of satellite reflectance data using high-frequency ground based hyperspectral canopy measurements for in-season estimation of grain yield and grain nitrogen status in winter wheat. *ISPRS J. Photogram. Remote Sens.* 149, 176–187. doi: 10.1016/j.isprsjprs.2019.01.023

Schächtl, J., Huber, G., Maidl, F. X., Sticksel, E., Schulz, J., and Haschberger, P. (2005). Laser-induced chlorophyll fluorescence measurements for detecting the nitrogen status of wheat (*Triticum aestium* L.) canopies. *Precis. Agric.* 6, 143–156. doi: 10.1007/s11119-004-1031-y

Schölkopf, B., Smola, A. J., Williamson, R. C., and Bartlett, P. L. (2000). New support vector algorithms. *Neural Comput.* 12, 1207–1245. doi: 10.1162/089976600300015565

Sims, D. A., and Gamon, J. A. (2002). Relationships between leaf pigment content and spectral reflectance across a wide range of species, leaf structures and developmental stages. *Remote Sens. Environ.* 81, 337–354. doi: 10.1016/S0034-4257(02)00010-X

Summers, D., Lewis, M., Ostendorf, B., and Chittleborough, D. (2009). Visible near-infrared reflectance spectroscopy as a predictive indicator of soil properties. *Ecol. Indic.* 11, 123–131. doi: 10.1016/j.ecolind.2009.05.001

Tahir Ata-Ul-Karim, S., Liu, X., Lu, Z., Yuan, Z., Zhu, Y., and Cao, W. (2016). In-season estimation of rice grain yield using critical nitrogen dilution curve. *Field Crops Res.* 195, 1–8. doi: 10.1016/j.fcr.2016.04.027

Tan, K., Ma, W. B., Wu, F. Y., and Du, Q. (2019). Random forest-based estimation of heavy metal concentration in agricultural soils with hyperspectral sensor data. *Environ. Monitor. Assessm.* 191:446. doi: 10.1007/s10661-019-7510-7514

Thomas, R. L., Shearad, R. W., and Moyer, J. R. (1967). Comparison of conventional and automated procedures for nitrogen, phosphorus, and potassium analysis of plant material using a single digestion. *Agron. J.* 59, 240–243. doi: 10.2134/agronj1967.00021962005900030010x

Thorp, K. R., Wang, G., Bronson, K. F., Badaruddin, M., and Mon, J. (2017). Hyperspectral data mining to identify relevant canopy spectral features for estimating durum wheat growth, nitrogen status, and grain yield. *Comput. Electron. Agric.* 136, 1–12. doi: 10.1016/j.compag.2017.02.024

Tian, H. Q., Shi, S. D., Wang, H., Li, F., Li, Z., and Alva, A. (2017). Estimating of sugar beet aboveground biomass by band depth optimization of hyperspectral canopy reflectance. *J. Indian Soc. Remote Sens.* 45, 795–803. doi: 10.1007/s12524-016-0632-z

Viña, A., Gitelson, A. A., Nguy-Robertson, A. L., and Peng, Y. (2011). Comparison of different vegetation indices for the remote assessment of green leaf area index of crops. *Remote Sens. Environ.* 115, 3468–3478. doi: 10.1016/j.rse.2011.08.010

Wang, F. M., Huang, J. F., and Lou, Z. H. (2011). A comparison of three methods for estimating leaf area index of paddy rice from optimal hyperspectral bands. *Precis. Agric.* 12, 439–447. doi: 10.1007/s11119-010-9185-9182

Wang, J., Shen, C. W., Liu, N., Jin, X., Fan, X. S., Dong, C. X., et al. (2017). Non-destructive evaluation of the leaf nitrogen concentration by in-field visible/near-infrared spectroscopy in pear orchards. *Sensors* 17:538. doi: 10.3390/s17030538

Weber, V. S., Araus, J. L., Cairns, J. E., Sanchez, C., Melchinger, A. E., and Orsini, E. (2012). Prediction of grain yield using reflectance spectra of canopy and leaves in maize plants grown under different water regimes. *Field Crops Res.* 128, 82–90. doi: 10.1016/j.fcr.2011.12.016

Wen, P. F., He, J., Ning, F., Wang, R., Zhang, Y. H., and Li, J. (2019). Estimating leaf nitrogen concentration considering unsynchronized maize growth stages with canopy hyperspectral technique. *Ecol. Indic.* 107:105590. doi: 10.1016/j.ecolind.2019.105590

Word, S., Sjöström, M., and Eriksson, L. (2001). Pls-regression: a basic tool of chemometrics. *Chemometr. Intellig. Lab. Syst.* 58, 109–130. doi: 10.1016/S0169-7439(01)00155-151

Wu, D., and Sun, D. W. (2013). Potential of time series-hyperspectral imaging (TS-HSI) for non-invasive determination of microbial spoilage of salmon flesh. *Talanta* 111, 39–46. doi: 10.1016/j.talanta.2013.03.041

Yao, X., Huang, Y., Shang, G. Y., Zhou, C., Cheng, T., Tian, Y. C., et al. (2015). Evaluation of six algorithms to monitor wheat leaf nitrogen concentration. *Remote Sens.* 7, 14939–14966. doi: 10.3390/rs71114939

Yao, X., Zhu, Y., Tian, Y. C., Feng, W., and Cao, W. X. (2010). Exploring hyperspectral bands and estimation indices for leaf nitrogen accumulation in wheat. *Intern. J. Appl. Earth Observ. Geoinform.* 12, 89–100. doi: 10.1016/j.jag.2009.11.008

Yao, X. F., Yao, X., Tian, Y. C., Ni, J., Liu, X. K., Cao, W. X., et al. (2013). A new method to determine central wavelength and optimal bandwidth for predicting plantnitrogen uptake in winter wheat. *J. Integr. Agric.* 12, 788–802. doi: 10.1016/S2095-3119(13)60300-60307

Zhao, B., Duan, A., Ata-Ul-karim, S. T., Liu, Z., Chen, Z., Gong, Z., et al. (2018). Exploring new spectral bands and vegetation indices for estimating nitrogen nutrition index of summer maize. *Eur. J. Agron.* 93, 113–125. doi: 10.1016/j.eja.2017.12.006

Zhao, B., Liu, Z., Ata-Ul-Karim, S. T., Xiao, J., Liu, Z., Qi, A., et al. (2016). Rapid and non-destructive estimation of the nitrogen nutrition index in winter barley using chlorophyll measurements. *Field Crops Res.* 185, 59–68. doi: 10.1016/j.fcr.2015.10.021

Conflict of Interest: The authors declare that the research was conducted in the absence of any commercial or financial relationships that could be construed as a potential conflict of interest.

frontiers in Plant Science

ORIGINAL RESEARCH
published: 06 October 2020
doi: 10.3389/fpls.2020.588994

Multi-Omics Analyses Reveal the Molecular Mechanisms Underlying the Adaptation of Wheat (*Triticum aestivum* L.) to Potassium Deprivation

Yong Zhao†, Ruoxi Sun†, Haodong Liu, Xiaowei Liu, Ke Xu, Kai Xiao, Shuhua Zhang, Xueju Yang and Cheng Xue**

State Key Laboratory of North China Crop Improvement and Regulation, Hebei Agricultural University, Baoding, China

OPEN ACCESS

Edited by:
Christoph Martin Geilfus, Humboldt University of Berlin, Germany

Reviewed by:
Yong Zhou, King Abdullah University of Science and Technology, Saudi Arabia
Yin Wang, Jilin Agricultural University, China

****Correspondence:***
Xueju Yang
shmyxj@126.com
Cheng Xue
xuechenghebau@hotmail.com; xuecheng@hebau.edu.cn

†These authors have contributed equally to this work

Specialty section:
This article was submitted to Plant Nutrition, a section of the journal Frontiers in Plant Science

Received: *30 July 2020*
Accepted: *14 September 2020*
Published: *06 October 2020*

Citation:
Zhao Y, Sun R, Liu H, Liu X, Xu K, Xiao K, Zhang S, Yang X and Xue C (2020) Multi-Omics Analyses Reveal the Molecular Mechanisms Underlying the Adaptation of Wheat (Triticum aestivum L.) to Potassium Deprivation. Front. Plant Sci. 11:588994. doi: 10.3389/fpls.2020.588994

Potassium (K) is essential for regulating plant growth and mediating abiotic stress responses. Elucidating the biological mechanism underlying plant responses to K-deficiency is crucial for breeding new cultivars with improved K uptake and K utilization efficiency. In this study, we evaluated the extent of the genetic variation among 543 wheat accessions differing in K-deficiency tolerance at the seedling and adult plant stages. Two accessions, KN9204 and BN207, were identified as extremely tolerant and sensitive to K-deficiency, respectively. The accessions were exposed to normal and K-deficient conditions, after which their roots underwent ionomic, transcriptomic, and metabolomic analyses. Under K-deficient conditions, KN9204 exhibited stronger root growth and maintained higher K concentrations than BN207. Moreover, 19,440 transcripts and 162 metabolites were differentially abundant in the roots of both accessions according to transcriptomic and metabolomic analyses. An integrated analysis of gene expression and metabolite profiles revealed that substantially more genes, including those related to ion homeostasis, cellular reactive oxygen species homeostasis, and the glutamate metabolic pathway, were up-regulated in KN9204 than in BN207 in response to low-K stress. Accordingly, these candidate genes have unique regulatory roles affecting plant K-starvation tolerance. These findings may be useful for further clarifying the molecular changes underlying wheat root adaptations to K deprivation.

Keywords: wheat, varietal diversity, ionome, transcriptome, metabolome, potassium utilization efficiency

INTRODUCTION

Potassium (K) is a critical inorganic nutrient for plants, wherein it has vital effects on several processes, including energy metabolism, protein synthesis, and solute transport, but especially enzyme activities, stomatal movement, and the maintenance of the cation–anion balance (Zed and Paul, 2008; Amtmann et al., 2005; White and Karley, 2010; Wang et al., 2013). Many agricultural soils worldwide lack sufficient K contents, which has restricted sustainable crop development. In China, over 25% of the arable land (30 million ha) is deficient in K. The application of K fertilizers

has effectively increased crop productivity in intensive cropping systems (Wu and Wang, 2015). However, the frequent and excessive use of K fertilizers has resulted in serious environmental problems, while also increasing farming costs (Laegreid et al., 1999). Therefore, further elucidating the molecular mechanisms underlying plant responses to K-starvation stress and breeding crop varieties that can more efficiently take up and use soil K are important for developing a more sustainable agricultural system.

Wheat has been cultivated in China for more than four millennia and is now grown in 10 major agro-ecological zones (Zhuang, 2003). Owing to a long evolutionary period and the artificial selection in different regions, the wheat germplasm in China exhibit regional genetic characteristics (He et al., 2001; Hao et al., 2008). Tolerance to K-deficiency is a complex quantitative trait, with strong interactions between genotypes and the environment. Additionally, there are the considerable differences in the K-deficiency tolerance among wheat species (Zhao et al., 2014). To date, there has been relatively little research conducted to characterize the K-deficiency tolerance of the available wheat germplasm at different growth stages. Therefore, an efficient characterization of wheat plants in terms of their tolerance to K-deficiency may produce important information for the development and cultivation of wheat genotypes exhibiting increased tolerance to insufficient K contents in soil.

Plant responses to K-deficiency stress are due to various complex gene regulatory networks that induce extensive changes in gene expression as well as protein and metabolite contents (Liang et al., 2013). The omics-based technologies, including ionomics, transcriptomics, proteomics, and metabolomics, have enabled high-throughput and efficient comprehensive analyses of K-deficiency stress-induced changes to ions and gene expression as well as protein and metabolite levels in plants (Hafsi et al., 2014). To date, there has been little research on ionomic responses to nutrient stress in wheat, but ionomics-based techniques are becoming powerful research tools for studying plant physiology (Wu et al., 2013; Zeng et al., 2015). Previously, the molecular mechanisms underlying plant responses to K-deficiency were dissected via transcriptomic and proteomic analyses, resulting in the identification of many K-responsive genes and proteins of *Triticum aestivum* (Ruan et al., 2015; Zeng et al., 2015; Quan et al., 2016; Li et al., 2017; Zhao et al., 2019). Additionally, metabolomics-based studies have revealed intermediate metabolites relevant to various plant physiological characteristics under different abiotic stress conditions. Zeng et al. (2018) identified 57 kinds of metabolites as well as differences in the phenylpropanoid metabolic pathway mediated by phenylalanine ammonia-lyase (PAL) among three genotypes, which may be closely associated with the genotypic differences in K-deficiency tolerance. However, there are few reports describing integrated analyses of the genes and metabolites involved in the K-deficiency stress response pathways in wheat.

This study was designed to evaluate the level of genetic variation among 543 wheat accessions (531 were Chinese wheat cultivars from 10 provinces) for K-deficiency tolerance at seedling and mature stages, with the aim to identify contrasting (K-deficiency tolerant and K-deficiency sensitive) genotypes for further breeding programs and genetic studies. The identified genotypes were further conducted ionomic, transcriptomic, and metabolomic analyses using the roots under normal or K-deficient conditions. The objectives of this study were to (1) determine the differences between the ionomes, transcriptomes, and metabolomes of two wheat accessions in response to low-K stress and (2) identify the signaling pathways and regulatory networks related to low-K tolerance, which further characterized the wheat root molecular responses enabling adaptations to K deprivation.

MATERIALS AND METHODS

Plant Materials

A total of 543 bread wheat germplasm accessions were used for evaluation of K-deficiency tolerance. Including 488 cultivars, 43 regional test lines from the 10 major wheat-growing Provinces of China, and 12 additional non-Chinese parental lines (Zhao et al., 2020).

Low-K Tolerance Evaluation

Hydroponic Test

The wheat germplasm accessions were hydroponically grown in a greenhouse at Hebei Agricultural University, Baoding, China. The plants in modified Hoagland's solution were screened at the seedling stage in a supported hydroponic system (Guo et al., 2012). The K treatment involved two concentrations prepared with K_2SO_4 in nutrient solution [2.0×10^{-3} mol/L as the control (CK) and 0.01×10^{-3} mol/L for the low-K (LK) treatment]. A completely randomized design was employed, with three replicates per treatment. Seeds (300 grains per wheat germplasm accession) were sterilized in 3% H_2O_2 for 5 min, rinsed three times with distilled water, and immersed in distilled water for 24 h. The uniformly germinated seeds were then transferred to Petri dishes containing three layers of filter paper and then incubated in an illuminated growth chamber at 20°C. Seven days later, the endosperm was removed from 30 uniformly and vigorously growing seedlings of each genotype. For each replication, 10 plants of each genotype were transferred to 25-L containers, which were placed in an illuminated growth chamber (20°C with a 12-h light/12-h dark cycle). Additionally, the nutrient solution was aerated continuously and renewed every 3 days for the duration of the experiment at which time the pH was re-adjusted to 6.0.

Wheat seedlings were harvested after 14 days of growth in the nutrient solution. Thirty seedlings (three replicates) were rinsed with distilled water and then divided into the roots and shoots. The shoot length (SL), leaf length (LL), and leaf width (LW) were measured and the leaf area (LA) was calculated. Root and shoot samples were dried in an oven at 105°C for 30 min and then at 80°C until they were completely dry (approximately 48 h). The total dry weight (TDW), shoot dry weight (SDW), and root dry weight (RDW) were measured, after

which the root-to-shoot dry weight (RSDW) ratio was calculated. The K concentration (SKCe, RKCe) was determined for the digested samples. Moreover, the K content (SKC, RKC) and K utilization efficiency (SKUE, RKUE) were calculated. Specific details regarding the methods used for analyzing samples are listed in **Supplementary Table 1**.

Pot Incubation Test

The pot experiments involving two treatment (180.00 mg/kg as the CK and 45.00 mg/kg for the LK treatment) were conducted under a movable transparent rain shelter at Hebei Agricultural University, Hebei, China. The experiments were conducted with a completely randomized design, with three replicates per treatment. Eighteen seeds were planted in plastic pots (20 cm diameter and 21 cm height) at a depth of 2 cm. The seedlings were thinned to 14 plantlets per pot at the three-leaf stage. Pots were filled with 6 kg sieved soil (0.90 g/kg organic matter, 0.17 g/kg total N, 17.95 g/kg total K, 535.00 mg/kg slowly available K, 4.18 mg/kg available P, and 45.00 mg/kg available K). The base fertilizer comprising 0.63 g urea (N 46.4%) and 0.94 g DAP (N 18.0%, P_2O_5 46.0%) per pot was applied before seeding, 1.53 g K_2SO_4 (K_2O 53.0%) was applied at the CK treatment. Additionally, the wheat plants in each pot were treated with 0.63 g urea during the reviving stage. Fungal diseases and insects were controlled by spraying growing wheat plants three times with a fungicide and once with the insecticide.

At the mature stage, three plants were randomly selected from each pot to measure the plant height (PH), LL, LW, and LA. After harvesting, the number of kernels per spike (KPS), SDW, 1,000-grain weight (TGW), grain yield (GY), and K concentration (SKCe, StKCe, GKCe) were determined. Moreover, the K content (SKC, StKC, GKC) and K utilization efficiency (SKUE, StKUE, GKUE) were calculated. Specific details regarding the methods used for analyzing samples are listed in **Supplementary Table 1**.

Principal Component Analysis and Comprehensive Evaluation

The low-K tolerance coefficient for each index was calculated as previously described (Yuan et al., 2005). The membership function value [U (x)], weight (w), and low-K tolerance comprehensive evaluation value (D) of each genotype was calculated using published methods (Zhou et al., 2003). The low-K tolerance coefficient was calculated as follows: mean measured value for the low-K stress/mean measured value for the control.

$$U\left(Xj\right) = \frac{Xj - Xj\min}{Xj\max - Xj\min}, \quad j = 1,\ 2,\ \text{and}\ 3 \qquad (1)$$

$U_{(Xj)}$ is the membership function value of the comprehensive index j; X_j is the measured value for the low-K tolerance coefficient of index j; $X_{j\ min}$ is the minimum value for the low-K tolerance coefficient of index j; X_{jmax} is the maximum value for the low-K tolerance coefficient of index j.

$$W_j = Pj \Big/ \sum_{j=1}^{n} Pj, \quad j = 1,\ 2,\ \text{and}\ 3 \qquad (2)$$

W_j is the weight of the comprehensive index j in all comprehensive indices; P_j is the contribution rate of the comprehensive index j of each genotype.

$$D = \sum_{j=1}^{n} \left[U(xj) \times Wj\right], \quad j = 1,\ 2,\ \text{and}\ 3 \qquad (3)$$

D is the low-K tolerance comprehensive index evaluation value.

X1–X13 respectively represent the following indices at the seedling stage: LL, LA, SL, SDW, RDW, TDW, RSDW, SKCe, RKCe, SKC, RKC, SKUE, and RKUE. Y1–Y13 respectively represent the following indices at the mature stage: PH, LL, LA, KPS, SDW, GY, TGW, StKCe, StKC, StKUE, GKCe, GKC, and GKUE.

Multi-Omics Analysis of Wheat Under Low-K Conditions

On the basis of the results for the above experiment, genotypes tolerant and sensitive to low-K stress (KN9204 and BN207, respectively) were selected for a low-K treatment under hydroponic culture conditions. The experiment was performed in triplicate for each treatment. After a 14-day LK treatment, the plants of each genotype were harvested for phenotypic and multi-omics analyses.

Elemental Content Analysis of Wheat

The harvested plants were dried in an oven at 105°C for 30 min and then at 80°C until reaching a constant mass. The plant samples were ground to a powder, after which 0.20 g ground sample was added to a tube for a digestion according to the nitric acid–perchloric acid method developed by Zasoski and Burau (1977). The clear and transparent digestion solution was transferred to a 50-mL volumetric flask containing deionized water. The N and P contents were measured with the Kjeldahl method and the vanadium aluminum yellow colorimetry method, respectively, whereas the K, Na, Ca, Mg, Fe, Mn, Cu, and Zn contents were determined with an atomic absorption spectrophotometer.

Transcriptomic Analysis of Wheat Under Low-K Conditions

After a 14-day LK treatment, the roots from 10 plants were collected, combined, immediately frozen in liquid nitrogen, and then stored at −80°C. Three biological replicates were collected for each treatment for the subsequent analysis. Total RNA was extracted from the frozen roots with the TRIzol reagent (Invitrogen, CA, United States) following the manufacturer's procedure. The total RNA quantity and purity were analyzed with the 2100 Bioanalyzer and the RNA 6000 Nano LabChip Kit (Agilent, CA, United States), with an RNA integrity number >7.0. Polyadenylated mRNA was purified from the high-quality total RNA with poly-T oligo-attached magnetic beads (Invitrogen). The cleaved RNA fragments were reverse-transcribed to create the final cDNA libraries with the mRNASeq sample preparation kit (Illumina, San Diego, CA, United States). The paired-end (150 bp) sequencing of the cDNA libraries was completed with the

Illumina HiSeq 4000 system at LC Sciences (United States) following the vendor's recommended protocol. Low-quality reads (e.g., poly-N sequences) and reads with adapters were removed from the raw data, and the remaining clean reads were retained for the subsequent analysis. The HISAT software was used to align clean reads to the wheat reference genome IWGSC[1] reference genome, and the transcripts were assembled based on the sequence alignment results (Kim et al., 2015). The edgeR program was used to analyze differentially expressed genes (DEGs), which were detected based on the following criteria: $|\log_2(\text{fold-change})| \geq 1$ and $p < 0.05$. The gene ontology (GO) and the Kyoto Encyclopedia of Genes and Genomes (KEGG) pathway enrichment analyses of the DEGs were completed with GOseqR and KOBAS, respectively.

Metabolomic Analysis of Wheat Under Low-K Conditions

The freeze-dried roots were ground to a powder, after which 100 mg powder was treated with 1.0 mL 70% aqueous methanol overnight at 4°C. Following a centrifugation at 10,000 × *g* for 10 min, the extracts were added to a CNWBOND Carbon-GCB SPE Cartridge (250 mg, 3 mL; ANPEL, Shanghai, China) and filtered (SCAA-104, 0.22 μm pore size; ANPEL) before the UPLC-MS analysis (Chen et al., 2013).

The sample extracts were analyzed with a UPLC-ESI MS/MS system (Shim-pack UFLC SHIMADZU CBM30A system and Applied Biosystems 6500 QTRAP mass spectrometer), with the following conditions: UPLC column, Waters ACQUITY UPLC HSS T3 C18 (1.8 μm, 2.1 mm × 100 mm); solvent system, water (0.04% acetic acid): acetonitrile (0.04% acetic acid); gradient program, 95:5 (v/v) at 0 min, 5:95 (v/v) at 11.0 min, 5:95 (v/v) at 12.0 min, 95:5 (v/v) at 12.1 min, and 95:5 (v/v) at 15.0 min; flow rate, 0.40 mL/min; temperature, 40°C; injection volume, 2 μL. MS/MS analysis was completed with an Applied Biosystems 6500 Q TRAP system (Chen et al., 2013).

On the basis of the internal database MWDB (metadata database), substances were qualitatively determined according to the second-order spectral information. The isotopic signal was removed during the analysis, including the repetitive signals of K^+, Na^+, and $NH4^+$ as well as the repetitive signal of the fragment ion, which has a relatively large molecular weight. Metabolites were quantified via the multiple reaction monitoring mode of the triple quadrupole mass spectrometer. The metabolites were identified by univariate analysis and orthogonal partial least squares discriminant analysis. The differentially abundant metabolites were screened according to the following criteria: variable importance in projection (VIP) ≥ 1 and a fold-change ≥2 or ≤0.5 (Zhao et al., 2019).

Statistical Analysis

The analysis of variance (ANOVA), the cluster analysis and the principal component analysis (PCA) were completed with SPSS (version 25.0) (Chicago, IL, United States). Means were compared with Duncan's multiple comparison tests with difference considered significant at $p < 0.05$.

[1]http://www.wheatgenome.org/

RESULTS

Analysis of Low-K Tolerance Traits at the Seedling and Mature Stages of Wheat

Low-K tolerance-related phenotypic traits of 543 wheat genotypes at the seedling and mature stages were compared under control and low-K conditions (**Tables 1**, **2**). In the hydroponic test, low-K stress significantly decreased the SL, LL, LA, SDW, RDW, TDW, SKCe, RKCe, SKC, and RKC, but increased the SKUE and RKUE relative to the control levels. The coefficient of variation (CV) of the different traits varied from 22.60 to 52.74% under low-K conditions. Regarding the pot incubation test, low-K stress decreased the PH, LL, LA, SDW, KPS, TGW, GY, SKCe, and SKC, but increased the SKUE. The CV of the different traits varied from 9.79 to 28.53% following the low-K treatment. These results revealed the substantial variations of most traits among the 543 wheat genotypes under low-K stress conditions during the two analyzed stages.

PCA and Comprehensive Evaluation of the Low-K Tolerance of Different Wheat Genotypes

Thirteen indices of the low-K tolerance of various wheat genotypes at the seedling and mature stages underwent a PCA (**Supplementary Tables 2**, **3**). The cumulative contribution of five principal components at the seedling stage was 89.69% (individual contributions of 24.21, 21.85, 17.27, 16.53, and 9.83%). Five independent comprehensive indices at the seedling stage were defined as the first to fifth principal components. The cumulative contribution of six principal components at the mature stage was 82.54% (individual contributions of 21.95, 15.45, 13.78, 12.88, 10.74, and 7.74). Six independent comprehensive indicators at the mature stage were defined as the first to sixth principal components. For both the seedling and mature stages, the PCA results are summarized in **Supplementary Tables 2**, **3**.

The principal component expression of different genotypes and the standardized low-K tolerance coefficient at the seedling and mature stages along with Eqs 1–3 were used to calculate the comprehensive index evaluation value (D value). The cluster analysis indicated that 7, 50, 238, and 248 genotypes were respectively tolerant, moderately tolerant, moderately sensitive, and sensitive to low-K stress at the seedling stage (**Supplementary Table 4**). The mean D values at the seedling and mature stages are provided in **Supplementary Figure 1**. The mean D value ranged from 0.77 (tolerant genotypes) to 0.46 (sensitive genotypes) (**Supplementary Figure 1A**), whereas the overall mean was 0.53. At the mature stage, 116, 214, 187, and 26 genotypes were respectively tolerant,

TABLE 1 | Phenotypic variations in the K utilization efficiency-related traits at the seedling stage.

Stage	Trait	Treatment	Mean	Max	Min	SD	CV (%)
Seedling	LL (cm)	CK	13.07	23.82	4.50	4.24	32.46
		LK	10.21	19.07	3.12	3.14	30.78
	LA (cm^2)	CK	2.99	5.81	0.86	1.09	36.67
		LK	2.09	4.31	0.40	0.79	37.65
	SL (cm)	CK	18.01	31.67	6.14	4.81	26.71
		LK	14.89	23.93	4.56	3.37	22.60
	SDW (mg $plant^{-1}$)	CK	21.36	39.62	6.50	5.79	27.09
		LK	17.22	29.42	4.47	4.48	26.04
	SKCe (g kg^{-1})	CK	24.44	48.27	8.27	8.38	34.31
		LK	6.93	12.16	2.22	1.87	27.01
	SKC (mg·$plant^{-1}$)	CK	1.02	1.43	0.10	0.24	46.02
		LK	0.28	0.95	0.02	0.07	52.13
	SKUE (mg^2 SDW·μg^{-1} SKC)	CK	0.99	2.43	0.24	0.50	50.33
		LK	2.61	5.46	0.36	1.09	41.89
	RDW (mg $plant^{-1}$)	CK	11.35	23.95	2.48	3.77	33.20
		LK	9.18	19.10	1.69	2.53	27.54
	RKCe (g kg^{-1})	CK	7.72	19.64	1.81	4.00	51.89
		LK	3.05	8.44	0.55	1.38	45.26
	RKC (mg $plant^{-1}$)	CK	0.08	0.27	0.01	0.04	53.79
		LK	0.03	0.09	0.01	0.01	52.74
	RKUE (mg^2 SDW·μg^{-1} SKC)	CK	1.95	6.09	0.20	1.28	65.50
		LK	3.52	8.37	0.36	1.72	48.93
	TDW (mg $plant^{-1}$)	CK	32.41	55.44	11.01	8.51	26.25
		LK	26.39	44.06	7.97	6.43	24.35

SL, LL, LA, SDW, RDW, and TDW are shoot length, leaf length, leaf area, shoot dry weight, root dry weight, and total dry weight at the seedling stage, respectively; SKCe and RKCe are the shoot and root K concentrations at the seedling stage, respectively; SKC and RKC are the shoot and root K contents, respectively; SKUE and RKUE are the shoot and root K utilization efficiencies at the seedling stage, respectively; CK and LK refer to the control and low-K stress conditions in the screening experiments, respectively; SD is standard deviation and CV is coefficient of variation.

moderately tolerant, moderately sensitive, and sensitive to low-K stress (**Supplementary Table 5**). The mean D value ranged from 0.69 (tolerant genotypes) to 0.43 (sensitive genotypes) (**Supplementary Figure 1B**), with an overall mean of 0.59. Two tolerant genotypes (KN9204 and Henong6119) (D value ranking >99th percentile) and one sensitive genotype (BN207) (D value ranking <1st percentile) exhibited consistent responses to low-K stress during the two analyzed stages (**Tables 3**, **4**).

Phenotypic Comparison of the Contrasting Genotypes

A comparison between a tolerant genotype (KN9204) and a sensitive genotype (BN207) treated with different K concentrations confirmed the low-K stress tolerance varied considerably between the two genotypes (**Figure 1**). In response to the low-K stress treatment, the BN207 leaves were chlorotic and scorched along the margins, unlike the KN9204 leaves, which were essentially symptomless (**Figure 1A**). The SL of KN9204 and BN207 exposed to low-K stress decreased relative to the control values, although the decrease was less for KN9204 (**Figure 1B**). The RL significantly decreased under LK stress conditions in BN207, but unchanged significantly in KN9204 (**Figure 1C**). After 14 days of low-K stress, the SDW and RDW also decreased for both genotypes relative to the control values, but the decrease was greater for BN207 (**Figures 1D,E**). These observations confirmed that KN9204 is more tolerant to low-K conditions than BN207.

Influence of Low-K Stress on the Shoot and Root Ionome of the Two Contrasting Genotypes

To reveal the effects of low-K stress on the uptake of K and other nutrients by wheat plants, the N, P, K, Ca, Mg, Na, Fe, Mn, Cu, and Zn contents in the roots and shoots were analyzed for plants that underwent a 14-day low-K stress treatment. The N, P, K, Fe, Mn, Cu, and Zn contents significantly decreased under LK stress conditions, with a greater decrease for BN207 than for KN9204 (**Table 5**). In response to the LK stress treatment of KN9204, the N, P, K, Fe, Mn, Cu, and Zn contents decreased. Specifically, the smallest decreases in the shoots and roots were for Mn (3.68%) and Fe (2.88%), respectively, whereas the largest decreases in the shoots and roots were for K (76.17 and 48.00%, respectively). Following the LK stress treatment of BN207, the N, P, K, Fe, Mn, Cu, and Zn contents also decreased. The smallest decreases in the shoots and roots were for Zn (6.70%) and Mn (14.35%), respectively. In contrast, the largest decreases in the shoots and roots were for K (78.87%) and P (84.23%), respectively.

TABLE 2 | Phenotypic variations in the K utilization efficiency-related traits at the mature stage.

Stage	Trait	Treatment	Mean	Max	Min	SD	CV (%)
Mature	PH (cm)	CK	46.07	73.00	30.00	6.14	13.32
		LK	40.49	64.68	24.33	6.05	14.95
	LL (cm)	CK	10.23	19.27	6.50	1.77	17.30
		LK	8.15	16.33	4.33	1.52	18.67
	LA (cm^2)	CK	6.71	15.03	3.88	1.48	22.05
		LK	4.33	8.92	1.41	1.16	27.04
	SDW (mg $plant^{-1}$)	CK	16.13	25.66	8.72	2.37	14.69
		LK	13.94	19.97	8.11	2.23	15.98
	KNPS	CK	12.26	17.33	8.67	1.20	9.79
		LK	10.53	13.67	4.67	1.48	14.02
	TGW (g)	CK	37.36	85.52	7.08	7.36	19.69
		LK	33.70	75.85	5.17	6.72	19.94
	GY (g pot^{-1})	CK	6.61	10.28	0.46	1.41	21.39
		LK	5.00	8.56	0.31	1.42	28.53
	SKCe (g kg^{-1})	CK	32.00	73.11	16.57	6.92	21.62
		LK	16.32	27.02	9.29	2.53	15.52
	SKC (mg $plant^{-1}$)	CK	0.52	1.10	0.23	0.13	25.17
		LK	0.23	0.38	0.11	0.05	20.20
	SKUE (mg^2 SDW·μg^{-1} SKC)	CK	0.53	1.17	0.13	0.13	24.95
		LK	0.88	1.52	0.36	0.21	23.48

PH, LL, LA, SDW, KNPS, TGW, and GY are height, leaf length, leaf area, shoot dry weight, number of kernels per spike, 1,000-grain weight, and grain yield at the mature stage, respectively; SKCe, SKC, and SKUE are shoot K concentration, K content, and K utilization efficiency at the mature stage, respectively; CK and LK refer to the control and low-K stress conditions in the screening experiments, respectively; SD is standard deviation and CV is coefficient of variation.

TABLE 3 | Low-K tolerant genotypes identified based on the D values in more than one growth stage.

Entry name	Seedling stage	Mature stage
	Tolerant	
Kenong9204	√	√
Henong6119	√	√
Han6172	√	
Jimai38	√	
Heng7228	√	
Cangmai119		√
Henong2552		√
Henong9204		√

The checkmark indicates whether the genotype is tolerant in the specific stage. The order of the genotypes is based on the D value rankings.

TABLE 4 | Low-K sensitive genotypes identified based on the D values in more than one growth stage.

Entry name	Seedling stage	Mature stage
	Sensitive	
Zhengyin4hao		√
Sanshumai		√
Jining6058		√
Jw1	√	
Shannongjian36-459	√	
Xu9158	√	
Pingan8hao	√	
Yanzhan4110		√
Bainong207	√	√

The checkmark indicates whether the genotype is sensitive in the specific stage. The order of the genotypes is based on the D value rankings.

In contrast, the Na, Ca, and Mg contents substantially increased in the roots and shoots under LK stress conditions (**Table 5**), with a greater increase in BN207 than in KN9204. Under low-K stress conditions, the Ca, Mg, and Na contents increased in KN9204 shoots by 17.77, 16.47, and 11.24%, respectively, and increased in KN9204 roots by 0.38, 3.23, and 5.66%, respectively. In response to the low-K stress treatment, the Ca, Mg, and Na contents increased in the BN207 shoots by 50.78, 16.77, and 10.22%, respectively, and increased in the BN207 roots by 121.31, 6.90, and 26.20%, respectively. Thus, there were obvious differences between the contrasting genotypes regarding the elemental content changes due to LK stress. The results of the tissue ionomic analysis provided additional evidence that KN9204 is more tolerant to low-K conditions than BN207.

Transcriptomic Analyses

Evaluation of the RNA-Seq Reads and Mapping Results

The sequencing of 12 libraries (four samples × three replicates) yielded approximately 50 million high-quality clean reads per library. An overview of the RNA-seq data for the 12 libraries is provided in **Supplementary Table 6**. The number of clean reads per library were as follows: 54,002,488 (TCK), 52,767,067 (TLK),

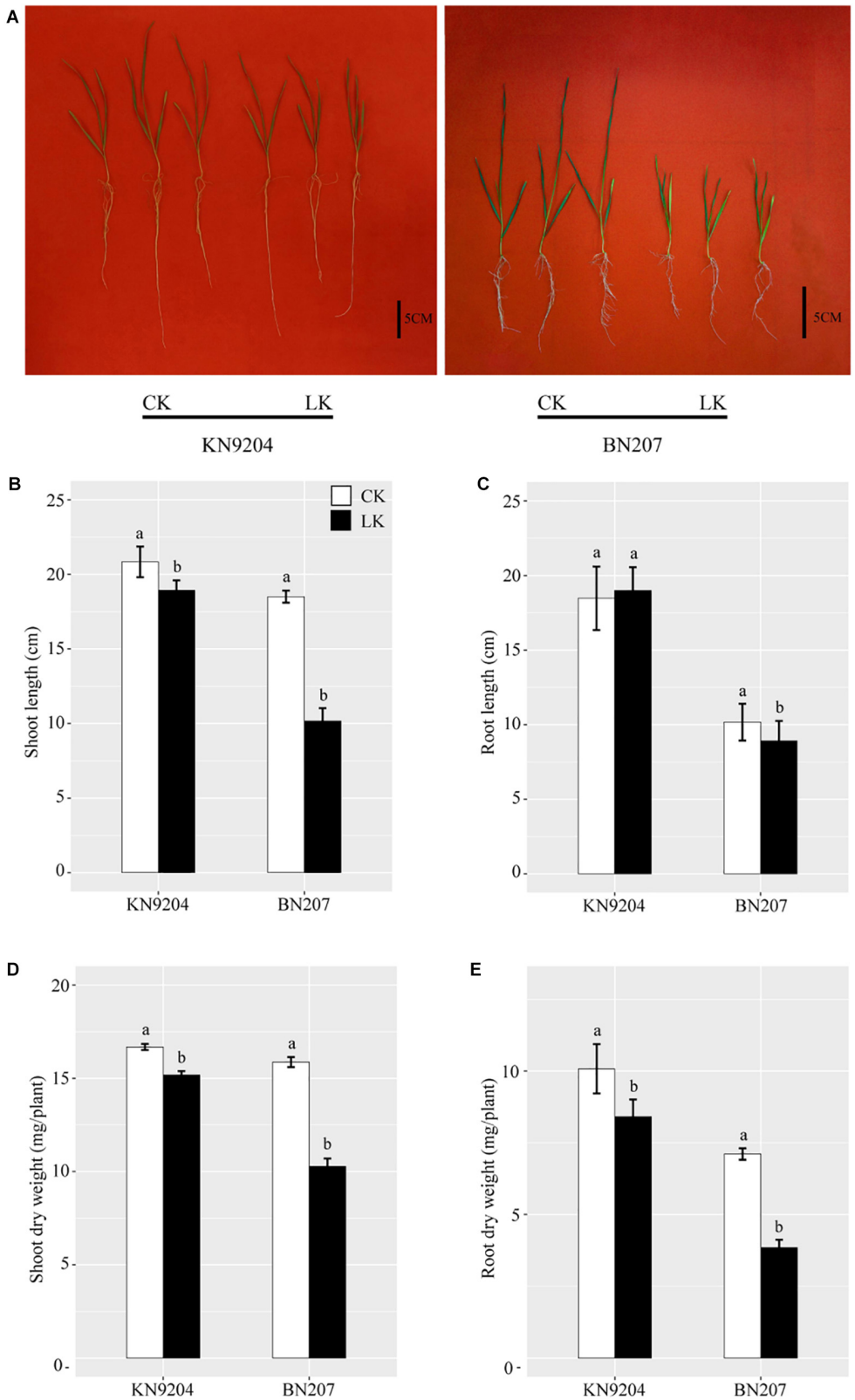

FIGURE 1 | Growth performance of KN9204 and BN207 after 14 days under control (CK) and low-K (LK) stress conditions. **(A)** KN9204 plants (left) and BN207 plants (right). Bar, 5 cm. **(B)** shoot length, **(C)** root length, **(D)** shoot dry weight, and **(E)** root dry weight of KN9204 and BN207 plants. Data are presented as the mean ± SD of three biological replicates ($n = 3$). Lowercase letters indicate significant differences ($p < 0.05$) as determined by a one-way ANOVA.

TABLE 5 | Elemental contents in different genotypes under control and low-K stress conditions.

Tissue	Treatment	Genotype	N (g/kg)	P (g/kg)	K (g/kg)	Ca (g/kg)	Mg (g/kg)	Na (g/kg)	Fe (mg/kg)	Mn (mg/kg)	Cu (mg/kg)	Zn (mg/kg)
Shoot	CK	KN9204	26.23Ab	8.59Aa	29.58Aa	3.94Aa	1.70Aa	2.58Ba	8.16Ab	9.23Aa	2.33Ab	31.83Aa
		BN207	31.82Aa	5.80Ab	26.60Ab	2.56Bb	1.55Aa	1.86Aa	18.19Aa	7.09Ab	5.82Aa	31.95Aa
	LK	KN9204	21.76Ba	7.80Aa	7.05Ba	4.64Aa	1.98Aa	2.87Aa	7.03Ab	8.89Aa	1.98Ab	30.35Ba
		BN207	16.14Bb	3.57Bb	5.62Bb	3.86Aa	1.81Aa	2.05Ab	15.04Ba	6.31Ab	4.64Aa	29.81Ba
Root	CK	KN9204	25.14Aa	4.21Aa	9.25Aa	2.63Aa	0.31Aa	2.65Aa	31.29Aa	4.58Ab	2.12Ab	35.06Aa
		BN207	23.37Ab	4.44Aa	7.00Ab	0.61Bb	0.29Aa	2.29Ba	23.77Ab	10.38Aa	6.10Aa	33.70Ab
	LK	KN9204	22.39Aa	3.40Aa	4.81Ba	2.64Aa	0.32Aa	2.80Aa	30.39Aa	3.83Ab	1.86Ab	31.09Ba
		BN207	15.07Bb	0.70Bb	1.40Bb	1.35Ab	0.31Aa	2.89Aa	19.61Bb	8.89Aa	5.12Aa	27.30Bb

CK and LK refer to the control and low-K stress conditions in the screening experiments, respectively. All experiments were replicated three times. Different uppercase letters (A and B) indicate significant difference among the same genotype between CK and LK at the 5% level, and different lowercase letters (a and b) indicate significant difference among different genotypes under the same treatment at the 5% level.

52,077,489 (SCK), and 53,631,401 (SLK). The proportion of the clean reads mapped to the wheat IWGSC[2] reference genome ranged from 87.11 to 92.20%. The GC content of the clean reads was approximately 53%. These values were within the range required for high-quality mRNA libraries.

Identification of DEGs

Gene expression profiles for the wheat roots under control (normal) and low-K conditions were analyzed. An analysis of the DEGs [$|\log_2(\text{fold-change})| > 1$ and $p < 0.05$] revealed 4,435 up-regulated and 4,612 down-regulated DEGs in KN9204 as well as 6,391 up-regulated and 9,319 down-regulated DEGs in BN207 (**Figure 2A**). Additionally, 2,270 up-regulated and 2,947 down-regulated genes were common to both genotypes (**Figures 2B,C**).

DEGs Related to Transporters and CBL-Interacting Protein Kinases

In the current study, 12 and 7 DEGs encoding K transporters and K channel proteins were identified, respectively, under low-K conditions (**Supplementary Table 7**). The expression levels of most of the DEGs encoding K transporters were up-regulated in the two genotypes. Notably, the expression levels of three DEGs (*TraesCS2A02G116700*, *TraesCS2B02G135900*, and *TraesCS2D02G118400*) were up-regulated in KN9204, but were unchanged in BN207. The expression levels of all seven DEGs encoding K channel proteins were up-regulated, but the up-regulated expression of three of them was detected only in KN9204. Seven DEGs encoding nitrate transporters were detected, implying that nitrate transporters contribute to the metabolic activities of wheat under low-K stress conditions. Additionally, nine DEGs encoding calcineurin B-like (CBL)-interacting protein kinases (CIPKs) were identified, including six DEGs in KN9204 (all up-regulated) and six DEGs in BN207 (three up-regulated and three down-regulated). Overall, more DEGs encoding transporters and CIPKs were up-regulated in KN9204 compared to BN207.

DEGs Related to Oxidative Stress

We identified 179 and 11 genes encoding peroxidase and glutathione S-transferase (GST), respectively, both of which are critical for eliminating reactive oxygen species (ROS) (**Supplementary Table 8**). The expression of five DEGs encoding peroxidase was up-regulated in both genotypes, whereas the expression levels of 111 and 174 DEGs encoding peroxidase were respectively down-regulated in KN9204 and BN207. Moreover, We identified five up-regulated DEGs encoding GST in the two varieties, among which one gene was only up-regulated in KN9204, as well as five DEGs with down-regulated and unchanged expression levels in BN207 and KN9204, respectively (**Supplementary Table 9**). There were more DEGs encoding peroxidase and GST with down-regulated expression levels in BN207 than in KN9204.

DEGs Related to Transcription Factors

Transcription factors (TFs) are essential gene expression regulators. In this study, 430 and 758 TF DEGs were identified

[2]http://www.wheatgenome.org/

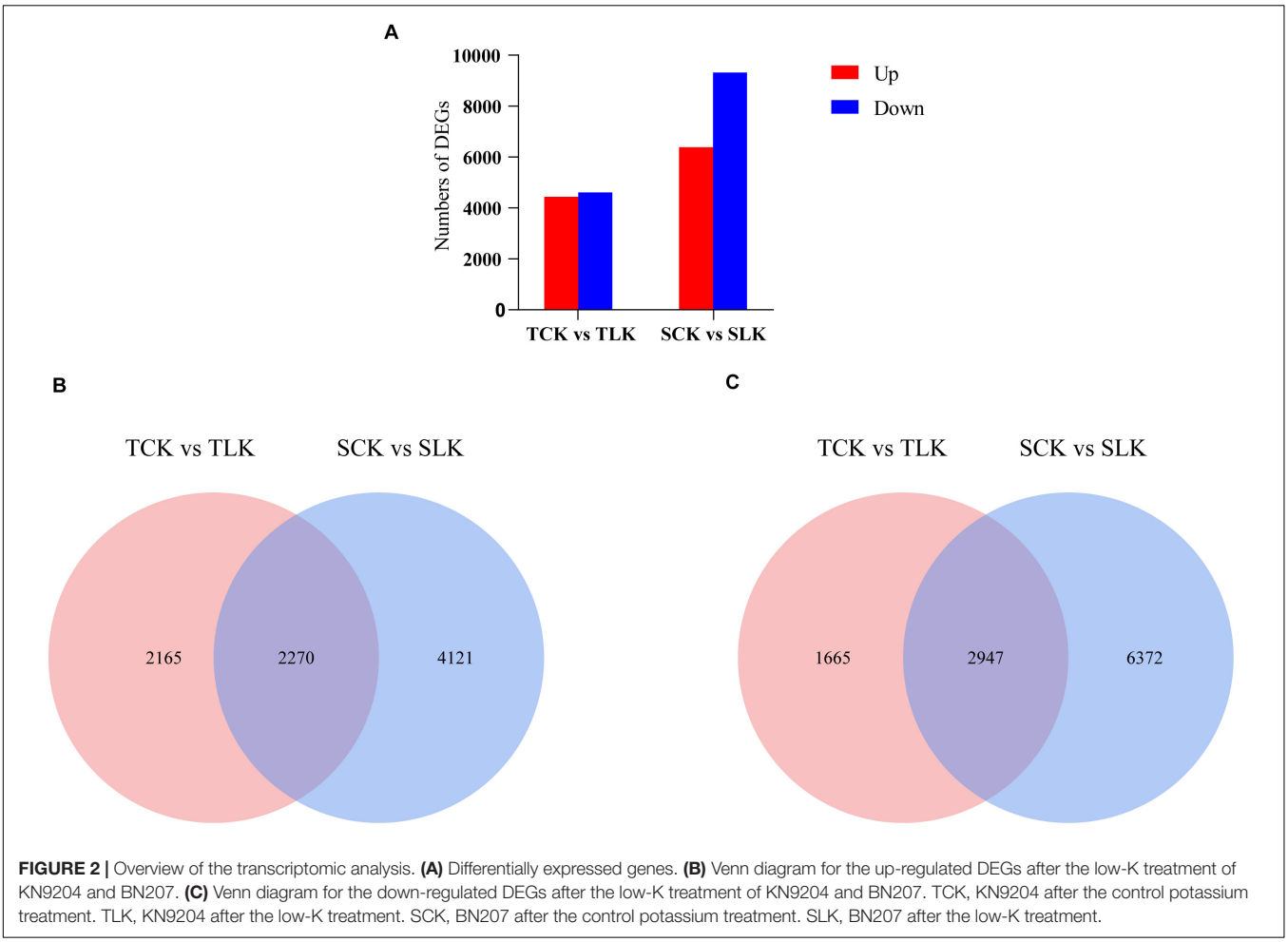

FIGURE 2 | Overview of the transcriptomic analysis. **(A)** Differentially expressed genes. **(B)** Venn diagram for the up-regulated DEGs after the low-K treatment of KN9204 and BN207. **(C)** Venn diagram for the down-regulated DEGs after the low-K treatment of KN9204 and BN207. TCK, KN9204 after the control potassium treatment. TLK, KN9204 after the low-K treatment. SCK, BN207 after the control potassium treatment. SLK, BN207 after the low-K treatment.

in KN9204 and BN207, respectively (**Supplementary Table 10**). These DEGs were from 35 different TF families, with more than half belonging to the CAMTA (88 in KN9204 and 104 in BN207), MYB (42 and 74), MYB_related (75 and 160), and WRKY (51 and 54) families. The DEGs also encoded members of other important TF families in plants, including bZIP, bHLH, and ERF. Among the identified TF DEGs, 409 had expression levels that were up-regulated in KN9204, but unchanged/down-regulated in BN207 or were unchanged in KN9204, but down-regulated in BN207 (**Supplementary Table 11**).

GO and KEGG Enrichment Analyses of DEGs

We selected the DEGs whose expression was significantly up-regulated in KN9204, but down-regulated/unchanged in BN207; or the DEGs whose expression was unchanged in KN9204, but down-regulated in BN207 for further analyses. Specifically, the 6,893 selected DEGs underwent a GO enrichment analysis (**Supplementary Figure 2**). Accordingly, the DEGs were divided into the following three main GO categories: biological process, cellular component, and molecular function. "Molecular function," "DNA binding," "protein binding," and "ATP binding" were the most enriched molecular function GO terms. Regarding biological processes, "biological process," "transcriptional regulation, DNA templating," and "redox process" were the most enriched GO terms. The DEGs related to low-K tolerance were also associated with diverse cell components. A KEGG pathway enrichment analysis assigned these same 6,893 DEGs to 41 pathways (**Supplementary Figure 3**), including those related to plant hormone signal transduction, phenylpropane biosynthesis, glutathione metabolism, as well as alanine, aspartic acid, and glutamic acid metabolism.

Metabolomic Analyses

Changes in the Metabolite Profiles of Two Contrasting Genotypes in Response to Low-K Stress

To clarify the differences in the metabolites of the two examined wheat genotypes under low-K stress conditions, we determined the metabolite contents of 12 samples, and detected 162 differentially abundant metabolites (**Supplementary Table 12**). The contents of 109 metabolites changed significantly in KN9204 (65 increased and 44 decreased). These metabolites included 20 amino acids and their derivatives, 18 lipids, 13 organic acids, and other substances. In BN207, the abundance of 91 metabolites changed significantly (29 increased and 62 decreased), including 24 organic acids, 19 amino acids and their derivatives, 15 nucleotides and their derivatives, and other substances. These

metabolites are mainly involved in amino acid synthesis and metabolism, the TCA cycle, and other metabolic processes. The synthesis of most amino acids increased in KN9204 after the low-K treatment, including L-ornithine (7.12-fold), L-citrulline (5.42-fold), L-cysteine (3.9-fold), and L-(+)-lysine (3.34-fold). In contrast, decreased amino acid synthesis was detected for only tyramine (0.36-fold), L-serine (0.47-fold), and L-(−)-cystine (0.1-fold). However, in BN207, more amino acid synthesis decreased, such as L-glutamine (0.43-fold), L-glutamate (0.42-fold), and L-alanine (0.37-fold) in response to the low-K stress. Moreover, the abundances of other metabolites, such as uridine (0.35-fold) and fumaric acid (0.45-fold), decreased in BN207, but were unchanged in KN9204. Overall, the synthesis of metabolites appeared to be inhibited more in BN207 than in KN9204.

Integration of the Transcriptomic and Metabolomic Profiles

An integrated analysis of the DEGs and differentially abundant metabolites responsive to low-K stress revealed several common enriched pathways, including glutamate metabolism (**Figure 3**). Glutamate, which is a precursor for proline, arginine, and γ-aminobutyric acid (GABA), is important for plant growth and development. The glutamate content in BN207 decreased significantly (0.42-fold), whereas significant changes were not detected in KN9204. The contents of some metabolites related to the glutamate biosynthesis pathway decreased significantly, including citric acid (0.35-fold in KN9204 and 0.09-fold in BN207), glutamine (1.15-fold and 0.43-fold), and CIS-aconitic acid (0.31-fold and 0.30-fold). An analysis of the RNA-seq data indicated the expression levels of most of the DEGs related to the glutamate biosynthesis pathway were up-regulated or not significantly changed in KN9204, whereas the expression levels of the DEGs in BN207 were down-regulated. For example, two DEGs (*TraesCS4B02G047400* and *TraesCS4A02G063800*) encoding glutamine synthetase (GS) had up-regulated expression levels in KN9204, but relatively unchanged expression in BN207. Moreover, the expression levels of the DEGs *TraesCS3B02G299800* and *TraesCS3D02G266400*, which encode glutamate synthase (GOGAT), were significantly down-regulated in BN207, but relatively unchanged in KN9204. The results of the integrated analysis of the transcriptome and metabolome indicated that glutamate biosynthesis and metabolism were inhibited in BN207.

DISCUSSION

Screening New Low-K Tolerant Genotypes Can Clarify the Complex Molecular Response of Wheat Under Low-K Stress Conditions

The availability of genetically diverse germplasm is important for the efficient breeding of new cultivars with desirable traits, including improved K uptake and K utilization efficiency. Screening new genotypes tolerant to low-K stress has enabled the identification of suitable donor parents with locally adapted genetic backgrounds in many crops (Dossougi et al., 2002; Tian et al., 2008; Wu et al., 2011). However, few studies have simultaneously evaluated low-K tolerance in more than one growth stage. In the current study, 543 wheat germplasm were evaluated regarding their tolerance to low-K stress at the seedling and mature stages. There were significant genetic differences related to the low-K tolerance traits between the germplasm at the two analyzed stages. Genotypes tolerant to low-K conditions may be used to breed for improved K utilization efficiency as well as for clarifying the genetic basis of wheat responses to K-deficiency stress. High-throughput omics-based techniques have been used to investigate complex molecular responses underlying low-K tolerance in crops (Ma et al., 2012; Fan et al., 2014; Ruan et al., 2015; Zeng et al., 2015; Quan et al., 2016; Li et al., 2017). However, no related study has been conducted to reveal the genotypic differences in wheat molecular responses to low-K stress. In the present study, we compared the ionomes, transcriptomes, and metabolomes of KN9204 (tolerant to low-K stress) and BN207 (sensitive to low-K stress) treated with different K concentrations.

Cooperative Uptake and Interactions of K-Cations Under Low-K Stress Conditions

Ion-related physiological and biochemical activities in different tissues change considerably during wheat growth and development. The available research regarding ionomic responses to low-K stress in different wheat genotypes is limited. Therefore, to investigate the mechanisms associated with K-cation interactions in wheat under low-K conditions is very important. Under K-deprivation conditions, K (osmoticum) in mature cells can be replaced by metabolites (sugars, organic acids, and compatible solutes), and other cations can assume the role of K^+ in the balancing of the vacuolar charge (White and Karley, 2010; Zhao et al., 2014). In the current study, we analyzed ten cations in the shoots and roots of two wheat genotypes that differed regarding their tolerance to low-K stress. The Ca, Mg, and Na contents increased significantly in the shoot and root tissues in response to low-K stress. These observations imply these cations can replace K to maintain specific physiological and biochemical activities. In contrast, the N, P, K, Fe, Mn, Cu, and Zn contents decreased significantly under low-K stress conditions, with a greater decrease in BN207 than in KN9204. Therefore, the high tolerance of KN9204 to low-K stress may be due to the active uptake and accumulation of K and other nutrients under low-K conditions.

The Expression Patterns of DEGs in the Two Genotypes Contribute to the Differences in the K Absorption Capacity Under Low-K Stress Conditions

Plant cells absorb K mainly through K transporters and K channels, which belong to high- and low-affinity uptake systems, respectively (Zeng et al., 2014). Several K transporters and channels have been functionally characterized in plants (Amtmann and Armengaud, 2009; Dreyer and Uozumi, 2011; Wang and Wu, 2013). Previous studies proved that K

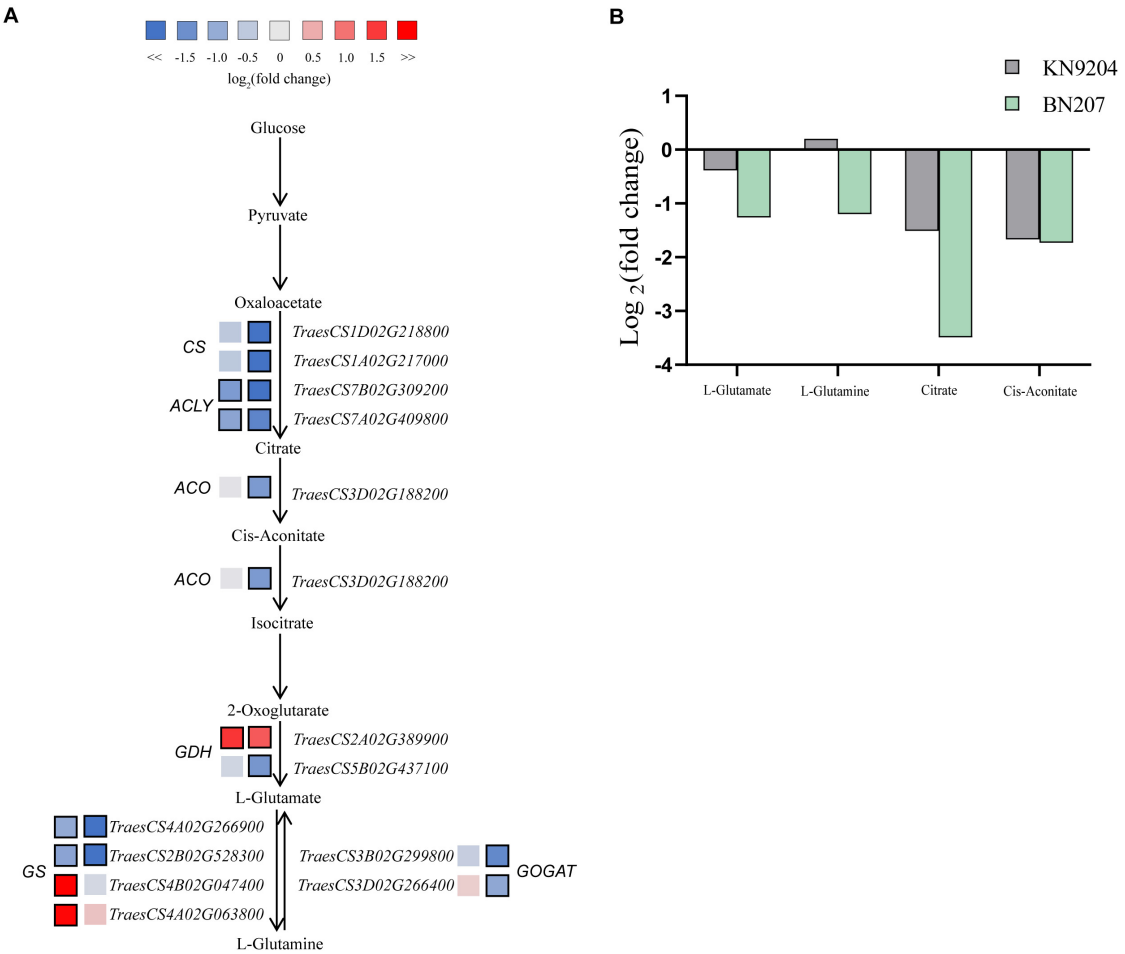

FIGURE 3 | Changes in the gene expression levels and metabolite contents associated with the glutamate biosynthesis pathway of BN207 and KN9204 after the low-K treatment. **(A)** Glutamate biosynthesis pathway. Log_2 fold-changes in DEG expression levels in KN9204 (left box) and BN207 (right box). Blue and red boxes respectively indicate the down- and up-regulated expression of the DEGs under low-K stress conditions. Bold margins indicate significant differences ($p < 0.05$) between treatments. **(B)** Changes to the metabolites in the glutamate biosynthesis pathway.

transporters and K channels help plants resist the adverse effects of K-deficiency (Xu et al., 2006; Pyo et al., 2010). In this study, the expression levels of 11 DEGs encoding K transporters and seven DEGs encoding K channels were up-regulated by low-K stress. However, the expression of some of these DEGs was up-regulated in KN9204, but was unchanged in BN207. Therefore, we speculate that KN9204 can absorb K under low-K conditions better than BN207, thereby helping to explain its greater low-K tolerance.

The CIPKs are plant-specific serine/threonine protein kinases that form protein complexes with the calcium sensor CBL protein (Shi et al., 1999; Liu et al., 2000). In Arabidopsis, CIPK23 interacts with CBL1 and CBL9 to activate AKT1-mediated K^+ uptake in roots under low-K^+ conditions (Lee et al., 2007). Another study confirmed that CIPK6 interacts with CBL4 to regulate the transfer of the K^+ channel AKT2 to the plasma membrane, where CIPK6 also enhances the AKT2 activity (Held et al., 2011). In the present study, the expression levels of three CIPK-encoding DEGs (*CIPK14*, *CIPK9*, and *CIPK27*) were up-regulated in KN9204, but were unchanged in BN207. Additionally, the expression of three other DEGs (*CIPK19*, *CIPK15*, and *CIPK29*) was down-regulated in BN207, but was unchanged in KN9204. We speculate that these different expression patterns of DEGs encoding CIPK between the two genotypes may contribute to the observed difference in low-K tolerance.

Low-K stress leads to excessive ROS accumulation, which can affect the functions of proteins, lipids, and even nucleic acids, leading to cell damage and even death (Mittler, 2017). Peroxidase and GST are essential for regulating ROS production and minimizing oxidative stress in plants. Armengaud et al. (2004) reported that the expression of *ATP19a*, which belongs to the peroxidase gene family, is significantly down-regulated in Arabidopsis roots under low-K stress conditions. Alka et al. (2017) observed that the expression of a GST-encoding gene is up-regulated in rice seedlings after a low-K treatment. In the current study, the expression levels of five peroxidase-related

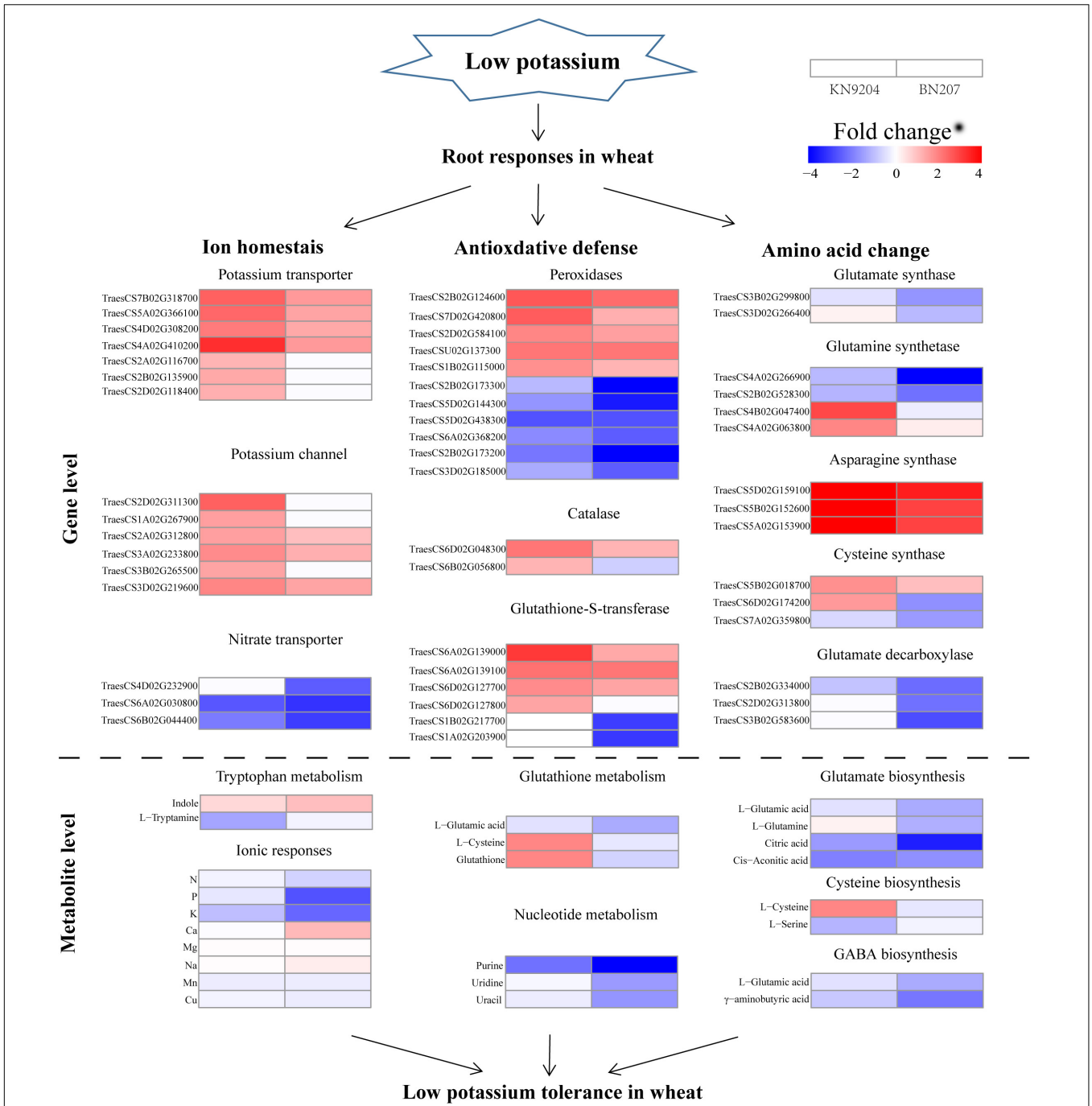

FIGURE 4 | Comparison of the transcriptomic and metabolomic profiles of the KN9204 and BN207 roots after the low-K stress treatment. Genes and metabolites involved in metabolic processes are classified into three main categories: ion homeostasis, antioxidative defense, and amino acid changes. Blue indicates decreased gene expression and metabolite contents, whereas red indicates increased gene expression and metabolite contents.

DEGs were up-regulated in the two genotypes, but the expression of the other DEGs encoding peroxidases was down-regulated. There were more DEGs with down-regulated expression in BN207 than in KN9204. Additionally, the expression of five GST-encoding DEGs was down-regulated in BN207, whereas it did not change significantly in KN9204. The differences in the peroxidase- and GST-related DEGs may enable KN9204 to maintain ROS homeostasis better than BN207, likely accounting for some of the genotypic difference in low-K tolerance.

Transcription factors bind to *cis*-regulatory elements in gene promoters to regulate expression (Lee and Young, 2000). Additionally, MYB is one of the largest TF families in plants,

with crucial functions in plant stress responses. Du et al. (2019) demonstrated that MYB59 is responsive to low-K stress and mediates root-to-shoot $K^+/NO3^-$ transport by regulating the expression of *NPF7.3* in Arabidopsis roots. In this study, 35 TF families responded to low-K stress, especially the MYB TFs. Therefore, we speculate that MYB TFs have key functions related to wheat resistance to low-K stress. The underlying molecular mechanism remains to be thoroughly characterized.

Many Metabolic Processes Are Responsive to Low-K Stress

Because K serves as a co-factor for enzymatic reactions and as a counter-ion for metabolite transport, K-deficiency can easily lead to metabolic disorders in plants (Armengaud et al., 2009). Armengaud et al. (2004) revealed that a low-K treatment of Arabidopsis alters carbohydrate metabolism, the TCA cycle, amino acid metabolism, and organic acid metabolism to varying degrees. In this study, we detected changes to many metabolites after a low-K treatment of wheat. The abundance of most analyzed amino acids increased in both genotypes, but some amino acid contents (e.g., L-glutamic acid, L-alanine, and GABA) decreased in BN207, but were relatively unchanged in KN9204. Our analyses also indicated that some organic acid contents decreased significantly in BN207, but not in KN9204 (e.g., D-galacturonic acid and fumaric acid). Moreover, the contents of some metabolites related to oxidative stress, such as glutathione, increased in KN9204, but did not change in BN207 (**Figure 4**). Glutathione is a key water-soluble antioxidant that scavenges ROS via the GSH-ascorbate cycle (Zagorchev et al., 2013). Our findings suggest that KN9204 may be able to cope with the metabolic disorders caused by low-K stress better than BN207.

Glutamic Acid Metabolism Influences Wheat Resistance to Low-K Stress

The transcriptomic and metabolomic analyses in this study revealed substantial changes to gene expression and glutamate metabolites. Glutamate is a precursor of many stress-adaptive metabolites, such as proline, arginine, and GABA, and it is also involved in nitrogen assimilation (Forde and Lea, 2007). Low-K stress inhibits nitrogen assimilation (Hu et al., 2017), which in turn affects the synthesis of amino acids and proteins. In the current study, the glutamate content decreased in BN207 exposed to low-K stress, whereas there was no significant change in KN9204. A similar trend was observed for glutamine, which is involved in glutamate metabolism. Glutamate and glutamine are important metabolites for plant nitrogen assimilation. Thus, decreases in the glutamate and glutamine contents in BN207 may have inhibited the nitrogen assimilation process in this genotype. The down-regulated expression of the genes encoding GS and GOGAT is consistent with this hypothesis. Moreover, there were no significant changes in the glutamate and glutamine contents in KN9204. We believe that the metabolites in the glutamine metabolic pathway and the changes in the expression of the related DEGs may be key factors explaining the difference in the low-K stress tolerance between the two analyzed wheat genotypes.

In conclusion, we evaluated the genetic variations among 543 wheat accessions differing in low-K tolerance at the seedling and adult plant stages. Accessions KN9204 and BN207, were identified as tolerant and sensitive to K-deficiency, respectively. On the basis of the ionomic, transcriptomic, and metabolomic analyses presented herein, we predicted that the low-K tolerance of KN9204 is mediated by enhancements to ion homeostasis, the antioxidant defense system, and the GS signaling pathway, all of which are conducive to strong root growth and the maintenance of high K concentrations under low-K stress conditions. These findings may be relevant for clarifying the molecular responses of wheat roots to K deprivation.

DATA AVAILABILITY STATEMENT

The datasets presented in this study can be found in online repositories. The names of the repository/repositories and accession number(s) can be found below: https://www.ncbi.nlm.nih.gov/, GSE155319.

AUTHOR CONTRIBUTIONS

YZ and XY conceived the project and set the scientific objectives. YZ, RS, HL, KXu, XL, and SZ conducted the experiments and analyzed the data. YZ and RS wrote the manuscript. CX and KXi revised the manuscript. All authors discussed the results as well as read and approved the final manuscript for publication.

FUNDING

This research was funded by the National Natural Science Foundation of China (31901539), the Hebei Basic Key Research Program (17966314D), and Science and Technology Planning Project of Hebei Province (16226320D).

SUPPLEMENTARY MATERIAL

The Supplementary Material for this article can be found online at: https://www.frontiersin.org/articles/10.3389/fpls.2020.588994/full#supplementary-material

Supplementary Figure 1 | Graphical representation of the studied genotypes based on the D value rankings. **(A)** D values of all 543 genotypes at the seedling stage. **(B)** D values of all 543 genotypes at the mature stage. The dotted line represents the mean D value for the entire population.

Supplementary Figure 2 | GO cluster analysis of DEGs.

Supplementary Figure 3 | Enriched KEGG pathways among the DEGs.

Supplementary Table 1 | Summary of the analyzed traits and how they were examined.

Supplementary Table 2 | Principal component analysis at the seedling stage.

Supplementary Table 3 | Principal component analysis at the mature stage.

Supplementary Table 4 | D value rankings for 543 genotypes at the seedling stage.

Supplementary Table 5 | D value rankings for 543 genotypes at the mature stage.

Supplementary Table 6 | Summary of sequencing data quality. TCK, KN9204 after the control K treatment; TLK, KN9204 after the low-K treatment; SCK, BN207 after the control K treatment; SLK, BN207 after the low-K treatment.

Supplementary Table 7 | Genes encoding transporters and CIPKs that were differentially expressed between genotypes under low-K stress conditions. "–" indicates no significant difference in gene expression.

Supplementary Table 8 | Genes encoding peroxidases that were differentially expressed between genotypes under low-K stress conditions. "–" indicates no significant difference in gene expression.

Supplementary Table 9 | Genes encoding glutathione S-transferase that were differentially expressed between genotypes under low-K stress conditions. "–" indicates no significant difference in gene expression.

Supplementary Table 10 | Transcription factors (TFs) identified among the differentially expressed genes.

Supplementary Table 11 | Transcription factors (TFs) that satisfied the screening criteria. The screening criteria was as follows: up-regulated in KN9204, but unchanged/down-regulated in BN207 or unchanged in KN9204, but down-regulated in BN207. "–" indicates no significant difference in gene expression.

Supplementary Table 12 | Fold-changes in the contents of detected metabolites in the roots of the two wheat genotypes under low-K stress conditions. "–" indicates no significant difference in content.

REFERENCES

Alka, S., Joel, L. F., Kanwaljeet, K., Manisha, S., Suman, K., Girdhar, K., et al. (2017). Rice phytoglobins regulate responses under low mineral nutrients and abiotic stresses in *Arabidopsis thaliana*. *Plant Cell Environ.* 41, 215–230. doi: 10.1111/pce.13081

Amtmann, A., and Armengaud, P. (2009). Effects of N, P, K and S on metabolism: new knowledge gained from multi-level analysis. *Curr. Opin. Plant Biol.* 12, 275–283. doi: 10.1016/j.pbi.2009.04.014

Amtmann, A., Hammond, J. P., Armengaud, P., and White, P. J. (2005). Nutrient sensing and signalling in plants: potassium and phosphorus. *Adv. Bot. Res.* 43, 209–257. doi: 10.1016/S0065-2296(05)43005-0

Armengaud, P., Breitling, R., and Amtmann, A. (2004). The potassium-dependent transcriptome of *Arabidopsis* reveals a prominent role of jasmonic acid in nutrient signaling. *Plant Physiol.* 136, 2556–2576. doi: 10.2307/4356610

Armengaud, P., Sulpice, R., Miller, A. J., Stitt, M., Amtmann, A., and Gibon, Y. (2009). Multilevel analysis of primary metabolism provides new insights into the role of potassium nutrition for glycolysis and nitrogen assimilation in *Arabidopsis* roots. *Plant Physiol.* 150, 772–785. doi: 10.1104/pp.108.133629

Chen, W., Gong, L. A., Guo, Z. L., Wang, W. S., Zhang, H. Y., Liu, X. Q., et al. (2013). A novel integrated method for large-scale detection, identification, and quantification of widely targeted metabolites: application in the study of rice metabolomics. *Mol. Plant* 6, 1769–1780. doi: 10.1093/mp/sst080

Dossougi, H. E., Claassen, N., and Stelngrobe, B. (2002). Potassium efficiency mechanisms of wheat, barley and sugar beet grown on a K fixing soil under controlled conditions. *J. Plant Nutr. Soil Sci.* 165, 732–737. doi: 10.1002/jpln.200290011

Dreyer, I., and Uozumi, N. (2011). Potassium channels in plant cells. *FEBS J.* 278, 4293–4303. doi: 10.1111/j.1742-4658.2011.08371.x

Du, X. Q., Wang, F. L., Li, H., Jing, S., Yu, M., Li, J., et al. (2019). The transcription factor MYB59 regulates K+/NO3- translocation in the *Arabidopsis* response to low K+ stress. *Plant Cell* 31, 699–714. doi: 10.1105/tpc.18.00674

Fan, M., Huang, Y., Zhong, Y., Kong, Q., Xie, J., Niu, M., et al. (2014). Comparative transcriptome profiling of potassium starvation responsiveness in two contrasting watermelon genotypes. *Planta* 239, 397–410.

Forde, B. G., and Lea, P. J. (2007). Glutamate in plants: metabolism, regulation, and signalling. *J. Exp. Bot.* 58, 2339–2358. doi: 10.1093/jxb/erm121

Guo, Y., Kong, F. M., Xu, Y. F., Zhao, Y., Liang, X., Wang, Y. Y., et al. (2012). QTL mapping for seedling traits in wheat grown under varying concentrations of N, P and K nutri-ents. *Theor. Appl. Genet.* 124, 851–865. doi: 10.1007/s00122-011-1749-7

Hafsi, C., Debez, A., and Abdelly, C. (2014). Potassium deficiency in plants: effects and signaling cascades. *Acta Physiol. Plant* 36, 1055–1070. doi: 10.1007/s11738-014-1491-2

Hao, C. Y., Dong, Y. C., Wang, L. F., You, G. X., Zhang, H. N., Ge, H. M., et al. (2008). Genetic diversity and construction of core collection in Chinese Wheat genetic resources. *Chin. Sci. Bull.* 53, 1518–1526. doi: 10.1007/s11434-008-0212-x

He, Z. H., Rajaram, S., Xin, Z. Y., and Huang, G. Z. (2001). A history of wheat breeding in China. *J. Comp. Neurol.* 523, 805–813. doi: 10.1002/cne.23713

Held, K., Pascaud, F., Eckert, C., Gajdanowicz, P., Hashimoto, K., Faillie, C. C., et al. (2011). Calcium-dependent modulation and plasma membrane targeting of the AKT2 potassium channel by the CBL4/CIPK6 calcium sensor/protein kinase complex. *Cell Res.* 21, 1116–1130. doi: 10.1038/cr.2011.50

Hu, W., Coomer, T. D., Loka, D. A., Oosterhuis, D. M., and Zhou, Z. G. (2017). Potassium deficiency affects the carbon-nitrogen balance in cotton leaves. *Plant Physiol. Biochem.* 115, 408–417. doi: 10.1016/j.plaphy.2017.04.005

Kim, D., Langmead, B., and Salzberg, S. L. (2015). HISAT: a fast spliced aligner with low memory requirements. *Nat. Methods* 12, 357–360. doi: 10.1038/nmeth.3317

Laegreid, M., Bockman, O. C., and Kaarstad, E. O. (1999). Agriculture, fertilizers and the environment. *Eur. J. Soil Sci.* 51, 541–549. doi: 10.1046/j.1365-2389.2000.00334-2.x

Lee, S. C., Lan, W. Z., Kim, B. G., Li, L. G., Cheong, Y. H., Pandey, G. K., et al. (2007). A protein phosphorylation/dephosphorylation network regulates a plant potassium channel. *Proc. Natl. Acad. Sci. U.S.A.* 104, 15959–15964. doi: 10.1073/pnas.0707912104

Lee, T. I., and Young, R. A. (2000). Transcription of eukaryotic protein-coding genes. *Annu. Rev. Genet.* 34, 77–137. doi: 10.1146/annurev.genet.34.1.77

Li, G. Z., Wu, Y. F., Liu, G. Y., Xiao, X. H., Wang, P. F., Gao, T., et al. (2017). Large-scale proteomics combined with transgenic experiments demonstrates an important role of jasmonic acid in potassium deficiency response in wheat and rice. *Mol. Cell. Proteom.* 16, 1889–1905. doi: 10.1074/mcp.ra117.000032

Liang, C. Y., Tian, J., and Liao, H. (2013). Proteomics dissection of plant responses to mineral nutrient deficiency. *Proteomics* 13, 624–636. doi: 10.1002/pmic.201200263

Liu, J. P., Ishitani, M., Halfter, U., Kim, C. S., and Zhu, J. K. (2000). The *Arabidopsis thaliana SOS2* gene encodes a protein kinase that is required for salt tolerance. *Proc. Natl. Acad. Sci. U.S.A.* 97, 3730–3734. doi: 10.1073/pnas.060034197

Ma, T. L., Wu, W. H., and Wang, Y. (2012). Transcriptome analysis of rice root responses to potassium deficiency. *BMC Plant Biol.* 12:161. doi: 10.1186/1471-2229-12-161

Mittler, R. (2017). ROS are good. *Trends Plant Sci.* 22, 11–19. doi: 10.1016/j.tplants.2016.08.002

Pyo, Y. J., Gierth, M., Schroeder, J. I., and Cho, M. H. (2010). High-affinity K+ transport in *Arabidopsis*: *AtHAK5* and *AKT1* are vital for seedling establishment and postgermination growth under low-potassium conditions. *Plant Physiol.* 153, 863–875. doi: 10.1104/pp.110.154369

Quan, X. Y., Zeng, J. B., Ye, L. Z., Chen, G., Han, Z. G., Shah, J. M., et al. (2016). Transcriptome profiling analysis for two Tibetan wild barley genotypes in responses to low nitrogen. *BMC Plant Biol.* 16:30. doi: 10.1186/s12870-016-0721-8

Ruan, L., Zhang, J. B., Xin, X. L., Zhang, C. Z., Ma, D. H., Chen, L., et al. (2015). Comparative analysis of potassium deficiency-responsive transcriptomes in low potassium susceptible and tolerant wheat (*Triticum aestivum* L.). *Sci. Rep.* 5:10090. doi: 10.1038/srep10090

Shi, J. R., Kim, K. N., Ritz, O., Albrecht, V., Gupta, R., Harter, K., et al. (1999). Novel protein kinases associated with calcineurin B-like calcium sensors in *Arabidopsis*. *Plant Cell* 11, 2393–2405. doi: 10.2307/3870963

Tian, X. L., Wang, G. W., Zhu, R., Yang, P. Z., Duan, L. S., and Li, Z. H. (2008). Conditions and indicators for screening cotton (*Gossypium hirsutum* L.) varieties tolerant to low potassium. *Acta Agron. Sin.* 34, 1435–1443. doi: 10.1016/s1875-2780(08)60050-4

Wang, M., Zheng, Q. S., Shen, Q. R., and Guo, S. W. (2013). The critical role of potassium in plant stress response. *Int. J. Mol. Sci.* 14, 7370–7390. doi: 10.3390/ijms1404730

Wang, Y., and Wu, W. H. (2013). Potassium transport and signaling in higher plants. *Annu. Rev. Plant Biol.* 64, 451–476. doi: 10.1146/annurev-arplant-050312-120153

White, P. J., and Karley, A. J. (2010). Potassium. *Plant Cell Monogr.* 17, 199–224. doi: 10.1007/978-3-642-10613-2_9

Wu, D. Z., Shen, Q. F., Cai, S. G., Chen, Z. H., Dai, F., and Zhang, G. P. (2013). Ionomic responses and correlations between elements and metabolites under salt stress in wild and cultivated barley. *Plant Cell Physiol.* 54, 1976–1988. doi: 10.1093/pcp/pct134

Wu, J. T., Zhang, X. Z., Li, T. X., Yu, H. Y., and Huang, P. (2011). Differences in the efficiency of potassium (K) uptake and use in barley varieties. *Agric. Sci. China* 10, 101–108. doi: 10.1016/S1671-2927(11)60312-X

Wu, W. H., and Wang, Y. (2015). Genetic approaches for improvement of the crop potassium acquisition and utilization efficiency. *Curr. Opin. Plant Biol.* 25, 46–52. doi: 10.1016/j.pbi.2015.04.007

Xu, J., Li, H. D., Chen, L. Q., Wang, Y., Liu, L. L., He, L., et al. (2006). A protein kinase, interacting with two calcineurin B-like proteins, regulates K+ transporter AKT1 in *Arabidopsis*. *Cell* 125, 1347–1360. doi: 10.1016/j.cell.2006.06.011

Yuan, J. H., Tu, N. M., Hu, M. H., and Yang, Z. Q. (2005). Comprehensive evaluation of drought resistance of upland and lowland rice. *Chin. Agric. Sci. Bull.* 21, 167–170. doi: 10.3969/j.issn.1000-6850.2005.06.048

Zagorchev, L., Seal, C. E., Kranner, I., and Odjakova, M. (2013). A central role for thiols in plant tolerance to abiotic stress. *Int. J. Mol. Sci.* 14, 7405–7432. doi: 10.3390/ijms14047405

Zasoski, R. J., and Burau, R. G. (1977). Rapid nitric-perchloric acid digestion method for multi-element tissue analysis. *Commun. Soil Sci. Plant Anal.* 8, 425–436. doi: 10.1080/00103627709366735

Zed, R., and Paul, M. D. (2008). Crops and genotypes differ in efficiency of potassium uptake and use. *Physiol. Plant* 133, 624–636. doi: 10.1111/j.1399-3054.2008.01079.x

Zeng, J. B., He, X. Y., Quan, X. Y., Cai, S. G., Han, Y., Nadira, U. A., et al. (2015). Identification of the proteins associated with low potassium tolerance in cultivated and Tibetan wild barley. *J. Proteom.* 126, 1–11. doi: 10.1016/j.jprot.2015.05.025

Zeng, J. B., He, X. Y., Wu, D. Z., Zhu, B., Cai, S. G., Nadira, U. A., et al. (2014). Comparative transcriptome profiling of two Tibetan wild barley genotypes in responses to low potassium. *PLoS One* 9:e100567. doi: 10.1371/journal.pone.0100567

Zeng, J. B., Quan, X. Y., He, X. Y., Cai, S. G., Ye, Z. L., Chen, G., et al. (2018). Root and leaf metabolite profiles analysis reveals the adaptive strategies to low potassium stress in barley. *BMC Plant Biol.* 18:187. doi: 10.1186/s12870-018-1404-4

Zhao, Y., Li, J. H., Zhao, R. L., Xu, K., Xiao, Y. R., Zhang, S. H., et al. (2020). Genome-wide association study reveals the genetic basis of cold tolerance in wheat. *Mol. Breed.* 40:30. doi: 10.1007/s11032-020-01115-x

Zhao, Y., Li, X. Y., Zhang, S. H., Wang, J., Yang, X. F., Tian, J. C., et al. (2014). Mapping QTLs for potassium-deficiency tolerance at the seedling stage in wheat (*Triticum aestivum* L.). *Euphytica* 192, 185–198. doi: 10.1007/s10681-014-1091-7

Zhao, Y., Zhou, M., Xu, K., Li, J. H., Li, S. S., Zhang, S. H., et al. (2019). Integrated transcriptomics and metabolomics analyses provide insights into cold stress response in wheat. *Crop J.* 7, 857–866. doi: 10.1016/j.cj.2019.09.002

Zhou, G. S., Mei, F. Z., Zhou, Z. Q., and Zhu, X. T. (2003). Comprehensive evaluation and forecast physiological indices of waterlogging resistance of different wheat varieties. *Sci. Agric. Sin.* 36, 1378–1382.

Zhuang, Q. S. (2003). *Chinese Wheat Improvement and Pedigree Analysis*. Beijing: China Agriculture Press.

Conflict of Interest: The authors declare that the research was conducted in the absence of any commercial or financial relationships that could be construed as a potential conflict of interest.

frontiers in Plant Science

ORIGINAL RESEARCH
published: 15 October 2020
doi: 10.3389/fpls.2020.568009

Root Morphological Traits of Seedlings Are Predictors of Seed Yield and Quality in Winter Oilseed Rape Hybrid Cultivars

Julien Louvieaux[1,2], Martin Spanoghe[3] and Christian Hermans[1]*

[1] Crop Production and Biostimulation Laboratory, Interfacultary School of Bioengineers, Université Libre de Bruxelles, Brussels, Belgium, [2] Laboratory of Applied Plant Ecophysiology, Haute Ecole Provinciale de Hainaut Condorcet, Centre pour l'Agronomie et l'Agro-Industrie de la Province de Hainaut, Ath, Belgium, [3] Laboratory of Biotechnology and Applied Biology, Haute Ecole Provinciale de Hainaut Condorcet, Mons, Belgium

The root system is responsible for soil resources acquisition. Hence, optimizing crop root characteristics has considerable implications for agricultural production. This study evaluated a panel of twenty-eight European modern cultivars of oilseed rape (*Brassica napus* L.) cultivated in laboratory and field environments. Root morphology was screened using a high-throughput hydroponic growth system with two divergent nitrogen supplies. The panel showed an important diversity for biomass production and root morphological traits. Differences in root and shoot dry biomasses and lateral root length were mainly explained by the genotype, and differences in primary root length by nitrogen nutrition. The cultivars were tested in a pluriannual field trial. The field variation for yield and seed quality traits attributed to the genotype was more important than the year or the genotype × year interaction effects. The total root length measured at the seedling stage could predict the proportion of nitrogen taken up from the field and reallocated to seed organs, a component of the nitrogen use efficiency. The genetic interrelationship between cultivars, established with simple sequence repeat markers, indicated a very narrow genetic base. Positive correlations were found between the genetic distance measures, root morphological traits during nitrogen depletion and yield components. This study illustrates a root phenotyping screen in the laboratory with a proof of concept evaluation in the field. The results could assist future genetic improvements in oilseed rape for desirable root characteristics to reduce nutrient losses in the environment.

Keywords: ***Brassica napus*, field performance, genetic diversity, hydroponics, root morphology**

OPEN ACCESS

Edited by:
Michael A. Grusak, Edward T. Schafer Agricultural Research Center (USDA-ARS), United States

Reviewed by:
Tao Ren, Huazhong Agricultural University, China
Ruilian Jing, Chinese Academy of Agricultural Sciences, China

****Correspondence:***
Julien Louvieaux
julien.louvieaux@condorcet.be

Specialty section:
This article was submitted to Plant Nutrition, a section of the journal Frontiers in Plant Science

Received: *31 May 2020*
Accepted: *22 September 2020*
Published: *15 October 2020*

Citation:
Louvieaux J, Spanoghe M and Hermans C (2020) Root Morphological Traits of Seedlings Are Predictors of Seed Yield and Quality in Winter Oilseed Rape Hybrid Cultivars. Front. Plant Sci. 11:568009. doi: 10.3389/fpls.2020.568009

INTRODUCTION

Nitrogen (N) is the nutrient required in the greatest amount for plant growth and the most determining one for crop yield (Lasisi et al., 2018; Qin et al., 2019). From the soil, plants can absorb mainly inorganic N forms (nitrate and ammonium) and N-containing organic compounds (amino acids and peptides) (Näsholm et al., 2009; Tegeder and Rentsch, 2010). In agricultural soils, inorganic N forms are prevailing (Jämtgård et al., 2010; Lonhienne et al., 2014). Since 1960, the

N fertilizer consumption has increased worldwide nearly ten times (IFASTAT, 2017), while the global crop demand is expected to double by 2050 (Tilman et al., 2011). Sustainable agriculture faces the challenge to produce more food while reducing the negative environmental impact of N fertilization. Cultural practices (e.g., precise fertilization, split doses or matching fertilizer forms) and crop genetic improvement are different levers for better use of N sources (Kant et al., 2011; Han et al., 2015). Besides, understanding the mechanisms of crop adaptation to N availability is crucial for improving Nitrogen Use Efficiency (NUE). The NUE has two main components: the Nitrogen Uptake Efficiency (NUpE) and the Nitrogen Utilization Efficiency (NUtE). These are, respectively, describing the capacity to acquire N from the soil and to utilize the absorbed N for producing harvestable organs (reviewed in Han et al., 2015). The latter one can be divided into the Nitrogen Assimilation Efficiency (NAE) and the Nitrogen Remobilization Efficiency (NRE).

Plant roots fulfill important functions as they not only provide anchorage but also forage soil for water and nutrients. The root system architecture defines the spatial distribution of roots in the soil expressing the ability of the plant to acquire soil resources and is plastic in response to N availability (Smith and De, 2012). In the model species *Arabidopsis thaliana*, a dual effect of nitrate on lateral root (LR) development is described by: (i) a systemic inhibition of uniformly elevated nitrate concentrations occurring on LR elongation at the post-emergence developmental stage and (ii) a localized stimulation of nitrate-rich patches triggering LR elongation of N-deficient plants, known as the foraging capacity (Zhang and Forde, 1998; Zhang et al., 1999; Ruffel et al., 2011). The repression of root development during important N input results in a suboptimal soil volume exploration (López-Bucio et al., 2003; Gruber et al., 2013; Qin et al., 2019). Modern crop breeding is exploiting the natural variation of root morphology to enhance crop productivity, nutrient and water use efficiencies, and to reduce N fertilizer input (Garnett et al., 2009; White et al., 2013; He et al., 2019).

Oilseed rape (*Brassica napus* L.) is the second most important oilseed crop worldwide after soybean, and the first one in Europe (Stahl et al., 2017). That crop requires an important N input and has poor NUE, with a low seed production per N unit applied (Rathke et al., 2005; Sylvester-Bradley and Kindred, 2009; Ulas et al., 2013). The recent domestication of oilseed rape has suffered from several genetic diversity bottlenecks, due to the selection of modern varieties with low concentrations of erucic acid and glucosinolate (Bouchet et al., 2016; Stahl et al., 2017; Hatzig et al., 2018). Surveys showed that crop yield gain has negatively impacted on root system size (Aziz et al., 2017; Pérez-Jaramillo et al., 2017; Bektas and Waines, 2018) and the green revolution unintentionally selected towards poor root morphological features (Voss-Fels et al., 2017). Some reports indicate that N-efficient oilseed rape cultivars are characterized by an important root density during the vegetative growth stage (Ulas et al., 2012). In addition, the genotypic variation of winter oilseed rape for NRE is less substantial than that of NUpE (Ulas et al., 2013), encouraging exploration of the second one. Only few reports associated the root phenome to the field performance of oilseed rape (White et al., 2013; Thomas et al., 2016b; Louvieaux et al., 2020).

This study was conducted with a diversity panel of 28 modern winter oilseed rape cultivars cultivated in laboratory and field environments. Our approach was (i) to explore the natural variation for root morphology at the seedling stage with two contrasting N supplies, and to identify root traits accounting for most of the variation (ii) to examine yield components in a pluriannual field trial (iii) to compare seedling with adult plant traits and to assess the predictiveness of laboratory observations for field performance and (iv) to evaluate relationships between genetic distances based on molecular markers and distances computed from phenotypic data.

MATERIALS AND METHODS

Plant Material

A panel of twenty-eight cultivars of winter oilseed rape (*Brassica napus* L.), registered in the European catalogs of plant species and varieties for less than 10 years, was assembled (**Supplementary Table 1**). Seeds were obtained from Terres Inovia (France). The cultivars were part of the trial network for the period covering 2015 to 2019 for post-registration evaluation of winter oilseed rape cultivars in northern France. The diversity panel reflects the trend of commercial oilseed rape varieties, with a prevalence of hybrids over the past two decades (Stahl et al., 2017). These genotypes undeniably outperform older ones for seed yield (Kessel et al., 2012; Koscielny and Gulden, 2012; Koeslin-Findeklee et al., 2014; Stahl et al., 2017). The mean seed weight at sowing (MSW) was determined by weighing three subsamples of 500 seeds of each cultivar.

Laboratory Culture

A pouch and wick hydroponic system was used for phenotyping root morphology of seedlings (Thomas et al., 2016b; Louvieaux et al., 2018). The seeds were placed on a blue germination paper (grade 194, Ahlstrom-Munksjö, Bärenstein, Germany) soaked in distilled water and then, stratified for 1 week at 4°C. Seeds were then transferred to a culture chamber (Growbank XXL2, CLF Plant Climatics, Wertingen, Germany), where the temperature was 21°C, the light period 16 h (150 μmol photons m^{-2} s^{-1})/8 h darkness and the relative humidity 70%. Two days after germination, six seedlings of uniform size were placed onto one blue paper sheet (20 cm × 30 cm), covered with a black microperforated rigid plate (Biplex®, IPB, Waregem, Belgium) to overshadow the root organs. The mounts (two per genotype, corresponding to twelve seedlings) were placed in containers filled with 10 L of nutrient solution. After 4 days, root and shoot organs were separated, and the root systems scanned at 300 dpi (HP Photosmart C4100). Images were analyzed with the RootNav software (Pound et al., 2013) to extract root morphological traits (**Table 1** and **Supplementary Figure 1**). Eventually, the dry weight of root and shoot organs was measured after 48 h at 70°C. The composition of the nutrient solution was adapted from Hermans et al. (2010). The nitrate concentration varied: the N−

TABLE 1 | Definition of biomass production and root morphological traits measured in hydroponically grown plants.

Abbreviation	Description
R	Root dry biomass (mg)
S	Shoot dry biomass (mg)
R+S	Total dry biomass (mg)
R:S	Root to shoot biomass ratio
L_{PR}	Length of primary root = L_{Z2}+L_{Z3}+L_{Z4} (cm)
L_{Z2}	Length of primary root zone 2, defined between the first and last lateral roots (cm)
L_{Z3}	Length of primary root zone 3, delimited between the hypocotyl junction and the first lateral root (cm)
L_{Z4}	Length of primary root zone 4, delimited between the last lateral root and the primary root tip (cm)
N_{LR}	Number of lateral roots >1 mm
ΣL_{LR}	Sum of lateral root lengths (cm)
D_{LR}-Z1	Density of lateral roots in zone 1 = N_{LR}/L_{PR} (cm^{-1})
D_{LR}-Z2	Density of lateral roots in zone 2 = $(N_{LR}-1)/L_{Z2}$ (cm^{-1})
TRL	Total root length = $L_{PR}+\Sigma L_{LR}$ (cm)
ML_{LR}	Mean length of lateral roots = $\Sigma L_{LR}/N_{LR}$ (cm)
SRL	Specific root length = $(L_{PR}+\Sigma L_{LR})/R$ ($cm\ mg^{-1}$)
MSW	Mean seed weight at sowing (mg)

Illustration of the different root zones is shown in ***Supplementary Figure 1****.*

TABLE 2 | Definition of field traits.

Abbreviation	Description
Seed yield and quality traits	
SY	Seed yield corrected to a standard water content of 9% ($t\ ha^{-1}$)
H	Humidity at harvest (%)
SW	Specific weight of seeds ($kg\ hl^{-1}$)
TSW	Thousand seed weight with moisture adjusted to 9% (g)
OilConc	Oil concentration in dry seeds (%)
ProtConc	Protein concentration in dry seeds (%)
NConc	Nitrogen concentration in dry seeds = ProtConc/6.25 (%)
GLS	Glucosinolate concentration in dry seeds ($\mu mol\ g^{-1}$)
OilY	Oil yield = OilConc × dry SY ($t\ ha^{-1}$)
ProteinY	Protein yield = ProtConc × dry SY ($t\ ha^{-1}$)
SNU	Seed nitrogen uptake = NConc × dry SY ($kg\ ha^{-1}$)
FLO	Earliness of flowering (%)
Optical indices measured at flowering	
CHL	Chlorophyll index
FLAV	Flavonol index
ANTH	Anthocyanin index
NBI	Nitrogen balance index

solution contained 0.2 mM nitrate [0.1 mM $Ca(NO_3)_2$ + 2.4 mM CaCl] and the N+ solution 5.0 mM nitrate [2.5 mM $Ca(NO_3)_2$].

Field Culture

The field trials were conducted over four growing seasons (2015–2019) at the CARAH experimental farm in Ath, Belgium (50°36′48.089″ N, 3°45′58.186″ E). Annual rainfall is typically 863 mm, spread evenly over the year, and annual average temperature is 10.4°C (reference period 1980–2010). The four-year-period was characterized by less important rainfall (ranging from 362 mm in 2018 to 533 mm in 2016) and higher temperature (ranging from 10.8°C in 2016 to 11.6°C in 2018) than average. The silt-loam soil is classified as Luvisol with a favorable drainage.

Preceding crop was winter wheat. The sowing density was 60 seeds m^{-2}. The culture received growth regulator and was protected against weeds, pests and diseases, as required. Each year, microplots of 1.5 m × 12 m in size were sown following a randomized complete block design with four replicates. Sowing dates were between August 28th and September 8th over the four-year-period. The field conditions were not N-limiting. Plots were fertilized with ammonium nitrate after winter, at vegetation stage BBCH 31–32. The fertilizer amount was adjusted on a yearly basis (ranging from 172 to 198 kg N ha^{-1} in 2016 and 2017, respectively), according to N absorbed in plant aerial biomass and mineral N in soil samples (0–90 cm profile) after winter, and using the predictive balance sheet method commonly used for the main arable crops (Makowski et al., 2005).

Cultivars were harvested at the same time, when the mean seed humidity (H) of the control varieties was less than 10% (between July 15th–30th over the 4-year period). To avoid side-effects, only the central parts of the microplots (1.5 m × 9 m) were harvested with a combine harvester (Wintersteiger Delta, Ried im Innkreis, Austria). Seed yield (SY) and seed quality traits are listed in **Table 2**. Subsamples of seeds from each replicate were analyzed for humidity at harvest (H), oil (OilConc), protein (ProtConc), and glucosinolate (GLS) concentrations by near infra-red spectroscopy (XDS NIR Analyzer, Foss, Hilleroed, Denmark). Specific weight of seeds (SW) was measured using a grain analyzer (GAC 2100, Dickey-John, Auburn, United States). A seed counter (Numigral, Chopin Technologies, Villeneuve-la-Garenne, France) was used to determine the thousand seed weight (TSW). Flowering earliness of cultivars (FLO) was visually estimated by the percentage of opened flowers on main inflorescences when control cultivars reached BBCH 65 (between April 10th–20th over the 4-year period). Within the same time window, the chlorophyll index (CHL), flavonol index (FLAV), anthocyanin index (ANTH) and the nitrogen balance index (NBI) were measured with a Dualex® Scientific + leafclip (Force-A, Orsay, France), based on pigment fluorescence (Padilla et al., 2018; Louvieaux et al., 2020). Within each microplot, measurements were conducted on the young mature leaves of five individuals. For adjusting the year effect, a data matrix was computed by normalizing field traits to the mean of three control genotypes (**Supplementary Table 1**). These cultivars were selected among the most marketed and having a wide range of earliness at harvest, as recommended by the French Permanent Technical Committee for Plant Breeding (CTPS) and following protocol for official examination of Value for Cultivation and Use (VCU) of agricultural crops (Animal and Plant Health Agency, United Kingdom, 2016; CTPS, 2017).

Genetic Survey

Genomic DNA was extracted from the cotyledons of two individuals per genotype, germinated in greenhouse conditions, using the DNeasy Plant Mini Kit following manufacturer's

protocol (Qiagen, Venlo, The Netherlands). The DNA samples were quantified with the ND-3300 NanoDrop spectrofluorometer (Thermo Fisher Scientific, Waltham, MA, United States).

Seventeen simple sequence repeat (SSR) markers were selected from the literature followed by in-depth internal testing based on the following criteria: (i) homogeneous repartition on the chromosomes; (ii) optimal amplification and resolution; (iii) capability to detect high rates of polymorphism; (iv) adequacy of observed fragment sizes with those reported in selected literature (Lowe et al., 2004; Cheng et al., 2009; Kim et al., 2009; Xu et al., 2010; Li et al., 2013; AAFC Consortium, 2016); and (v) suitability to be used in a multiplexed PCR reaction, according to the step-by-step protocol by Henegariu et al. (1997). These were amplified in two multiplex PCR sets of nine and eight SSR markers, respectively. The forward primer 5' of each pair was labeled with a fluorescent dye (6-FAM, VIC, NED, or PET dyes) (**Table 3**). The PCR amplification was performed using the Kapa2G HotStart Multilocus Amplification Kit (Kapa Biosystems, Boston, United States) in 25 μl volumes containing 1.5× Kapa2G HotStart PCR Buffer, 0.2 mM dNTP, 0.1–0.2 μM of each primer (Thermo Fisher Scientific, Waltham, MA, United States), 1 unit of KAPA2G Fast HotStart DNA Polymerase and 15 ng of DNA template. All amplifications were done in the same conditions with the SimpliAmp Thermal Cycler (Applied Biosystems, Waltham, MA, United States). The PCR cycling parameters were as follows: initial denaturing step of 2 min at 95°C, 30 cycles of 15 s at 95°C, 30 s at 55°C (Ta), 12 s at 72°C, followed by a hold step of 2 min at 72°C for final extension. After amplification, 0.7 μl of PCR products for each multiplex PCR reaction were transferred into 14.3 μl HiDi (Applied Biosystems) containing 2% of GeneScan™ 500 LIZ™ dye Size Standard (Applied Biosystems), then denatured at 95°C for 3 min and quenched on ice. The denatured samples were run on the SeqStudio™ Genetic Analyzer System (Applied Biosystems), following standard run module parameters. Estimations of PCR product lengths were determined using GeneMapper™ Software 6.0 (Applied Biosystems).

Polymorphism Information Content (PIC) was calculated for each marker as PIC = $1-\Sigma Pi^2$, where Pi is the frequency of the ith allele detected in the subset, according to the Nei's statistic (Nei, 1973). Allelic frequency, observed heterozygosity, and PIC were computed using Cervus software v 3.0 (Kalinowski et al., 2007). Genotyping data was treated based on a hierarchical clustering analysis with the unweighted Neighbor Joining (NJ) methodology using the program DARwin 6.0 (Perrier and Jacquemoud-Collet, 2006) from a dissimilarity matrix beforehand computed by pair-wise comparisons based on simple matching of allelic data.

Statistical Analysis

A two-way analysis of variance (ANOVA) was used to isolate the genotypic effect from the environment/nutrition effect in the laboratory experiment and from the year effect in field trials, as well as their interaction and residual effects. Furthermore, a principal component analysis (PCA) with laboratory and field traits was performed for capturing traits influencing the most the observed variability. Both ANOVA and PCA were executed using R software (R Core Team, 2014) with FactoMinerR (Lê et al., 2008), factoextra (Kassambara and Mundt, 2017), and corrplot (Wei and Simko, 2017) packages. Assumptions for ANOVA were verified with a D'Agostino-Pearson normality test. Correlations between traits were established with Pearson's correlation method

TABLE 3 | Genetic diversity information of the 17 SSR markers used for genotyping of 28 winter oilseed rape cultivars.

Marker Name	Multiplex set	Dye	Linkage group	Allele size range (bp)	No. of alleles	Ho	PIC
BrGMS4028[a]	1	VIC	A01	162–178	2	0.07	0.12
BrGMS0667[a]	1	PET	A02	173	1	0.00	0.00
sN2025[b]	1	6-FAM	A04	128–136	2	0.61	0.37
BrGMS0070[a]	1	NED	A05	188–227	7	0.82	0.76
BrGMS3750[a]	1	6-FAM	A06	209–214	2	0.29	0.28
BrGMS3837[a]	1	NED	A07	299	1	0.00	0.00
BnGMS0281[c]	1	PET	A09	277–295	6	0.61	0.57
BrGMS0086[a]	1	6-FAM	A10	298–314	3	0.43	0.34
BnGMS027[c]	1	VIC	C01	304–312	3	0.25	0.21
cnu_m250a[d]	2	NED	A03	203–264	5	0.54	0.48
Na14-G02[e]	2	6-FAM	A03	183–195	3	0.29	0.23
BrGMS0742[a]	2	NED	A08	131–139	3	0.39	0.34
BnGMS0347[f]	2	6-FAM	C04	272–278	4	0.57	0.47
Na12D10[e]	2	PET	C05	173	1	0.00	0.00
BnGMS0353[c]	2	PET	C06	286–302	4	0.14	0.13
Na12F03[e]	2	VIC	C07	305–315	5	0.61	0.56
Ol12D05[e]	2	VIC	C08	127	1	0.00	0.00
				Average:	**3.12**	**0.33**	**0.29**
				Total:	**53**		

Ho, observed heterozygosity; PIC, polymorphism information content. Detailed marker information is available in: [a]Xu et al., 2010; [b]AAFC Consortium, 2016; [c]Cheng et al., 2009; [d]Kim et al., 2009; [e]Lowe et al., 2004; [f]Li et al., 2013.

on R software, at significant level $\alpha = 0.05$. Correlation plots were drawn with the corrplot package.

The Mantel test was used to investigate the relations between genetic dissimilarities matrix, computed from genotyping analysis, and trait dissimilarities matrices calculated as Euclidean distances from laboratory and field assays. Data were computed using ade4 package on R software at significance level $\alpha = 0.05$ (parameter: 9999 permutations) (Chessel et al., 2004; Dray and Dufour, 2007; Dray et al., 2007; Bougeard and Dray, 2018).

RESULTS

Laboratory Assays

Influence of the Nitrate Supply on Biomass Production and Root Morphology in a Laboratory Environment

A panel of 28 winter oilseed rape cultivars was grown hydroponically to measure biomass production and root morphological traits (**Table 1**), in response to the nitrate supply. Mean seed weight at sowing (MSW) showed large genotypic variation and was almost double between Bonanza and DK Expertise cultivars (**Supplementary Table 1**). Representative root organs of genotypes cultivated with 0.2 mM (N−) or 5.0 mM (N+) nitrate supplies are presented in **Figure 1**. On average for the diversity panel, the shoot biomass (S, +17.8%) and the total biomass (R+S, +14.5%) increased, the root-to-shoot biomass ratio (R:S, −18.2%) decreased, whereas the root biomass (R) was not different in seedlings treated with N+ compared to those with N−. The length of primary root (L_{PR}, +30.5%), the length of primary root zone 4 (L_{Z4}, +44.9%), the sum of lateral root lengths (ΣL_{LR}, +25.8%), the mean length of lateral roots (ML_{LR}, +40.5%), the total root length (TRL, +26.3%), and the specific root length (SRL, +21.8%) were more important, the densities of lateral roots in zone 1 (D_{LR}-Z1, −31.7%) and in zone 2 (D_{LR}-Z2, −12.7%) were less important, whereas the lengths of primary root zone 2 and 3 (L_{Z2}, L_{Z3}) and the number of lateral roots (N_{LR}) did not change during N− compared to N+ conditions (**Figures 1**, **2C**). All mentioned differences between treatments were significant ($P < 0.01$). Root morphology greatly varied among genotypes. For instance, the percentage differences between the two most extreme genotypes were in the range of 28% (Angus *vs.* ES Mambo) and 58% (ES Navigo *vs.* DK Exentiel) for L_{PR}, and of 139% (Cristal *vs.* ES Mambo) and 140% (DK Exclamation *vs.* ES Mambo) for ΣL_{LR}, respectively, at N− and N+ (**Figures 1**, **2A,B**). The responsiveness of cultivars to N depletion (i.e., increase/decrease of one trait value in response to N−) was also assessed (**Figure 2C**). A large variation in phenotypic plasticity was observed, with cultivars poorly or greatly responsive to N supply for L_{PR} (e.g., ES Vito *vs.* Angus) and ΣL_{LR} (e.g., Fernando KWS *vs.* ES Vito).

Variance and Multivariate Analyses With Traits Measured in Laboratory Environment

A global analysis of variance (ANOVA) assessed the effect of (i) the genotype/cultivar, (ii) the environment/nutrition, (iii) the interaction between the genotype and the environment, and (iv) the residual in the variation of phenotypic traits. The biomass traits (R, S, and R+S) were predominantly influenced by the genotype (54–69% of the total variation), while the R:S ratio by the environment (41%) (**Figure 3A**). The length of the primary root, and notably L_{Z4}, was largely dependent on the environment (67%), while L_{Z2} and L_{Z3} were more reliant on the genotype (38 and 29%, respectively). The remaining traits were also depending on the genotype but generally to a lesser extent. Overall, the interaction (genotype × environment) effect was weak.

A principal component analysis (PCA) captured the variation in phenotypic traits across the 28 cultivars and the two N treatments (**Figures 4A,B**). The three first components (PCs), respectively, explained 35.2, 33.6, and 12.9% of the total variation. Some root length traits (TRL, ΣL_{LR}, L_{Z2}, ML_{LR}) and R had mainly loads on PC1 (63%), while other traits (D_{LR}-Z1, L_{Z4}, S, R+S and L_{PR}) on PC2 (61%) and MSW on PC3 (18%).

In-Field Assays

Performance in Field Environment

Field trials were implemented in a complete randomized block design with four replicates, using three control genotypes (DK Exception, DK Expansion, and DK Exstorm) to normalize the data. The field performance of these genotypes during the 4-year trial is given in **Table 4**. The seed yield and quality trait values were falling in the range of trials conducted for the last 10 years at the CARAH experimental station (min 4.37 t ha^{-1} in 2007, max 6.65 t ha^{-1} in 2015; unpublished data) and of other surveys (Stahl et al., 2017). On average for the panel of cultivars, the seed yield (SY) varied by 38% between the two most contrasting years (2017 and 2019). Smaller variations between the years were observed for the protein (ProtConc) and the oil (OilConc) concentrations in dry seeds (14 and 6%, respectively). Large genotypic variations were found within a range of 140% for the earliness of flowering (FLO) and 25% for the nitrogen balance index (NBI) between the two most contrasting cultivars (**Figure 2D**).

Variance and Multivariate Analyses With Traits Measured in Field Environment

The data set of the pluriannual field trial was examined with an ANOVA considering the following effects: (i) genotype, (ii) year, (iii) interaction between genotype and year, and (iv) residuals (**Figure 3B**). The percentage of variation attributed to the genotype varied between 19% for the anthocyanin index (ANTH) and 68% for FLO. The year effect was generally low, except for the thousand seed weight (TSW) for which it accounted for 35%. The genotype × year interaction was overall more important than the year effect and reached 30% for SY. The PCA with field traits revealed three first components explaining, 35, 19.3, and 13% of the total variation respectively. The oil yield (OilY), protein yield (ProteinY), seed nitrogen uptake (SNU), and SY, mainly influenced PC1 (60%) (**Figures 4C,D**), while PC2 was mostly attributed to the glucosinolate concentration in dry seeds (GLS), the

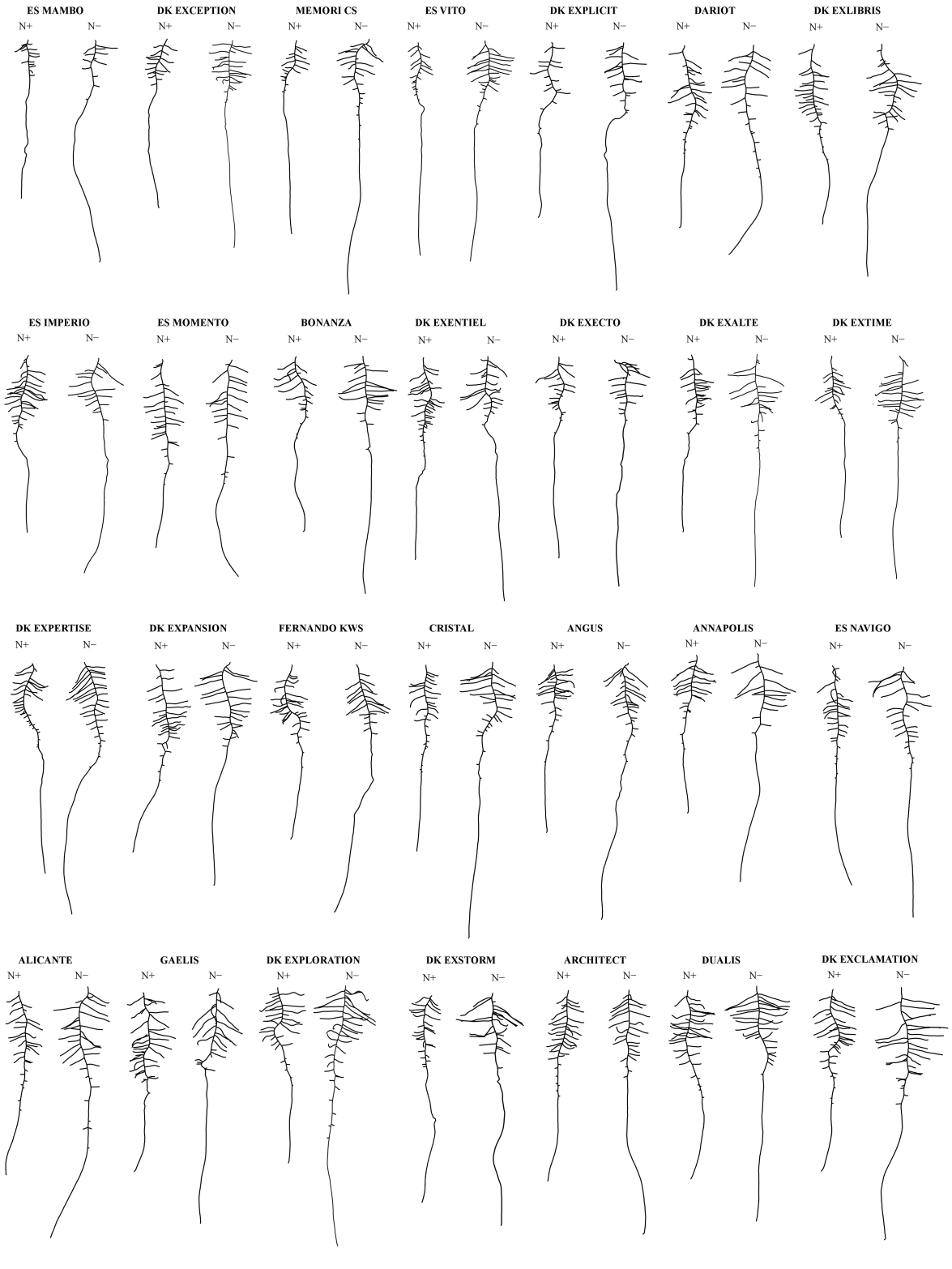

FIGURE 1 | Representative root morphologies of 28 winter oilseed rape cultivars grown in hydroponics. Seedlings grew in the hydroponic pouch-and-wick system with 0.2 mM (N–) or 5.0 mM (N+) nitrate supplies (12 seedlings observed). Representative items for each cultivar-N concentration pair were selected from individuals being closest to the median value for both the primary root length (LPR) and the total root length (TRL). Cultivars are ordered by increasing total root length (TRL) measured at N–. Scale bar = 5 cm.

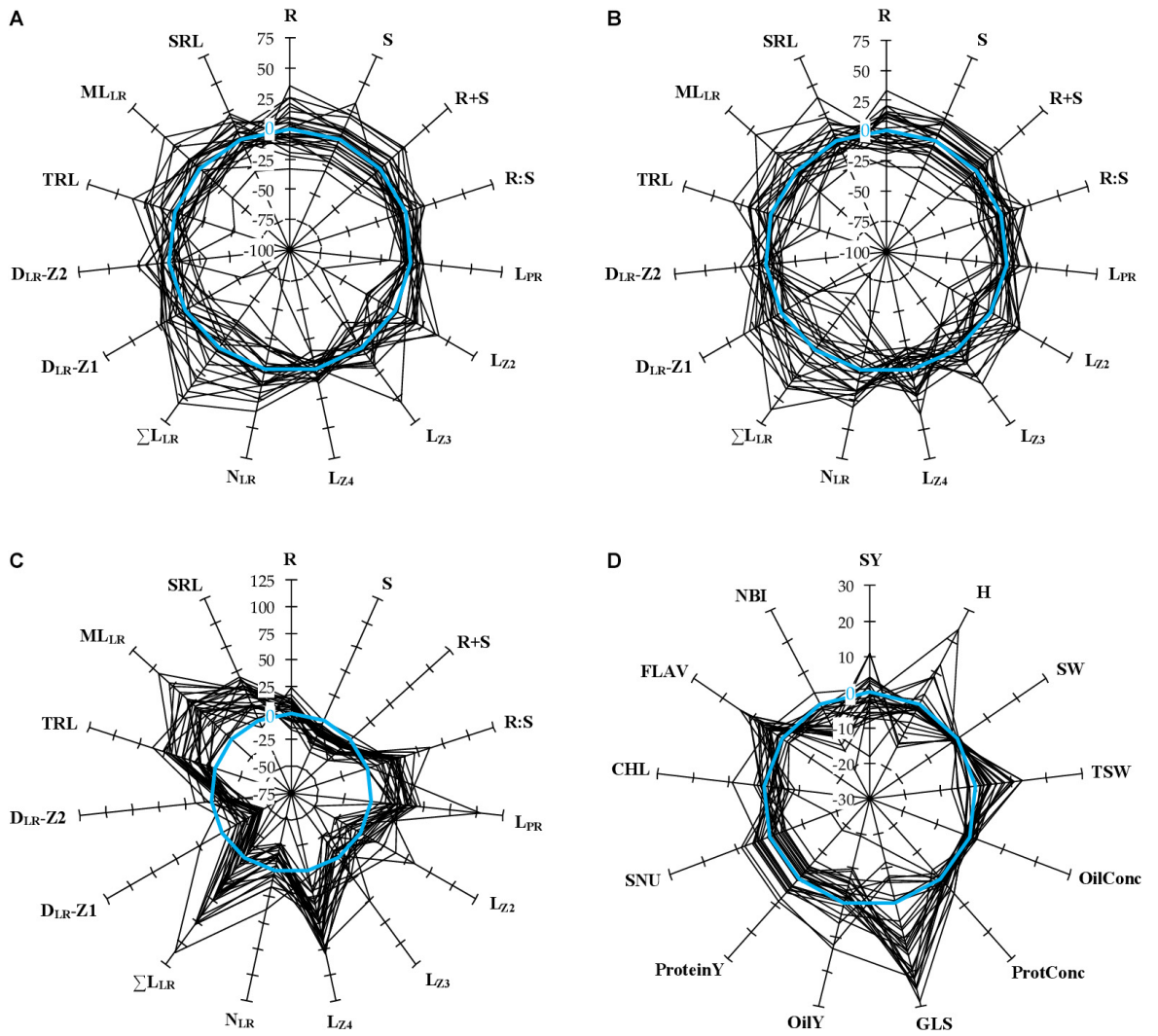

FIGURE 2 | Relative variation of phenotypic traits measured in 28 winter oilseed rape cultivars. **(A,B)** The spider plots show the percentage variation of biomass production and root morphological traits for every cultivar, normalized by the mean value of the panel, measured during N– **(A)** or N+ **(B)** conditions. Zero percent (blue circle) indicates no difference compared to the mean value of the panel in one condition. **(C)** The spider plot shows the percentage variation of biomass production and root morphological traits for every cultivar grown under N– conditions, normalized by the value observed under N+ conditions. This defines the responsiveness of one trait to N depletion. Zero percent indicates no difference compared to N+ conditions. **(D)** The spider plot shows the percentage variation of field traits for every cultivar, normalized to the mean value of three reference cultivars (DK Exception, DK Expansion, and DK Exstorm) over four growing seasons. Zero percent indicates no difference compared to the reference cultivars.

nitrogen balance index (NBI), the specific weight of seeds (SW) and TSW (57%), and PC3 to OilConc and ProtConc at harvest (49%).

Correlations Between Traits Measured in Laboratory and Field Environments

Correlations were established firstly between all traits measured in one culture environment, and secondly between all traits measured in laboratory and field environments (**Supplementary Table 2**). Only traits with important loads on PCs in both environments were considered for drawing the correlograms (**Figure 5**). Pearson's correlation matrices were generated considering the two N treatments separately and then the responsiveness to N. In hydroponics, biomass traits (R, S) and root morphological traits associated with lateral roots (N_{LR}, ΣL_{LR}, ML_{LR}, D_{LR}-Z1) were positively correlated to each other during both N conditions. These traits were positively correlated with L_{PR} at N−, and negatively correlated with L_{Z4} at N+. The MSW was correlated to R and S in both environments and only to some length parameters (L_{PR}, TRL) at N−. In field conditions, FLO was negatively correlated with H. All yield traits were implicitly correlated with SY, while the ProtConc was negatively correlated with OilConc and SY. The nitrogen balance index (NBI), an optical index measured at flowering, was negatively correlated with the seed humidity at harvest (H).

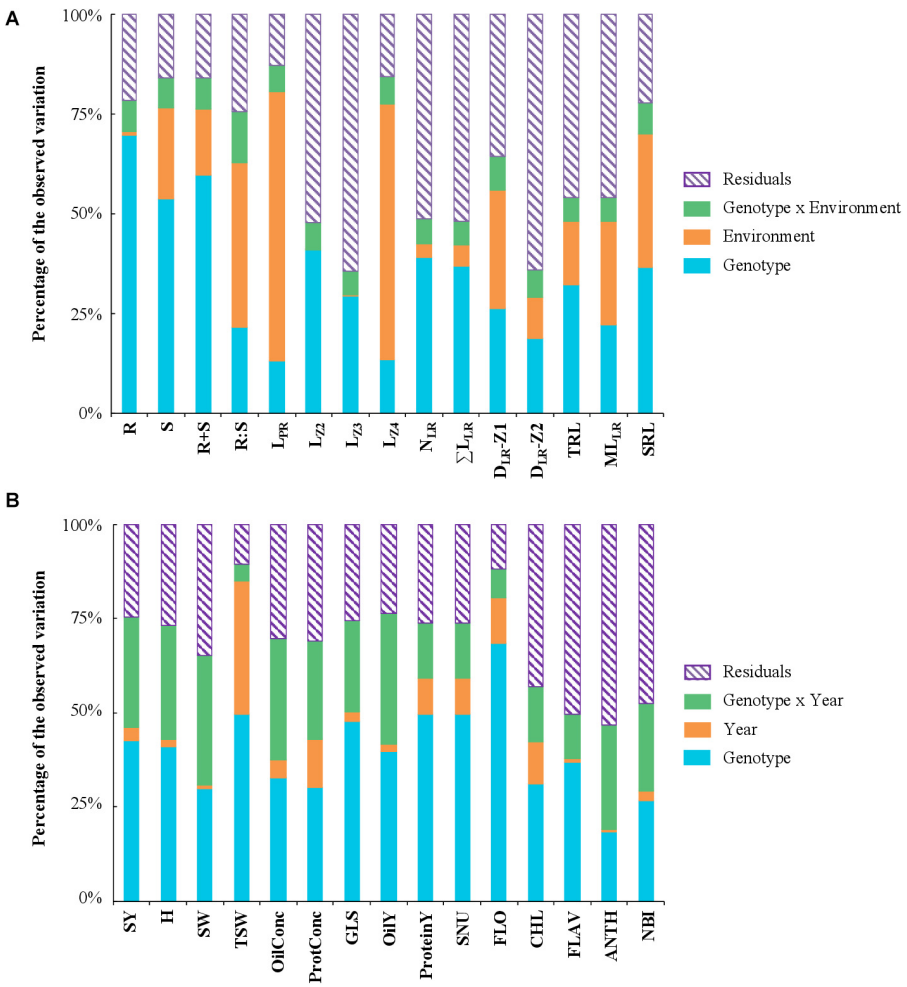

FIGURE 3 | Variance component analysis with phenotypic traits measured in 28 winter oilseed rape cultivars. The histograms show the schematic ANOVA representation for traits measured in hydroponic **(A)** or in field **(B)** conditions. The components of phenotypic variance are **(A)** the genotype/cultivar, environment/nutrition, and interaction (genotype × environment) and residuals as a percentage of the observed variation, and **(B)** genotype/cultivar, year and interaction (genotype × year) and residuals as a percentage of the observed variation. Traits are defined in **Tables 1**, **2**.

Some root related traits (N_{LR}, D_{LR}-Z1, R) measured under N− were positively correlated with ProtConc, while ΣL_{LR} and ML_{LR} under N+ were positively correlated with SY. Some other root morphological traits (ΣL_{LR}, TRL) measured during both N treatments were positively correlated with the seed N uptake (SNU). The responsiveness to N depletion of some traits related to lateral roots (N_{LR}, D_{LR}-Z1, ΣL_{LR}) was positively correlated with ProtConc, and the responsiveness of S negatively with FLO. No significant ($P > 0.05$) correlation was found between TSW and seedling root traits during both N treatments.

Genetic Survey of Winter Oilseed Rape Cultivars

The genetic interrelationships among the 28 cultivars were established using 17 polymorphic SSR markers to eventually identify relationships between genetic distances and measured trait distances in laboratory and field environments. A total of 53 alleles were detected in the diversity panel and the number of alleles per marker ranged from 1 to 7, with an average of 3.12 (**Table 3**). Four markers (BrGMS0667, BrGMS3837, Na12D10 and O112D05) were monomorphic. The allele frequency varied from 1.8% (rare) to 92.9% (common), while the mean was 26.5%. Fifteen out of the 53 total alleles were regarded as rare ones (<5%). The polymorphism information content (PIC) values for all markers ranged from 0.00 to 0.76, with a mean value of 0.29. Only three markers (BrGMS0070, BnGMS0281, and Na12F03) had a PIC value above 0.50. The observed heterozygosity varied from 0.00 to 0.82, with an average of 0.33. The hierarchical clustering using Neighbor-Joining (NJ) generated a radial tree (**Figure 6**) that set together the most closely related cultivars on common branches, and apart those more genetically distant. When reporting the length of the tree branches between the accession pairs to the scale bar, it appeared that the genetic distances within the panel were overall short.

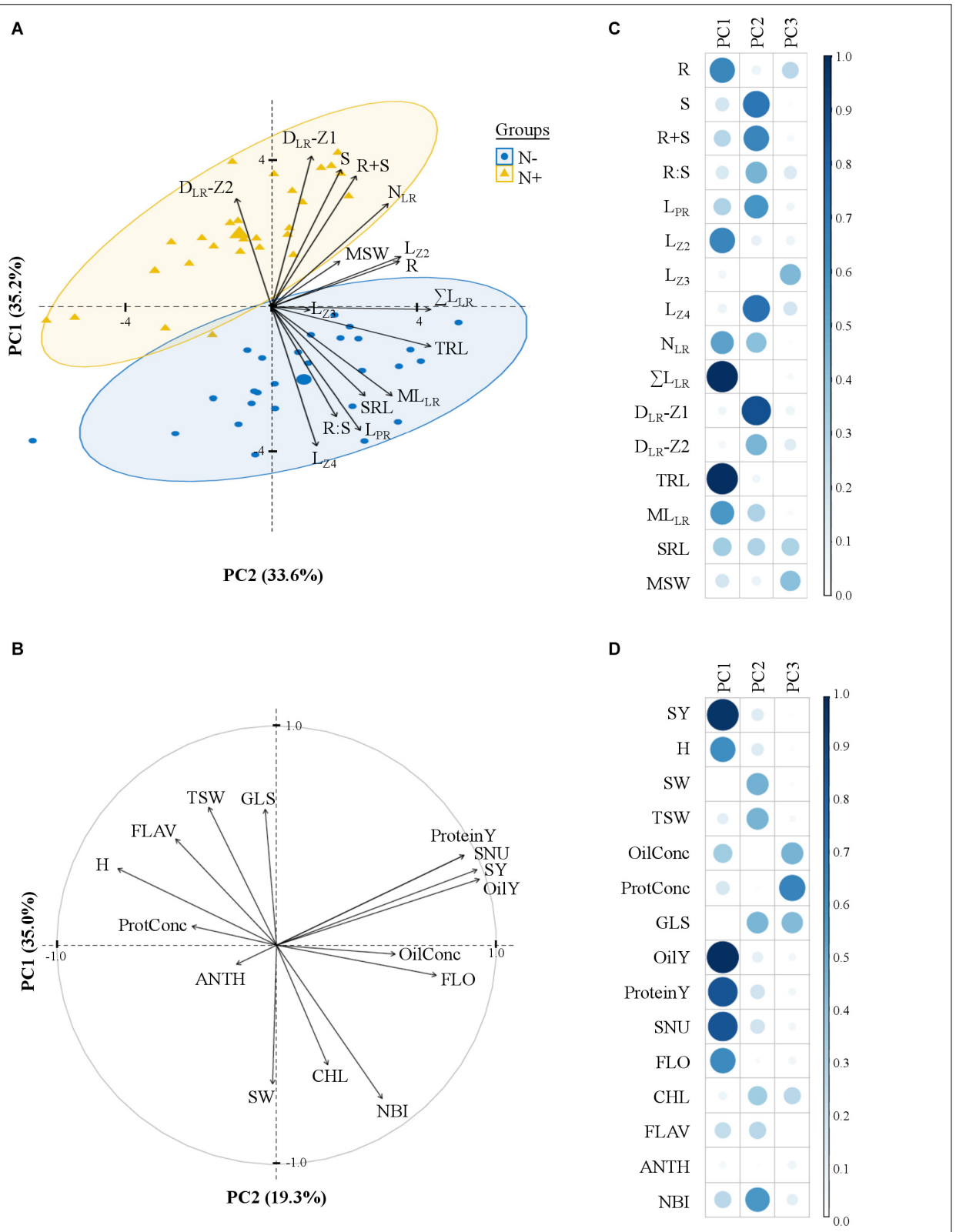

FIGURE 4 | Principal component analysis of traits measured in laboratory and field environments. The biplot graph **(A)** shows 16 variables and 28 cultivars grown in laboratory environment with 5.0 mM (N+) or 0.2 mM (N–) nitrate supplies and the correlation circle **(B)** 15 variables in field environment, with the two first dimensions. Percentages under brackets are those contributed by the first and second principal components. **(C,D)** Representation quality of the variables on the dimensions (values = squared cosines). Traits are defined in **Tables 1**, **2**.

TABLE 4 | Seed yield and quality traits of the control cultivars for the four-year trial.

Harvest Year	SY (t ha^{-1})	H (%)	SW (kg hl^{-1})	TSW (g)	ProtConc (%)	OilConc (%)
2016	5.06 ± 0.19	9.1 ± 0.4	65.6 ± 0.5	3.81 ± 0.15	19.7 ± 0.5	47.2 ± 1.1
2017	6.33 ± 0.33	9.8 ± 0.2	66.4 ± 0.3	4.22 ± 0.20	19.2 ± 0.4	48.0 ± 0.5
2018	4.94 ± 0.32	8.1 ± 1.7	64.2 ± 1.2	5.01 ± 0.55	22.1 ± 0.3	45.1 ± 0.4
2019	4.32 ± 0.22	7.7 ± 0.5	64.8 ± 0.2	4.52 ± 0.22	20.9 ± 0.6	45.6 ± 0.3
	GLS (μmol g^{-1})	**ProteinY (t ha^{-1})**	**OilY (t ha^{-1})**	**SNU (kg ha^{-1})**		
2016	12.3 ± 0.9	0.91 ± 0.02	2.17 ± 0.13	145 ± 2.5		
2017	10.4 ± 1.6	1.11 ± 0.04	2.76 ± 0.16	177 ± 6.7		
2018	15.5 ± 0.1	1.00 ± 0.07	2.03 ± 0.15	159 ± 11.0		
2019	13.1 ± 1.1	0.82 ± 0.02	1.79 ± 0.14	131 ± 3.3		

Mean values (4 replicates ± S.D.) for the three control genotypes (DK Exception, DK Expansion, and DK Exstorm). Traits are defined in ***Table 2****.*

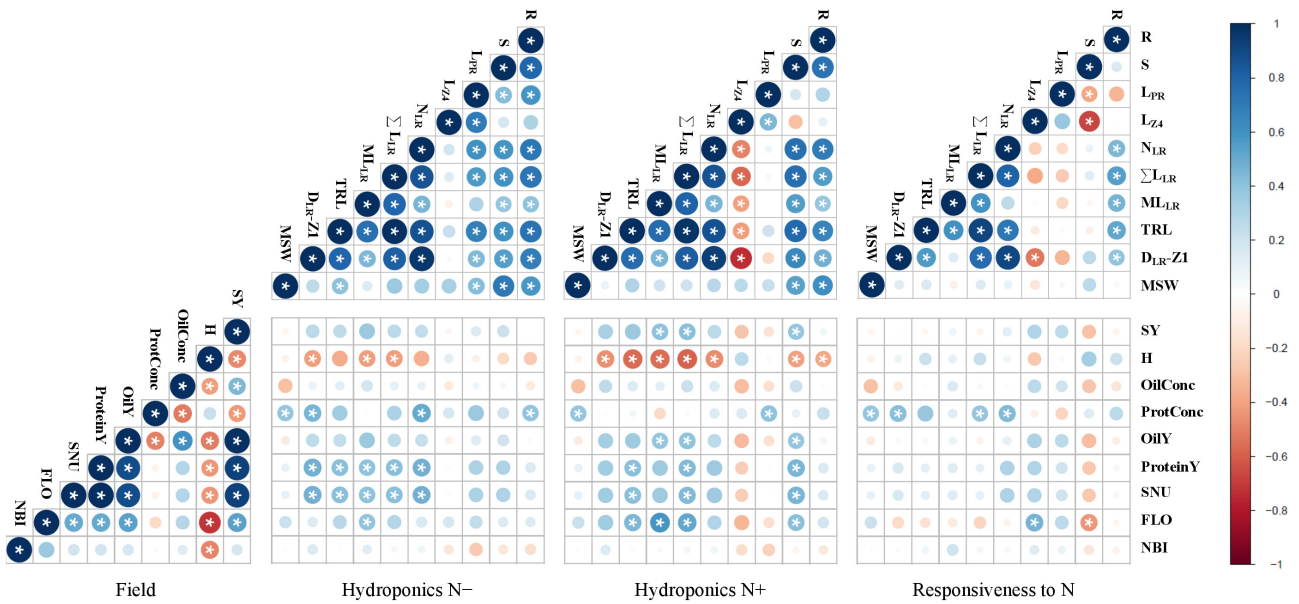

FIGURE 5 | Inter-trait phenotypic correlations in winter oilseed rape genotypes. Biomass production and root morphological traits were measured at 0.2 mM nitrate (N–) or 5 mM nitrate (N+) in hydroponics. Seed yield and seed quality traits as well as optical indices were measured in the field. Circle area and color intensity indicate the strength of the Pearson's correlation. Blue or red colors indicate positive or negative correlations. Star indicates a correlation coefficient significantly ($P < 0.05$) different from zero. Traits are defined in **Tables 1**, **2**.

Correlations Between Genetic Distance and Phenotypic Trait Distance Matrices

Euclidean distances matrices between cultivars were first calculated for each of the traits measured in hydroponic or field conditions and then, correlated to the genetic dissimilarity matrix computed from the genotyping data, using a Mantel test (**Supplementary Table 3**). Significant correlations ($P < 0.05$) were observed between genetic dissimilarities and distances among root morphological traits like S ($r = 0.24$), R+S ($r = 0.19$), L_{PR} ($r = 0.33$), L_{Z2} ($r = 0.33$), L_{Z4}; ($r = 0.30$), and SRL ($r = 0.26$) measured in N− conditions. Significant correlations were also found between genetic dissimilarities and distances among field traits like SY; ($r = 0.35$), ProtConc ($r = 0.20$), GLS ($r = 0.17$), OilY ($r = 0.33$), SNU ($r = 0.30$), and FLO ($r = 0.21$).

DISCUSSION

There is a growing awareness among crop breeders concerning research on root being neglected compared to shoot and reproductive organs. Optimizing root morphology is an important strategy for increasing water and nutrient uptake and coping with soil fertility problems (Den Herder et al., 2010; Lynch, 2013). This study explored the genetic diversity of root morphology in a panel of modern winter oilseed rape cultivars, using a laboratory set-up, and was followed with field validation.

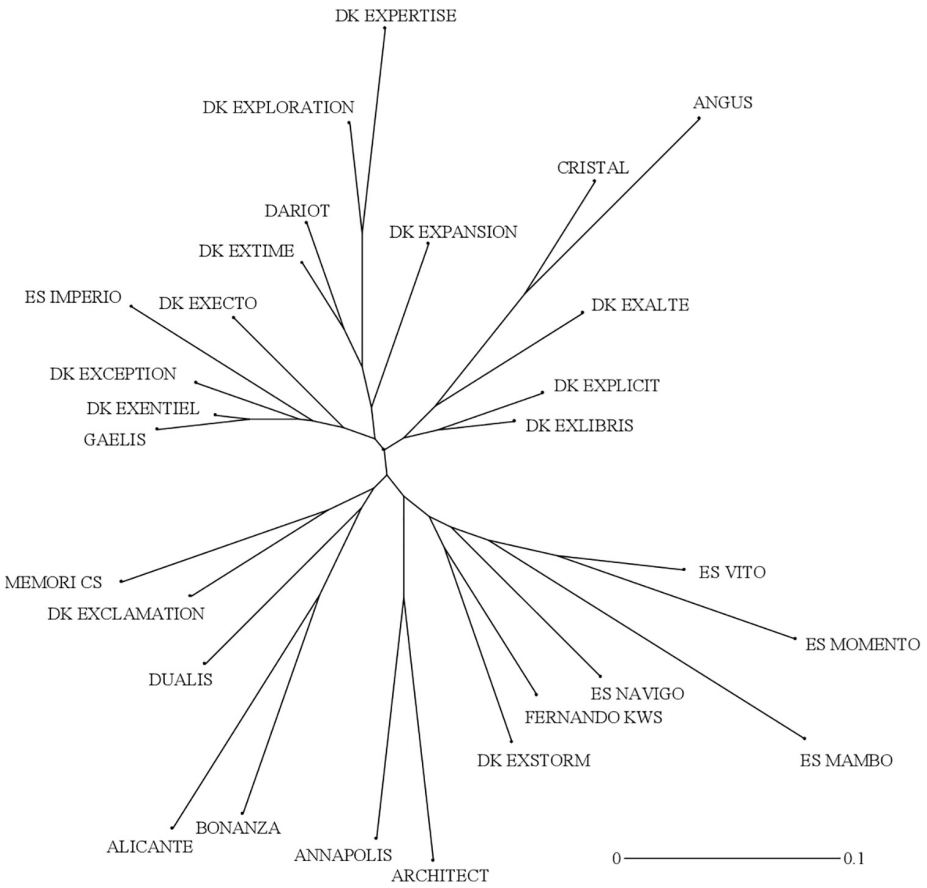

FIGURE 6 | Unweighted Neighbor-Joining (NJ) radial tree showing genetic interrelationships of 28 winter oilseed rape cultivars. The pairwise comparisons were based on dissimilarity coefficients computed from simple matching of allelic data using 17 SSR markers.

The results, discussed hereafter, strengthen the premise that root morphological traits could be successful indicators of field performance. Furthermore, phenotypic and marker-trait correlations launch some prospects for crop breeding programs.

The Root to Shoot Biomass Allocation Is a Key Adaptive Strategy to Nitrogen Availability but Does Not Show Trade-Off Among Cultivars

The root morphological traits of rapeseed are rapidly responding to N availability, with differences reported as early as two days after N depletion (Qin et al., 2019). Nonetheless, seed nutrition may support the growth of seedlings, and attenuate differences between N treatments. This high-throughput hydroponic culture system envisages sequentially a two-day germination step with distilled water (to deplete N storage) and a four-day culture with two divergent N supplies. Hence, the method is suitable for discriminating root organ morphologies at a young development stage (**Figure 1**). Some traits were more depending on the genotype (e.g., R, N_{LR}), while other ones on the N nutrition (e.g., R:S, L_{PR}). Several authors share the foundation that a profuse crop root system exploring a large volume of soil would limit N leaching (Lynch, 2013; Li et al., 2016; Thorup-Kristensen and Kirkegaard, 2016). However, conflicting opinions may be expressed regarding to a possible trade-off between large root system size, contributing to N absorption capacity, and the metabolic costs associated with the growth and maintenance of that organ, which can *in fine* have an impact on NUpE. Results showed increased root to shoot biomass ratio during N− conditions, but a positive correlation between root biomass production and root length, and shoot biomass production across the two N treatments (**Figure 5**). The responsiveness of shoot and root dry biomass production to N deprivation were not correlated. This indicates a positive impact of increased root production on above ground biomass while comparing cultivars. An allometric effect cannot be excluded, where plants with greater biomass having greater root morphological features (Niklas, 2004). The length of primary (especially L_{Z4}) and of lateral roots responded distinctly to N availability (Louvieaux et al., 2018; Qin et al., 2019). The inverse relationship between L_{Z4} and other lateral root related traits (N_{LR}, ΣL_{LR}, D_{LR}-Z1, ML_{LR}) at N+, point out different strategies deployed to modulate horizontal or vertical expansions of the root system. The N responsiveness of L_{PR} and L_{Z4} (i.e., an increase of L_{PR} and L_{Z4} in response to N−) was negatively correlated with S biomass

responsiveness (i.e., a decrease of S biomass in response to N−) (**Figure 5**). This indicates that cultivars with invariable rooting depth could produce more shoot biomass during N depletion.

Root Traits Observed at a Seedling Stage Are Predictors of Field Performance

The cultivars were tested in a pluri-annual field trial for determining some NUE and yield components. The N taken up by roots and utilized for producing seeds (SNU) was considered as a proxy for NUE. The data showed the genotype effect was overall the most important and that genotype × year interaction generally greater than the year effect (**Figure 3**). Indeed, cultivars performed differently from year to year, and this highlights the importance of conducting trials over several seasons. FLO was negatively correlated with H and positively with SY (**Figure 5**). This implies that early-flowering cultivars achieved seed maturity sooner and performed better than late-flowering ones.

Some traits observed at a young developmental stage in laboratory conditions were significantly correlated with field parameters. The positive correlation between lateral root traits (ΣL_{LR}, ML_{LR}) measured in hydroponics during N+ and in-field SY (**Figure 5**), evokes that rapid lateral root development of seedlings is a desirable field characteristic, as stated by Ulas et al. (2012) and Thomas et al. (2016b). Seed germination vigor and rapid radicle growth may enhance seedling survival and ultimately yield (Hatzig et al., 2015; Thomas et al., 2016b; Boter et al., 2019). In this study, the seed weight at sowing had no marked influence neither on seedling root size neither on yield components (**Figures 4**, **5**), in line with Hatzig et al. (2015) but contrary to Thomas et al. (2016a).

Besides, root traits (ΣL_{LR}, TRL) measured under both N treatments were positively correlated with SNU, signifying that root phenotypes could be considered for screening NUE components. Measurements of root system morphology and total biomass at harvest (roots, stems, leaves, pods, and seeds) should be considered in future field trials to better evaluate the total N uptake and the reallocation to seed organs, but this is hardly achievable in field conditions. The 4-year trial was marked with a severe rain deficit, in such conditions root traits may also be important for water absorption and maintaining yield under drought conditions (Den Herder et al., 2010; Comas et al., 2013).

The lateral root traits (N_{LR}, ΣL_{LR}, D_{LR}-Z1) were correlated positively with FLO and negatively with H (**Figure 5**). The seed maturation is marked by H decreased (Elias and Copeland, 2001; Sadeghi et al., 2010). Since harvest was simultaneously done under the same climatic conditions, a low H value reflects an early seed maturity. Presumably, plants with greater root development reach more rapidly seed maturity. Genotypes flowering early better synchronize N mobilization with the pods demand and potentially have an extended seed filling period (Malagoli et al., 2005; Stahl et al., 2016). Therefore, optimizing flowering time is an important breeding target (Schiessl et al., 2014).

Breeding efforts to select modern varieties achieving great oil yield could possibly be the reason for which SY and OilConc traits are intricated (Stahl et al., 2016, 2017). The SY was negatively correlated with ProtConc, but positively with ProteinY (**Figure 5**). This confirms that yield *per se* is more decisive than seed N concentration with the purpose of improving ProteinY and seed N uptake (SNU). However, ProtConc was positively correlated with root traits measured during N− (N_{LR}, D_{LR}-Z1, R) and N+ (L_{PR}) conditions.

The N responsiveness of ΣL_{LR} (i.e., an increase of this trait in response to N−) was positively correlated with ProtConc (**Figure 5**), meaning that cultivars with important lateral root growth plasticity have greater protein concentration in seeds. The N responsiveness of S biomass (i.e., a decrease of S in response to N−) and the N responsiveness of L_{Z4} (i.e., an increase of L_{Z4} in response to N−) were negatively and positively correlated with FLO, respectively (**Figure 5**). This indicates that cultivars with major impact on S biomass and profound impact on L_{Z4} during N depletion were flowering early.

These results corroborate recent reports on oilseed rape, but also on other crops like maize and wheat, in which root traits observed at a seedling stage could predict field performance (Canè et al., 2014; Ali et al., 2015; Thomas et al., 2016b).

The Genetic Variability of Root Traits Can Be Exploited to Develop Markers for Assisted Breeding to Improve Soil Resource Capture

The assessment of the genetic diversity among the hybrid varieties with SSR markers indicated a rather narrow genetic basis (**Table 3** and **Figure 6**). Four markers were monomorphic, despite filling internal tests with different germplasms (our unpublished data). Besides, the PIC values and the observed heterozygosity were lower than in other reports using the same markers (Li et al., 2013; Chen et al., 2017, 2020). The small number of detected alleles per marker and the high disparities occurring in the allelic frequencies between common and rare alleles, explained together the lower PIC scores in the present study (**Table 3**). However, the great variability of biomass production and of root morphology within that nested gene pool of modern cultivars, indicates that these traits may constitute an exploitable resource in a breeding effort to ameliorate NUE. Furthermore, the weak relationships between the genetic dissimilarities and phenotypic distances data measured during N− conditions, are encouraging us to extend the study to more genotypes from more diverse origins using denser molecular markers. Mapping approaches in a wider *B. napus* gene pool could be adopted to characterize the allelic variation. Such traits could be incorporated in superior cultivars by genomic and marker-assisted selection strategies.

This report with a small panel of modern winter oilseed rape cultivars compared root phenotypes, field harvest and NUE components. Similar investigation sought to evaluate genotypic variation for root systems and NUE were successfully conducted in core sets of other crop species (Yang et al., 2019; Iqbal et al., 2020). To strengthen this pilot experiment, further studies with a larger diversity panel should assess yield stability in multi-environment trials and across N rates (Thorup-Kristensen and Kirkegaard, 2016; Stahl and Snowdon, 2018). Selection of

seedling root traits that could predict field performance, would open a cost-effective way to facilitate introgression of root morphology in rapeseed breeding programs.

CONCLUSION

Below-ground phenotyping of the root organ can be tedious in breeding programs. Root traits measured in laboratory culture were to a certain degree predictive of field performance. Such high-throughput screen could be applied to a larger mapping population to identify genes and alleles shaping root morphology, for selection targets in breeding programs to use soil resources more efficiently. This exploratory work is supporting possible genetic improvements for the root morphology of modern oilseed rape cultivars.

DATA AVAILABILITY STATEMENT

The raw data supporting the conclusions of this article will be made available by the authors, without undue reservation.

AUTHOR CONTRIBUTIONS

CH and JL contributed to the conceptualization and funding acquisition. JL contributed to the methodology, field and laboratory investigations, formal analysis, and writing-original draft. MS contributed to the genotyping investigation. CH, MS, and JL contributed to the writing-review and editing. All authors contributed to the article and approved the submitted version.

FUNDING

This research was funded by MIS and PDR T.0116.19 grants from Fonds de la Recherche Scientifique (F.R.S.-FNRS).

ACKNOWLEDGMENTS

CH is F.R.S.-FNRS research associate. The authors thankfully acknowledge the Centre pour l'Agronomie et l'Agro-Industrie de la Province de Hainaut (CARAH), Olivier Mahieu for management of the field trials, Camille Dekuijper for DNA extraction, Antoine Leclercq and Katja Keržič for conducting hydroponic culture.

SUPPLEMENTARY MATERIAL

The Supplementary Material for this article can be found online at: https://www.frontiersin.org/articles/10.3389/fpls.2020.568009/full#supplementary-material

REFERENCES

AAFC Consortium (2016). Available online at: http://brassica.agr.gc.ca/index_e.shtml (accessed December 22, 2019).

Ali, M. L., Luetchens, J., Nascimento, J., Shaver, T. M., Kruger, G. R., and Lorenz, A. J. (2015). Genetic variation in seminal and nodal root angle and their association with grain yield of maize under water-stressed field conditions. *Plant Soil* 397, 213–225. doi: 10.1007/s11104-015-2554-x

Animal and Plant Health Agency, UK (2016). Available online at: https://www.gov.uk/guidance/vcu-protocols-and-procedures-for-testing-agricultural-crops#protocols (accessed December 22, 2019).

Aziz, M. M., Palta, J. A., Siddique, K. H. M., and Sadras, V. O. (2017). Five decades of selection for yield reduced root length density and increased nitrogen uptake per unit root length in Australian wheat varieties. *Plant Soil* 413, 181–192. doi: 10.1007/s11104-016-3059-y

Bektas, H., and Waines, J. G. (2018). Root and shoot traits in parental, early and late generation Green Revolution wheats (*Triticum* spp.) under glasshouse conditions. *Genet. Resour. Crop Evol.* 65, 2003–2012. doi: 10.1007/s10722-018-0673-y

Boter, M., Calleja-Cabrera, J., Carrera-Castaño, G., Wagner, G., Hatzig, S. V., Snowdon, R., et al. (2019). An integrative approach to analyze seed germination in *Brassica napus*. *Front. Plant Sci.* 10:1342. doi: 10.3389/fpls.2019.01342

Bouchet, A.-S., Laperche, A., Bissuel-Belaygue, C., Snowdon, R., Nesi, N., and Stahl, A. (2016). Nitrogen use efficiency in rapeseed. A review. *Agron. Sustain. Dev.* 36:38. doi: 10.1007/s13593-016-0371-0

Bougeard, S., and Dray, S. (2018). Supervised multiblock analysis in R with the ade4 package. *J. Stat. Softw.* 86, 1–17. doi: 10.18637/jss.v086.i01

Canè, M. A., Maccaferri, M., Nazemi, G., Salvi, S., Francia, R., Colalongo, C., et al. (2014). Association mapping for root architectural traits in durum wheat seedlings as related to agronomic performance. *Mol. Breed.* 34, 1629–1645. doi: 10.1007/s11032-014-0177-1

Chen, R., Hara, T., Ohsawa, R., and Yoshioka, Y. (2017). Analysis of genetic diversity of rapeseed genetic resources in Japan and core collection construction. *Breed. Sci.* 67, 239–247. doi: 10.1270/jsbbs.16192

Chen, R., Shimono, A., Aono, M., Nakajima, N., Ohsawa, R., and Yoshioka, Y. (2020). Genetic diversity and population structure of feral rapeseed (*Brassica napus* L.) in Japan. *PLoS One* 15:e0227990. doi: 10.1371/journal.pone.0227990

Cheng, X., Xu, J., Xia, S., Gu, J., Yang, Y., Fu, J., et al. (2009). Development and genetic mapping of microsatellite markers from genome survey sequences in *Brassica napus*. *Theor. Appl. Genet.* 118, 1121–1131. doi: 10.1007/s00122-009-0967-8

Chessel, D., Dufour, A., and Thioulouse, J. (2004). The ade4 package – I: one-table methods. *R News* 4, 5–10.

Comas, L. H., Becker, S. R., Cruz, V. M. V., Byrne, P. F., and Dierig, D. A. (2013). Root traits contributing to plant productivity under drought. *Front. Plant Sci.* 4:442. doi: 10.3389/fpls.2013.00442

CTPS (2017). *Règlement Technique D'examen des Variétés de Colza Oléagineux en vue de leur Inscription au Catalogue Officiel Français*. Available online at: https://info.agriculture.gouv.fr/gedei/site/bo-agri/document_administratif-e7c591c7-5dca-44ef-be62-57e6da03d35c/telechargement (accessed January 15, 2020).

Den Herder, G., van Isterdael, G., Beeckman, T., and de Smet, I. (2010). The roots of a new green revolution. *Trends Plant Sci.* 15, 600–607. doi: 10.1016/j.tplants.2010.08.009

Dray, S., and Dufour, A. (2007). The ade4 package: implementing the duality diagram for ecologists. *J. Stat. Softw.* 22, 1–20. doi: 10.18637/jss.v022.i04

Dray, S., Dufour, A., and Chessel, D. (2007). The ade4 package – II: two-table and K-table methods. *R News* 4, 5–10.

Elias, S. G., and Copeland, L. O. (2001). Physiological and harvest maturity of canola in relation to seed quality. *Agron. J.* 93, 1054–1058. doi: 10.2134/agronj2001.9351054x

Eu Plant Variety Database (2019). Available online at: http://ec.europa.eu/food/plant/plant_propagation_material/plant_variety_catalogues_databases/search/public/index.cfm?event=SearchForm&ctl_type=A (accessed December 08, 2019).

Garnett, T., Conn, V., and Kaiser, B. N. (2009). Root based approaches to improving nitrogen use efficiency in plants. *Plant Cell Environ.* 32, 1272–1283. doi: 10.1111/j.1365-3040.2009.02011.x

Gruber, B. D., Giehl, R. F. H., Friedel, S., and von Wirén, N. (2013). Plasticity of the Arabidopsis root system under nutrient deficiencies. *Plant Physiol.* 163, 161–179. doi: 10.1104/pp.113.218453

Han, M., Okamoto, M., Beatty, P. H., Rothstein, S. J., and Good, A. G. (2015). The genetics of nitrogen use efficiency in crop plants. *Annu. Rev. Genet.* 49, 269–289. doi: 10.1146/annurev-genet-112414-055037

Hatzig, S., Breuer, F., Nesi, N., Ducournau, S., Wagner, M.-H., Leckband, G., et al. (2018). Hidden effects of seed quality breeding on germination in oilseed rape (*Brassica napus* L.). *Front. Plant Sci.* 9:419. doi: 10.3389/fpls.2018.00419

Hatzig, S. V., Frisch, M., Breuer, F., Nesi, N., Ducournau, S., Wagner, M.-H., et al. (2015). Genome-wide association mapping unravels the genetic control of seed germination and vigor in *Brassica napus*. *Front. Plant Sci.* 6:221. doi: 10.3389/fpls.2015.00221

He, Y., Hu, D., You, J., Wu, D., Cui, Y., Dong, H., et al. (2019). Genome-wide association study and protein network analysis for understanding candidate genes involved in root development at rapeseed seedling stage. *Plant Physiol. Biochem.* 137, 42–52. doi: 10.1016/j.plaphy.2019.01.028

Henegariu, O., Heerema, N. A., Dlouhy, S. R., Vance, G. H., and Vogt, P. H. (1997). Multiplex PCR: critical parameters and step-by-step protocol. *Biotechniques* 23, 504–511. doi: 10.2144/97233rr01

Hermans, C., Vuylsteke, M., Coppens, F., Craciun, A., Inzé, D., and Verbruggen, N. (2010). Early transcriptomic changes induced by magnesium deficiency in *Arabidopsis thaliana* reveal the alteration of circadian clock gene expression in roots and the triggering of abscisic acid-responsive genes. *New Phytol.* 187, 119–131. doi: 10.1111/j.1469-8137.2010.03258.x

IFASTAT. (2017). *International Fertilizer Association*. Available online at: https://www.ifastat.org/ (accessed December 31, 2019).

Iqbal, A., Qiang, D., Zhun, W., Xiangru, W., Huiping, G., Hengheng, Z., et al. (2020). Growth and nitrogen metabolism are associated with nitrogen-use efficiency in cotton genotypes. *Plant Physiol. Biochem.* 149, 61–74. doi: 10.1016/j.plaphy.2020.02.002

Jämtgård, S., Näsholm, T., and Huss-Danell, K. (2010). Nitrogen compounds in soil solutions of agricultural land. *Soil Biol. Biochem.* 42, 2325–2330. doi: 10.1016/j.soilbio.2010.09.011

Kalinowski, S. T., Taper, M. L., and Marshall, T. C. (2007). Revising how the computer program CERVUS accommodates genotyping error increases success in paternity assignment. *Mol. Ecol.* 16, 1099–1106. doi: 10.1111/j.1365-294X.2007.03089.x

Kant, S., Bi, Y. M., and Rothstein, S. J. (2011). Understanding plant response to nitrogen limitation for the improvement of crop nitrogen use efficiency. *J. Exp. Bot.* 62, 1499–1509. doi: 10.1093/jxb/erq297

Kassambara, A., and Mundt, F. (2017). *Factoextra: Extract and Visualize the Results of Multivariate Data Analyses (version 1.0.7)*. Available online at: https://cran.r-project.org/web/packages/factoextra/index.html (accessed June 15, 2020).

Kessel, B., Schierholt, A., and Becker, H. C. (2012). Nitrogen use efficiency in a genetically diverse set of winter oilseed rape (*Brassica napus* L.). *Crop Sci.* 52, 2546–2554. doi: 10.2135/cropsci2012.02.0134

Kim, H., Choi, S. R., Bae, J., Hong, C. P., Lee, S. Y., Haossain, M. J., et al. (2009). Sequenced BAC anchored reference genetic map that reconciles the ten individual chromosomes of *Brassica rapa*. *BMC Genomics* 10:432. doi: 10.1186/1471-2164-10-432

Koeslin-Findeklee, F., Meyer, A., Girke, A., Beckmann, K., and Horst, W. J. (2014). The superior nitrogen efficiency of winter oilseed rape (*Brassica napus* L.) hybrids is not related to delayed nitrogen starvation-induced leaf senescence. *Plant Soil* 384, 347–362. doi: 10.1007/s11104-014-2212-8

Koscielny, C. B., and Gulden, R. H. (2012). Seedling root length in *Brassica napus* L. is indicative of seed yield. *Can. J. Plant Sci.* 92, 1229–1237. doi: 10.4141/cjps2012-070

Lasisi, A. A., Akinremi, O. O., Tenuta, M., and Cattani, D. (2018). Below-ground plant biomass and nitrogen uptake of perennial forage grasses and annual crops fertilized with pig manures. *Agric. Ecosyst. Environ.* 268, 1–7. doi: 10.1016/j.agee.2018.08.006

Lê, S., Josse, J., and Husson, F. (2008). FactoMineR: an R package for multivariate analysis. *J. Stat. Softw.* 25, 1–18. doi: 10.18637/jss.v025.i01

Li, H., Younas, M., Wang, X., Li, X., Chen, L., Zhao, B., et al. (2013). Development of a core set of single-locus SSR markers for allotetraploid rapeseed (*Brassica napus* L.). *Theor. Appl. Genet.* 126, 937–947. doi: 10.1007/s00122-012-2027-z

Li, X., Zeng, R., and Liao, H. (2016). Improving crop nutrient efficiency through root architecture modifications. *J. Integr. Plant Biol.* 58, 193–202. doi: 10.1111/jipb.12434

Lonhienne, T. G. A., Trusov, Y., Young, A., Rentsch, D., Näsholm, T., Schmidt, S., Paungfoo-Lonhienne, C. (2014). Effects of externally supplied protein on root morphology and biomass allocation in Arabidopsis. *Sci. Rep.* 4:5055. doi: 10.1038/srep05055

López-Bucio, J., Cruz-Ramírez, A., and Herrera-Estrella, L. (2003). The role of nutrient availability in regulating root architecture. *Curr. Opin. Plant Biol.* 6, 280–287. doi: 10.1016/S1369-5266(03)00035-9

Louvieaux, J., De Gernier, H., and Hermans, C. (2018). "Exploiting genetic variability of root morphology as a lever to improve nitrogen use efficiency in oilseed rape," in *Engineering Nitrogen Utilization in Crop Plants*, eds A. Shrawat, A. Zayed, and D. A. Lightfoot (Cham: Springer International Publishing), 185–206. doi: 10.1007/978-3-319-92958-3_11

Louvieaux, J., Leclercq, A., Haelterman, L., and Hermans, C. (2020). In-field observation of root growth and nitrogen uptake efficiency of winter oilseed rape. *Agronomy* 10:105. doi: 10.3390/agronomy10010105

Lowe, A. J., Moule, C., Trick, M., and Edwards, K. J. (2004). Efficient large-scale development of microsatellites for marker and mapping applications in Brassica crop species. *Theor. Appl. Genet.* 108, 1103–1112. doi: 10.1007/s00122-003-1522-7

Lynch, J. P. (2013). Steep, cheap and deep: an ideotype to optimize water and N acquisition by maize root systems. *Ann. Bot.* 112, 347–357. doi: 10.1093/aob/mcs293

Makowski, D., Maltas, A., Morison, M., and Reau, R. (2005). Calculating N fertilizer doses for oil-seed rape using plant and soil data. *Agron. Sustain. Dev.* 25, 159–161. doi: 10.1051/agro:2004052

Malagoli, P., Lainé, P., Rossato, L., and Ourry, A. (2005). Dynamics of nitrogen uptake and mobilization in field-grown winter oilseed rape (*Brassica napus*) from stem extension to harvest: I. Global N flows between vegetative and reproductive tissues in relation to leaf fall and their residual N. *Ann. Bot.* 95, 853–861. doi: 10.1093/aob/mci091

Näsholm, T., Kielland, K., and Ganeteg, U. (2009). Uptake of inorganic nitrogen by plants. *New Phytol.* 182, 31–48. doi: 10.1111/j.1469-8137.2008.02751.x

Nei, M. (1973). Analyses of gene diversity in subdivided populations. *Proc. Natl. Acad. Sci. U.S.A.* 70, 3321–3323. doi: 10.1073/pnas.70.12.3321

Niklas, K. J. (2004). Plant allometry: is there a grand unifying theory? *Biol. Rev.* 79, 871–889. doi: 10.1017/s1464793104006499

Padilla, F. M., Gallardo, M., Peña-Fleitas, M. T., de Souza, R., and Thompson, R. B. (2018). Proximal optical sensors for nitrogen management of vegetable crops: a review. *Sensors* 18:2083. doi: 10.3390/s18072083

Pérez-Jaramillo, J. E., Carrión, V. J., Bosse, M., Ferrão, L. F. V., de Hollander, M., Garcia, A. A. F., et al. (2017). Linking rhizosphere microbiome composition of wild and domesticated *Phaseolus vulgaris* to genotypic and root phenotypic traits. *ISME J.* 11, 2244–2257. doi: 10.1038/ismej.2017.85

Perrier, X., and Jacquemoud-Collet, J. P. (2006). *DARwin software*. Available online at: http://darwin.cirad.fr/darwin (accessed March 13, 2020).

Pound, M. P., French, A. P., Atkinson, J. A., Wells, D. M., Benett, M. J., and Pridmore, T. (2013). RootNav: navigating images of complex root architectures. *Plant Physiol.* 162, 1802–1814. doi: 10.1104/pp.113.221531

Qin, L., Walk, T. C., Han, P., Chen, L., Zhang, S., Li, Y., et al. (2019). Adaptation of roots to nitrogen deficiency revealed by 3D quantification and proteomic analysis. *Plant Physiol.* 179, 329–347. doi: 10.1104/pp.18.00716

R Core Team (2014). *R: A Language and Environment for Statistical Computing*. Vienna: R Foundation for Statistical Computing.

Rathke, G. W., Christen, O., and Diepenbrock, W. (2005). Effects of nitrogen source and rate on productivity and quality of winter oilseed rape (*Brassica napus* L.) grown in different crop rotations. *Field Crop Res.* 94, 103–113. doi: 10.1016/j.fcr.2004.11.010

Ruffel, S., Krouk, G., Ristova, D., Shasha, D., Birnbaum, K. D., and Coruzzi, G. M. (2011). Nitrogen economics of root foraging: transitive closure of the nitrate–cytokinin relay and distinct systemic signaling for N supply vs. demand. *Proc. Natl. Acad. Sci. U.S.A.* 108, 18524–18529. doi: 10.1073/pnas.1108684108

Sadeghi, H., AghaAlikhani, M., Khazaei, F., and Sharafi Nezhad, M. (2010). Investigation of seed moisture content at harvest time as an empirical index

for improving viability and seed vigour of two oil-seed rape cultivars. *ARPN J. Agric. Biol. Sci.* 6, 20–26.

Schiessl, S. V., Samans, B., Hüttel, B., Reinhard, R., and Snowdon, R. J. (2014). Capturing sequence variation among flowering-time regulatory gene homologs in the allopolyploid crop species. *Front. Plant Sci.* 5:404. doi: 10.3389/fpls.2014.00404

Smith, S., and De, S. I. (2012). Root system architecture: insights from *Arabidopsis* and cereal crops. *Philos. Trans. R. Soc. Lond. B. Biol. Sci.* 367, 1441–1452. doi: 10.1098/rstb.2011.0234

Stahl, A., Freidt, W., Wittkop, B., and Snowdon, R. J. (2016). Complementary diversity for nitrogen uptake and utilization efficiency reveals broad potential for increased sustainability of oilseed rape production. *Plant Soil* 400, 245–262. doi: 10.1007/s11104-015-2726-8

Stahl, A., Pfeifer, M., Frisch, M., Wittkop, B., and Snowdon, R. J. (2017). Recent genetic gains in Nitrogen Use Efficiency in oilseed rape. *Front. Plant Sci.* 8:963. doi: 10.3389/fpls.2017.00963

Stahl, A., and Snowdon, R. (2018). "Genetic improvement of nitrogen use efficiency in oilseed rape," in *Engineering Nitrogen Utilization in Crop Plants*, eds A. Shrawat, A. Zayed, and D. A. Lightfoot (Cham: Springer International Publishing), 207–232. doi: 10.1007/978-3-319-92958-3_12

Sylvester-Bradley, R., and Kindred, D. R. (2009). Analysing nitrogen responses of cereals to prioritize routes to the improvement of nitrogen use efficiency. *J. Exp. Bot.* 60, 1939–1951. doi: 10.1093/jxb/erp116

Tegeder, M., and Rentsch, D. (2010). Uptake and partitioning of amino acids and peptides. *Mol. Plant* 3, 997–1011. doi: 10.1093/mp/ssq047

Thomas, C. L., Alcock, T. D., Graham, N. S., Hayden, R., Matterson, S., Wilson, L., et al. (2016a). Root morphology and seed leaf ionomic traits in *Brassica napus* L. diversity panel show wide phenotypic variation and are characteristic of crop habits. *BMC Plant Biol.* 16:214. doi: 10.1186/s12870-016-0902-5

Thomas, C. L., Graham, N. S., Hayden, R., Meacham, M. C., Neugebauer, K., Nightingale, M., et al. (2016b). High-throughput phenotyping (HTP) identifies seedling root traits linked to variation in seed yield and nutrient capture in field-grown oilseed rape (*Brassica napus* L.). *Ann. Bot.* 118, 655–665. doi: 10.1093/aob/mcw046

Thorup-Kristensen, K., and Kirkegaard, J. (2016). Root system-based limits to agricultural productivity and efficiency: the farming systems context. *Ann. Bot.* 118, 573–592. doi: 10.1093/aob/mcw122

Tilman, D., Balzer, C., Hill, J., and Befort, B. L. (2011). Global food demand and the sustainable intensification of agriculture. *Proc. Natl. Acad. Sci. U.S.A.* 108, 20260–20264. doi: 10.1073/pnas.1116437108

Ulas, A., Behrens, T., Wiesler, F., Horst, W. J., and Schulte auf'm Erley, G. (2013). Does genotypic variation in nitrogen remobilisation efficiency contribute to nitrogen efficiency of winter oilseed-rape cultivars (*Brassica napus* L.)? *Plant Soil* 371, 463–471. doi: 10.1007/s11104-013-1688-y

Ulas, A., Schulte auf'm Erley, G., Kamh, M., Wiesler, F., and Horst, W. J. (2012). Root-growth characteristics contributing to genotypic variation in nitrogen efficiency of oilseed rape. *J. Plant Nutr. Soil Sci.* 175, 489–498. doi: 10.1002/jpln.201100301

Voss-Fels, K. P., Qian, L., Parra-Londono, S., Uptmoor, R., Frisch, M., Keeble-Gagnère, G., et al. (2017). Linkage drag constrains the roots of modern wheat. *Plant Cell Environ.* 40, 717–725. doi: 10.1111/pce.12888

Wei, T., and Simko, V. (2017). *R Package "corrplot": Visualization of a Correlation Matrix (version 0.84)*. Available online at: https://github.com/taiyun/corrplot (accessed May 20, 2020).

White, P. J., George, T. S., Gregory, P. J., Bengough, G., Hallett, P. D., and McKenzie, B. M. (2013). Matching roots to their environment. *Ann. Bot.* 112, 207–222. doi: 10.1093/aob/mct123

Xu, J., Qian, X., Wang, X., Li, R., Cheng, X., Yang, Y., et al. (2010). Construction of an integrated genetic linkage map for the A genome of *Brassica napus* using SSR markers derived from sequenced BACs in *B. rapa*. *BMC Genomics* 11:594. doi: 10.1186/1471-2164-11-594

Yang, J. T., Schneider, H. M., Brown, K. M., and Lynch, J. P. (2019). Genotypic variation and nitrogen stress effects on root anatomy in maize are node specific. *J. Exp. Bot.* 70, 5311–5325. doi: 10.1093/jxb/erz293

Zhang, H., and Forde, B. G. (1998). An Arabidopsis MADS box gene that controls nutrient-induced changes in root architecture. *Science* 279, 407–409. doi: 10.1126/science.279.5349.407

Zhang, H., Jennings, A., Barlow, P. W., and Forde, B. G. (1999). Dual pathways for regulation of root branching by nitrate. *Proc. Natl. Acad. Sci. U.S.A.* 96, 6529–6534. doi: 10.1073/pnas.96.11.6529

Conflict of Interest: The authors declare that the research was conducted in the absence of any commercial or financial relationships that could be construed as a potential conflict of interest.

frontiers in Plant Science

ORIGINAL RESEARCH
published: 24 November 2020
doi: 10.3389/fpls.2020.589692

Biodiversity in Tomatoes: Is It Reflected in Nutrient Density and Nutritional Yields Under Organic Outdoor Production?

*Cut Erika[1†], Stefanie Griebel[2], Marcel Naumann[1] and Elke Pawelzik[1]**

[1] Division Quality of Plant Products, Department of Crop Sciences, Faculty of Agricultural Sciences, University of Göttingen, Göttingen, Germany, [2] Division Plant Breeding Methodology, Department of Crop Sciences, Faculty of Agricultural Sciences, University of Göttingen, Göttingen, Germany

OPEN ACCESS

Edited by:
Christoph Martin Geilfus, Humboldt University of Berlin, Germany

Reviewed by:
Xiaokun Li, Huazhong Agricultural University, China
Paloma Koprovski Menguer, Federal University of Rio Grande do Sul, Brazil

***Correspondence:**
Elke Pawelzik
epawelz@gwdg.de

†Present address:
Cut Erika, Department of Agricultural Product Technology, Faculty of Agriculture, University of Syiah Kuala, Banda Aceh, Indonesia

Specialty section:
This article was submitted to Plant Nutrition, a section of the journal Frontiers in Plant Science

Received: 31 July 2020
Accepted: 21 October 2020
Published: 24 November 2020

Citation:
Erika C, Griebel S, Naumann M and Pawelzik E (2020) Biodiversity in Tomatoes: Is It Reflected in Nutrient Density and Nutritional Yields Under Organic Outdoor Production? Front. Plant Sci. 11:589692. doi: 10.3389/fpls.2020.589692

In many regions of the world, human nutrition is still characterized by an insufficient intake of essential nutrients like minerals such as iron (Fe) and zinc (Zn). In view of decreasing resources and a growing world population, the efficiency and the sustainability of cultivation systems should be considered not only in terms of crop yield and profit margin but also in terms of the yield of essential nutrients. Tomatoes are the most consumed vegetable in the world. Organic outdoor tomato cultivation is generally characterized by a higher diversity of varieties and lower fertilization input compared to conventional production. A 2-year field experiment with a set of 20 cultivars was performed to evaluate their variation regarding fruit mineral concentrations [potassium (K), calcium (Ca), magnesium (Mg), phosphorous (P), Fe, and Zn], their contribution to the dietary reference intake (DRI), and the nutritional yields (adults ha^{-1} $year^{-1}$). Results show that mineral concentrations differed significantly by cultivar and by year. However, even though significant genotype-by-year effects appear, several cultivars exhibit high genotype stability across years for the single traits studied. Taking this together with medium-to-high heritability, genetics strongly controls most studied traits. Among the cultivars, the contribution of 100 g fresh fruits varied from 4.5 to 7.7% for K, 0.8 to 1.8% for Ca, 2.3 to 4.4% for Mg, 3 to 6.6% for P, 3.1 to 6.9% for Fe, and 1.9 to 4.2% for Zn to meet daily requirements. Based on average fruit yields per hectare, the cultivars varied with regard to the nutritional yields for all the studied minerals, but most strongly for Fe (44–120 adults ha^{-1} $year^{-1}$) and Zn (22–84 adults ha^{-1} $year^{-1}$). In terms of contribution to the DRI and nutritional yield for Fe, the cocktail cultivar "Bartelly F1" produced the highest results, while for Zn the salad cultivar "Bocati F1" showed the highest values. Our results show that the targeted use of tomato biodiversity in organic outdoor production can be suitable to achieve high fruit yields as well as to produce high nutritional yields per unit area, thus contributing to more effective land use and improved food security. These findings also provide valuable insights for tomato breeders to improve the tomato fruit quality while maintaining yield.

Keywords: tomato, biodiversity, nutrients, nutritional yield, dietary reference intake, genotypic stability

INTRODUCTION

The demand-oriented nutrition of a growing world population with a simultaneous reduction in the area of arable land per inhabitant and the shortage of other resources is one of the greatest challenges in the coming years (Springmann et al., 2018). In the past, increasing yields through improved nutrient utilization (e.g., Branca et al., 2013), crop protection, and cultivation techniques (Pretty and Bharucha, 2014) as well as breeding (Tieman et al., 2017) have been the main focus. Intensive land use has contributed to the increase in many environmental problems, such as rising emissions ((Foley et al., 2011) as well as the contamination of soil and water with residues (Ridoutt et al., 2017). In global terms, there is still no substantial improvement in the nutritional situation, but rather many forms of malnutrition: on the one hand malnutrition due to a deficiency in micronutrients and obesity and diet-related diseases on the other hand (Fears et al., 2019). A major cause of this is the one-sided focus on the production of nutritional energy and protein, which has led to a steady decrease in the number of cultivated crops (FAOSTAT, 2019) and varieties within crops (Martin et al., 2019). Using FAO data, Martin et al. (2019) have compiled the changes in the number of cultivars for human nutrition over the period 1961–2014. In Western Europe, the number of tomato cultivars decreased by 78% and of potato cultivars by 77%, while for wheat they increased by 43%. Continuing concerns about global food security and food quality, particularly for increased nutrient content, need to be improved with reduced inputs (Tester and Langridge, 2010). While the biodiversity on and around agricultural land may be higher, organic agriculture may require more land than conventional to produce the same yield (Schrama et al., 2018).

Based on the increasing recognition of the link between sustainable land use and food security, more comprehensive evaluation parameters are necessary. The aim is not to consider the crop yield per hectare or calorie uptake as assessment criteria but the nutrients produced per hectare and the number of people who can be fed for a full year from the nutrients produced per hectare (De Fries et al., 2015). Nutritional yield (NY) was introduced, in the form described here, by De Fries et al. (2015) and is calculated on the basis of nutrient yield per hectare and the recommended food intake. This also allows the nutritional quality of the cultivated species to be considered. There are some studies on the NY of minerals in cereals (De Fries et al., 2015, 2016; Moreira-Ascarrunz et al., 2016), legumes (Graham et al., 2018), or of the constituents in several types of plant and animal foods (De Ruiter et al., 2018). Individual vegetable species, which are frequently consumed due to their easy availability and popularity, have not yet been examined in detail under the aspect of NY.

Globally, tomato (*Solanum lycopersicum* L.) is a major cultivated and consumed fruit vegetable with per capita consumption of either fresh or processed type of about 21 kg in 2017 or around 19% of the total vegetable consumption per year (FAOSTAT, 2020). It is a rich source of macro- and micronutrients (Bauchet and Causse, 2012), vitamins, and phytochemicals for human diet (Viskelis et al., 2015; Uluisik et al., 2016; Tieman et al., 2017). In Germany, tomato production covered, in 2019, an area of 385.63 hectares, and organic production accounted for 21% of those cultivated (Statistisches Bundesamt, 2020). However, the quantities are expected to increase (Zörb et al., 2020) due to consumers' growing attention to organic systems for reasons of health, safety, and environmental benefits (Ordóñez-Santos et al., 2011; Johansson et al., 2014).

Tomatoes have been cultivated for about 400 years, and substantial breeding activities have been implemented for only eight decades. So far, more than 10,000 tomato cultivars have been developed (Bhattarai et al., 2018). Beginning in the 20th century, through intensive breeding activities, scientists and breeders worldwide created a wide array of morphologically different cultivars from the single species *S. lycopersicum* to modern tomato varieties with high variation in fruit weight, fruit size and shapes, and colors (Bai and Lindhout, 2007).

The focus of modern breeding programs for fresh market use of tomato have usually laid emphasis on resistance, yield, and quality attributes such as firmness, color, texture, and traits related to fruit appearance (Foolad, 2007) rather than on sustainable production and nutritional quality (Mata-Nicolás et al., 2020).

In the present study, the approach of NY was applied to assess the trade-off between yields and nutrients, and the potential of tomato cultivars differing in fruit size and color to meet the human nutritional requirements of mineral nutrients. The objectives of the present work were (i) to estimate the production potential and contribution of the cultivars differing in their fruit type to meet human dietary needs for several nutrients, (ii) to assess the NY of the cultivars grown in a 2-year field experiment for selected macro- and micronutrients, and (iii) to evaluate the heritability of traits and the genotypic value and stability of the cultivars. The macronutrients K, Ca, Mg, and P are the major elements in the tomato fruit (Hernández Suárez et al., 2007), and Fe and Zn, as indispensable micronutrients, are involved in various metabolic processes (Costa et al., 2011; Jha and Warkentin, 2020).

The example of tomato will be used to investigate how a diversity of varieties is reflected in mineral composition and how this is expressed in NY. Selecting a cultivar with a greater NY will increase the contribution of tomato for human diet, with efficient use of land while still providing adequate amounts of nutrients and achieving agricultural sustainability.

MATERIALS AND METHODS

Plant Material and Cultural Practice

Twenty indeterminate tomato cultivars (**Table 1**) were grown in organic low-input conditions in the field under a well-ventilated rainout shelter. The study was carried out during summer 2015 and 2016 at the experimental research station of the University of Göttingen, Germany. The 20 cultivars included 12 cocktail and 8 salad cultivars and were grouped within their fruit type on the basis of the average fruit weight. The main determinant of the tomato type definition is not well specified in the scientific

literature, although the traits related to fruit size and shape seem to be the most important factors for the fruit type classification (Lázaro, 2018). Cocktail tomatoes were described as small-sized type of tomatoes—they are hybrids of cherry tomatoes with normal-sized cultivars, e.g., salad tomatoes (Kagan-Zur and Mizrahi, 1993). In this study, cultivars with fruit weight less than 52 g were classified as cocktail tomatoes, while cultivars with higher fruit weight were categorized as salad tomatoes. The main selection criteria for these cultivars were the yield and the parameters that determine the taste and the aroma formation.

The seeds were germinated in the substrate "Anzuchtsubstrat Organisch" (Kleeschulte GmbH & Co. KG, Germany) on March 30, and the seedlings were potted after 20 days in the substrate "Hawita Fruhstorfer Bio-Aussaat-und Kräutererde" (HAWITA-Gruppe GmbH, Germany). The seedlings were maintained under greenhouse conditions (20°C day, 18°C night, 16/8 h) before being transplanted to the field. The field trials were established in a randomized complete block design with eight replications. The cultivars were assessed with one plant per plot in 2015 and two plants per plot in 2016. All the plants were cultivated and spaced at 50 cm within the row and spaced at 100 cm at a population of two plants per square meter. In both years, the plants were grown under organic low-input conditions without fertilization and moderate irrigation. Further information on the growth conditions in the field is described in **Table 2**.

TABLE 1 | Overview of the tested cultivars.

Cultivar	Fruit type[a]	Fruit color	Fruit weight[b] (g)	
			2015	2016
Goldita	Cocktail	Orange	15.6	17.2
Supersweet 100 F1	Cocktail	Red	15.7	13.7
Resi	Cocktail	Red	17.3	20.4
Bartelly F1	Cocktail	Red	18.4	14.9
Benarys Gartenfreude	Cocktail	Red	18.5	19.1
Primavera	Cocktail	Red	21.3	21.6
Black Cherry	Cocktail	Red-brown	23.0	25.2
Sakura F1	Cocktail	Red	23.7	24.1
Primabella	Cocktail	Red	28.1	27.8
Tastery F1	Cocktail	Red	33.5	32.1
Annamay F1	Cocktail	Red	46.0	48.2
Amoroso F1	Cocktail	Red	50.8	47.4
Campari F1	Salad	Red	63.3	62.5
Auriga	Salad	Orange	71.5	75.1
Harzfeuer F1	Salad	Red	76.4	72.1
Roterno F1	Salad	Red	106.7	104.6
Lyterno F1	Salad	Red	115.9	115
Bocati F1	Salad	Red	124.4	114.4
Cappricia F1	Salad	Red	131.5	124.1
Green Zebra	Salad	Green-yellow	153.0	136.4

[a]*Fruit type is defined by an average fruit weight of <52 g for cocktail cultivars and >52 g for salad cultivars.*
[b]*Fruit weight was calculated as the average single fruit weight of each cultivar for each year derived from eight biological replicates.*

Determination of Fruit Yield

At full maturity, the fruits were harvested at 2-week intervals, starting from 9 weeks after planting (WAP) in 2015 and 8 WAP in 2016. All the plants of each block from eight biological replications were harvested and weighed by pooled replications to obtain the total yield (kg plant^{-1}) of fully ripe healthy fruits. Next, the mean fruit weight for each of the 20 evaluated plants was used to calculate the fruit yield per hectare and converted to fruit yield in tons per hectare (tons ha^{-1}).

Determination of Minerals in Fruits

Samples from two harvest dates for both years (2015: 13 WAP and 18 WAP; 2016: 14 WAP and 19 WAP) were used for the determination of mineral concentration. At harvest, the fully ripe fruits of eight biological replicates were combined into four pooled replicates for further analysis. Each 10 fruits of cocktail cultivars and 3 fruits of salad cultivars were cut into wedges. The fruits were freeze-dried (EPSILON 2-40, Christ, Osterode am Harz, Germany) for 4 days and were later ground by using a ball mill (45 s at 30 Hz; Retsch, model: MM 400, Germany) to get fine powder of up to 0.5 mm in particle size. The mineral concentration was determined according to Koch et al. (2019), with minor changes. In total, 100 mg of the ground fruit material was weighed in a Teflon vessel and digested in 4 ml of 65% (v/v) concentrated HNO_3 and 2 ml of 30% concentrated H_2O_2 (Carl Roth GmbH & Co. KG, Germany) for 75 min at 200°C and 40 bar in a microwave oven (ETHOS Professional Microwave System, MLS GmbH, Germany). After microwave digestion, the

TABLE 2 | Information about field location and cultural practices in 2015 and 2016.

	2015	2016
Location	51°30′17.6″ N, 9°55′16.2″ E	
District/region	Göttingen, Lower Saxony	
Experimental design	RCBD, eight replicates	
Soil type/properties	Fluventic Eutrochrept soil	
Average temperature (°C)[a]	19 ± 4.6	19 ± 7.0
Average relative humidity (%)[a]	75 ± 10.7	75 ± 18.9
Pre-crop	Faba bean (*Vicia faba*)	Winter wheat (*Triticum aestivum*)
Soil pH	7	6.9
Humus content (%)	1.89	1.87
Phosphorus (mg 100 g^{-1} soil)	7	6
Magnesium (mg 100 g^{-1} soil)	4	7
Potassium (mg 100 g^{-1} soil)	9	9
Planting date	May 20	May 20
Planting arrangement	One plant per plot	Two plants per plot
Plant density (plants ha^{-1})	20.000	
Weed control	Space between rows were covered with plastic layers	
Main shoot pruning	Weekly, hand pruning	
Frequency/total amount of irrigation	Weekly/150 l m^{-2}	

[a]*Data were recorded every 30 min from planting to final harvest using an EBI 20-TH Data Logger (ebro Electronic GmbH & Co. KG).*
RCBD, randomized complete block design.

samples were transferred to volumetric flasks and filled up with distilled water to a total volume of 25 ml. The concentrations of macronutrients (Ca, K, Mg, and P) and micronutrients (Fe and Zn) were analyzed using inductively coupled plasma-optical emission spectrometry (Vista-RL, Variance Inc., Palo Alto, CA, United States). The concentrations of minerals were expressed in mg/100 g fresh weight (FW).

Calculations and Statistical Analysis

In this study, the fraction of the dietary reference intake (DRI) was defined as the percentage of the nutrient requirement provided by 100 g of tomatoes based on the assessed mineral concentration for each cultivar. The DRIs are derived from the values released by the Food and Nutrition Board of the Institute of Medicine (IOM) and have been widely used in recommending quantitative estimates of nutrient intakes for the United States and Canadian populations (Institute of Medicine, 2006). The fraction of DRI is calculated as grams of a mineral divided by the DRI values. The values for DRI*i* are taken either from the recommended daily allowance or the adequate intake for average adult males and females (not pregnant or lactating) aged between 19 and 50 years (**Supplementary Table 1**). The fraction of DRI of each mineral *i* from a tomato cultivar *j* was calculated as:

$$\text{fraction DRI} = \frac{g_i/100\,g_j}{\text{DRI}_i} \quad (1)$$

where $g_i/100\,g_j$ is the value for grams of a mineral *i* in 100 g of a tomato cultivar *j*.

The NY weighs the conventional yield measure (ton ha^{-1}) by its nutritional content, and this value is divided by the dietary requirement necessary for 1 year (De Fries et al., 2016). This metric estimates the number of adults (average for male and female between 19 and 50 years old) who can fulfill 100% of their DRI for selected nutrients from 1 ha for 1 year (De Fries et al., 2016).

Therefore, the NY of a mineral *i* from a tomato cultivar *j* was calculated as:

$$NY_{ij} = \text{fraction of DRI}_i/100g_j \times \text{tons}_j/\text{ha/year} \times 10^4/365 \quad (2)$$

where the fraction of $\text{DRI}_i/100g_j = g_i/100g_j/\text{DRI}_i$

The fraction of DRI of nutrient *i*, provided by 100 g of cultivar *j*, was calculated as grams of each mineral *i* in 100 g of each tomato cultivar *j* divided by the daily dietary requirement for the respective mineral *i* (g_i/100 g_j)/DRI_i. For example, a tomato's NY for K is derived from the fraction of DRI for K supplied by 100 g of tomato (which is grams of K in 100 g of tomatoes divided by the daily dietary requirement for K) multiplied by the yield for the respective cultivar.

Four replications of each cultivar were maintained in each year of cultivation. The data were presented as means of each cultivar over two cultivation years. The effect of cultivar and year on the mineral concentration was evaluated by means of analysis of variance. The variances between the cultivar and the treatment means for all the traits were separated by pairwise means comparisons with Tukey's test at $p < 0.05$ by using the STATISTIX statistical software (Version 8.0).

The heritability and the genotypic values were calculated for single years based on a linear, fully randomized model using the R package lme4 (Bates et al., 2015). Heritability (H^2) was calculated as broad sense heritability for single years:

$$H^2 = \frac{\delta^2 g}{\delta^2 g + \delta^2 e} \quad (3)$$

Where $\delta^2 g$ was the estimated genetic variance and $\delta^2 e$ was the residual variance. Best linear unbiased predictors (BLUPs) extracted from the model were reported as genotypic values. The genotypic values and the grand mean were summed up to obtain the predicted means of a trait for a single cultivar. Pearson and Spearman's rank correlations were calculated between each year's BLUPs of a single trait.

RESULTS

Fruit Mineral Concentrations and Their Contribution to the Dietary Reference

The concentrations of macronutrients in the fruits of the cocktail cultivars ranged on the basis of FW for K between 211 mg 100 g^{-1} ("Roterno F1") and 361 mg 100 g^{-1} ("Supersweet 100 F1"), for Ca between 7.9 mg 100 g^{-1} ("Auriga") and 17.7 mg 100 g^{-1} ("Resi"), for Mg between 8.4 mg 100 g^{-1} ("Cappricia F1") and 16 mg 100 g^{-1} ("Supersweet 100 F1"), and for P between 20.9 mg 100 g^{-1} ("Roterno F1") and 46.1 mg 100 g^{-1} ("Resi"). The contents for Zn ranged between 0.18 mg 100 g^{-1} ("Cappricia F1") and 0.40 mg 100 g^{-1} ("Resi"), while the Fe content varied from 0.41 mg 100 g^{-1} ("Cappricia F1") to 0.90 mg 100 g^{-1} ("Resi"). The traits with a higher coefficient of variation (CV) were the concentrations of Zn (43.9%), Fe (37.4%), and Ca (23.2%), while the lowest CV was found in the concentrations of K, Mg, and P. Considering the fruit type, i.e., cocktail versus salad, it was found that the cocktail cultivars tended to have higher concentrations of all the nutrients studied. Based on the averaged sums of all nutrients, the cocktail cultivars contained about 20% higher contents than the salad cultivars (**Table 3**).

Overall, the nutrient densities of the determined minerals were lower in 2015 than in 2016, except for Zn. The cultivar had a very strong effect on the variance of all nutrient concentrations, followed by the effect of year—except for Ca. In general, the cultivar was dependent on the year of cultivation at different significance levels.

Over all cultivars and years, the study showed that tomatoes can contribute for K with 6.1% at most to the DRI of this nutrient, and it varied from 4.5% ("Roterno F1") to 7.7% ("Supersweet 100 F1"). The cultivars can meet the need of the DRI of Ca on average with 1.2% within a range from 0.8% ("Auriga") to 1.8% ("Resi"). Fresh consumption of 100 g of the studied cultivars will provide Mg from 2.3% ("Cappricia F1") to 4.4% ("Resi" and "Supersweet 100 F1") and P from 3.0% ("Roterno F1") to 6.6% ("Resi") of the DRI (**Table 4**). Based on the presented data, the consumption of 100 g tomato fruits will provide on average 3.4 and 4.3% of the DRI of Mg and P, respectively. When the fruit type was considered, it was shown that cocktail cultivars

TABLE 3 | Fruit concentrations of K, Ca, Mg, P, Fe, and Zn (mg 100 g^{-1} FW) by cultivar.

Cultivar	Concentration (mg 100 g^{-1} FW)					
	K	Ca	Mg	P	Fe	Zn
Goldita	312 ± 32	16.1 ± 4.2	14.0 ± 2.0	32.3 ± 6.4	0.76 ± 0.37	0.38 ± 0.25
Supersweet 100 F1	361 ± 45	10.2 ± 2.1	16.0 ± 1.2	40.8 ± 4.6	0.79 ± 0.27	0.39 ± 0.15
Resi	340 ± 63	17.7 ± 4.0	15.8 ± 3.7	46.1 ± 8.5	0.90 ± 0.15	0.40 ± 0.16
Bartelly F1	323 ± 37	14.6 ± 3.3	14.2 ± 1.5	35.8 ± 4.8	0.69 ± 0.21	0.34 ± 0.08
Benarys Gartenfreude	336 ± 64	8.8 ± 2.5	13.2 ± 3.5	36.1 ± 7.7	0.82 ± 0.54	0.37 ± 0.20
Primavera	278 ± 27	12.2 ± 2.2	11.2 ± 1.3	29.9 ± 3.2	0.73 ± 0.30	0.39 ± 0.37
Black Cherry	263 ± 59	11.1 ± 2.9	12.4 ± 2.7	27.7 ± 6.3	0.68 ± 0.22	0.31 ± 0.08
Sakura F1	305 ± 41	12.1 ± 3.0	13.6 ± 2.1	31.8 ± 3.5	0.63 ± 0.25	0.32 ± 0.08
Primabella	324 ± 39	11.5 ± 3.6	14.2 ± 1.7	35.8 ± 5.1	0.78 ± 0.19	0.33 ± 0.14
Tastery F1	271 ± 28	11.9 ± 2.8	12.2 ± 1.4	29.4 ± 4.0	0.62 ± 0.13	0.30 ± 0.13
Annamay F1	299 ± 29	13.3 ± 2.4	13.5 ± 1.3	29.3 ± 3.1	0.62 ± 0.15	0.35 ± 0.20
Amoroso F1	244 ± 23	12.4 ± 2.0	10.6 ± 1.1	27.7 ± 2.3	0.61 ± 0.21	0.28 ± 0.10
Campari F1	278 ± 34	12.0 ± 2.3	12.0 ± 1.4	29.2 ± 4.1	0.60 ± 0.43	0.26 ± 0.12
Auriga	282 ± 34	7.9 ± 1.3	13.2 ± 1.3	27.3 ± 3.2	0.49 ± 0.16	0.22 ± 0.04
Harzfeuer F1	294 ± 34	11.1 ± 3.0	10.7 ± 1.1	26.1 ± 3.2	0.54 ± 0.23	0.24 ± 0.06
Roterno F1	211 ± 58	12.4 ± 4.0	8.6 ± 2.4	20.9 ± 6.3	0.42 ± 0.12	0.19 ± 0.04
Lyterno F1	232 ± 23	12.8 ± 3.6	9.3 ± 0.6	24.3 ± 3.4	0.44 ± 0.12	0.21 ± 0.06
Bocati F1	217 ± 35	11.9 ± 2.7	9.1 ± 1.4	21.6 ± 3.6	0.43 ± 0.15	0.19 ± 0.05
Cappricia F1	236 ± 41	13.9 ± 3.1	8.4 ± 1.0	23.3 ± 4.8	0.41 ± 0.17	0.18 ± 0.07
Green Zebra	290 ± 34	12.3 ± 2.1	14.1 ± 1.5	29.4 ± 3.4	0.55 ± 0.17	0.24 ± 0.08
Mean	285.2	12.3	12.3	30.3	0.6	0.3
CV (%)	12.9	23.2	13.0	14.8	37.4	43.9
HSD	46.20	3.57	2.00	5.61	0.29	0.16
Year						
2015	274 ± 43.4	12.0 ± 3.8	11.7 ± 2.2	29.6 ± 6.4	0.53 ± 0.26	0.34 ± 0.20
2016	296 ± 66.2	12.6 ± 3.4	13.0 ± 3.3	31.0 ± 8.8	0.69 ± 0.28	0.25 ± 0.08
Source of variation						
Cultivar	***	***	***	***	***	***
Year	***	ns	***	**	***	***
Cultivar × year	***	*	***	***	*	*

*The cultivars are arranged according to their average single fruit weight (see **Table 1**); cocktail cultivars are indicated in italics; the others are salad cultivars.*
Mean values are given for each of the 20 cultivars as mean from both years and from each year ± standard deviation.
CV, coefficient of variation; HSD, honestly significant difference at $p \leq 0.05$; ns, not significant.
$^{*}p \leq 0.05$, $^{**}p \leq 0.01$, $^{***}p \leq 0.001$.

contributed more to the DRI than salad cultivars; i.e., "Resi" contributed at most to the Ca, Mg, and P requirements in human nutrition, while "Supersweet 100 F1" was the highest contributor for providing K and Mg.

The studied cultivars can contribute with an average of 4.8% for Fe and 3.1% for Zn to the DRI. Among the cultivars, the fraction of DRI for Fe ranged between 3.1% in "Cappricia F1" and 6.9% in "Resi." For Zn, the lowest contribution to the DRI with 1.9% was found in "Cappricia F1" and the highest with 4.2% in "Resi" (**Table 4**).

Fruit Yield and Its Variation in Nutritional Yield Across Years

The cultivars showed a large variation in average fruit yield and NY (**Table 5**). The cultivar with the highest average fruit yield across the 2 years was the salad cultivar "Roterno F1" (116 tons ha^{-1}), followed by other salad cultivars "Lyterno F1" (110.3 tons ha^{-1}), "Bocati F1" (112.7 tons ha^{-1}), and "Cappricia F1" (112.1 tons ha^{-1}). The lowest average fruit yield showed the cocktail cultivar "Resi" (22.7 tons ha^{-1}), which significantly differed from all the other investigated cultivars. On average, the cultivars produced 70.4 tons ha^{-1} in 2015 and 77.4 tons ha^{-1} of ripe fruits in 2016. Although in both cultivation years the mean temperature (19°C) and relative humidity (75%) in the field were similar (**Table 2**), low temperatures (less than 10°C) occurred at early 18th WAP in 2015 and persisted for several days, while in 2016 temperatures below 10°C were only observed later than 18th WAP (**Supplementary Figures 1.1** and **1.2**).

The NYs of Ca, K, Mg, and P varied significantly among the cultivars. The variations of NY for the different minerals were as follows: K (46–155 adults $year^{-1}$ ha^{-1}), Ca (11–43 adults $year^{-1}$ ha^{-1}), Mg (28–88 adults $year^{-1}$ ha^{-1}), and P (42–114 adults $year^{-1}$ ha^{-1}). As shown in **Table 5**, "Bartelly F1" was the highest yielding cultivar among cocktail tomatoes and showed the

TABLE 4 | Contribution of cultivars to the dietary reference intake (DRI) for K, Ca, Mg, P, Fe, and Zn.

Cultivar	DRI (%)					
	K	Ca	Mg	P	Fe	Zn
Goldita	6.6 ± 0.7	1.6 ± 0.4	3.9 ± 0.5	4.6 ± 0.9	5.9 ± 2.8	4.0 ± 2.6
Supersweet 100 F1	7.7 ± 1.0	1.0 ± 0.2	4.4 ± 0.3	5.8 ± 0.7	6.1 ± 2.1	4.1 ± 1.5
Resi	7.2 ± 1.3	1.8 ± 0.4	4.4 ± 1.0	6.6 ± 1.2	6.9 ± 1.2	4.2 ± 1.6
Bartelly F1	6.9 ± 0.8	1.5 ± 0.3	3.9 ± 0.4	5.1 ± 0.7	5.3 ± 1.6	3.6 ± 0.8
Benarys Gartenfreude	7.2 ± 1.4	0.9 ± 0.2	3.6 ± 1.0	5.2 ± 1.1	6.3 ± 4.1	3.9 ± 2.2
Primavera	5.9 ± 0.6	1.2 ± 0.2	3.1 ± 0.4	4.3 ± 0.5	5.6 ± 2.3	3.1 ± 0.6
Black Cherry	5.6 ± 1.3	1.1 ± 0.3	3.4 ± 0.7	4.0 ± 0.9	5.2 ± 1.7	3.2 ± 0.9
Sakura F1	6.5 ± 0.9	1.2 ± 0.3	3.7 ± 0.6	4.5 ± 0.5	5.4 ± 2.8	3.3 ± 0.9
Primabella	6.9 ± 0.8	1.1 ± 0.4	3.9 ± 0.5	5.1 ± 0.7	6.0 ± 1.5	3.5 ± 1.4
Tastery F1	5.8 ± 0.6	1.2 ± 0.3	3.4 ± 0.4	4.2 ± 0.6	4.7 ± 1.0	3.2 ± 1.3
Annamay F1	6.4 ± 0.6	1.3 ± 0.2	3.7 ± 0.4	4.2 ± 0.5	4.8 ± 1.2	3.6 ± 2.1
Amoroso F1	5.2 ± 0.5	1.2 ± 0.2	2.9 ± 0.3	4.0 ± 0.3	4.7 ± 1.6	3.0 ± 1.0
Campari F1	5.9 ± 0.7	1.2 ± 0.2	3.3 ± 0.4	4.2 ± 0.6	4.6 ± 3.3	2.7 ± 1.3
Auriga	6.0 ± 0.7	0.8 ± 0.1	3.6 ± 0.4	3.9 ± 0.5	3.8 ± 1.2	2.3 ± 0.4
Harzfeuer F1	6.3 ± 0.7	1.1 ± 0.3	3.0 ± 0.3	3.7 ± 0.5	4.1 ± 1.8	2.5 ± 0.7
Roterno F1	4.5 ± 1.2	1.2 ± 0.4	2.4 ± 0.7	3.0 ± 0.9	3.2 ± 1.0	2.0 ± 0.5
Lyterno F1	4.9 ± 0.5	1.3 ± 0.4	2.6 ± 0.2	3.5 ± 0.5	3.4 ± 0.9	2.2 ± 0.6
Bocati F1	4.6 ± 0.7	1.2 ± 0.3	2.5 ± 0.4	3.1 ± 0.5	3.3 ± 1.2	1.9 ± 0.6
Cappricia F1	5.0 ± 0.9	1.4 ± 0.3	2.3 ± 0.3	3.3 ± 0.7	3.1 ± 1.3	1.9 ± 0.7
Green Zebra	6.2 ± 0.7	1.2 ± 0.2	3.9 ± 0.4	4.2 ± 0.5	4.2 ± 1.3	2.5 ± 0.8
Mean	6.1	1.2	3.4	4.3	4.8	3.1
CV	12.9	23.2	13.0	14.8	38.8	35.3
HSD	0.98	0.36	0.55	0.80	2.94	1.37
Year						
2015	5.8 ± 0.9	1.2 ± 0.4	3.2 ± 0.6	4.2 ± 0.9	4.18 ± 2.10	3.48 ± 1.77
2016	6.3 ± 1.4	1.3 ± 0.3	3.6 ± 0.9	4.4 ± 1.3	5.35 ± 2.17	2.61 ± 0.84

*The DRI is the fraction (%) of mineral requirement provided by 100 g fresh tomato fruit based on the mineral concentration for each cultivar (see **Table 3**). The cultivars are arranged according to average single fruit weight (see **Table 1**); cocktail cultivars are indicated in italics; the others are salad cultivars.*
Mean values are given for each of the 20 cultivars as mean from both years and from each year ± standard deviation.
CV, coefficient of variation; HSD, honestly significant difference at $p \leq 0.05$.

highest NY for all nutrients. "Resi," known as the lowest yielding cultivar in the present investigation, had also the lowest NY for all the studied minerals.

The salad varieties showed a slightly greater variation in relation to NY. While "Auriga" produced the lowest NY for all the other nutrients with the exception of K ("Green Zebra") and Mg ("Harzfeuer F1"), the highest NYs were achieved as follows: by "Cappricia F1" for K and Ca, by "Lyterno F1" for Mg, P, and Fe, by "Roterno F1" for Fe, and by "Bocati F1" for Zn. As compared to the NY of macronutrients, higher CV was found for Fe and Zn with values of 37.1 and 31.8%, respectively (**Table 5**).

Looking at the variation in fruit yield and NY as a function of fruit type, the spectrum of cultivars examined showed different variations in minimum and maximum values. Among the cocktail cultivars, "Resi" had the lowest yield with 22.7 tons ha^{-1}, clearly far away from the other cocktail cultivars, while "Bartelly F1" produced a yield 3.5 times higher. This was also reflected in the NYs, where "Resi" produced the lowest NY for all nutrients and "Bartelly F1" the highest; the NYs were 2.7 (P) to 3.3 (K) times higher than in "Resi." Also, for Fe and Zn, "Bartelly F1" produced 2.7- and 3.3-fold higher NY. For salad cultivars, it was found that, in terms of fruit yield, "Roterno F1" produced about twice as much as "Green Zebra," the cultivar with the lowest fruit yield. With regard to NY, the differences between the cultivars with the lowest values ("Green Zebra" for K; "Auriga" for Ca, P, Fe, and Zn; "Harzfeuer F1" for Mg) and the highest values ("Cappricia F1" for K and Ca, "Lyterno F1" for Mg and P, "Roterno F1" and "Lyterno F1" for Fe, and "Bocati F1" for Zn) were 0.2 (Mg) to 2.9 (Ca) times higher than those with the lowest values. For the micronutrients Fe and Zn, the maximum values in the above-mentioned cultivars were 0.5 and 2 times higher than in "Auriga."

Heritabilities of Traits and Genotypic Values of Cultivars and Their Stability Across Years

The heritabilities and genotypic values of cultivars were calculated for each trait on a single year basis (**Tables 6**, **7**). For the majority of traits such as fruit yield [H^2 = 0.86 (2015), 0.95 (2016)] and densities of K [H^2 = 0.51 (2015), 0.61 (2016)], P [H^2 = 0.54 (2015), 0.74 (2016)], Fe [H^2 = 0.24 (2015), 0.31 (2016)], and Zn [H^2 = 0.21 (2015), 0.43 (2016)], the heritabilities increased in 2016, as expected, since up to four

TABLE 5 | Variation of fruit yield and nutritional yield (adults year^{-1} ha^{-1}) for K, Ca, Mg, P, Fe, and Zn by cultivar.

Cultivar	Fruit yield (tons ha^{-1})	Nutritional yield (adults year^{-1} ha^{-1})					
		K	Ca	Mg	P	Fe	Zn
Goldita	42.5 ± 5.6	78 ± 16.6	19 ± 6.0	45 ± 9.0	54 ± 14.1	71 ± 37.4	44 ± 15.1
Supersweet 100 F1	58.0 ± 7.9	123 ± 27.3	16 ± 3.7	70 ± 13.4	93 ± 17.3	100 ± 38.9	55 ± 26.4
Resi	22.7 ± 5.1	46 ± 17.2	11 ± 4.5	28 ± 11.7	42 ± 15.6	44 ± 13.0	22 ± 11.0
Bartelly F1	81.5 ± 5.4	154 ± 23.1	32 ± 7.0	88 ± 13.2	114 ± 19	120 ± 38.8	72 ± 20.7
Benarys Gartenfreude	56.5 ± 5.3	112 ± 30.6	14 ± 4.2	57 ± 20.0	81 ± 23.8	102 ± 72.8	45 ± 15.9
Primavera	76.6 ± 6.2	125 ± 19.7	26 ± 6.3	65 ± 11.4	90 ± 13.9	118 ± 48.3	61 ± 16.6
Black Cherry	62.8 ± 4.1	96 ± 22.8	19 ± 5.3	59 ± 13.4	68 ± 15.8	91 ± 30.5	49 ± 19.6
Sakura F1	66.3 ± 7.2	118 ± 21.6	22 ± 6.3	68 ± 14.2	83 ± 14.5	89 ± 38.3	57 ± 12.6
Primabella	59.1 ± 12.5	113 ± 30.8	19 ± 8.8	64 ± 17.1	83 ± 21.6	95 ± 22.2	49 ± 20
Tastery F1	71.5 ± 4.2	113 ± 13.8	23 ± 5.5	66 ± 8.0	82 ± 10.9	93 ± 18.2	68 ± 21.2
Annamay F1	73.7 ± 12.9	129 ± 26.4	27 ± 6.6	75 ± 16.7	85 ± 18.1	99 ± 32.9	68 ± 8.1
Amoroso F1	68.6 ± 10.3	98 ± 18.3	23 ± 3.9	55 ± 11.0	74 ± 10.7	88 ± 32.1	60 ± 23.6
Campari F1	74.4 ± 10.2	121 ± 25.4	24 ± 5.7	68 ± 13.3	85 ± 18.2	93 ± 55.6	52 ± 15.2
Auriga	67.9 ± 8.9	111 ± 17.4	15 ± 3.1	67 ± 9.1	72 ± 10.4	71 ± 26.7	44 ± 20.3
Harzfeuer F1	80.3 ± 10.8	137 ± 21.7	24 ± 5.1	65 ± 9.5	82 ± 14.3	89 ± 35.9	62 ± 16.2
Roterno F1	116.0 ± 7.6	143 ± 40.5	39 ± 13.1	75 ± 21.1	95 ± 28.5	103 ± 31.3	75 ± 18.6
Lyterno F1	110.3 ± 18.5	150 ± 29.3	39 ± 13.6	78 ± 15.2	104 ± 18.4	103 ± 31.8	70 ± 23.1
Bocati F1	112.7 ± 6.7	143 ± 23.3	37 ± 9.1	77 ± 12.8	95 ± 16.8	102 ± 37.1	84 ± 17.7
Cappricia F1	112.1 ± 13.7	155 ± 31.3	43 ± 10.7	71 ± 11.8	103 ± 24.6	98 ± 46.0	76 ± 35.1
Green Zebra	63.9 ± 10.1	110 ± 19.6	22 ± 4.9	70 ± 12.6	75 ± 12.8	76 ± 27.1	47 ± 13.9
Mean	73.9	119	25	66	83	91	58
CV	10.7	17.7	28.6	16.9	18.6	37.1	31.8
HSD	9.9	26.3	8.9	13.9	19.3	42.3	23.2
Year							
2015	70.4 ± 26.1	109 ± 34.4	23 ± 12.0	59 ± 17.1	77 ± 23.5	75 ± 35.9	61 ± 22.5
2016	77.4 ± 23.6	128 ± 33.3	26 ± 10.2	72 ± 17.2	88 ± 22.4	107 ± 38.4	56 ± 24.6

*The nutritional yield is the number of adult males and females who can obtain 100% of the annual recommended dietary allowance from 1 ha of land per year. The cultivars are arranged according to average single fruit weight (see **Table 1**); cocktail cultivars are indicated in italics; the others are salad cultivars.*
Mean values are given for each of the 20 cultivars as mean from both years and from each year ± standard deviation.
CV, coefficient of variation; HSD, honestly significant difference at $p \leq 0.05$.

plants were included in the pooled replicates for the traits' analyses instead of only two plants in 2015. For the traits' Mg density [$H^2 = 0.76$ (2015), 0.66 (2016)] and Ca density [$H^2 = 0.40$ (2015), 0.37 (2016)], the heritabilities remained more or less the same. Traits with the lowest heritabilities were Ca, Fe, and Zn density, respectively.

To make conclusions about genotypic stability across years, the genotypic values were presented as BLUPs and ranked for single years, and correlations were calculated (**Tables 6**, **7**). High correlations between BLUPs of each year for single traits can be observed, and cultivar ranks do not change much across years. This was observed for fruit yield, K, Mg, and P densities, all having medium-high heritability combined with a strong correlation between genotypic values (fruit yield: 0.88 Spearman's, 0.95 Pearson; K density: 0.80 Spearman's, 0.83 Pearson; Mg density: 0.80 Spearman's, 0.82 Pearson; P density: 0.89 Spearman's, 0.89 Pearson). The traits Ca density (0.55 Spearman's, 0.66 Pearson), Fe density (0.52 Spearman's, 0.49 Pearson), and Zn density (0.64 Spearman's, 0.66 Pearson) have medium-high correlations, resulting in moderate genotype stabilities since the ranks change likely due to genotype-by-year effects but not completely across years. Ca, Fe, and Zn are also reported with larger CV values than those of the other traits under study (**Table 3**).

DISCUSSION

Nutrient Concentration

Vegetables are an important part of daily diet, and therefore the concentrations of mineral nutrients in them could contribute significantly to the mineral nutrient intake in human diet (Marles, 2017). The present study confirms that mineral concentrations in tomato fruits were strongly influenced by the cultivar (Kapoulas et al., 2013), and the influence of the cultivar on both macro- and micronutrients depends only to some extent on the cultivation year. A high correlation between genotypic values of each year for a single trait showed that, even though there were significant genotype-by-year effects, the cultivar ranks did not change much (**Tables 6**, **7**). A strong correlation of genotypic values across years together with a high heritability of the trait shows that genetics control the trait strongly and genotypes are stable across environments. Thus, the cultivars exhibit a good genotype stability across years for the traits K, Mg, and P density, respectively. The traits Ca density, Fe density, and Zn density exhibited medium-strong correlations and medium heritabilities and therefore resulted in moderate genotype stability. Overall, most cultivars have relatively high genotype stability for different traits across years. It may be that

TABLE 6 | Genetic parameters [heritability as broad sense heritability (H^2) and genotypic values (best linear unbiased predictors)] of macronutrient densities (Ca, K, Mg, and P) created from a linear fully randomized model on a yearly basis.

	Ca density (mg 100 g^{-1} FW)		K density* (mg 100 g^{-1} FW)		Mg density* (mg 100 g^{-1} FW)		P density (mg 100 g^{-1} FW)	
	2015	2016	2015	2016	2015	2016	2015	2016
H (broad sense)	0.40	0.37	0.51	0.61	0.76	0.66	0.54	0.74
Grand mean (±standard error)	12.07 (±0.66)	12.55 (±0.57)	273.64 (±7.46)	296.18 (±12.16)	11.64 (0.45)	12.97 (0.62)	29.51 (±1.14)	30.99 (±1.77)
Spearman's rank correlation rho	0.55 *p*-value = 0.01351		0.80 *p*-value = 2.833e-05		0.80 *p*-value = 2.603e-05		0.89 *p*-value < 2.2e-16	
Pearson's correlation	0.66 *p*-value = 0.001449		0.83 *p*-value = 5.666e-06		0.82 *p*-value = 1.024e-05		0.89 *p*-value = 1.649e-07	

Cultivar = genotype	Geno typic value	Mean (predi-cted)	Rank	Geno typic value	Mean (predi-cted)	Rank	Geno typic value	Mean (predi-cted)	Rank	Geno typic value	Mean (predi-cted)	Rank	Geno typic value	Mean (predi-cted)	Rank	Geno typic value	Mean (predi-cted)	Rank	Geno typic value	Mean (predi-cted)	Rank	Geno typic value	Mean (predi-cted)	Rank
Amoroso F1	0.753	12.820	7	−0.574	11.979	13	−28.457	245.183	16	−46.150	250.030	16	−1.287	10.348	15	−2.005	10.968	16	−1.228	28.280	13	−3.523	27.464	15
Annamay F1	1.247	13.313	6	0.377	12.931	7	16.265	289.905	7	9.872	306.052	8	1.453	13.088	7	0.791	13.764	9	−0.204	29.304	10	−1.553	29.434	9
Auriga	−4.035	8.031	20	−3.264	9.290	20	4.639	278.279	11	−11.042	285.138	11	1.002	12.638	8	0.649	13.622	10	−2.392	27.116	15	−3.163	27.824	13
Bartelly F1	2.468	14.534	4	1.346	13.899	3	36.079	309.719	2	33.506	329.686	6	1.812	13.447	3	1.756	14.729	6	4.526	34.034	4	5.777	36.764	4
Benarys Gartenfreude	−3.447	8.620	19	−2.401	10.153	19	8.060	281.700	9	86.933	383.113	1	−1.213	10.423	14	2.822	15.795	3	0.311	29.819	8	10.852	41.839	2
Black Cherry	−1.023	11.043	14	−0.914	11.640	17	−16.916	256.724	15	−23.949	272.231	14	0.136	11.771	11	0.051	13.023	11	−1.495	28.013	14	−3.229	27.758	14
Bocati F1	0.066	12.132	10	−0.749	11.805	16	−44.697	228.943	19	−78.557	217.623	19	−2.130	9.506	17	−4.006	8.967	18	−5.911	23.597	19	−10.233	20.754	19
Campari F1	0.120	12.186	9	−0.605	11.948	14	4.249	277.889	12	−16.367	279.813	13	0.059	11.695	12	−0.588	12.385	12	0.124	29.632	9	−2.083	28.904	10
Cappricia F1	2.496	14.563	3	0.344	12.897	8	−40.778	232.862	17	−49.669	246.511	17	−3.432	8.203	20	−4.108	8.865	19	−5.225	24.283	18	−7.485	23.502	18
Goldita	4.583	16.649	1	1.773	14.327	2	20.635	294.275	6	29.590	325.770	7	1.562	13.198	5	1.623	14.596	7	2.090	31.598	5	1.658	32.645	7
Green Zebra	−0.323	11.743	12	0.165	12.718	9	21.710	295.350	5	−13.052	283.128	12	2.370	14.006	2	1.096	14.068	8	0.986	30.494	6	−2.563	28.424	12
Harzfeuer F1	−2.685	9.382	18	0.642	13.195	6	7.915	281.555	10	9.359	305.539	9	−1.412	10.224	16	−1.609	11.364	15	−3.648	25.860	16	−4.049	26.938	16
Lyterno F1	1.423	13.489	5	−0.530	12.023	12	−42.979	230.661	18	−52.890	243.290	18	−2.605	9.031	18	−3.130	9.843	17	−4.364	25.144	17	−6.814	24.173	17
Primabella	−1.567	10.499	17	0.123	12.676	10	27.919	301.559	3	43.660	339.840	4	1.673	13.308	4	1.979	14.952	5	4.873	34.381	3	5.422	36.409	5
Primavera	−0.950	11.117	13	0.730	13.284	5	−10.619	263.021	14	−0.904	295.276	10	−1.165	10.471	13	−0.936	12.037	14	−1.035	28.473	12	0.486	31.473	8
Resi	3.059	15.126	2	5.828	18.382	1	22.657	296.297	4	78.903	375.083	3	1.557	13.193	6	5.087	18.060	1	9.715	39.223	1	19.999	50.986	1
Roterno F1	0.217	12.284	8	−0.146	12.407	11	−53.413	220.227	20	−80.999	215.181	20	−2.948	8.687	19	−4.157	8.816	20	−6.781	22.727	20	−10.681	20.306	20
Sakura F1	−1.172	10.894	15	0.883	13.436	4	2.471	276.111	13	35.221	331.401	5	0.261	11.896	10	2.146	15.119	4	−0.597	28.911	11	3.530	34.517	6
Supersweet 100 F1	−1.285	10.781	16	−2.297	10.257	18	57.020	330.660	1	81.075	377.255	2	3.600	15.235	1	3.372	16.345	2	9.425	38.933	2	10.182	41.169	3
Tastery F1	0.055	12.122	11	−0.732	11.822	15	8.240	281.880	8	−34.539	261.641	15	0.705	12.341	9	−0.833	12.140	13	0.829	30.337	7	−2.529	28.458	11

The genotypic values were ranked for single years, and correlations between both years were calculated.

**Could not estimate Pooled Rep cause of singularity but we kept it in the model. After checking, it did not change the model results.*

there is a stronger environmental influence on the density of micronutrients (Fe and Zn) than for most of the macronutrients.

Micronutrient density, defined as the amount of a nutrient per unit weight in a food, is important to achieve an optimal micronutrient status in human diet (Miller and Welch, 2013). Basically, the analysis of the mineral concentration of tomatoes in the present study shows that these cultivars can potentially provide essential nutrients to a large population (**Table 3**). From the present study, data for K, Mg, P, Fe, and Zn concentrations were comparable to those from other studies for organically grown tomatoes (Hernández Suárez et al., 2007; Ordóñez-Santos et al., 2011; Kapoulas et al., 2013; Mohammed et al., 2019). However, the range of the Ca concentration in our tomato cultivars (7.9–17.7 mg 100 g^{-1} FW) was lower than the range of earlier experiments with 28 cultivars (11.2–24.5 mg 100 g^{-1} FW) (Mohammed et al., 2019), but, with the exception of the concentration in one cultivar, it was higher than the range presented by Kapoulas et al. (2013) (8.1–9.0 mg 100 g^{-1} FW) as well as for three tomato cultivars grown in a greenhouse and for five cultivars in open-field cultivation (5.9–7.0 mg 100 g^{-1} FW) (Hernández Suárez et al., 2007). Ca is a mineral with the lowest levels of adequately estimated intake worldwide (Beal et al., 2017).

Potassium is the most abundant mineral nutrient in fresh tomato fruits (Sager, 2017; Labate et al., 2018), while Mg is the mineral nutrient most frequently lacking in the human diet (White and Broadley, 2005). Phosphorus is one of the 17 key elements required in plant metabolism (Dixon et al., 2020) and is essential for human nutrition, but dietary P deficiency occurs very rarely, as it is contained in many foods and is well absorbed (Vorland et al., 2017). High fruit K concentrations (211–361 mg 100 g^{-1} FW), which exceed the range presented by others (Hernández Suárez et al., 2007; Kapoulas et al., 2013; Mohammed et al., 2019; Ordóñez-Santos et al., 2011), were determined in the present study. The achieved result showed a higher maximum content of Mg (16 mg 100 g^{-1} FW) than in other studies (Ordóñez-Santos et al., 2011; Mohammed et al., 2019). The maximum value of P in our tomato cultivars (46.1 mg 100 g^{-1} FW) was slightly higher than those previously reported by Mohammed et al. (2019), who had found P contents up to 43.7 mg 100 g^{-1} FW and far higher than the one presented by Hernández Suárez et al. (2007) (27.1 mg 100 g^{-1} FW). The differences in the range of mineral concentrations reported in different studies may result from variations in the number of the cultivars studied, the type of genetic materials used, the location, and the growing environment evaluated. Regardless of their variation in nutrient concentration, the reductions in the levels of K, Ca, and Mg as well as the increasing concentrations of P and Fe in tomatoes grown in the 1930s and the 1980s [UK Government's Composition of Foods tables, cited in Mayer (1997)] were reported by Mayer (1997). The author noted that the average concentration of K, Ca, and Mg in tomato fruits decreased from 288 to 250 mg 100 g^{-1} FW, 13.3 to 7 mg 100 g^{-1} FW, and 11 to 7 mg 100 g^{-1} FW, respectively, whereas the concentration of P had witnessed a slight increase from 21 to 24 mg 100 g^{-1} FW over an approximate 50-year period.

Several agrobiodiversity-related studies have focused on improving diets or dietary quality, including intake of key nutrients, dietary diversity, and consumption of micronutrient-rich foods (e.g., Powell et al., 2015; Herrero et al., 2017). From the nutritional perspective, Fe and Zn are essential micronutrients for both humans and plants, but they remain deficient in the diets of the global population (Li et al., 2017). As reported in earlier studies (Ordóñez-Santos et al., 2011; Kapoulas et al., 2013; Mohammed et al., 2019), Fe is identified as a major micronutrient in the tomato fruit. Comparing the micronutrient contents in tomato fruits between the 1930s and 1980s, only Fe was found in higher concentrations in the fruits, with an increase of 16% in tomatoes cultivated 50 years later (Mayer, 1997). In the present study, the range of Fe concentrations was lower than the one measured by Mohammed et al. (2019) and Ordóñez-Santos et al. (2011). On the other hand, the range of the Zn concentration exceeds the range presented by Hernández Suárez et al. (2007); Kapoulas et al. (2013), and Mohammed et al. (2019).

Different values of CV between the traits for the nutrient concentration and also for the fraction of DRI and NY were observed in the present study (**Tables 3**, **4**, and **5**). The CV, a mean-standardized measure of variation, is often used to compare the variability of quantitative traits, and higher CVs are ascribed to a greater relative variability (Ogunniyan and Olakojo, 2014; Pélabon et al., 2020). For nutrient concentrations, the highest CV was obtained for Zn followed by Fe (**Table 3**). The genetic parameters support these findings as Zn and Fe densities exhibit the lowest heritabilities (**Table 7**). High CVs (**Table 3**) are related to low heritabilities (**Tables 6**, **7**). These results imply that the concentration of the micronutrients had higher variability than those for macronutrients among the studied parameters. These high CV values of the traits were adequate to distinguish the cultivars. With the CVs between 20 and 30%, Ca had high data dispersion around the mean, thereby reflecting a relatively higher genetic variation (Ene et al., 2016), while K, Mg, and P traits showed the lowest CVs within the range of 10 to 20% (**Table 3**) and highest heritabilities (**Table 6**). No CV was lower than 10%—this means that the observed traits in the study displayed moderate to high variability. The variations for CV and the genetic parameters calculated in the present study confirm that the traits were often more controlled by the cultivar (genotype) than by the environment (Kapoulas et al., 2013).

Contribution of Tomatoes to the DRI of Mineral Nutrients

The contribution of tomato, in terms of macro- and micronutrients, to daily requirements is not very high due to the low dry matter content of the fruit. It was not the primary purpose of this study to evaluate the contribution of the cultivars investigated, but the fraction of DRI was determined in order to calculate the NY. However, the variations in the variety spectrum are also reflected here, so the contribution to the intake of the minerals was rather low, except for K and Fe (**Table 4**). Our result indicated that 100 g of "Supersweet 100 F1" contributed up to 7.7% of the DRI of K, which agrees with the data reported by Mohammed et al. (2019) after recalculation of the data.

TABLE 7 | Genetic parameters [heritability as broad sense heritability (H^2) and genotypic values (best linear unbiased predictors)] of micronutrient densities (Fe and Zn) and fruit yield created from a linear fully randomized model on a yearly basis.

	Fe density (mg 100 g^{-1} FW)		Zn density (mg 100 g^{-1} FW)		Fruit yield (kg/pooled rep)	
	2015	2016	2015	2016	2015	2016
H (broad sense)	0.24	0.31	0.21	0.43	0.86	0.95
Grand mean (±standard error)	0.54 (±0.04)	0.70 (±0.05)	0.35 (±0.03)	0.25 (±0.01)	3.52 (±0.29)	3.87 (±0.28)
Spearman's rank correlation rho	0.52 *p*-value = 0.02098		0.64 *p*-value = 0.002778		0.88 *p*-value < 2.2e-16	
Pearson's correlation	0.49 *p*-value = 0.02709		0.66 *p*-value = 0.001582		0.95 *p*-value = 2.582e-10	

Cultivar = genotype	Genotypic value	Mean (predicted)	Rank	Genotypic value	Mean (predicted)	Rank	Genotypic value	Mean (predicted)	Rank	Genotypic value	Mean (predicted)	Rank	Genotypic value	Mean (predicted)	Rank	Genotypic value	Mean (predicted)	Rank
Amoroso F1	0.036	0.574	7	−0.050	0.646	13	0.004	0.351	10	−0.020	0.228	13	−0.454	3.065	14	−0.054	3.814	9
Annamay F1	0.000	0.539	10	−0.034	0.662	12	0.099	0.447	4	−0.002	0.246	11	−0.222	3.297	11	0.209	4.077	6
Auriga	−0.097	0.442	18	−0.092	0.604	15	−0.083	0.264	17	−0.025	0.223	15	−0.209	3.310	10	−0.373	3.495	14
Bartelly F1	−0.006	0.533	11	0.100	0.796	4	0.016	0.363	9	0.057	0.305	3	0.357	3.876	6	0.386	4.254	5
Benarys Gartenfreude	−0.014	0.525	12	0.302	0.998	1	0.027	0.374	8	0.086	0.333	1	−0.889	2.630	17	−0.803	3.065	18
Black Cherry	0.006	0.545	9	0.075	0.771	8	−0.008	0.340	11	0.035	0.283	6	−0.408	3.111	12	−0.678	3.190	17
Bocati F1	−0.086	0.452	15	−0.199	0.497	20	−0.088	0.260	18	−0.082	0.166	20	2.192	5.711	1	1.588	5.456	4
Campari F1	−0.083	0.456	14	0.068	0.764	9	−0.071	0.277	16	0.019	0.267	8	0.047	3.566	8	0.003	3.871	8
Cappricia F1	−0.149	0.389	20	−0.168	0.529	17	−0.101	0.247	20	−0.064	0.184	18	1.845	5.364	3	1.879	5.747	3
Goldita	0.094	0.633	3	0.099	0.795	5	0.115	0.463	1	0.017	0.265	9	−1.523	1.996	19	−1.537	2.331	19
Green Zebra	0.028	0.567	8	−0.140	0.556	16	−0.036	0.312	13	−0.052	0.196	16	−0.637	2.882	15	−0.330	3.538	13
Harzfeuer F1	−0.095	0.444	17	−0.021	0.675	11	−0.068	0.280	14	−0.019	0.228	12	0.850	4.369	5	−0.233	3.635	11
Lyterno F1	−0.081	0.458	13	−0.185	0.511	18	−0.069	0.279	15	−0.062	0.186	17	1.511	5.029	4	2.047	5.915	1
Primabella	0.210	0.749	2	0.024	0.720	10	0.039	0.387	6	0.015	0.263	10	−1.008	2.511	18	−0.426	3.442	15
Primavera	0.076	0.615	5	0.076	0.772	7	0.103	0.451	2	0.035	0.283	7	0.125	3.644	7	0.141	4.009	7
Resi	0.222	0.760	1	0.168	0.864	2	0.103	0.451	3	0.050	0.297	4	−2.421	1.098	20	−2.562	1.306	20
Roterno F1	−0.108	0.431	19	−0.193	0.504	19	−0.096	0.252	19	−0.067	0.181	19	2.175	5.694	2	1.929	5.797	2
Sakura F1	−0.095	0.444	16	0.081	0.777	6	−0.009	0.339	12	0.046	0.294	5	−0.409	3.110	13	−0.329	3.539	12
Supersweet 100 F1	0.093	0.632	4	0.156	0.852	3	0.084	0.432	5	0.057	0.305	2	−0.886	2.633	16	−0.660	3.208	16
Tastery F1	0.051	0.589	6	−0.066	0.630	14	0.039	0.387	7	−0.024	0.224	14	−0.035	3.484	9	−0.198	3.670	10

The genotypic values were ranked for single years, and correlations between both years were calculated.

**Could not estimate Pooled Rep cause of singularity but we kept it in the model. After checking, it did not change the model results.*

Consumption of one serving of tomato (∼200 g) provided 10% of the DRI of K (Labate et al., 2018). Compared to Ca, a greater contribution of Mg and P in the cultivars was observed, with maximal contribution of 100 g fresh fruits up to 4.4 and 6.6% of the DRI reference value for average adult male and female, respectively. These results are important because the intake of minerals, particularly K, Ca, and Mg, in human diets is below healthful levels and often insufficient (Labate et al., 2018).

Interestingly, the cocktail cultivar "Resi" contributed the most to the DRI among the investigated minerals—except for K, thereby showing a valuable performance of this cultivar in terms of nutritional value. In spite of its low fruit productivity, "Resi" has excellent fruit quality and moderate resistance against *Phytophthora infestans* (Zörb et al., 2020).

Fruit Yield and Its Variation in the Nutritional Yields of the Cultivars

The trait fruit yield exhibits a strong correlation between the genotypic values of both years, and even though significant genotype-by-year effects may appear, the cultivars' ranks across years do not change much (**Table 7**). A strong correlation together with a high heritability of fruit yield shows that genetics strongly control the trait. Thus, the cultivars exhibit a high genotype stability for fruit yield across years. The mean fruit yield of the 20 studied cultivars (73.9 ton ha^{-1}) exceeded the estimated average yield of global tomato released by FAO (2018), which was about 42 tons ha^{-1} (FAOSTAT, 2020), and higher than the mean of 14 tomato landraces (34.2 ton ha^{-1}) reported by Firas et al. (2012). Considering the average yields among all the tested cultivars, "Roterno F1," "Lyterno F1," "Bocati F1," and "Cappricia F1" exhibited the highest fruit yields in both cultivation years (**Table 5**). These four salad cultivars may represent good materials for tomato production under outdoor organic conditions for fruit yield. "Bartelly F1" showed the highest fruit yield among all cocktail cultivars across the 2 years, and it is, therefore, considered a feasible plant material for cocktail fruit-type tomato production.

With respect to NY, the present study identifies open-field tomato cultivars suitable for organic production with high NYs for the minerals Ca, K, Mg, P, Fe, and Zn (**Table 5**). The NY incorporates measures of two important dimensions for future food systems: the production of nutritious food and the efficient use of land (De Fries et al., 2015). The present study shows a high variation of the NY of Zn and Fe within the 20 tomato cultivars, thereby indicating a wide variability for these traits in the fruits. Several studies for the organic production of tomatoes (Ordóñez-Santos et al., 2011; Kapoulas et al., 2013; Pavithra et al., 2015) confirm that the genotype has important effects on most of the variations in the micronutrient content (e.g., Fe and Zn), while environmental effects have only a small impact. The metrics of NY opens up options to compare the usefulness of different production systems for food production to feed the growing global population (Moreira-Ascarrunz et al., 2016). Hence, a comparison of the mean average NYs of macronutrients (Ca, K, Mg, and P) and micronutrients (Fe and Zn) of the studied tomato cultivars with the calculated NYs for vegetables under organic production was performed, i.e., for eggplant (Raigón et al., 2010), potato tuber (Hajšlová et al., 2005; Järvan and Edesi, 2009), and tomato (Kapoulas et al., 2013) (**Table 8**). The means of NY of the eggplant (Raigón et al., 2010) and potato varieties (Järvan and Edesi, 2009) were considerably lower for all the studied nutrients compared to that of the tomato cultivars from the present study (**Table 8**). The NYs of Fe and Zn calculated from eight potato varieties during 3 years of cultivation (Hajšlová et al., 2005) also only amounted to one third of the NY obtained in the tomato cultivars that we studied. Compared to the study of Kapoulas et al. (2013) with three tomato cultivars, the mean of NYs in the present study showed 1.03-fold higher NY for Fe and 1.66-fold higher NY for Zn. Although the tomato cultivars in the present study had substantially higher NYs for K and Ca, the NYs for Mg and P of the tomato cultivars calculated based on the data in Kapoulas et al. (2013) were 1.70- and 1.52-fold higher than the NY generated from the present study (**Table 8**). The reasons for the different results are, on the one hand, the different cultivars and, on the other hand, the cultivation conditions. In contrast to our experiment, the trials described in Kapoulas et al. (2013) were carried out under greenhouse conditions and with a higher nutrient supply (including for P). Among different crop species compared from the cited studies, the tomato cultivars that we studied were leading in the NYs for Fe and Zn, and eggplant was the lowest micronutrient-yielding vegetable crop (**Table 8**).

It is notable in the present investigation that the cultivars with the highest yield ("Roterno F1," "Lyterno F1," "Bocati F1," and "Cappricia F1") were not the cultivars with the highest concentrations (expressed in mg 100 g^{-1} FW) of the six minerals studied. Conversely, the cultivar with the highest mineral concentrations, such as "Resi," did not show a high yield and was even recorded as the lowest-yielding cultivar. Thus, the results generally show significant antagonism effects of yield trait and mineral concentrations, which means that the positive effect of a high fruit yield is diminished by a decreased nutrient concentration in the fruits. Earlier studies already reported the negative relationship between yield components and mineral concentrations among tomato cultivars (Costa et al., 2011; Chávez-Servia et al., 2018). Davis (2009) reveals inverse relationships between crop yield and mineral concentration, suggesting the presence of the so-called dilution effect, which commonly occurs when selective breeding successfully increases crop yields. The dilution effect of an increased crop yield or harvest index without a proportional increase in the mineral concentration has been well documented in several vegetable and grain crops (Marles, 2017). In this study, we use the metrics of NY which weigh the conventional yield measure (tons/ha) by its nutritional content, and therefore our selected tomato cultivars are supposed to be adequately dense in mineral nutrients to fulfill the requirements with a high yield potential.

The data from the present study shows that 1 ha of land of cultivated "Bartelly F1" can annually produce Mg for 88 adults, P for 114 adults, and Fe for 120 adults. Despite having fewer metric tons per hectare compared to the salad cultivar "Cappricia F1" and other high-yielding cultivars, the cocktail cultivar "Bartelly F1" was excellent in providing Mg, P, and Fe for a high number of people. Nevertheless, "Cappricia F1" was an excellent salad

TABLE 8 | Nutritional yield (adults ha^{-1} year^{-1}) of macro- and micronutrients from different vegetables (organically cultivated) in comparison with the data of the present study.

Study	Species	Year of cultivation	Number of cultivars	Nutritional yield (adults ha^{-1} year^{-1})					
				Ca	K	Mg	P	Fe	Zn
Raigón et al., 2010	Eggplant	2008	3	11	69	29	50	19	26
Hajšlová et al., 2005	Potato	1996–1998	8	–	–	–	–	30	18
Järvan and Edesi, 2009	Potato	2007–2008	2	8	57	46	52	30	18
Kapoulas et al., 2013	Tomato	2008–2010	3	17	66	112	126	88	35
Present study	Tomato	2015–2016	20	25	119	66	83	91	58

The nutritional yield values of other studies were calculated based on the given data in the cited studies.

cultivar to supply the dietary intake of Ca, K, and Zn with NYs of 43, 155, and 76 adults year^{-1} ha^{-1}, respectively. The determined NY can influence the choice of varieties if both a high fruit yield and a high nutrient density per unit area are to be produced. Moreover, this study provides information about the number of people that can be fed according to their need for different nutrients with the respective tomato cultivars for 1 year from 1 ha of land. In addition, the NY might be an additional metric considered in exploiting the diversity of tomato to satisfy the nutritional needs of an increasing population.

In terms of contribution to the DRI and NY for Fe, the cocktail cultivar "Bartelly F1" produced the highest results, while the salad cultivar "Bocati F1" showed the highest values for Zn. Thus, to gain both maximum agronomic productivity in terms of fruit yield and Fe and Zn NYs, choosing "Bartelly F1" and "Bocati F1" as genotypes for breeding and/or selection in terms of micronutrients would be more feasible. Nevertheless, it should not be interpreted as implying that those cultivars were the sole source of any given nutrient since other cultivars also had significantly high concentrations of Fe and Zn. For example, "Lyterno F1" and "Roterno F1" did not differ significantly from "Bartelly F1" in the NY of Fe, and "Cappricia F1" and "Roterno F1" did not vary significantly with "Bocati F1" for the NY of Zn. However, if we compare the cultivars within the group of fruit type, it is clear that, among cocktail tomatoes, "Bartelly F1" produced the highest NY for both Fe and Zn. Incidentally, while comparing within the salad tomatoes, "Bocati F1" would be the best choice because it had the highest NY for both Fe and Zn.

Across the 2-year investigation, our data indicate that the cocktail cultivar "Resi" accounted for three- to fourfold lower NY values as compared to the highest-performing salad cultivars of the respective determined nutrients—for instance, the NY for Zn of "Bocati F1" (84 adults year^{-1} ha^{-1}) was about fourfold higher than that measured in "Resi" (22 adults year^{-1} ha^{-1}). Therefore, it might be possible to increase the mineral concentrations in tomatoes by incorporating the micronutrient-dense cultivars in breeding programs that have a higher ability to accumulate the Fe and Zn contents in the fruits. Even though the NY covers both yield and nutrient concentration, it should not imply that a single crop be consumed as the sole source of any given nutrient (Graham et al., 2018) as monotonous diets are likely to increase the risk of various nutrient deficiencies (Arimond et al., 2010). The NY should rather be considered as a policy tool to emphasize how any number of agronomic decisions are implicitly biased against either yield or nutrient concentration (Graham et al., 2018).

The current study reveals that a cultivar with the highest fruit yield was not automatically the cultivar with the highest NY. However, high yielding-cultivars with considerable nutrient contents were likely to have higher NYs. Similarly, the cultivar with the highest nutrient content did not always show a high NY. The results show that it is a challenge to evaluate genotypes for breeding and/or selection in terms of overall nutritional quality (Moreira-Ascarrunz et al., 2016; Gascuel et al., 2017) because no single cultivar might be rich in all relevant compounds or nutrients (Vicente et al., 2009), and no parent is a good general combiner for all desirable traits (Agarwal et al., 2017). Nonetheless, the metric of NY could be useful for plant breeders and growers in the selection, development, and choice of cultivars, and on the global scale, it provides another perspective for policymakers in projections of food demand and requirements of nutrients (De Fries et al., 2015). The results of this study regarding DRI and NY, together with the high genotypic stability of several cultivars for yield and micro- and macronutrients across years, provide valuable input to growers' and plant breeders' decisions. However, consumer demand will still determine the growers' choice on tomato cultivars and influence the plant breeders' cultivar development program.

The NYs of the micronutrients mentioned in the present study were much higher and satisfying in comparison with the NYs of tomatoes and other vegetables calculated from previous reports. In fact, the comparison with other plant species should consider the effects of diverse cultivation systems. Data for both mineral contents and crop yields are also lacking in many studies. The results show that the tomato biodiversity used in the present study can contribute to satisfying the nutritional needs of the ever-growing human population while minimizing the negative impact on the environment. Hence, the metrics of NY can also be useful in selecting the cultivar with improved nutrients to increase food security and conserve the biodiversity of tomato in organic outdoor production.

DATA AVAILABILITY STATEMENT

The original contributions presented in the study are included in the article/**Supplementary Material**,

further inquiries can be directed to the corresponding author.

AUTHOR CONTRIBUTIONS

CE, MN, and EP planned and designed the experimental setup. CE performed the experiments. CE and SG analyzed the data. All the authors wrote the manuscript.

FUNDING

CE received a scholarship from the Ministry of Research, Technology, and Higher Education of the Republic of Indonesia (RISTEK-DIKTI).

ACKNOWLEDGMENTS

We thank the Section of Genetic Resources and Organic Plant Breeding team for providing tomato cultivars and field assistance (Bernd Horneburg and Barbara Wedemeyer-Kremer). We express our special thanks to Janna Henrike Groeneveld for her contribution on-farm and to Bettina Egger from the Division Quality of Plant Products for technical assistance.

SUPPLEMENTARY MATERIAL

The Supplementary Material for this article can be found online at: https://www.frontiersin.org/articles/10.3389/fpls.2020.589692/full#supplementary-material

REFERENCES

Agarwal, A., Sharma, U., Ranjan, R., and Nasim, M. (2017). Combining ability analysis for yield, quality, earliness, and yield-attributing traits in tomato. *Int. J. Veget. Sci.* 23, 605–615. doi: 10.1080/19315260.2017.1355864

Arimond, M., Wiesmann, D., Becquey, E., Carriquiry, A., Daniels, M. C., Deitchler, M., et al. (2010). Simple food group diversity indicators predict micronutrient adequacy of women's diets in 5 diverse, resource-poor settings. *J. Nutr.* 140, 2059S–2069S. doi: 10.3945/jn.110.123414

Bai, Y., and Lindhout, P. (2007). Domestication and breeding of tomatoes: what have we gained and what can we gain in the future? *Ann. Bot.* 100, 1085–1094. doi: 10.1093/aob/mcm150

Bates, D., Mächler, M., Bolker, B., and Walker, S. (2015). Fitting linear mixed-effects models using lme4. *J. Stat. Soft.* 67:18637. doi: 10.18637/jss.v067.i01

Bauchet, G., and Causse, M. (2012). "Genetic diversity in tomato (Solanum lycopersicum) and its wild relatives," in *Genetic Diversity in Plants*, ed. M. Caliskan, (London: InTech), doi: 10.5772/33073

Beal, T., Massiot, E., Arsenault, J. E., Smith, M. R., and Hijmans, R. J. (2017). Global trends in dietary micronutrient supplies and estimated prevalence of inadequate intakes. *PLoS One* 12:e0175554. doi: 10.1371/journal.pone.0175554

Bhattarai, K., Sharma, S., and Panthee, D. R. (2018). Diversity among modern tomato genotypes at different levels in fresh-market breeding. *Int. J. Agron.* 2018, 1–15. doi: 10.1155/2018/4170432

Branca, G., Lipper, L., McCarthy, N., and Jolejole, M. C. (2013). Food security, climate change, and sustainable land management. A review. *Agron. Sustain. Dev.* 33, 635–650. doi: 10.1007/s13593-013-0133-1

Chávez-Servia, J., Vera-Guzmán, A., Linares-Menéndez, L., Carrillo-Rodríguez, J., and Aquino-Bolaños, E. (2018). Agromorphological traits and mineral content in tomato accessions from El Salvador, Central America. *Agronomy* 8, 1–14. doi: 10.3390/agronomy8030032

Costa, F., de Lurdes Baeta, M., Saraiva, D., Verissimo, M. T., and Ramos, F. (2011). Evolution of mineral contents in tomato fruits during the ripening process after harvest. *Food Anal. Methods* 4, 410–415. doi: 10.1007/s12161-010-9179-8

Davis, D. R. (2009). Declining fruit and vegetable nutrient composition: what is the evidence? *Horticult. Sci.* 44, 15–19.

De Ruiter, H., Macdiarmid, J. I., Matthews, R. B., and Smith, P. (2018). Moving beyond calories and protein: micronutrient assessment of UK diets and land use. *Global Environ. Change* 52, 108–116. doi: 10.1016/j.gloenvcha.2018.06.007

De Fries, R., Fanzo, J., Remans, R., Palm, C., Wood, S., and Anderman, T. L. (2015). Metrics for land-scarce agriculture. *Science* 349, 238–240. doi: 10.1126/science.aaa5766

De Fries, R., Mondal, P., Singh, D., Agrawal, I., Fanzo, J., Remans, R., et al. (2016). Synergies and trade-offs for sustainable agriculture: nutritional yields and climate-resilience for cereal crops in Central India. *Global Food Secur.* 11, 44–53. doi: 10.1016/j.gfs.2016.07.001

Dixon, M., Simonne, E., Obreza, T., and Liu, G. (2020). Crop response to low phosphorus bioavailability with a focus on tomato. *Agronomy* 10:617. doi: 10.3390/agronomy10050617

Ene, C. O., Ogbonna, P. E., Agbo, C. U., and Chukwudi, U. P. (2016). Studies of phenotypic and genotypic variation in sixteen cucumber genotypes. *Chilean J. Agric. Res.* 76, 307–313. doi: 10.4067/S0718-58392016000300007

FAO, (2018). *Tomato [WWW Document]*. Available online at: http://www.fao.org/faostat/en/#data/QC/ (accessed August 16, 2018).

FAOSTAT, (2019). *Food and Agriculture Organisation of the United Nations [WWW Document]*. Available online at: http://www.fao.org/faostat/en/?#data (accessed April 14, 2019).

FAOSTAT, (2020). *FAOSTAT [WWW Document]*. Available online at: http://www.fao.org/faostat/en/#data (accessed June18, 2020).

Fears, R., Ter Meulen, V., and Von Braun, J. (2019). Global food and nutrition security needs more and new science. *Sci. Adv.* 5:eaba2946. doi: 10.1126/sciadv.aba2946

Firas, A.-A., Hussein, K., Mahmood, S., Mahmood, A.-Z., and Mohammad, A. A.-N. (2012). Genetic analysis and correlation studies of yield and fruit quality traits in tomato (Solanum lycopersicum L.). *N. Y. Sci. J.* 5, 42–145.

Foley, J. A., Ramankutty, N., Brauman, K. A., Cassidy, E. S., Gerber, J. S., Johnston, M., et al. (2011). Solutions for a cultivated planet. *Nature* 478, 337–342. doi: 10.1038/nature10452

Foolad, M. R. (2007). Genome mapping and molecular breeding of tomato. *Int. J. Plant Genom.* 2007, 1–52. doi: 10.1155/2007/64358

Gascuel, Q., Diretto, G., Monforte, A. J., Fortes, A. M., and Granell, A. (2017). Use of natural diversity and biotechnology to increase the quality and nutritional content of tomato and grape. *Front. Plant Sci.* 8:652. doi: 10.3389/fpls.2017.00652

Graham, C., Beck, R., and Thavarajah, D. (2018). Dietary reference intake and nutritional yield of lentils in the Northern Great Plains. *Crop Sci.* 58, 1–7. doi: 10.2135/cropsci2017.10.0617

Hajšlová, J., Schulzová, V., Slanina, P., Janné, K., Hellenäs, K. E., and Andersson, C. (2005). Quality of organically and conventionally grown potatoes: Four-year study of micronutrients, metals, secondary metabolites, enzymic browning and organoleptic properties. *Food Addit. Contamin.* 22, 514–534. doi: 10.1080/02652030500137827

Hernández Suárez, M., Rodríguez Rodríguez, E. M., and Díaz Romero, C. (2007). Mineral and trace element concentrations in cultivars of tomatoes. *Food Chem.* 104, 489–499. doi: 10.1016/j.foodchem.2006.11.072

Herrero, M., Thornton, P. K., Power, B., Bogard, J. R., Remans, R., Fritz, S., et al. (2017). Farming and the geography of nutrient production for human use: a transdisciplinary analysis. *Lancet Planet. Health* 1, e33–e42. doi: 10.1016/S2542-5196(17)30007-4

Institute of Medicine, (2006). *DRI, Dietary Reference Intakes: The Essential Guide to Nutrient Requirements*. Washington, DC: National Academies Press.

Järvan, M., and Edesi, L. (2009). The effect of cultivation methods on the yield and biological quality of potato. *Agron. Res.* 7, 289–299.

Jha, A. B., and Warkentin, T. D. (2020). Biofortification of pulse crops: status and future perspectives. *Plants* 9:73. doi: 10.3390/plants9010073

Johansson, E., Hussain, A., Kuktaite, R., Andersson, S., and Olsson, M. (2014). Contribution of organically grown crops to human health. *Int. J. Environ. Res. Public Health* 11, 3870–3893. doi: 10.3390/ijerph110403870

Kagan-Zur, V., and Mizrahi, Y. (1993). Long shelf-life small sized (cocktail) tomatoes may be picked in bunches. *Sci. Horticult.* 56, 31–41.

Kapoulas, N., Ilić, Z. S., Milenković, L., and Mirecki, N. (2013). Effects of organic and conventional cultivation methods on mineral content and taste parameters intomato fruit. *Agricult. Fores.* 59, 23–34.

Koch, M., Busse, M., Naumann, M., Jákli, B., Smit, I., Cakmak, I., et al. (2019). Differential effects of varied potassium and magnesium nutrition on production and partitioning of photoassimilates in potato plants. *Phys. Plant.* 166, 921–935. doi: 10.1111/ppl.12846

Labate, J. A., Breksa, A. P., Robertson, L. D., King, B. A., and King, D. E. (2018). Genetic differences in macro-element mineral concentrations among 52 historically important tomato varieties. *Plant Genet. Resour.* 16, 343–351. doi: 10.1017/S1479262117000417

Lázaro, A. (2018). Tomato landraces: an analysis of diversity and preferences. *Plant Genet. Resour.* 16, 315–324. doi: 10.1017/S1479262117000351

Li, H., Lian, C., Zhang, Z., Shi, X., and Zhang, Y. (2017). Agro-biofortification of iron and zinc in edible portion of crops for the global south. *Adv. Plants Agric. Res.* 6, 52–54. doi: 10.15406/apar.2017.06.00210

Marles, R. J. (2017). Mineral nutrient composition of vegetables, fruits and grains: the context of reports of apparent historical declines. *J. Food Compos. Anal.* 56, 93–103. doi: 10.1016/j.jfca.2016.11.012

Martin, A. R., Cadotte, M. W., Isaac, M. E., Milla, R., Vile, D., and Violle, C. (2019). Regional and global shifts in crop diversity through the Anthropocene. *PLoS One* 14:e0209788. doi: 10.1371/journal.pone.0209788

Mata-Nicolás, E., Montero-Pau, J., Gimeno-Paez, E., Garcia-Carpintero, V., Ziarsolo, P., Menda, N., et al. (2020). Exploiting the diversity of tomato: the development of a phenotypically and genetically detailed germplasm collection. *Hortic Res* 7:66. doi: 10.1038/s41438-020-0291-7

Mayer, A. (1997). Historical changes in the mineral content of fruits and vegetables. *Br. Food J.* 99, 207–211. doi: 10.1108/00070709710181540

Miller, B. D. D., and Welch, R. M. (2013). Food system strategies for preventing micronutrient malnutrition. *Food Policy* 42, 115–128. doi: 10.1016/j.foodpol.2013.06.008

Mohammed, A. E., Smit, I., Pawelzik, E., Keutgen, A. J., and Horneburg, B. (2019). Organically grown outdoor tomato: fruit mineral nutrients and plant infection by Phytophthora infestans. *Org. Agr.* 10, 125–134. doi: 10.1007/s13165-019-00253-7

Moreira-Ascarrunz, S., Larsson, H., Prieto-Linde, M., and Johansson, E. (2016). Mineral nutritional yield and nutrient density of locally adapted wheat genotypes under organic production. *Foods* 5, 1–18. doi: 10.3390/foods5040089

Ogunniyan, D. J., and Olakojo, S. A. (2014). Genetic variation, heritability, genetic advance and agronomic character association of yellow elite inbred lines of maize (Zea mays L.). *Nigerian J. Genet.* 28, 24–28. doi: 10.1016/j.nigjg.2015.06.005

Ordóñez-Santos, L. E., Vázquez-Odériz, M. L., and Romero-Rodríguez, M. A. (2011). Micronutrient contents in organic and conventional tomatoes (Solanum lycopersicum L.): micronutrient contents of tomato. *Int. J. Food Sci. Technol.* 46, 1561–1568. doi: 10.1111/j.1365-2621.2011.02648.x

Pavithra, G. J., Salimath, M., Geetha, K. N., and Shankar, A. G. (2015). Genetic variability studies in tomato germplasm for zinc and iron content and its relationship with growth and yield parameters. *Eco. Env. Cons* 21, AS355–AS360.

Pélabon, C., Hilde, C. H., Einum, S., and Gamelon, M. (2020). On the use of the coefficient of variation to quantify and compare trait variation. *Evolut. Lett.* 4, 180–188. doi: 10.1002/evl3.171

Powell, B., Thilsted, S. H., Ickowitz, A., Termote, C., Sunderland, T., and Herforth, A. (2015). Improving diets with wild and cultivated biodiversity from across the landscape. *Food Sec.* 7, 535–554. doi: 10.1007/s12571-015-0466-5

Pretty, J., and Bharucha, Z. P. (2014). Sustainable intensification in agricultural systems. *Ann. Bot.* 114, 1571–1596. doi: 10.1093/aob/mcu205

Raigón, M. D., Rodríguez-Burruezo, A., and Prohens, J. (2010). Effects of organic and conventional cultivation methods on composition of eggplant fruits. *J. Agric. Food Chem.* 58, 6833–6840. doi: 10.1021/jf904438n

Ridoutt, B. G., Hendrie, G. A., and Noakes, M. (2017). Dietary strategies to reduce environmental impact: a critical review of the evidence base. *Adv. Nutr.* 8, 933–946. doi: 10.3945/an.117.016691

Sager, M. (2017). Main and trace element contents of tomatoes grown in Austria. *J. Food Sci. Eng.* 7, 239–248. doi: 10.17265/2159-5828/2017.05.002

Schrama, M., De Haan, J. J., Kroonen, M., Verstegen, H., and Van der Putten, W. H. (2018). Crop yield gap and stability in organic and conventional farming systems. *Agricult. Ecosyst. Environ.* 256, 123–130. doi: 10.1016/j.agee.2017.12.023

Springmann, M., Clark, M., Mason-D'Croz, D., Wiebe, K., Bodirsky, B. L., Lassaletta, L., et al. (2018). Options for keeping the food system within environmental limits. *Nature* 562, 519–525. doi: 10.1038/s41586-018-0594-0

Statistisches Bundesamt, (2020). *Betriebe, Anbauflächen, Erträge und Erntemengen von Gemüse [WWW Document]. Statistisches Bundesamt*. Available online at: https://www.destatis.de/DE/Themen/Branchen-Unternehmen/Landwirtschaft-Forstwirtschaft-Fischerei/Obst-Gemuese-Gartenbau/Tabellen/betriebe-anbau-erntemenge-gemuese.html (accessed May 7, 2020).

Tester, M., and Langridge, P. (2010). Breeding technologies to increase crop production in a changing world. *Science* 327, 818–822. doi: 10.1126/science.1183700

Tieman, D., Zhu, G., Resende, M. F. R., Lin, T., Nguyen, C., Bies, D., et al. (2017). A chemical genetic roadmap to improved tomato flavor. *Science* 355, 391–394. doi: 10.1126/science.aal1556

Uluisik, S., Chapman, N. H., Smith, R., Poole, M., Adams, G., Gillis, R. B., et al. (2016). Genetic improvement of tomato by targeted control of fruit softening. *Nat. Biotechnol.* 34, 950–952. doi: 10.1038/nbt.3602

Vicente, A., Manganaris, G., Sozzi, G., and Crisosto, C. (2009). "Nutritional quality of fruits and vegetables," in *Postharvest Handling: A Systems Approach, Food Science and Technology*, eds W. J. Florkowski, R. Shewfelt, B. Brueckner, and S. Prussia, (Burlington, MA: Academic Press).

Viskelis, P., Radzevicius, A., Urbonaviciene, D., Viskelis, J., Karkleliene, R., and Bobinas, C. (2015). "Biochemical parameters in tomato fruits from different cultivars as functional foods for agricultural, industrial, and pharmaceutical uses," in *Plants for the Future*, ed. H. El-Shemy, (London: InTech), 45–77. doi: 10.5772/60873

Vorland, C. J., Stremke, E. R., Moorthi, R. N., and Hill Gallant, K. M. (2017). Effects of excessive dietary phosphorus intake on bone health. *Curr. Osteoporos Rep.* 15, 473–482. doi: 10.1007/s11914-017-0398-4

White, P., and Broadley, M. (2005). Biofortifying crops with essential mineral elements. *Trends Plant Sci.* 10, 586–593. doi: 10.1016/j.tplants.2005.10.001

Zörb, C., Piepho, H.-P., Zikeli, S., and Horneburg, B. (2020). Heritability and variability of quality parameters of tomatoes in outdoor production. *Research* 2020, 1–9. doi: 10.34133/2020/6707529

Conflict of Interest: The authors declare that the research was conducted in the absence of any commercial or financial relationships that could be construed as a potential conflict of interest.

frontiers in Plant Science

ORIGINAL RESEARCH
published: 23 December 2020
doi: 10.3389/fpls.2020.602065

Early Changes in Nitrate Uptake and Assimilation Under Drought in Relation to Transpiration

Vít Gloser[1], Michaela Dvorackova[1], Daniel Hernandez Mota[1], Bojana Petrovic[1], Patricia Gonzalez[2] and Christoph Martin Geilfus[2]*

[1]*Department of Experimental Biology, Faculty of Science, Masaryk University, Brno, Czechia,* [2]*Division of Controlled Environment Horticulture, Faculty of Life Sciences, Albrecht Daniel Thaer-Institute of Agricultural and Horticultural Sciences, Humboldt-University of Berlin, Berlin, Germany*

Soil drying combined with nitrogen (N) deficiency poses a grave threat to agricultural crop production. The rate at which nitrate (NO_3^-) is taken up depends partly on the uptake and transpiration of water. Rapid changes in nitrate assimilation, in contrast to other N forms, may serve as a component of the plant stress response to drought because nitrate assimilation may lead to changes in xylem pH. The modulation of xylem sap pH may be relevant for stomata regulation *via* the delivery of abscisic acid (ABA) to guard cells. In several factorial experiments, we investigated the interactions between nitrate and water availability on nitrate fate in the plant, as well as their possible implications for the early drought-stress response. We monitored the short-term response (2–6 days) of nitrate in biomass, transport to shoot and reduction in *Pisum sativum*, *Hordeum vulgare*, *Vicia faba*, and *Nicotiana tabacum* and correlated this with sap pH and transpiration rates (TRs). Cultivation on inorganic substrate ensured control over nutrient and water supply and prevented nodulation in legume species. NO_3^- content in biomass decreased in most of the species under drought indicating significant decline in NO_3^- uptake. *Hordeum vulgare* had the highest NO_3^- concentrations in all organs even under drought and low NO_3^- treatment. This species can likely respond much better to the combined adverse effects of low NO_3^- and water scarcity. Nitrate reductase activity (NRA) was reduced in both roots and leaves of water deficient (WD) plants in all species except *H. vulgare*, presumably due to its high NO_3^- contents. Further, transient reduction in NO_3^- availability had no effect on sap pH. Therefore, it seems unlikely that NRA shifts from shoot root leading to the supposed alkalization of sap. We also did not observe any interactive effects of NO_3^- and water deficiency on transpiration. Hence, as long as leaf NO_3^- content remains stable, NO_3^- availability in soil is not linked to short-term modulation of transpiration.

Keywords: nitrate transport, nitrogen deficiency, nitrate reductase, pH, xylem, apoplast

OPEN ACCESS

Edited by:
Carla S. Santos, Catholic University of Portugal, Portugal

Reviewed by:
Yordan Muhovski, Walloon Agricultural Research Centre, Belgium
Jaime Puertolas, Lancaster University, United Kingdom

****Correspondence:***
Vít Gloser
vitgloser@sci.muni.cz

Specialty section:
This article was submitted to Plant Nutrition, a section of the journal Frontiers in Plant Science

Received: *02 September 2020*
Accepted: *04 December 2020*
Published: *23 December 2020*

Citation:
Gloser V, Dvorackova M, Mota DH, Petrovic B, Gonzalez P and Geilfus CM (2020) Early Changes in Nitrate Uptake and Assimilation Under Drought in Relation to Transpiration. Front. Plant Sci. 11:602065. doi: 10.3389/fpls.2020.602065

INTRODUCTION

Nitrate (NO_3^-) is a very important nitrogen (N) source for almost all plants, particularly crop plants. Fluctuations in NO_3^- availability considerably alter both rates of NO_3^- transport and assimilation (i.e., reduction) within the plant (Peuke et al., 1996; Lips, 1997). When external NO_3^- availability decreases, its transport to the plant and to the shoot is typically reduced (Hachiya and Sakakibara, 2017). Low NO_3^- availability can also lower the transpiration rate

(TR; Wilkinson et al., 2007) and consequently affect water use by crops. Araus et al. (2020) showed that changes in NO_3^- availability may lead to changes in the expression of drought-response genes; this response also involves the drought stress hormone abscisic acid (ABA). An interesting detail is that nitrogen supply to roots enhances stomatal opening, provided that plants are well watered (Wilkinson et al., 2007; Matimati et al., 2014). Conversely, nitrogen deficiency can cause rapid reduction of gas exchange (Chapin et al., 1988). This response can occur without any change in leaf water potential (WP); it is mediated by increased ABA production and a consequent decrease in gas exchange similar to the response to water deficiency (Chapin, 1991). The N status of the plant also influences gas exchange because N is involved in many processes related to photosynthesis (Lu and Zhang, 2000). The variation in the rate of carbon fixation and, consequently in leaf intercellular CO_2 concentration, strongly affects stomatal aperture (Roelfsema et al., 2002, 2006). Additionally, the rate of ATP generation in the primary processes of photosynthesis is also one of the regulators of stomatal conductance (Tezara et al., 1999; Tominaga et al., 2001).

Thus, there seems to be a link between nitrogen (NO_3^-) availability and the response to drought. Moreover, decreasing water availability in soil can negatively affect NO_3^- uptake and assimilation (Lawlor and Cornic, 2002; Azedo-Silva et al., 2004). Nevertheless, it is not completely clear whether these early changes in NO_3^- metabolism can also serve as a component of the plant stress response system. For an overall summary of the interdependence of water and nitrogen use, the reader is referred to the recent review by Plett et al. (2020).

Experimental evidence also indicates that changes in NO_3^- availability even within the non-deficient range may have a rapid regulatory effect on stomatal opening (Wilkinson et al., 2007). The underlying mechanism may involve changes in xylem sap pH, which is relevant for the compartmental distribution of ABA between mesophyll cells and the guard cell apoplast (Wilkinson et al., 1998; Davies et al., 2002; Geilfus et al., 2015). This ABA is likely being produced in the shoot (Dodd et al., 2009; McAdam et al., 2016; Li et al., 2018). For example, apoplastic alkalization during drought or other environmental stresses promotes ABA accumulation in the guard cell apoplast and triggers stomatal closure (Wilkinson and Davies, 2002; Geilfus et al., 2017). Notably, increasing NO_3^- levels was also reported to increase leaf apoplast pH (Jia and Davies, 2007). This could be due to altered NO_3^- assimilation, *via* altered NO_3^- reductase activity (NRA; Wilkinson, 2004).

Nitrate assimilation is a relevant factor for apoplastic pH because of the number of electrons required to reduce NO_3^- to NH_4^+. As a result, strongly basic hydroxides are formed, which are buffered by newly synthesized organic acids (i.e., malic acid) as otherwise the alkalizing hydroxides can drastically alter cytosolic pH (Dijkshoorn, 1962). Transporting organic acid anions (e.g., malate^{2-}), into the apoplast is considered as the cause for the depletion of free apoplast protons. In the slightly acidified apoplast, free protons associate with the malate anion, thereby increasing the pH. Nonetheless, the relevance of drought for this apoplastic pH-modulating effect is still unclear. Drought is known to increase apoplastic pH, as shown for field bean (Karuppanapandian et al., 2017), sunflower (Gollan et al., 1992), asiatic dayflower (*Commelina communis*; Wilkinson and Davies, 1997), or maize (Goodger et al., 2005). Drought also has a significant effect on NRA in some species (Larsson et al., 1989; Azedo-Silva et al., 2004; Correia et al., 2005). Limited availability of NO_3^- as substrate for NRA due to the reduced uptake and transport under drought is one possible explanation for the downregulation of NRA (Azedo-Silva et al., 2004). NRA may also decrease due to lower NR activation under drought (Brewitz et al., 1996; Foyer et al., 1998). Moreover, the response of NRA to water availability may differ between species that differ in the primary site of NO_3^- reduction (root vs. leaves), but to our knowledge no data on this has been published so far.

Given that resource availability in the environment fluctuates greatly over time, rapid plant responses to any fluctuations may significantly impact productivity. The interrelation between water availability and both uptake and reduction of NO_3^- could be relevant for transpiration by modulating xylem sap pH – a factor that is linked to controlling plant transpiration and gas exchange in general. Besides the role of NO_3^- in plant metabolism, in contrast to other N forms available in the soil, is its uptake more tightly linked to water movement toward plant roots (Marschner, 1995). Any assessment of the hypothesis on the relevance of NO_3^- for transpiration must consider species-specific differences in the ability to take up and reduce NO_3^- under drought. Thus, four species were evaluated that contrast in their nitrogen uptake and assimilation: *Pisum sativum*, *Hordeum vulgare*, *Vicia faba*, and *Nicotiana tabacum*. Moreover, the differential ability of diverse species to change xylem sap pH under drought stress is also certainly relevant (Sharp and Davies, 2009; Gloser et al., 2016). In this paper, we describe a series of experiments where we investigated the interactions between NO_3^- availability and water availability and their implication for the early drought-stress response. The possible effect of the dominant site of NO_3^- assimilation inside the plant on its drought response is also discussed.

MATERIALS AND METHODS

Plant Material and Cultivation

Four species were used in experiments: green pea (*P. sativum* cv. *Premium*), spring barley (*H. vulgare cv. Heris*), bean (*V. faba cv. Merkur*), and tobacco (*N. tabacum cv. GAT*). Species differ in the distribution of NRA between roots and leaves (Andrews, 1986), as well as in the changes of xylem sap composition under water deficiency (Gloser et al., 2016). Plants were cultivated with the inorganic substrate Profile Porous Ceramic (PPC, PROFILE Products LLC, Buffalo Grove, IL, United States). This was done to ensure full control of nutrient availability. In all experiments, plants were initially grown in a greenhouse with temperature and humidity control. Five days before the drying treatment started, plants were moved to a growth chamber with 16/8 h light/dark photoperiod and the following conditions: mean photosynthetic photon flux density

400 µmol m^{-2} s^{-1}, average temperature of 22°C (light) and 20°C (dark), and relative humidity 60% (constant). The position of plants for different treatments in the chamber was randomized. Due to the supply of NO_3^-, there were no nodules on roots of the legumes *V. faba* and *P. sativum*.

Five days after moving the plants to the growth chamber (day 0), two different experiments were started. In experiment 1, 40 plants of each of the four species were separated into two treatments. Irrigation was stopped in the water deficient (WD) treatment for 10 days, whereas well-watered (WW) plants were irrigated daily to full water holding capacity of the substrate with nutrient solution containing: 1.21 mM $Ca(NO_3)_2$, 1.6 mM KNO_3, 380 µM KH_2PO_4, 540 µM $MgSO_4$, 4 µM $MnSO_4$, 1.7 µM $ZnSO_4$, 0.3 µM $CuSO_4$, 40 µM, H_3BO_3, 0.5 µM Na_2MoO_4, and 81 µM FeNa-EDTA (4 mM NO_3^- N in total). Experiment 2 was a two-factorial experiment with water and nitrogen availability as factors. About 60 plants of *V. faba* and *P. sativum* were divided into the same two treatments as experiment 1 at day 0, i.e., in 30 WW and 30 WD plants. The 30 plants of each water treatment were then separated into two group's á 15 plants. At day 0, in order to wash out the remaining nitrogen, containers of the plants that were supposed to experience lack of nitrogen were flushed with a large amount of nitrogen solution containing: 60.3 µM $Ca(NO_3)_2$, 79.5 µM KNO_3, 750 µM K_2SO_4, 1.14 mM $CaCl_2$, 380 µM KH_2PO_4, 540 µM, $MgSO_4$, 4 µM $MnSO_4$, 1.7 µM $ZnSO_4$, 0.3 µM $CuSO_4$, 40 µM, H_3BO_3, 0.5 µM Na_2MoO_4, and 81 µM FeNa-EDTA [0.2 mM NO_3^- N in total; plants from this experimental group are named "low nitrogen (LN) plants"]. The missing NO_3^- in LN solution was replaced with sulphate to retain both ionic and osmotic parity between treatments. Plants in "full nitrogen (FN) treatment" were watered with the initial solution described above. Model calculations based on solution volume retained (or additionally supplied) in each container, and composition of the solution showed large differences in total nitrate potentially available to plants during the experimental period when drying was applied, particularly between HN and LN treatments: WWHN: 3.1 mmol, WDHN 1.7 mmol, WWLN: 0.15 mmol, and WDLN: 0.08 mmol. Plant response was monitored regularly for up to 10 days after the start of treatments, making three harvests every 2–3 days.

Measurements of Soil and Plant Water Relations

Substrate water content (SWC) was monitored using a ThetaProbe connected to a HH2 meter (Delta-T Devices, Cambridge, United Kingdom). SWC was also measured in each pot immediately prior to harvesting. The relationship between substrate WP and SWC is shown in **Supplementary Figure S1** (**Supplementary Material**). Whole plant TR was determined gravimetrically prior to xylem sap collection. TR was measured at least for 1 h under normal cultivation conditions, and plant containers were covered with a plastic bag to prevent evaporation from the substrate. Plant leaf area was determined at the end of sampling using a scanner and the image analysis software ImageJ (NIMH, Bethesda, MD, United States). WP of the plant was measured either on young fully developed leaves or on the top part of the shoot (depending on the species), using the pressure chamber method before xylem sap sampling (see below).

Xylem Sap Collection and Analysis

The collection of xylem sap and the measurement of leaf/stem WP (Boyer, 1967) and xylem sap pH were conducted between 2 and 7 h from photoperiod start. Xylem sap was collected either from leaf (*N. tabacum*) or stems (*P. sativum*, *H. vulgare*, and *V. faba*) using a pressure chamber (PWSC 3005, Soilmoisture Equipment Corp., Santa Barbara, CA, United States). Sap was sampled from the second or third fully developed leaf of *N. tabacum*. After cutting, the cut surface of the petiole/stem was rinsed with distilled water to remove contaminants from the cut cells and the petiole/stem was sealed in the pressure chamber. The first drop of xylem sap was discarded and the pressure was noted as the WP. Pressure was gradually increased up to approx. Around 0.2 MPa above the balancing pressure and 10–40 µl of xylem sap was collected from each leaf (or shoot) over approximately 10 min. The pH of xylem sap was taken by a pH microelectrode (Microelectrodes Inc., Bedford, MA, United States) connected to an MP220 pH meter (Mettler Toledo, Switzerland). Samples were stored at −20°C immediately after pH measurement, until further analysis.

Determination of Nitrate in Biomass and Sap, Calculation of Delivery Rates

Nitrate was extracted from 50 mg of fresh biomass in 1 ml of hot (95°C) DI water for 30 min. NO_3^- concentration in the extract as well as in the xylem sap samples was consequently assayed by a spectrophotometric method (Cataldo et al., 1975). The delivery rate of NO_3^- was calculated as sap NO_3^- concentration multiplied by water flux to leaves (g h^{-1}) derived from the gravimetric TR measurement of the respective plant shortly before sap sampling.

Nitrate Reductase Activity

Nitrate reductase activity was estimated in leaves and roots with an *in vivo* assay (Black et al., 2002). Four subsamples of leaf disks (~100 mg) or finely chopped roots (~200 mg) were combined with 5 ml of assay buffer (200 mol m^{-3} KNO_3 and 5% propanol in 100 mol m^{-3} potassium phosphate buffer, pH 7.5) in 20 ml glass vials. The vials were closed and placed in the dark at 25°C on a shaker. Two replicate vials for each sample were removed from the shaker after 10 and 90 min and placed in boiling water for 15 min. The vials were cooled to room temperature and aliquots of assay buffer were collected and stored at −20°C. To determine nitrite concentration, 500 ml of 1% sulphanilamide in 3 M HCl and 500 ml of 0.02% N-naphthyl-ethylene-diamine hydrochloride in water were added to the thawed samples and kept in the dark at room temperature for 20 min, and the absorbance measured at 540 nm. Enzyme activity was calculated by comparing the amount of nitrite produced after 90-min incubation with that detected after 10 min (Black et al., 2002). We took the mean of two replicates and expressed NRA as µmol nitrite produced g (Fresh Mass)$^{-1}$ (fine roots or leaves) h^{-1}.

Statistical Evaluation

The effect of drought was tested on WD and WW control plants. However, the different species and the various treatments differed in drying rates. To enable meaningful comparison across treatments and species, we used information about SWC and TR of each plant shortly before harvest. Plants were grouped such that both SWC and TR of WD plants were significantly lower than those of WW plants. WD treatment typically included plants with SWC 0.6 g g^{-1} and lower. Statistical analyses were performed using STATISTICA 12 (TIBCO Software Inc., Palo Alto, CA, United States). In the first group of results – comparison of the response to drought under full NO_3^- supply – significant differences between means WW and WD treatments were tested by a *t*-test separately for species and parameter. In experiments with a two-factorial design, the combined effects of drought and N-deficiency were tested by a two-way ANOVA for each species separately. Normality of data and homogeneity of variances were tested prior to analysis and non-homogeneous datasets were log transformed. Spearman's correlation analysis was used to evaluate the significance of correlations between the measured parameters. Correlation analyses included data of all harvested plants of each species.

RESULTS

Effect of Water Availability on Plant Water Relations

A fall in water availability to approximately 50–60% of the maximum substrate water holding capacity (SWC = 1.1 g g^{-1}) led to a significant decrease in the TR and the leaf WP in all examined species (**Table 1**). The decrease was particularly pronounced (approximately 50%) in *N. tabacum* and *P. sativum*. *Nicotiana tabacum* showed a significant decrease in WP with the value being three times lower relative to WW-conditions.

Effect of Water Availability on NO_3^- Content

Water deficient treatment significantly reduced NO_3^- content in roots and leaves in three of the examined species and they also differed considerably in their response (**Table 2**). In *V. faba*,

TABLE 1 | Mean soil water content (SWC), whole plant TR and the leaf WP of plants with full water supply (well-watered; WW) and plant exposed to gradual drying of substrate for several days (water-deficient; WD).

Species	Treatment	SWC (g g^{-1})	TR (g $m^{-2}h^{-1}$)	WP (MPa)
Vicia	WW	0.86 ± 0.2 a	159.15 ± 8.4 a	−0.24 ± 0.04 a
faba	WD	0.49 ± 0.2 b	121.80 ± 10.51 b	−0.41 ± 0.05 b
Nicotiana	WW	0.84 ± 0.02 a	76.5 ± 7.7 a	−0.20 ± 0.04 a
tabacum	WD	0.49 ± 0.04 b	35.8 ± 8.1 b	−0.65 ± 0.05 b
Pisum	WW	1.01 ± 0.01 a	263.72 ± 6.3 a	−0.52 ± 0.02 a
sativum	WD	0,43 ± 0.1 b	152.50 ± 18.5 b	−0.75 ± 0.09 b
Hordeum	WW	0.92 ± 0.04 a	146.9 ± 14.3 a	−0.54 ± 0.05 a
vulgare	WD	0.42 ± 0.1 b	96.6 ± 14.2 b	−0.70 ± 0.05 b

Presented are means and SEs of *Vicia faba* (n = 13), *Nicotiana tabacum* (n = 17), *P. sativum* (n = 31), and *H. vulgare* (n = 13). Significant differences ($p \leq 0.05$) between treatments were tested separately for each species and are marked by different letters.

TABLE 2 | Mean NO_3^- content in the biomass of leaves ($[NO_3^-]_L$) and roots ($[NO_3^-]_R$), NO_3^- concentration in the xylem sap ($[NO_3^-]_S$) and the delivery rate of NO_3^- to the shoot (DR); NRA in leaves (NRAL) and roots (NRAR) and the ratio of NRA in leaves and roots (NRAR/L), pH of the xylem sap (pHSAP).

Species	Treatment	$[NO_3^-]_L$ (µmol g^{-1})	$[NO_3^-]_R$ (µmol g^{-1})	$[NO_3^-]_S$ (µmol g^{-1})	DR (µmol h^{-1})	pH_{SAP}	NRA_L (nmol $g^{-1}h^{-1}$)	NRA_R (nmol $g^{-1}h^{-1}$)	$NRA_{R/L}$
Vicia	WW	10.31 ± 1.2 a	21.45 ± 3.8 a	3.49 ± 0.4 a	7.23 ± 1.0 a	5.95 ± 0.1 a	158.27 ± 21 a	227.90 ± 33.5 a	1.44
faba	WD	6.21 ± 0.8 b	10.10 ± 1.7 b	1.59 ± 0.4 b	1.37 ± 0.6 b	5.64 ± 0.1 b	85.47 ± 17 b	84.47 ± 17.2 b	0.99
Nicotiana	WW	5.66 ± 0.9 a	10.25 ± 1.1 a	9.09 ± 1.4 a	12.23 ± 1.5 a	6.96 ± 0.1 a	206.15 ± 34 a	49.29 ± 6.1 a	0.24
tabacum	WD	3.75 ± 0.4 b	5.65 ± 0.7 b	2.14 ± 0.9 b	2.83 ± 1.2 b	6.89 ± 0.1 a	147.89 ± 33 b	29.36 ± 3.8 b	0.20
Pisum	WW	5.08 ± 0.3 a	11.21 ± 0.9 a	2.14 ± 0.2 a	3.69 ± 0.5 a	6.07 ± 0.1 a	319.29 ± 35 a	376.51 ± 55.6 a	1.18
sativum	WD	3.95 ± 0.3 b	4.80 ± 0.7 b	1.05 ± 0.2 b	2.44 ± 0.8 b	5.84 ± 0.1 b	190.93 ± 24 b	125.96 ± 27.7 b	0.66
Hordeum	WW	93.06 ± 1.0 a	78.92 ± 11 a	7.87 ± 0.8 a	19.40 ± 1.7 a	6.26 ± 0.1 a	554.88 ± 66 a	324.18 ± 61 a	0.58
vulgare	WD	98.04 ± 6.8 a	82.47 ± 10 a	5.81 ± 0.9 a	12.17 ± 2.1 b	6.33 ± 0.1 a	655.02 ± 61 a	305.56 ± 56 a	0.47

Plants fully supplied with water (WW) or exposed to gradual drying of substrate for several days (WD). The table shows means ± SE for *V. faba* (n = 13), *N. tabacum* (n = 17), *P. sativum* (n = 31), and *H. vulgare* (n = 13). Significant differences (p = 0.05) between treatments were tested separately for each species and are marked by different letters.

N. tabacum and *P. sativum*, NO_3^- content was reduced both in leaves and roots in response to WD treatment (**Table 2**), but leaf NO_3^- content was not significantly affected in *H. vulgare*. The concentration of NO_3^- in xylem sap was also reduced in all species except *H. vulgare* (**Table 2**). The calculated delivery rates of NO_3^- to leaves were significantly reduced (by 40–80%) in all species (**Table 2**). NRA significantly declined in WD treatment (**Table 2**) but the magnitude of the response was different among the different species. NRA in roots was greatly reduced (by 35–75%) in all species. NRA in leaves decreased in *V. faba*, *P. sativum*, and *N. tabacum* but not in *H. vulgare* (**Table 2**).

Impact of Nitrogen Deficiency Under Drought

In *P. sativum* and *H. vulgare*, we studied the combined effects of water scarcity and lowered nitrogen availability in more detail. Contrary to expectations, reduction in NO_3^- availability for several days had no negative effect on TR in either species (**Figure 1**; **Table 3**). Reduced NO_3^- availability caused a significant reduction of NO_3^- content in roots of both species but leaf content was not reduced in *P. sativum* (**Figure 2**; **Table 3**). The fall in TR under drought was similar under full or reduced NO_3^- supply (**Figure 1**). WP of *P. sativum* decreased under water limitation, but in *H. vulgare* the decrease was not significant (**Figure 3**; **Table 3**).

Regression analysis revealed that the WP decrease in FN treatment occurred under higher SWC (**Figure 3B**) than in LN

TABLE 3 | Significance of the experimental factors and their interaction was analyzed by two-way ANOVA.

Trait	*Pisum sativum*			*Hordeum vulgare*		
	Water	Nitrogen	W × N	Water	Nitrogen	W × N
TR	0.000	0.683	0.251	0.000	0.536	0.618
WP	0.000	0.460	0.550	0.115	0.561	0.059
$[NO_3^-]_L$	0.197	0.960	0.082	0.718	0.000	0.472
$[NO_3^-]_R$	0.000	0.000	0.854	0.698	0.000	0.420
NRA_L	0.104	0.003	0.030	0.901	0.000	0.425
NRA_R	0.000	0.000	0.021	0.396	0.027	0.603
$[NO_3^-]_S$	0.000	0.002	0.676	0.179	0.000	0.781
Sap pH	0.004	0.870	0.953	0.201	0.714	0.439

TR, whole plant transpiration rate; WP, leaf water potential; [NO3-]L and [NO3-]R, NO3- content in the biomass of leaves and roots; [NO3-]S, concentration of NO3- in xylem sap; NRAL and NRAR, NO3- reductase activity in leaves and roots; and sap pH, pH of the xylem sap.

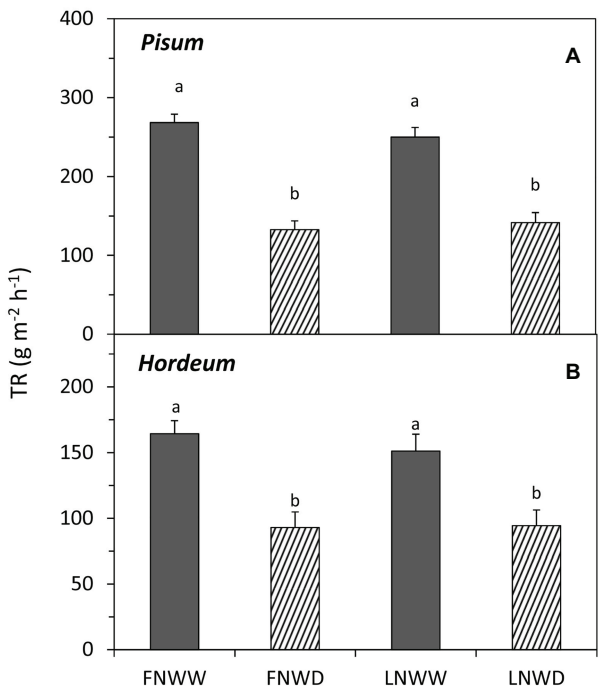

FIGURE 1 | Mean transpiration rates (TRs) of *Pisum sativum* **(A)** and *Hordeum vulgare* **(B)** plants after 2–6 days treatment with different water and nitrogen availability. FNWW plants received 4 mM nitrate ($NO3^-$) daily, FNWD plants received 4 mM $NO3^-$ at the start but no water during the sampling period, LNWW plants received 0.2 mM $NO3^-$ daily, and LNWD plants received 0.2 mM $NO3^-$ at the start but no water during the sampling period. The graph shows means ± SE (n = 6–17). Significant differences ($p \leq 0.05$) between treatments were tested separately for each species and are marked by different letters. FN, full nitrogen; LN, low nitrogen; WW, well-watered; and WD, water deficient.

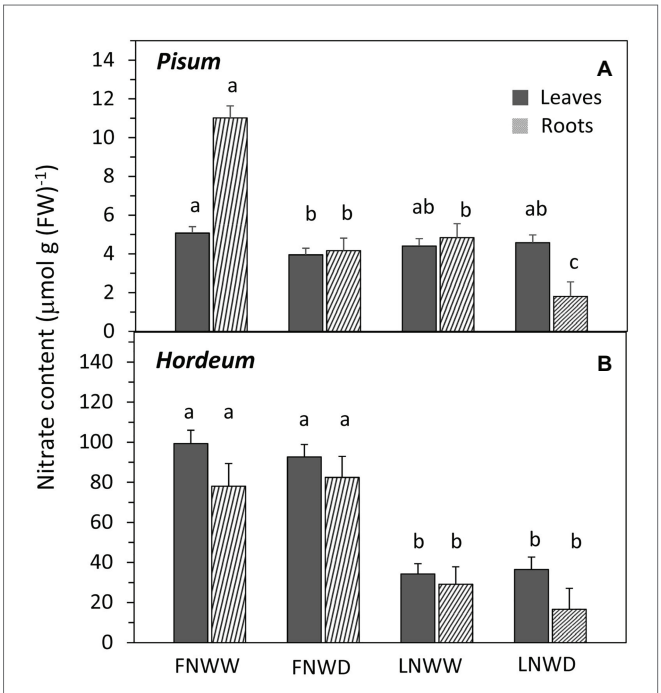

FIGURE 2 | Mean $NO3^-$ content in leaf and root biomass of *P. sativum* **(A)** and *H. vulgare* **(B)** plants after 2–6 days treatment with different water and nitrogen availability. FNWW plants received 4 mM $NO3^-$ daily, FNWD plants received 4 mM $NO3^-$ at the start but no water during the sampling period, LNWW plants received 0.2 mM $NO3^-$ daily, and LNWD plants received 0.2 mM $NO3^-$ at the start but no water during the sampling period. The graph shows means ± SE (n = 6–17). Significant differences ($p \leq 0.05$) between treatments were tested separately for each organ of respective species separately and are marked by different letters. FN, full nitrogen; LN, low nitrogen; WW, well-watered; and WD, water deficient.

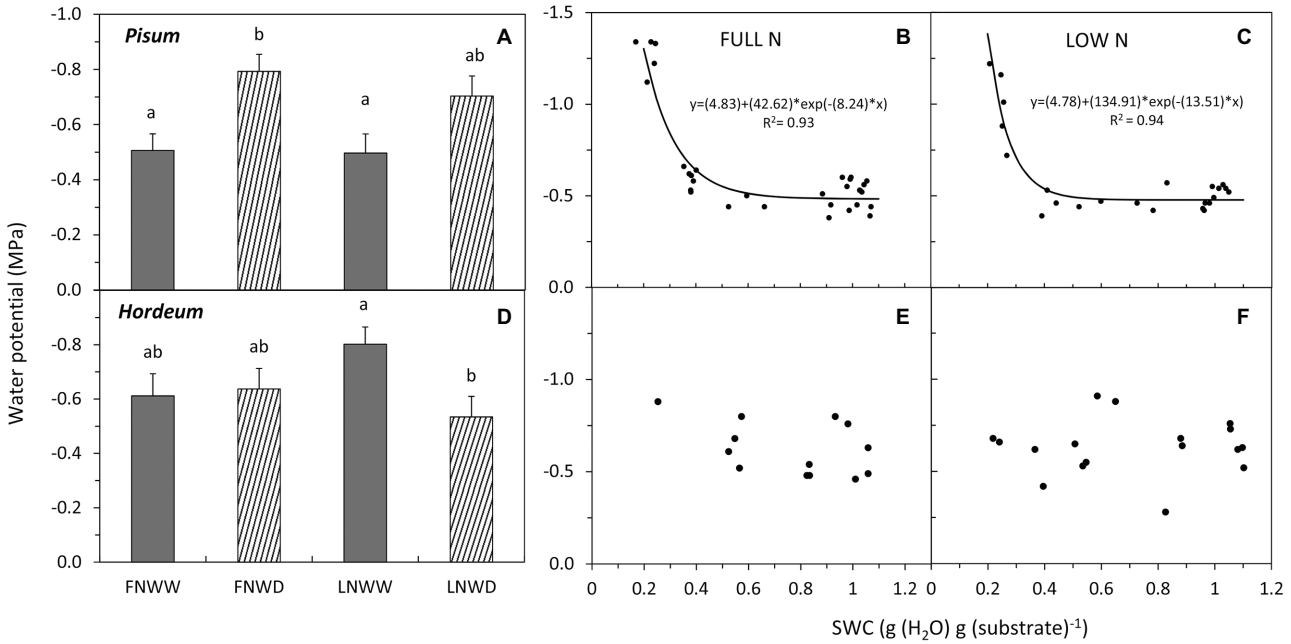

FIGURE 3 | Mean water potential (WP) of *P. sativum* **(A,B,C)** shoots and *H. vulgare* **(D,E,F)** leaves after 2–6 days treatment with different water and nitrogen availability. FNWW plants received 4 mM $NO3^-$ daily, FNWD plants received 4 mM $NO3^-$ at the start but no water during the sampling period, LNWW plants received 0.2 mM $NO3^-$ daily, and LNWD plants received 0.2 mM $NO3^-$ at the start but no water during the sampling period. The graph **(A,D)** shows means in each treatment ± SE (n = 6–17). Significant differences ($p \leq 0.05$) between treatments were tested separately for each species and are marked by different letters. Dynamic changes of WP with declining substrate water content (SWC) are shown in **(B,C)** for P. sativum; **(E,F)** for H. vulgare under full $NO3^-$ (FN) and low $NO3^-$ (LN) availability. Significant relationships are marked by a regression line with the corresponding equation. FN, full nitrogen; LN, low nitrogen; WW, well-watered; and WD, water deficient.

treated plants, where the decrease under low SWC was steeper (**Figure 3C**). Drought had a significant negative effect on NO_3^- content in roots of *P. sativum* but no interaction of these factors was detected (**Figure 2A, Table 3**). NRA was significantly reduced in roots and leaves of both species in LN treatment (**Figure 4**). The negative effect of drought on NRA was observed only in *P. sativum* roots, and the negative effects of LN and reduced water availability were synergistic (**Table 3**), resulting in a much greater decrease of NRA of roots when both stress factors were applied simultaneously (**Figure 4**). Reduced NO_3^- availability significantly reduced NO_3^- transport in shoot xylem of both species (**Figures 5A,D**). From the group comparison, it is clear that the effect of drought was significant only under FN treatment in *P. sativum* (**Figure 5A**).

The relationship between changes in sap NO_3^- concentration and SWC revealed two interesting findings. Firstly, under FN treatment, substrate drying led to a gradual decrease in NO_3^- concentration in the sap, but this effect was not apparent in LN treated plants (**Figures 5C,F**). Secondly, in *P. sativum*, we observed a transient increase in NO_3^- concentration in moderately dry substrate (approx. 0.7–0.8 g g^{-1} = 60–70% of the field water capacity, **Figure 5B**). The initial increase of sap NO_3^- was confirmed also by a separate linear regression analysis of sap NO_3^- concentrations when SWC was above 0.7 g g^{-1} ($p \geq 0.003$). Xylem sap pH decreased in response to reduced water availability in *P. sativum* (**Figure 6A**; **Table 3**) but no significant response was detected in *H. vulgare* (**Figure 6D**; **Table 3**). Moreover, the relationship between pH and SWC showed a transient increase in *P. sativum* xylem sap pH, with this effect being apparent in both FN and LN treatments (**Figures 6B,C**). The range of SWC over which the pH increased was similar to that observed for the increase in sap NO_3^- concentration. No such a response was observed in *H. vulgare* plants (**Figures 6E,F**).

DISCUSSION

Water Availability and Nitrate Utilization by Plant

Drought Has a Negative Effect on NO_3^- Availability and NO_3^- Content

Under drought, the NO_3^- content in biomass decreased in the majority of species we examined, implying a significant decline in NO_3^- uptake (**Table 2**). This effect is probably due to a reduction of mass flow or diffusion-driven uptake of NO_3^- from soil to root. It is known that short drought periods do not cause a decline in N-uptake due to low carbon (energy) supply from the shoot (Buljovcic and Engels, 2001). Decrease of SWC hinders the movement of soil solutions, due to increased hydraulic resistance as well as the reduced root surface area in contact with soil solution (Ehlers and Goss, 2016). Root shrinkage might also reduce the contact area (Nobel and Cui, 1992). The combined effect is decreased

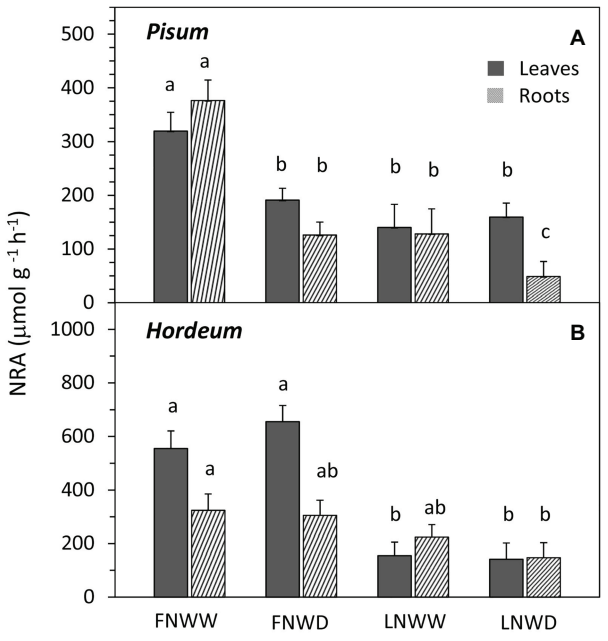

FIGURE 4 | Mean nitrate reductase activity (NRA) in leaf and root biomass of *P. sativum* **(A)** and *H. vulgare* **(B)** plants after 2–6 days treatment with different water and nitrogen availability. FNWW plants received 4 mM $NO3^-$ daily, FNWD plants received 4 mM $NO3^-$ at the start but no water during the sampling period, LNWW plants received 0.2 mM $NO3^-$ daily, and LNWD plants received 0.2 mM $NO3^-$ at the start but no water during the sampling period. Presented are means ± SE (n = 6–17). Significant differences ($p \leq 0.05$) between treatments were tested separately for each species and are marked by different letters. FN, full nitrogen; LN, low nitrogen; WW, well-watered; and WD, water deficient.

delivery of NO_3^- to the root rhizodermis and its lowered uptake, unless the plant responds synthesizing new transport proteins, as suggested by Buljovcic and Engels (2001) and others (Bassett et al., 2014; Duan et al., 2016). Our results reveal a drought-induced reduction in NO_3^--uptake, as indicated by changes in the NO_3^- content in the biomass, for *V. faba*, *N. tabacum*, and *P. sativum* but not for *H. vulgare*. Barley had the highest NO_3^- concentrations by far, and this did not change in response to drought. Moreover, it did not change much when only 0.2 mM NO_3^- was supplied (**Figure 2B**). We do not know exactly why barley is unlike other species in this respect, but it is likely due to the result of selection by breeders who have attempted to increase nitrogen uptake efficiency for barley. These selection efforts have led to changes that combine favorable root morphology with more efficient NO_3^- transporters (Bingham et al., 2012). Species with extensive root systems (e.g., Poaceae) typically show better NO_3^- acquisition (Lainé et al., 1993).

We observed a transient but significant increase of NO_3^- concentration in *P. sativum* xylem sap in the early phase of drying when fully supplied (FN) with NO_3^- (**Figure 5**). No such increase was detected in plants supplied with LN. This suggests that this transient increase is linked to greater NO_3^- uptake from substrate and cannot be explained only by NO_3^- mobilization from root cell reserves. Moreover, evaporation of water from soil might potentiate short term NO_3^- uptake by roots in as the soil concentration of NO_3^- increases when water evaporates. Nevertheless, the contribution of this effect has never been properly evaluated. This mechanism could explain the previously observed transient increase in xylem NO_3^- concentration following increased osmotic pressure of the solution (Larsson et al., 1989) or during the course of gradual drying (Wilkinson et al., 2007).

Drought Affects the Distribution of Nitrate in the Plant

Typically, higher NO_3^- concentrations were observed in roots than in leaves of the species we examined (**Table 2**). Lower SWC led to a relatively greater reduction in NO_3^- in roots than in leaves. The leaf NO_3^- pool was significantly reduced in WD plants of all species except *H. vulgare*. Again, this might be attributable to better nitrogen uptake efficiency relative to other species. Field bean and pea are legumes that can fix atmospheric nitrogen (in our experiment, we used a rooting substrate that does not harbor the suitable N_2-fixing symbiotic bacteria and no nodulation was observed). It is salient to note that legumes are not bred for higher abundances of root NO_3^- transporters. Tobacco is a plant that is not primarily bred for the amount but rather the quality of its biomass. In tobacco, high contents of NO_3^- or nitrile are undesirable because they are precursors of carcinogenic nitrosamines (Tso, 1972). In other words, breeding programs for nitrogen uptake efficiency are more common for barley and less relevant for the other crops. In their analysis of improvements in the nitrogen use efficiency of barley, Bingham et al. (2012) showed that over 75 years of breeding the nitrogen content of barley has increased as a result of both increased N uptake and utilization efficiencies. Barley might possess a more optimal composition of transporters for NO_3^- uptake enabling enough nitrogen to be taken up when the available concentration of NO_3^- is relatively low (0.2 mM), even in combination with reduced water availability. This is not only reflected as high NO_3^- concentration in *H. vulgare* shoots but also as high sap concentrations in WD plants (**Table 2**). The first conclusion drawn by the results is that *H. vulgare*, in comparison to *P. sativum*, seems to maintain its capacity to take up NO_3^- although NO_3^- and water availability are low. It should be noted that under the water limited conditions applied in our experiments, *H. vulgare* did not show signs of severe drought stress such as a significantly lower WP (**Figure 3**). Also, it is well known that there are large differences in response to nitrogen availability and other environmental factors affecting productivity among plant cultivars (Giles et al., 2017). Therefore, the conclusions presented here may not be readily applicable to all varieties of examined species and this fact should be considered in future experiments.

Drought Negatively Affects Nitrate Assimilation

Many studies have demonstrated the strong negative effect of water deficit on NRA in leaves (Shaner and Boyer, 1976;

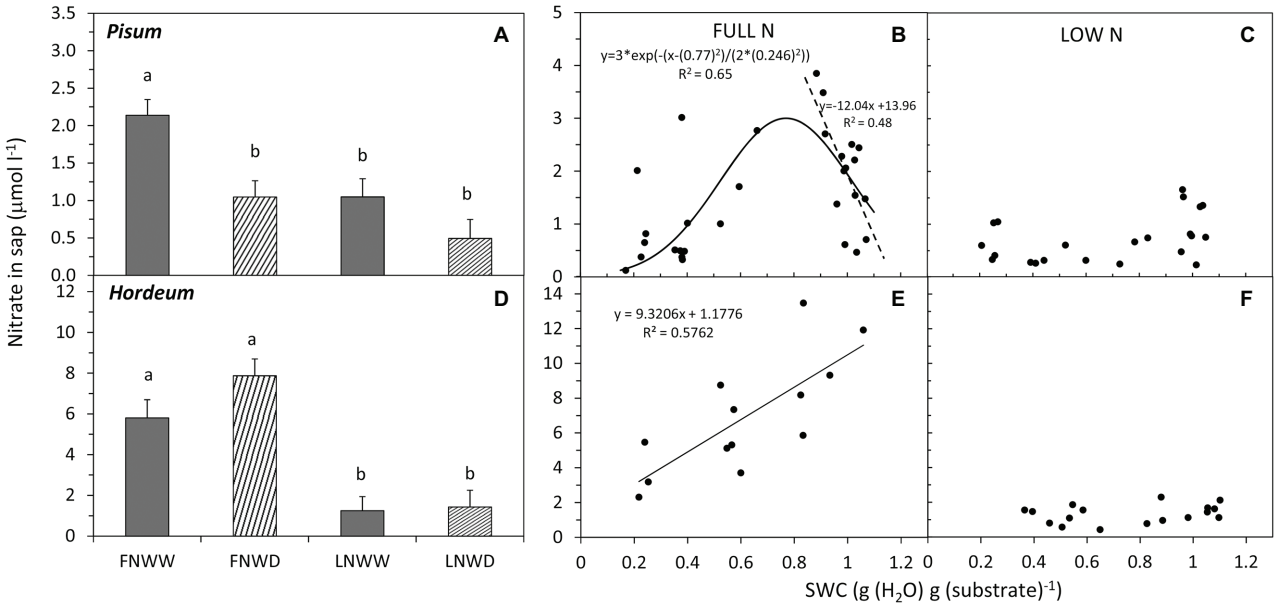

FIGURE 5 | Mean $NO3^-$ concentration in xylem sap of *P. sativum* **(A,B,C)** and *H. vulgare* **(D,E,F)** plants after 2–6 days treatment with different water and nitrogen availability. FNWW plants received 4 mM $NO3^-$ daily, FNWD plants received 4 mM $NO3^-$ at the start but no water during the sampling period, LNWW plants received 0.2 mM $NO3^-$ daily, and LNWD plants received 0.2 mM $NO3^-$ at the start but no water during the sampling period. The graphs **(A,D)** show means in each treatment ± SE (n = 6–17). Significant differences ($p \leq 0.05$) between treatments were tested separately for each species and are marked by different letters. Dynamic changes of $NO3^-$ concentration in sap with declining substrate water content (SWC) are shown in **(B,C)** for *P. sativum*; **(E,F)** for *H. vulgare* under full (FN) and low (LN) $NO3^-$ availability. Significant relationships are marked by a regression line with the corresponding equation. In graph **(B)**, the separate linear regression line was fitted only to SWC above 0.7 $g.g^{-1}$ (significant at $p \leq 0.003$). FN, full nitrogen; LN, low nitrogen; WW, well-watered; and WD, water deficient.

Larsson et al., 1989; Foyer et al., 1998) and roots (Azedo-Silva et al., 2004). That water deficit has a more significant impact on NO_3^- assimilation than on NO_3^- uptake was suggested by Lawlor and Cornic (2002) as they observed a sharp decline in NRA under drought conditions, which was correlated with a reduction of relative water content. In our experiments, NRA was always reduced in roots and leaves of WD treated plants – with the salient exception of barley (**Table 2**). The major difference between barley and the other three species was that NO_3^- content was not reduced by a water deficit. This clearly indicates that availability of the NR substrate (NO_3^-) is more relevant for NR activity as opposed to other drought-related regulatory signals. Shaner and Boyer (1976) showed that decline in transport of NO_3^- to shoot can be more closely related to NRA than total content of NO_3^- in leaf biomass of maize. In WD treatment of our experiments was NO_3^- delivery to leaves also reduced. Possible "buffering effect" of high NO_3^- in biomass and relatively smaller decrease in delivery rate in comparison to other examined species can be possible explanation of this different result. Besides NO_3^- availability (Kaiser et al., 2002), the availability of carbohydrates (Larios et al., 2001), or products of nitrogen assimilation (Scheible et al., 1997) may have also been shown to have a regulatory effect on NRA. More detailed analysis of the relationship between NO_3^- transport and NRA, including other regulatory signals, represents the next logical step in clarifying uncertainties related to the early impact of drought on nitrogen assimilation in barley.

Nitrate Availability and Plant Response to Drought

Early Response to Drought and Nitrate Assimilation

In our experiments, we tested the hypothesis that NO_3^- availability is not only affected by reduced water availability in the substrate but it can also modulate the plant drought response. Lips (1997) proposed a model explaining how NO_3^- can be involved in the plant drought response. Declining water availability would reduce NO_3^- uptake and transport to the shoot. This change then triggers a relatively larger decrease of NRA in the shoot rather than the root. Consequently, the increased proportion of NRA in roots would increase xylem sap pH due to the export of organic acids anions from the symplast into the apoplast (organic acid anions are formed during NO_3^- reduction; see Introduction for details). Our experiments with four species indeed show that NO_3^- concentration in organs and NO_3^- transport to the shoot are mostly reduced even in the early phase of drought (**Tables 2, 3**), presumably due to restricted NO_3^- uptake. On the other hand, under drought conditions, NRA was always more reduced in roots than in leaves. This was the case in all species that differed in the primary contribution of leaves and roots to plant NO_3^- assimilation –

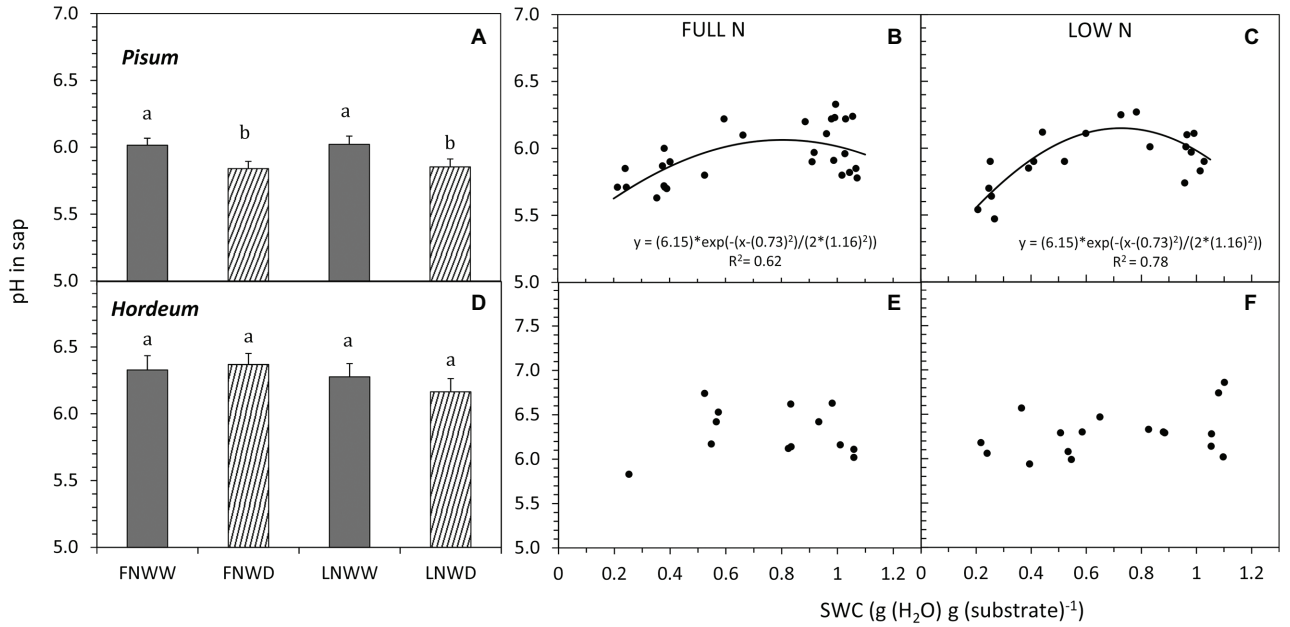

FIGURE 6 | Mean pH in xylem sap (pH in sap) of *P. sativum* **(A,B,C)** and *H. vulgare* **(D,E,F)** plants after 2–6 days of treatments with different water and nitrogen availability. FNWW plants received 4 mM $NO3^-$ daily, FNWD plants received 4 mM $NO3^-$ at the start but no water during the sampling period, LNWW plants received 0.2 mM $NO3^-$ daily, and LNWD plants received 0.2 mM $NO3^-$ at the start but no water during the sampling period. The graphs **(A,D)** show means in each treatment ± SE (n = 6–17). Significant differences ($p \leq 0.05$) between treatments were tested separately for each species and are marked by different letters. Dynamic changes of pH in sap with declining SWC are shown in **(B,C)** for *P. sativum*; **(E,F)** for *H. vulgare* under full (FN) and low (LN) $NO3^-$ availability. Significant relationships are marked by a regression line with the corresponding equation. FN, full nitrogen; LN, low nitrogen; WW, well-watered; and WD, water deficient.

legumes with relatively higher NRA in roots vs. non-legumes with rather equal distribution of NRA (**Table 2**). Therefore, the increased sap pH due to a shift of NRA from leaves to roots seems unlikely, just like the sequence of events that lead to pH-driven ABA accumulation as described above. In fact, we did not observe sap alkalization in any of the examined species when we compared only WW and WD treatments. On the contrary, *V. faba* and *P. sativum* responded to drought by sap acidification. Correlation analysis of data also did not find any relationship between NRA either in leaves or in roots and sap pH in *P. sativum*, *H. vulgare*, and *N. tabacum*. This result fits well with our previous multi-species study, which showed that the dominant site of NO_3^- reduction has no effect on sap pH under drought (Gloser et al., 2016). On the other hand, reduced NO_3^- uptake and transport under declining SWC can lead to changes in sap pH. Changes of sap pH of both *P. sativum* and *H. vulgare* were, however, similar in both FN and LN treatments (**Figure 6**), suggesting that a short-term reduction in NO_3^- availability has little or no effect on sap pH. Thus, we can clearly say that our data collected from four different species do not support the model proposed by Lips (1997).

Consequences of Short-Term Low Nitrogen Treatment Under Drought

We used two species, namely *P. sativum* and *H. vulgare*, for follow-up experiments where the combined effects of short-term deficiency of both water and nitrogen were analyzed in detail. For both species, there were no short-term effects of NO_3^- availability on the whole plant TR (**Figure 1**). This is not surprising considering that leaf NO_3^- concentration was stable over the experimental time frame in *P. sativum* plants that were supplied with 0.2 mM NO_3^- relative to plants supplied with 4 mM NO_3^- (**Figure 2**). In *H. vulgare*, there was a significant decrease in NO_3^-, and yet leaf NO_3^- concentration was eight times higher compared to *P. sativum* leaves (**Figure 1**). In other words, we assume that the reduction in leaf NO_3^- amount in the LN treatment of plants in solid media was not strong and fast enough over the duration of the experiment. It could explain different conclusions of Chapin et al. (1988) where NO_3^- content in the leaves of plants rapidly transferred to N-free solution decreased to 30–40% of control plants within 2 days. They also observed a simultaneous decrease in TR, probably as a consequence of higher ABA concentration in leaves.

In our short-term experiments, we also did not observe any interactive effects of NO_3^- and water deficiency on TR. We found a transient increase of sap pH in *P. sativum*. This pattern of pH change has been previously observed in some other species (Gloser et al., 2016) but the origin and the regulatory implications for the leaf apoplast remain unclear. We therefore conclude that NO_3^- availability in soil is not linked to the modulation of transpiration in the short-term (up to 2–6 days) as long as leaf NO_3^- levels remain stable. Lower NO_3^- levels in leaves, however, may

contribute to stomatal regulation over longer periods of N-starvation as suggested by Chapin et al. (1988).

DATA AVAILABILITY STATEMENT

The raw data supporting the conclusions of this article will be made available by the authors, to any qualified researcher after request.

AUTHOR CONTRIBUTIONS

VG and CG conceptualized the main research questions, designed experiments and wrote the manuscript. VG, MD, DM, BP, and PG collected data. VG and MD performed the data analyses. All authors contributed to the article and approved the submitted version.

FUNDING

This work supported by the German Academic Exchange Service and The Czech Ministry of Education Youth and Sports *via* the bilateral project MOBILITY grant (reg. no. 8J19DE007) and by a BMBF research grant (CUBES Circle 031B0733A), which is gratefully acknowledged.

ACKNOWLEDGMENTS

We thank Oldřich Jůza for valuable technical assistance.

SUPPLEMENTARY MATERIAL

The Supplementary Material for this article can be found online at: https://www.frontiersin.org/articles/10.3389/fpls.2020.602065/full#supplementary-material

REFERENCES

Andrews, M. (1986). The partitioning of nitrate assimilation between root and shoot of higher plants. *Plant Cell Environ.* 9, 511–519. doi: 10.1111/1365-3040.ep11616228

Araus, V., Swift, J., Alvarez, J. M., Henry, A., and Coruzzi, G. M. (2020). A balancing act: how plants integrate nitrogen and water signals. *J. Exp. Bot.* 71, 4442–4451. doi: 10.1093/jxb/eraa054

Azedo-Silva, J., Osório, J., Fonseca, F., and Correia, M. J. (2004). Effects of soil drying and subsequent re-watering on the activity of nitrate reductase in roots and leaves of *Helianthus annuus*. *Funct. Plant Biol.* 31, 611–621. doi: 10.1071/FP04018

Bassett, C. L., Baldo, A. M., Moore, J. T., Jenkins, R. M., Soffe, D. S., Wisniewski, M. E., et al. (2014). Genes responding to water deficit in apple (*Malus* × domestica Borkh.) roots. *BMC Plant Biol.* 14:182. doi: 10.1186/1471-2229-14-182

Bingham, I. J., Karley, A. J., White, P. J., Thomas, W. T. B., and Russell, J. R. (2012). Analysis of improvements in nitrogen use efficiency associated with 75 years of spring barley breeding. *Eur. J. Agron.* 42, 49–58. doi: 10.1016/j.eja.2011.10.003

Black, B. L., Fuchigami, L. H., and Coleman, G. D. (2002). Partitioning of nitrate assimilation among leaves, stems and roots of poplar. *Tree Physiol.* 22, 717–724. doi: 10.1093/treephys/22.10.717

Boyer, J. S. (1967). Leaf water potentials measured with a pressure chamber. *Plant Physiol.* 42, 133–137. doi: 10.1104/pp.42.1.133

Brewitz, E., Larsson, C. -M., and Larsson, M. (1996). Responses of nitrate assimilation and N translocation in tomato (*Lycopersicon esculentum* mill) to reduced ambient air humidity. *J. Exp. Bot.* 47, 855–861. doi: 10.1093/jxb/47.7.855

Buljovcic, Z., and Engels, C. (2001). Nitrate uptake ability by maize roots during and after drought stress. *Plant Soil* 229, 125–135. doi: 10.1023/A:1004879201623

Cataldo, D. A., Haroon, M., Schrader, L. E., and Youngs, V. L. (1975). Rapid colorimetric determination of nitrate in plant tissue by nitration of salicylic acid. *Commun. Soil Sci. Plant Anal.* 61, 71–80. doi: 10.1080/00103627509366547

Chapin, F. S. III. (1991). Integrated responses of plants to stress. *Bioscience* 41, 29–36. doi: 10.2307/1311538

Chapin, F. S. III., Walter, C. H., and Clarkson, D. T. (1988). Growth response of barley and tomato to nitrogen stress and its control by abscisic acid, water relations and photosynthesis. *Planta* 173, 352–366. doi: 10.1007/BF00401022

Correia, M. J., Fonseca, F., Azedo-Silva, J., Dias, C., David, M. M., Barrote, I., et al. (2005). Effects of water deficit on the activity of nitrate reductase and content of sugars, nitrate and free amino acids in the leaves and roots of sunflower and white lupin plants growing under two nutrient supply regimes. *Physiol. Plant.* 124, 61–70. doi: 10.1111/j.1399-3054.2005.00486.x

Davies, W. J., Wilkinson, S., and Loveys, B. (2002). Stomatal control by chemical signalling and the exploitation of this mechanism to increase water use efficiency in agriculture. *New Phytol.* 153, 449–460. doi: 10.1046/j.0028-646X.2001.00345.x

Dijkshoorn, W. (1962). Metabolic regulation of the alkaline effect of nitrate utilization in plants. *Nature* 194, 165–167. doi: 10.1038/194165a0

Dodd, I. C., Theobald, J. C., Richer, S. K., and Davies, W. J. (2009). Partial phenotypic reversion of ABA-deficient flacca tomato (*Solanum lycopersicum*) scions by a wild-type rootstock: normalizing shoot ethylene relations promotes leaf area but does not diminish whole plant transpiration rate. *J. Exp. Bot.* 60, 4029–4039. doi: 10.1093/jxb/erp236

Duan, J., Tian, H., and Gao, Y. (2016). Expression of nitrogen transporter genes in roots of winter wheat (*Triticum aestivum* L.) in response to soil drought with contrasting nitrogen supplies. *Crop Past Sci.* 67, 128–136. doi: 10.1071/CP15152

Ehlers, W., and Goss, M. (2016). *Water dynamics in plant production. 2nd Edn*. Wallingford, Boston: CABI.

Foyer, C. H., Valadier, M. H., Migge, A., and Becker, T. H. (1998). Drought-induced effects on nitrate reductase activity and mRNA and on the coordination of nitrogen and carbon metabolism in maize leaves. *Plant Physiol.* 117, 283–292. doi: 10.1104/pp.117.1.283

Geilfus, C. M., Mithöfer, A., Ludwig-Müller, J., Zörb, C., and Muehling, K. H. (2015). Chloride-inducible transient apoplastic alkalinizations induce stomata closure by controlling abscisic acid distribution between leaf apoplast and guard cells in salt-stressed *Vicia faba*. *New Phytol.* 208, 803–816. doi: 10.1111/nph.13507

Geilfus, C. M., Tenhaken, R., and Carpentier, S. C. (2017). Transient alkalinization of the leaf apoplast stiffens the cell wall during onset of chloride salinity in corn leaves. *J. Biol. Chem.* 292, 18800–18813. doi: 10.1074/jbc.M117.799866

Giles, C. D., Brown, L. K., Adu, M. O., Mezeli, M. M., Sandral, G. A., Simpson, R. J., et al. (2017). Response-based selection of barley cultivars and legume species for complementarity: root morphology and exudation in relation to nutrient source. *Plant Sci.* 255, 12–28. doi: 10.1016/j.plantsci.2016.11.002

Gloser, V., Korovetska, H., Martin-Vertedor, A. I., Hájíčková, M., Prokop, Z., Wilkinson, S., et al. (2016). The dynamics of xylem sap pH under drought: a universal response in herbs? *Plant Soil* 409, 259–272. doi: 10.1007/s11104-016-2962-6

Gollan, T., Schurr, U., and Schulze, E. D. (1992). Stomatal response to drying soil in relation to changes in the xylem sap composition of *Helianthus annuus*. I. the concentration of cations, anions, amino acids in, and pH of, the xylem sap. *Plant Cell Environ.* 155, 551–559. doi: 10.1111/j.1365-3040.1992.tb01488.x

Goodger, J. Q. D., Sharp, R. E., Marsh, E. L., and Schachtman, D. P. (2005). Relationships between xylem sap constituents and leaf conductance of well-watered and water-stressed maize across three xylem sap sampling techniques. *J. Exp. Bot.* 56, 2389–2400. doi: 10.1093/jxb/eri231

Hachiya, T., and Sakakibara, H. (2017). Interactions between nitrate and ammonium in their uptake, allocation, assimilation, and signaling in plants. *J. Exp. Bot.* 68, 2501–2512. doi: 10.1093/jxb/erw449

Jia, W., and Davies, W. J. (2007). Modification of leaf apoplastic pH in relation to stomatal sensitivity to root-sourced abscisic acid signals. *Plant Physiol.* 143, 68–77. doi: 10.1104/pp.106.089110

Kaiser, W. M., Weiner, H., Kandlbinder, A., Tsai, C. -B., Rockel, P., Sonoda, M., et al. (2002). Modulation of nitrate reductase: some new insights, an unusual case and a potentially important side reaction. *J. Exp. Bot.* 53, 875–882. doi: 10.1093/jexbot/53.370.875

Karuppanapandian, T., Geilfus, C. M., Muehling, K. H., Novák, O., and Gloser, V. (2017). Early changes of the pH of the apoplast are different in leaves, stem and roots of *Vicia faba* L. under declining water availability. *Plant Sci.* 255, 51–58. doi: 10.1016/j.plantsci.2016.11.010

Lainé, P., Ourry, A., Macduff, J., Boucaud, J., and Salette, J. (1993). Kinetic parameters of nitrate uptake by different catch crop species: effects of low temperatures or previous nitrate starvation. *Physiol. Plant.* 88, 85–92. doi: 10.1111/j.1399-3054.1993.tb01764.x

Larios, B., Aguera, E., de la Haba, P., Perez-Vicente, R., and Maldonado, J. M. (2001). A short-term exposure of cucumber plants to rising atmospheric CO_2 increases leaf carbohydrate content and enhances nitrate reductase expression and activity. *Planta* 212, 305–312. doi: 10.1007/s004250000395

Larsson, M., Larsson, C. M., Whitford, P. N., and Clarkson, D. T. (1989). Influence of osmotic stress on nitrate reductase activity in wheat (*Triticum aestivum* L.) and the role of abscisic acid. *J. Exp. Bot.* 40, 1265–1271. doi: 10.1093/jxb/40.11.1265

Lawlor, D. W., and Cornic, G. (2002). Photosynthetic carbon assimilation and associated metabolism in relation to water deficits in higher plants. *Plant Cell Environ.* 25, 275–294. doi: 10.1046/j.0016-8025.2001.00814.x

Li, W., de Ollas, C., and Dodd, I. C. (2018). Long-distance ABA transport can mediate distal tissue responses by affecting local ABA concentrations. *J. Integr. Plant Biol.* 60, 16–33. doi: 10.1111/jipb.12605

Lips, S. H. (1997). The role of inorganic nitrogen ions in plant adaptation processes. *Russ. J. Plant Physiol.* 44, 421–431.

Lu, C., and Zhang, J. (2000). Photosynthetic CO_2 assimilation, chlorophyll fluorescence and photoinhibition as affected by nitrogen deficiency in maize plants. *Plant Sci.* 151, 135–143. doi: 10.1016/S0168-9452(99)00207-1

Marschner, H. (1995). *Mineral nutrition of higher plants*. Cambridge: Academic Press, 889.

Matimati, I., Verboom, G. A., and Cramer, M. D. (2014). Nitrogen regulation of transpiration controls mass-flow acquisition of nutrients. *J. Exp. Bot.* 65, 159–168. doi: 10.1093/jxb/ert367

McAdam, S. A., Manzi, M., Ross, J. J., Brodribb, T. J., and Gómez-Cadenas, A. (2016). Uprooting an abscisic acid paradigm: shoots are the primary source. *Plant Signal. Behav.* 11, 652–659. doi: 10.1080/15592324.2016.1169359

Nobel, P. S., and Cui, M. (1992). Shrinkage of attached roots of *Opuntia ficus-indica* in response to lowered water potentials—predicted consequences for water uptake or loss to soil. *Ann. Bot.* 70, 485–491. doi: 10.1093/oxfordjournals.aob.a088508

Peuke, A. D., Glaab, J., Kaiser, W. M., and Jeschke, W. D. (1996). The uptake and flow of C, N and ions between roots and shoots in *Ricinus communis* L. IV. Flow and metabolism of inorganic nitrogen and malate depending on nitrogen nutrition and salt treatment. *J. Exp. Bot.* 47, 377–385. doi: 10.1093/jxb/47.3.377

Plett, D. C., Ranathunge, K., Melino, V. J., Kuya, N., Uga, Y., and Kronzucker, H. J. (2020). The intersection of nitrogen nutrition and water use in plants: new paths toward improved crop productivity. *J. Exp. Bot.* 71, 4452–4468. doi: 10.1093/jxb/eraa049

Roelfsema, M. R. G., Hanstein, S., Felle, H. H., and Hedrich, R. (2002). CO_2 provides an intermediate link in the red light response of guard cells. *Plant J.* 32, 65–75. doi: 10.1046/j.1365-313X.2002.01403.x

Roelfsema, M. R. G., Konrad, K. R., Marten, H., Psaras, G. K., Hartung, W., and Hedrich, R. (2006). Guard cells in albino leaf patches do not respond to photosynthetically active radiation, but are sensitive to blue light, CO_2 and abscisic acid. *Plant Cell Environ.* 29, 1595–1605. doi: 10.1111/j.1365-3040.2006.01536.x

Scheible, W. R., Gonzalez-Fontes, A., Morcuende, R., Lauerer, M., Geiger, M., Glaab, J., et al. (1997). Tobacco mutants with a decreased number of functional *nia* genes compensate by modifying the diurnal regulation of transcription, post-translational modification and turnover of nitrate reductase. *Planta* 203, 304–319. doi: 10.1007/s004250050196

Shaner, D. L., and Boyer, J. S. (1976). Nitrate reductase activity in maize (*Zea mays* L.) leaves. II. Regulation by nitrate flux at low leaf potential. *Plant Physiol.* 58, 505–509. doi: 10.1104/pp.58.4.505

Sharp, R. G., and Davies, W. J. (2009). Variability among species in the apoplastic pH signalling response to drying soils. *J. Exp. Bot.* 60, 4363–4370. doi: 10.1093/jxb/erp273

Tezara, W., Mitchell, V. J., Driscoll, S. D., and Lawlor, D. W. (1999). Water stress inhibits plant photosynthesis by decreasing coupling factor and ATP. *Nature* 401, 914–917.

Tominaga, M., Kinoshita, T., and Shimazaki, K. (2001). Guard-cell chloroplasts provide ATP required for H1 pumping in the plasma membrane and stomatal opening. *Plant Cell Physiol.* 42, 795–802. doi: 10.1093/pcp/pce101

Tso, T. C. (1972). *Physiology and biochemistry of tobacco plants*. Stroudsburg: Dowden, Hutchinson & Ross, Inc.

Wilkinson, S. (2004). "Water use efficiency and chemical signalling" in *Water use efficiency in plant biology*. ed. M. A. Bacon (Oxford: Blackwell Publishing Ltd), 75–112.

Wilkinson, S., Bacon, M. A., and Davies, W. J. (2007). Nitrate signalling to stomata and growing leaves: interactions with soil drying, ABA and xylem sap pH in maize. *J. Exp. Bot.* 58, 1705–1716. doi: 10.1093/jxb/erm021

Wilkinson, S., Corlett, J. E., Oger, L., and Davies, W. J. (1998). Effects of xylem pH on transpiration from wild-type and flacca tomato leaves: a vital role for abscisic acid in preventing excessive water loss even from well-watered plants. *Plant Physiol.* 117, 703–709. doi: 10.1104/pp.117.2.703

Wilkinson, S., and Davies, W. J. (1997). Xylem sap pH increase: a drought signal received at the apoplastic face of the guard cell that involves the suppression of saturable abscisic acid uptake by the epidermal symplast. *Plant Physiol.* 113, 559–557. doi: 10.1104/pp.113.2.559

Wilkinson, S., and Davies, W. J. (2002). ABA-based chemical signalling: the co-ordination of responses to stress in plants. *Plant Cell Environ.* 25, 195–210. doi: 10.1046/j.0016-8025.2001.00824.x

Conflict of Interest: The authors declare that the research was conducted in the absence of any commercial or financial relationships that could be construed as a potential conflict of interest.

frontiers in Plant Science

ORIGINAL RESEARCH
published: 18 January 2021
doi: 10.3389/fpls.2020.601455

Soilless Cultivation: Dynamically Changing Chemical Properties and Physical Conditions of Organic Substrates Influence the Plant Phenotype of Lettuce

*Annika Nerlich and Dennis Dannehl**

Division Biosystems Engineering, Faculty of Life Sciences, Albrecht Daniel Thaer-Institute of Agricultural and Horticultural Sciences, Humboldt University of Berlin, Berlin, Germany

OPEN ACCESS

Edited by:
Christoph Martin Geilfus, Humboldt University of Berlin, Germany

Reviewed by:
Cheng Xue, Agricultural University of Hebei, China
Asif Naeem, Nuclear Institute for Agriculture and Biology, Pakistan

***Correspondence:**
Dennis Dannehl
dennis.dannehl@hu-berlin.de; dennis.dannehl@agrar.hu-berlin.de

Specialty section:
This article was submitted to Plant Nutrition, a section of the journal Frontiers in Plant Science

Received: *01 September 2020*
Accepted: *18 December 2020*
Published: *18 January 2021*

Citation:
Nerlich A and Dannehl D (2021) Soilless Cultivation: Dynamically Changing Chemical Properties and Physical Conditions of Organic Substrates Influence the Plant Phenotype of Lettuce. Front. Plant Sci. 11:601455. doi: 10.3389/fpls.2020.601455

In agriculture, the increasing scarcity of arable land and the increase in extreme weather conditions has led to a large proportion of crops, especially vegetables, being cultivated in protected soilless cultivation methods to provide people with sufficient and high-quality food. Rockwool has been used for decades as a soil substitute in soilless cultivation. Since rockwool is not biodegradable, it is disposed in landfills after its use, which nowadays leads to ecological concerns and drives the search for alternative substrates, especially organic materials. The objectives of this study were to investigate the effects of organic materials (wood chips, sphagnum moss, and hemp fibers) in relation to rockwool substrate on plant growth and quality of lettuce as a result of physical and chemical properties of the mentioned substrates. We were able to show that sphagnum moss is a suitable substitute substrate for lettuce cultivation, contrary to hemp. All investigated substrates presented good physical properties, but differed in their decomposition stability. Within 8 weeks, 30% of the hemp and about 10% of both sphagnum and wood materials were degraded. It was concluded that the increased microbiological activity immobilized nitrogen and led to oxygen deficiency in the rhizosphere and resulted in increased phenolic acid contents in lettuce but poor yield on hemp. Sphagnum caused a pH decrease and accumulation of ammonium in the nutrient solution and allowed the highest yield for lettuce at moderate phenolic acid contents. Low yields were obtained on wood, which could possibly be increased by optimized nutrient solution, so that wood as an alternative to rockwool was not excluded. By applying used organic substrates as soil additives on arable land, the nutrients accumulated in it might fertilize the open field crops, thus saving mineral fertilizers. This, together with the avoidance of waste, would contribute to a greater sustainability.

Keywords: sphagnum moss, oxygen, lettuce, phenolic acids, nitrogen immobilization, rockwool substitutes, organic substrates, soilless cultivation

INTRODUCTION

Soilless cultivation is a modern cultivation system of plants that uses either inert organic or inorganic growing substrates, mostly in combination with nutrient solution to supply nutrients to plants. In this protected cultivation system, the yield and quality of horticultural crops can be significantly improved compared to conventional soil culture by managing the quantity and composition of the nutrient solution as well as the growing medium (Massantini et al., 1988; Xu et al., 1995). Rockwool which offers optimum physical and chemical properties has been used in greenhouse cultivation for decades (Sonneveld, 1991). An estimated area of more than 10,000 ha is cultivated in rockwool slabs worldwide, including 6,000 ha greenhouse area in Europe (Blok and Urrestarazu, 2010). The growing awareness that the disposal of rockwool substrates is not only expensive but also difficult due to their non-biodegradability and the strong negative effects on human health (Benoit and Ceustermans, 1995; Quantis, 2012) had led to the search for alternative materials. The suitability of various organic substrates as a substitute for rockwool substrates, such as wood, coconut fibers, hemp, bark, and sawdust, etc., has been investigated by many researchers (Allaire et al., 2005; Dannehl et al., 2015; Xiong et al., 2017). For a successful soilless cultivation of horticultural crops, differences in specific properties of each substrate must be considered. Various vegetable and ornamental plants have been successfully grown in bark (Wilson, 1984; Shaw et al., 2004), but also phenolic compounds with a phytotoxic effect could be extracted from the substrate (Politycka et al., 1985). Gruda (2009) noted that the activity of microorganisms should be considered when comparing potential substrates, such as bark, wood fibers, paper, and straw, to assess their suitability as growing media. Increased microbial activity can lead to nitrogen immobilization, as mineral nitrogen from the nutrient solution, is used during the mineralization of organic matter (Jansson, 1958). This reduces the nitrogen availability for plants, which in turn can lead to possible losses in product quality (Gruda, 2009). In general, several properties of a substrate, e.g., particle size, water and nutrient holding capacities, cation exchange capacity and nutrient content influence the retention, movement and availability of mineral nutrients in the root-zone (Islam et al., 2002; Sahin et al., 2002; Ao et al., 2008). Consequently, depending on the substrate properties, an adjustment of the mineral content of the applied nutrient solution should be considered in order to meet the nutrient requirements of the crops.

To produce plants in an environmentally friendly way, suitable organic substrates must be used as a substitute for rockwool. This is the only way to avoid high energy consumption and thus CO_2 emissions during the production of rockwool. In the current study, three organic substrates were used. Wood chips were chosen because they are a waste product of wood processing. Sphagnum seems also to be a good candidate for further investigations because it was shown in a previous study by Dannehl et al. (2015) that this material has optimal physical properties for use as a growing medium. As a third option, the focus was on hemp fibers, as these give the impression of a stable and compact connection after processing. These properties could be advantageous when used as growing medium in the hydroponic system. Based on this selection, the objectives of this study were to investigate the effects of dynamically changing chemical properties and physical conditions of the mentioned organic materials in relation to rockwool substrate on plant growth and quality of lettuce. Of particular interest were physical characteristics gained from water-retention curves, substrate mineralization stability and field capacities of the substrates as well as chemical characteristics in terms of nitrogen dynamics, pH, electrical conductivity (EC) and oxygen concentrations within the different substrates.

We have chosen lettuce (*Lactuca sativa*, variety Descartes RZ) for our pot experiment because on the one hand it grows fast and on the other it is the most common salad vegetable consumed worldwide. Lettuce is known to be a good source of health-promoting compounds, especially phenolic compounds (Llorach et al., 2008; Kim et al., 2016). Usually salad is eaten raw, so that many ingredients are preserved. Substitute substrates for rockwool should not negatively influence the content of valuable ingredients and should, for example, maintain a high phenolic acid content in lettuce.

MATERIALS AND METHODS

Experimental Set-Up and Plant Cultivation

Experiments were conducted in a Venlo-type greenhouse at Humboldt-University Berlin, Germany (Latitude 52° 46′ 74″, Longitude 13° 31′ 16″) from October 16th until December 13th 2019. Organic materials tested for their suitability as growth substrates were dried sphagnum moss, wood chips, and hemp fibers. Rockwool as an established substrate was used as a control.

Seeds of lettuce (*L. sativa*, variety Descartes RZ) were sown on October 16th in perlite and transferred to pots with different substrates on October 29th. All pots contained 52 *g* of one of the organic materials or 32 *g* of rockwool. Nine replicates per substrate were prepared and arranged in three randomized blocks. Initially all pots (d = 13 cm, v = 1 L) received 20 ml nutrient solution containing 540 mg/l $Ca(NO_3)_2$, 850 mg/l KNO_3, 128 mg/l $MgSO_4$, 180 mg KH_2PO_4, and 60 mg/l Fe-Chelate (Fetrilon Combi 1, Compo Expert, Münster). Further fertilization occurred successively during irrigation by supplying 76, 27, 18, 21, and 6 mg nitrate 23, 30, 37, 44, and 51 days after sowing (DAS).

As such, each pot received a total of 265 ml of nutrient solution containing 147 mg nitrate during the cultivation. Irrigation was carried out twice a week and three times a week for the last 2 weeks, recording the weights of the pots to determine the water used before replenishing them to their field capacity (FC). The average daytime temperature was set to 19°C, the average night-time temperature to 17°C during the first 33 DAS and from 34 DAS to 22°C daytime temperature and 20°C at night to accelerate growth. Additional light (63 μmol m^{-2} s^{-1}) was

distributed evenly over all 3 blocks from 6 am to 6 pm by high-pressure sodium lamps.

Characterization of Growing Media Utilized for Lettuce Cultivation

Water-Retention Curves (pF – Curves)

The substrates to be used were first examined with regard to different physical parameters, such as total pore space (TPS), air volume (AV), bulk density (BD), and easily available water (EAW). For this purpose, metal rings with a volume of 100 cm^3 were filled with the respective substrates, completely saturated with water and placed on a ceramic pressure plate connected to a manometer. Increasing negative pressure levels (pF-values) were used to drain different pore sizes of the previously water-saturated soil sample (pF 0). The amount of water released at each pressure stage (in our case pF 1.0 and pF 1.8) indicated the pore water volume of a defined pore size range. In this way it was possible to determine the water volume proportions [volumetric water content; θ_V (Eq. 1)] of different sizes of soil pores and thus their percentage shares in the soil. The density of water was assumed to be 1 mg cm^{-3}.

$$\theta_V[Vol\,\%] = \theta_g[g\,g^{-1}] \times \mathrm{BD}[g\,\mathrm{cm}^{-3}] \times 100 \quad (1)$$

The gravimetric water content (θ_g) is given in $g\ g^{-1}$ and is the amount of water in g at each suction point per g substrate (Eq. 2).

$$\theta_g\ \left[g\ g^{-1}\right] = \frac{m_{H_2O}\ [g]}{m_{\mathrm{substrate}}\ [g]} \quad (2)$$

Bulk density indicates the dry mass of the substrate per 100 cm^3 (Eq. 3).

$$\mathrm{BD}\ [g\ \mathrm{cm}^{-3}] = \frac{m_{\mathrm{substrate}}\ [g]}{100\ \mathrm{cm}^{-3}} \quad (3)$$

According to De Boodt and Verdonck (1972) moisture content at zero suction (pf 0) is defined as TPS stated in Vol % and is the product of gravimetric water content (θ_g) and the BD (Eq. 4).

$$\mathrm{TPS}\ [Vol\,\%] = \theta_{g\,(pf0)}\ \left[g\ g^{-1}\right] \times \mathrm{BD}\ [g\ \mathrm{cm}^{-3}] \times 100 \quad (4)$$

The AV is the difference of the gravimetric water content at pF 0 and pF 1 (Eq. 5), the easy available water the difference of the gravimetric water content at pF 1 and pF 1,8 (Eq. 6).

$$\mathrm{AV}\ [Vol\,\%] = \theta_{g(pf0)}\ \left[g\ g^{-1}\right] - \theta_{g(pf1)}\ [g\ g^{-1}] \quad (5)$$

$$\mathrm{EAW}\ [Vol\,\%] = \theta_{g(pf1)}\ \left[g\ g^{-1}\right] - \theta_{g(pf1,8)}\ [g\ g^{-1}] \quad (6)$$

All physical parameters were determined in 5 replicates per substrate.

Field Capacity

To determine the FC, 11 pots per substrate were filled with 32 *g* rockwool, or 52 *g* of the organic substrates and saturated with water overnight. When no more water leaked from the covered pots, the difference in weight between water-filled and dry pots was used to calculate how many *g* of water per *g* of substrate was kept, representing the field capacity (Veihmeyer and Hendrickson, 1931). Means of 11 pots per substrate were calculated and used for irrigation of the plants to ensure no undesired elution of solution and nutrients from the pots. The mean pot weights at field capacity were 310 *g* for hemp, 260 *g* for wood, 530 *g* for sphagnum, and 365 *g* for rockwool. Due to the plant biomass formed or organic substrate mineralized, the target weights of the pots were adjusted to 300 *g*, 280 *g*, 550 *g*, and 385 *g* for hemp, wood, sphagnum and rockwool, respectively, on December 2nd 2019 (47 DAS).

Substrate Mineralization

The determination of the dry mass of all substrate pots by drying in a ventilated oven at 60°C (Heraeus, Hanau, Germany) for 7 days at the beginning and end of lettuce cultivation allowed the calculation of the mineralized organic matter during the experiment. This method was applied according to the method described by Dannehl et al. (2015). The weight reduction that occurred was expressed as percentage (%), with the root biomass not removed. The increase in weight in the rockwool substrates allowed an approximate idea of the root biomass formed in the organic substrates in which plants formed a comparable above-ground biomass as in rockwool substrates.

Substrate Solution Characteristics

Irrigation and fertilization of the substrates creates a "substrate solution" in the pots, which can be influenced by the organic materials used and could thus also influence the growth of the lettuce plants. The properties of the substrate solution that were studied included EC, pH-value, oxygen content and contents of ammonium, and nitrate. To obtain the substrate solution, all pots were filled with tap water to field capacity once a week and then 50 ml of tap water was added to elute excess liquid from pots. Eluates from three pots per substrate and block were collected and combined into one sample. In each sample the pH/EC value was determined according to the manufacturer's instructions using HI9811-5 Portable pH/EC/TDS/Temperature Meter [Hanna Instruments (M), Petaling Jaya, Selangor, Malaysia] and oxygen content was determined using O_2-Meter CG 867 (Schott Geräte GmbH, Hofheim, Germany). The substrate solution was then stored at −20°C until the ammonium and nitrate contents were analyzed with the San++ Continuous-Flow Analysator (Skalar Analytic GmbH, Erkelenz, Germany). Nitrate determination was based on a reaction with hydrazinium sulfate, sulfanilamide and N-(1-naphthyl) ethylenediamine dihydrochloride which results in the formation of a highly colored azo dye which is measured at 540 nm. The determination of ammonium was based on the chlorination of ammonium to monochloramine, which reacts with salicylate to form 5-aminosalicylate. After oxidation and oxidative coupling, a green-colored complex is formed whose absorbance is measured at 660 nm.

Documented Plant Parameters

Water Usage per Plant Biomass

When the plants were watered twice a week, the weights of all pots were documented before they were refilled to

field capacity to determine water consumption by evaporation and transpiration during the growing season. The yield at the harvest date and the summed-up water use was used to calculate the water use efficiency expressed as gram biomass per gram water applied.

Chlorophyll Contents by SPAD Meter

Chlorophyll content of leaves was nondestructively measured with a SPAD-502P portable, measuring device (Minolta Camera Co., Ltd, Osaka, Japan). The numerical SPAD value is proportional to the concentration of chlorophyll present in the leaf and is calculated from measured absorbance of a leaf in the red and near-infrared regions. Since chlorophyll content increases with the amount of nitrogen, a higher SPAD value indicates better nitrogen nutrition of the plant. Based on the plant development, readings were taken on young leaves (hemp: $n = 3$, other substrates $n = 5$) from 9 plants per substrate. SPAD values were documented starting from November 8th (23 DAS) for 6 consecutive weeks.

Yield, Leaf Number, Leaf Area, Dry Matter Content

Yield was determined as fresh mass per lettuce head at the end of the cultivation from 9 plants per substrate. Additionally, leaf number was counted and leaf area (LA) in cm^2 per lettuce head was determined using a leaf area meter (Model LI 3100, LAMBDA Inst. Corp; United States) from 6 plants per substrate.

Three plants from each substrate variant and block were mixed to one sample resulting in 3 samples per substrate for further analysis. Dry mass was determined after freeze-drying (Christ Alpha 1–4, Christ; Osterrode, Germany) for 5 days. The dry matter content expressed in % was calculated by the ratio of the dry mass to the fresh mass.

Extraction and Determination of Phenolic Acids and Flavonoids

The freeze-dried lettuce leaves were ground to a fine powder (MM 30, Retsch GmbH, Haan, Germany) and stored at −80°C until analysis. Extraction and determination of phenolic acids and flavonoids was performed as described by Förster et al. (2015). For analysis a HPLC (Ultimate 3000, Thermo Scientific) equipped with a 150 × 2.1 mm C16 column (AcclaimPA, 3 μm, Thermo Scientific) was used. Commercially available standards of single compounds were utilized as references. The following determined response factors (RF) were used to correct the absorption differences between the internal standard 4-methoxycinnamic acid (1 mM, Sigma Aldrich; RF = 1) and the detected phenolic acids and flavonoids: RF = 1.42 for caffeoyltartaric acid (CT; Sigma-Aldrich) and di CT (Sigma-Aldrich), RF = 1.58 for caffeoylquinic acid (CQ; Sigma-Aldrich) and dicaffeoylquinic acid (diCQ; Sigma-Aldrich), RF = 2.16 for caffeoylmalic acid (CM; Phytolab), and RF = 2.15 for quercetin 3-*O*-(6″-malonylglucoside; Sigma-Aldrich).

Statistical Methods

Data were statistically analyzed using agricolae package (de Mendiburu, 2020) in RStudio Version 1.2.5033 (R Core Team, 2020). The data were first tested for normal distribution and variance homogeneity before an analysis of variance (ANOVA) was applied and a *post hoc* analysis was performed using HSD test. Significant differences between the substrates with respect to their physical properties and influences on the substrate solution properties as well as the resulting different performances of lettuce in terms of yield and quality were calculated. Significance of statistical analyses in this research was concluded for $p < 0.05$ for a given test.

RESULTS

Characteristics of Materials Used as Growing Substrates for Lettuce Cultivation

Physical Properties of the Different Materials Used as Substrates

In pots 52 *g* of the organic substrates and 32 *g* of the rock wool were filled up to 1 cm to the upper edge. The resulting BD per substrate and the proportion of air and water at different humidity levels in them were investigated by water-retention curves (pF curves). Results are depicted in **Table 1**.

The BD of wood and hemp substrates were each 0.10 *g* cm^{-3} and thus higher than the BD of sphagnum (0.08 *g* cm^{-3}) and twice as high as for rockwool (0.05 *g* cm^{-3}). Sphagnum moss and rockwool had the highest TPS with 87 vol% and 90 vol%, respectively, followed by wood with a lower TPS of 81 vol% and hemp with the lowest TPS of 76 vol%. The AV was almost twice as high in wood (29.6 vol%) as in the other substrates used (Hemp 13.9 vol%, sphagnum 12.6 %, and rockwool 18.9 vol%). The proportion of EAW was highest in rockwool (70 vol%) and significantly lower in hemp (41 vol%) followed by wood and sphagnum showing the lowest share of EAW with ∼ 20 vol%. If one compares the measured parameters with the corresponding reference values, all of them are mostly within the recommended limits.

In addition to the water-retention curve, it was also investigated how much water can be stored per g substrate. The amount of water held per g substrate, depicted as field capacity (FC) in **Table 1**, varies significantly for each substrate. Although significantly different, Rockwool (10.4 *g* H_2O/g) and sphagnum (9.2 *g* H_2O/g) could hold similar amounts of water per g substrate. Hemp (4.9 *g* H_2O/g) and wood (3.8 *g* H_2O/g) exhibit half of the FC of rockwool and sphagnum.

Apart from the water and air balance of the substrates, their degradation stability must also be considered, as organic materials, unlike rockwool, can be mineralized during their utilization. **Table 1** shows the mineralized proportion of substrate in %. 30.6% of hemp, 11.3% of wood, and 9.5% of sphagnum were mineralized during 58 days of cultivation. In the case of rockwool, an increase in the mass can be recognized by the negative sign, which is due to the roots of the lettuce plants growing into the substrate. It should be noted that the roots could not be removed from the substrates at the end of the experiment, because they were to firmly anchored in the substrates.

TABLE 1 | Characteristics of the air and water contents in the investigated materials used as growing substrates for lettuce cultivation.

	Hemp	Wood	Sphagnum	Rockwool	Reference*
BD ($g\ cm^{-3}$)	0.10 ± 0.00^a	0.10 ± 0.01^a	0.08 ± 0.01^b	0.05 ± 0.01^c	<0.4
TPS (Vol %)	75.9 ± 2.9^c	81.4 ± 2.0^b	87.4 ± 1.6^a	90.4 ± 2.6^a	75–85
AV (Vol %)	13.9 ± 3.3^b	29.6 ± 2.0^a	12.6 ± 2.7^b	18.9 ± 5.1^b	10–30
EAW (Vol %)	41.4 ± 2.0^b	22.4 ± 1.4^c	21.0 ± 1.5^c	70.3 ± 5.2^a	20–30
FC ($g\ H_2O/g$)	4.9 ± 0.1^c	3.8 ± 0.1^d	9.2 ± 0.2^b	10.4 ± 1.0^a	
Mineralized (%)	30.6 ± 1.0^a	11.3 ± 1.0^b	9.5 ± 1.5^c	-1.7 ± 0.7	

Differences between the substrates in bulk density (BD, n = 5), total pore space (TPS, n = 5), air volume (AV, n = 5), easy available water (EAW, n = 5) Field Capacity (FD, n = 11), and Proportion of mineralized organic material within the 58 days of the experiment (Mineralized, n = 11) are indicated by different lower case letters (HSD-Test, $p < 0.05$, Mean ± Standard deviation).

**Reference values for evaluation of our results were taken from the publication by Dannehl et al. (2015).*

Influence of Different Substrates on pH, Electric Conductivity, Oxygen Concentration and Concentrations of Ammonium and Nitrate Within Substrate Solution

Several properties of the nutrient solution can influence the yield and/or quality of lettuce, including EC, pH-value, oxygen concentration of the solution and the concentration of nutrients or chemical forms of the elements. Since it was expected that the different substrates would change the properties of the nutrient solution added to the substrate pots, part of the solution contained in the pots (substrate solution) was eluted and analyzed weekly for 6 consecutive weeks.

Looking at the pH values in **Figure 1A**, it is noticeable that at all times the pH values of the sphagnum substrate solution were the lowest and ranged between 4.5 and 5.5, whereas the pH values of the rock wool substrate solution were the highest at all times and ranged between 7.6 and 8.1. At the time points 30, 37, and 44 days after sowing, there was no significant difference in the pH value of the substrate solution between rockwool, hemp and wood. In the last 2 weeks, the pH value in the substrate solution of hemp and wood decreased significantly compared to rockwool and in the last week in substrate solution of wood more strongly than in hemp.

Regarding the EC values in **Figure 1B**, it is striking that this was highest for rockwool at all times and seemed to increase over time, starting from 1.87 mS cm^{-1} and finish at 2.66 mS cm^{-1}. At the beginning, the EC in hemp substrate solution (1.71 mS cm^{-1}) was similar to that in rockwool, but in the following weeks it was always significantly lower than in rockwool, ranging between 1.41 mS cm^{-1} and 1.89 mS cm^{-1}. During the first 3 weeks, the lowest EC values were always in substrate solutions of wood and sphagnum with values between 1.13 mS cm^{-1} and 1.49 mS cm^{-1}. In the following weeks EC of hemp, wood and sphagnum substrate solutions leveled off to a similar degree.

The oxygen concentration in substrate solutions of hemp was lowest at all measured time points, starting at 4.2 mg/l and declining to almost zero at 44 days after sowing (DAS) before increasing again to 2.6 mg/l at the last date (**Figure 1C**). Substrate solutions from the other substrates contained similar oxygen concentrations, but significantly higher oxygen concentrations than hemp solution at all dates, ranging between 6.4 and 9.0 mg/l (**Figure 1C**).

Equal amount of nitrogen was added successively to each pot during the experiment in the form of nitrate. Because we used organic materials as substrate, the substrate solution could contain released ammonium from the organic substance in addition to the fertilized nitrate. Therefore, the amounts of ammonium and nitrate per pot were determined in 6 consecutive weeks (**Figure 2**). The amount of nitrate per pot was highest in the rockwool variety and corresponded to the weekly nutrient doses, which first increased up to 108 mg nitrate per pot till the 3rd week and then decreased to 2 mg nitrate per pot in the last week. In Sphagnum solutions lower amounts of nitrate than in rockwool solutions were measured during the first 4 weeks peaking at the 5th week at a similar amount of nitrate (56 mg) as in rockwool solutions. Lower amounts in nitrate were found in pots of wood from the 3rd week onward constant decreasing from 11.5 mg per pot to 1 mg at the end. Nitrate in hemp samples was below the lower detection limit almost at every date analyzed. At the final monitoring point, all substrate solutions contained similarly low nitrate contents.

All pots contained equal low amounts of ammonium at the start of the measurements, between 0.17 and 0.44 mg per pot. While wood, hemp and rockwool maintained similarly low levels of ammonium per pot throughout the 6 weeks, in sphagnum the ammonium content increased continuously from the second week and reached its highest level of 3.81 mg at 44 DAS before starting to decrease.

Influence of Different Growth Substrates on Plant Growth, Yield and Quality

Early on in the experiment, it became apparent that plant growth in the different substrates was clearly different. On the one hand by the size and number of leaves of the lettuce (data not shown) and on the other hand by the different green coloring of the leaves. Results of documented plant parameters are described in detail in the following sections.

Influence of Different Growth Substrates on Water Use Efficiency

When lettuce was grown on different substrates, water usage differed significantly among variants (**Figure 3**). From the beginning till the end, plants grown on sphagnum used most water followed by rockwool grown plants. Hemp and wood grown plants used similar amounts of water, but significantly

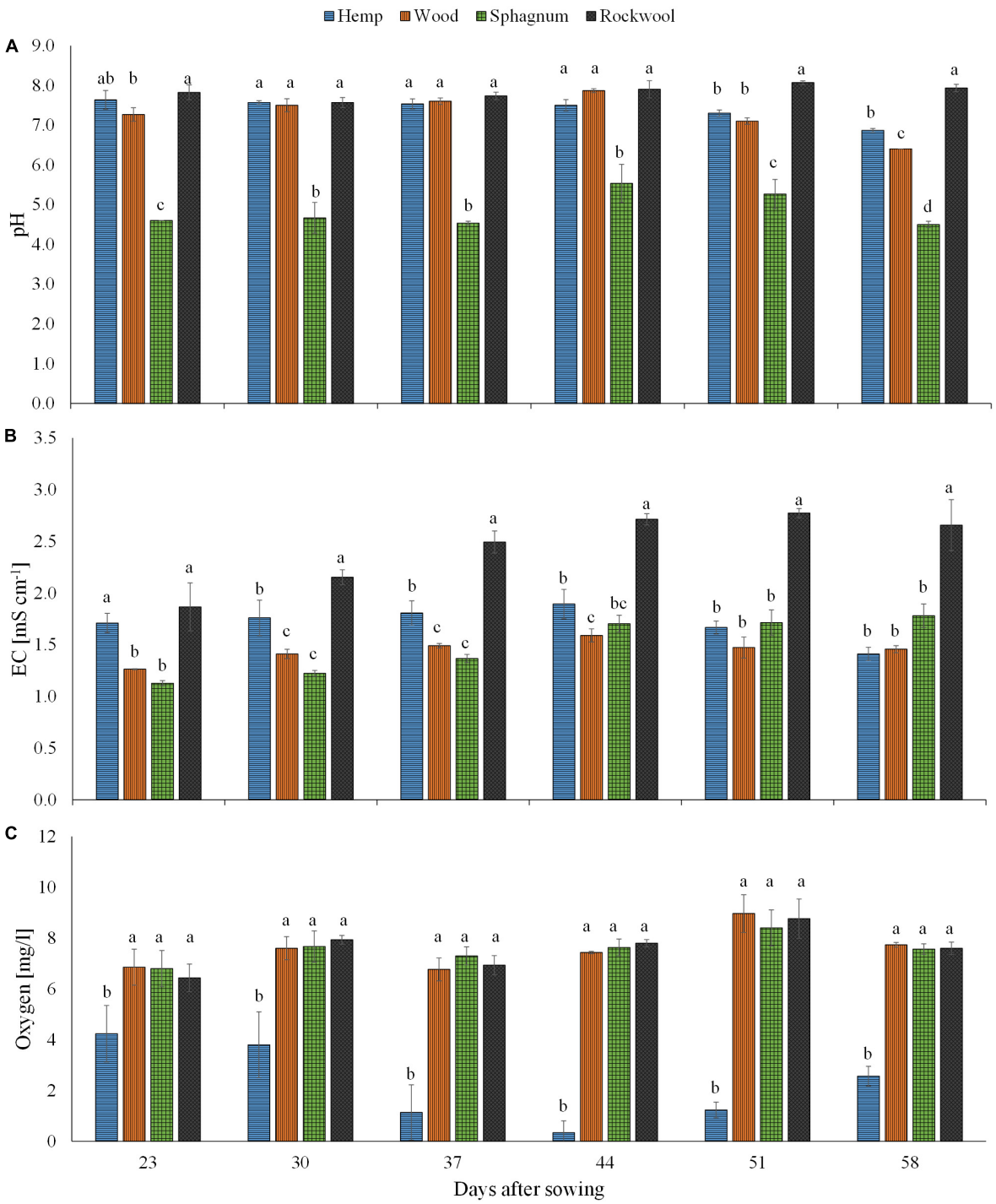

FIGURE 1 | Measured pH **(A)**, EC **(B)**, and oxygen concentration **(C)** in substrate solution eluted from pots filled with different substrates for cultivation of lettuce. Measurements were taken during 6 consecutive weeks until harvest. Significant differences between the substrates are indicated by different lower case letters (HSD-Test, $p < 0.05$, Mean ± Standard deviation, and $n = 3$) EC: electrical conductivity.

less than those from sphagnum and rockwool. Finally, plants grown on sphagnum were irrigated with 965 *g*, on rockwool with 748 *g*, on wood with 482 *g*, and on hemp with 496 *g* water. As the plants exhibited different growth on the substrates, it was useful to compare the biomass produced per given amount of water, as this is the productive part of the water consumption in contrast to the evaporation from the substrates. As can be seen in **Table 2**, the plants on rockwool and sphagnum

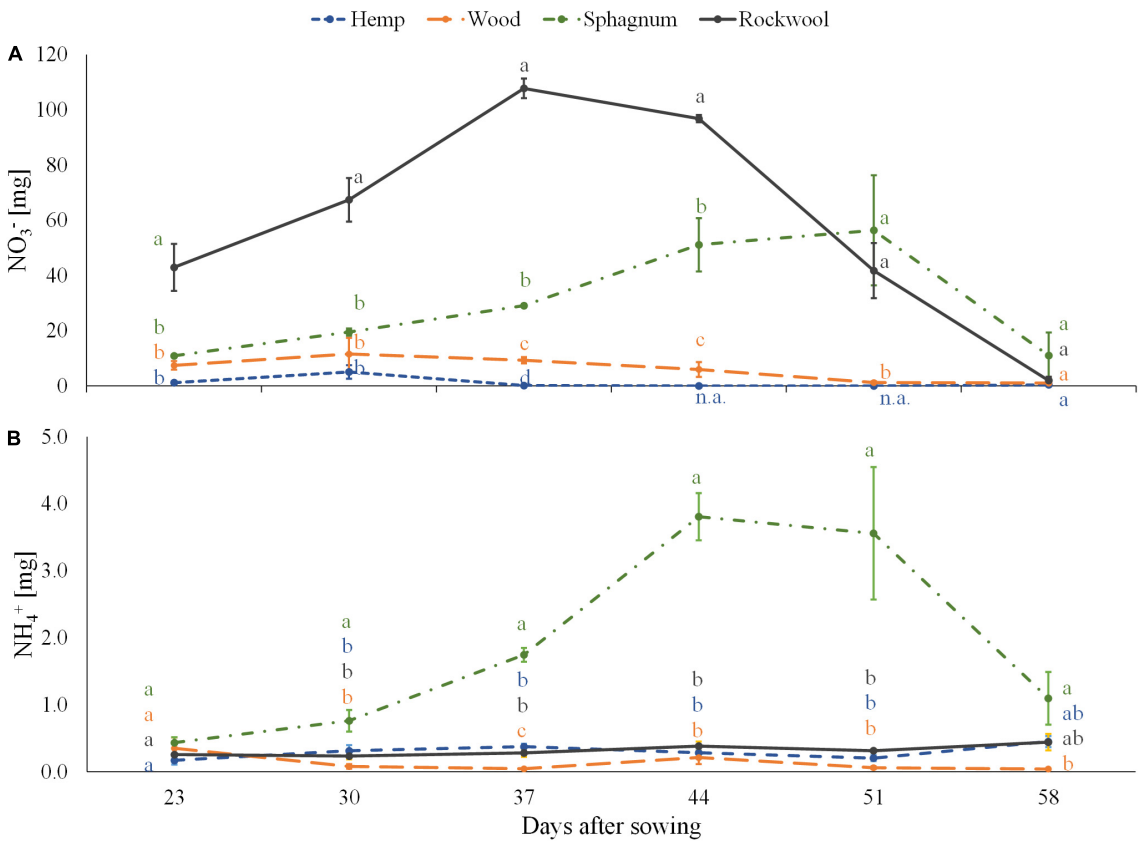

FIGURE 2 | Ammonium **(A)** and nitrate **(B)** contents in substrate solution eluted from pots filled with different substrates for cultivation of lettuce. Measurements were taken during 6 consecutive weeks until harvest. Significant differences between the substrates are indicated by different lower case letters (HSD-Test, $p < 0.05$, Mean ± Standard deviation, and $n = 3$) n.a.: not available (below detection limit).

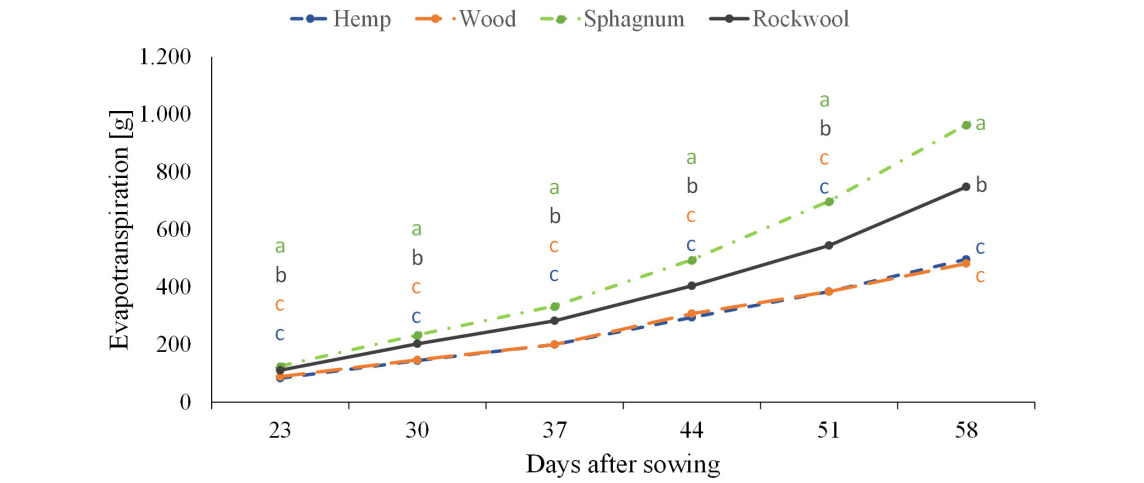

FIGURE 3 | Influence of different substrates on evapotranspiration of lettuce plants grown in pots. Measurements were taken twice a week. Significant differences between the substrates are indicated by different lower case letters (HSD-Test, $p < 0.05$, Mean ± Standard deviation, and $n = 9$).

were most effective in forming fresh mass with 23.24 *g* FM and 25.45 *g* FM per *g* of water, respectively. Wood grown plants could synthesize 6.36 *g* FM per g water, yielding just a quarter of biomass compared to sphagnum. In hemp substrates, plants were extremely retarded in growth and just reached 0.39 *g* FM per g water.

TABLE 2 | Effects of different growth substrates on leaf number, leaf area, yield, dry matter content, and fresh mass (FM) per *g* irrigated water of lettuce heads.

	Hemp	Wood	Sphagnum	Rockwool
Leaf number	7 ± 1^{c}	24 ± 2^{b}	54 ± 4^{a}	50 ± 3^{a}
Leaf Area (cm^2)	7 ± 2^{d}	175 ± 23^{c}	873 ± 160^{a}	692 ± 53^{b}
Yield (*g* FW)	0.2 ± 0.1^{d}	3.1 ± 1.0^{c}	24.6 ± 3.6^{a}	17.2 ± 1.9^{b}
DM content (%)	17.1 ± 3.2^{a}	8.8 ± 0.5^{b}	5.4 ± 0.1^{b}	5.4 ± 0.3^{b}
FM (g)/H_2O (g)	0.39 ± 0.11^{c}	6.36 ± 2.17^{b}	25.45 ± 2.94^{a}	23.24 ± 3.20^{a}

Significant differences between the substrates are indicated by different lower case letters [HSD-Test, $p < 0.05$, Mean ± Standard deviation, $n = 9$, for DM content $n = 3$, for FM (g) H_2O (g) $^{-1}$: $n = 6$].

Influence of Different Growth Substrates on Chlorophyll Content in Lettuce

To confirm the impression of the previously mentioned observed different green colorations, the SPAD values of all plants were recorded weekly and are depicted in **Figure 4**. During the experiment, the lowest SPAD values were measured in leaves of hemp grown plants at each measurement time, which also decreased continuously over time from 14.6 to 7.8. In contrast, the SPAD values of lettuce leaves grown on rockwool were always highest and ranged from 16.4 to 21.6. The SPAD values of lettuce grown on wood or sphagnum did not significantly differ from SPAD values of the rockwool variety, except at 29 and 35 DAS. At 29 and 35 DAS, SPAD values were increasing in the order hemp < wood < sphagnum < rockwool.

Influence of Different Growth Substrates on Yield

Hemp plants were strongly reduced in growth, exhibiting the lowest leaf number (7), leaf area (7 cm^2) and yield (0.2 *g* FW) and the highest DM content (17.1%) from all varieties (**Table 2**). Lettuce plants from wood performed slightly better than plants from hemp with 24 leaves, 175 cm^2 leaf area and 3.1 *g* yield. Leaf number of plants from rockwool (50) and sphagnum (54) were similar and highest, but significantly different in leaf area (rockwool: 692 cm^2; sphagnum: 873 cm^2) and thus yield (rockwool: 17.2 *g*; sphagnum: 24.6 *g*). The dry matter content of plants grown on wood (8.8%) seems to be higher than that of plants grown on rockwool (5.4%) and sphagnum (5.4%), but this was not significant different.

Influence of Different Growth Substrates on Secondary Metabolites in Lettuce

As nutritionally valuable ingredients, secondary metabolites such as phenolic acids and flavonoids are important for the quality of lettuce. We were able to detect the following phenolic acids in lettuce: caffeoyltartaric acid (CT), caffeoylquinic acid (CQ), caffeoylmalic acid (CM), dicaffeoyltartaric acid (diCT), and diCQ. Quercetin 3-O-(600-malonylglucoside; QM-glucoside) was also found as representative of flavonoids (**Table 3**). Total flavonoid concentration was highest in hemp leaves (0.50 mg/*g* DM) followed by wood leaves (0.18 mg/*g* DM). In plants from rockwool (0.05 mg/*g* DM) and sphagnum (0.06 mg/*g* DM) comparable low concentration of flavonoids were found. A similar result was found for total phenolic acids, which concentration were much higher than concentrations of flavonoids. Plants grown on hemp and wood substrates had concentrations of about 20 mg, twice as high as plants grown on sphagnum or rockwool. The most abundant phenolic acid was diCT. In comparison within the substrate variants, the concentration of diCT is highest in plants cultivated on hemp and wood and lowest in plants of rockwool and sphagnum. DiCQ was the least detectable compared to the other phenolic acids considered and was significantly higher in lettuce grown on hemp than in plants of all other substrates. Concentration of CQ was highest in plants from the hemp variant, followed by wood. Least concentrations of CQ were found in plants from rockwool and sphagnum. Regarding CT, concentrations ranged from 2.17 mg/*g* DM in wood, to 1.24 mg/*g* DM in Hemp and almost 1.7 mg/*g* DM in plants from sphagnum and rockwool. Concentrations of CM was the lowest in plants from hemp and sphagnum, higher in plants from wood and highest in plants from rockwool.

Comparing the proportion of individual phenolic acids, a clear shift is visible in plants grown on hemp from diCT, CT, and CM toward diCQ and CQ when comparing the phenolic acid profiles

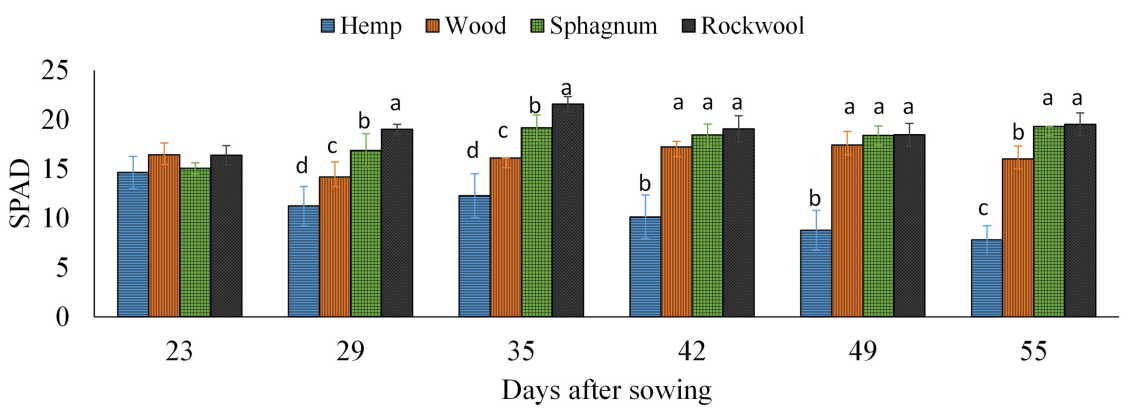

FIGURE 4 | Measured SPAD values in lettuce plants grown in different substrates. Mean SPAD values measured on 6 consecutive weeks. Significant differences between the substrates are indicated by different lower case letters (HSD-Test, $p < 0.05$, Mean ± Standard deviation, and $n = 9$).

TABLE 3 | Concentrations of phenolic acids and flavonoids in lettuce caused by different substrates.

	Hemp	Wood	Sphagnum	Rockwool
		Phenolic acids (mg/*g* DM)		
Caffeoyltartaric acid	1.24 ± 0.17^{c}	2.17 ± 0.05^{a}	1.68 ± 0.06^{b}	1.66 ± 0.14^{b}
Caffeoylquinic acid	6.17 ± 0.27^{a}	4.23 ± 0.22^{b}	1.50 ± 0.15^{c}	1.06 ± 0.14^{c}
Caffeoylmalic acid	0.45 ± 0.06^{c}	0.71 ± 0.01^{b}	0.65 ± 0.10^{bc}	0.93 ± 0.07^{a}
Dicaffeoyltartaric acid	10.69 ± 0.79^{a}	12.59 ± 0.56^{a}	6.69 ± 0.49^{b}	5.97 ± 0.60^{b}
Dicaffeoylquinic acid	2.63 ± 0.17^{a}	0.19 ± 0.05^{b}	0.19 ± 0.08^{b}	0.10 ± 0.03^{b}
Total phenolic acids Σ	21.18 ± 0.96^{a}	19.89 ± 0.52^{a}	10.72 ± 0.60^{b}	9.72 ± 0.97^{b}
		Flavonoids (mg/*g* DM)		
Quercetin 3-*O*-(6′′-malonylglucoside)	0.50 ± 0.05^{a}	0.18 ± 0.03^{b}	0.06 ± 0.00^{c}	0.05 ± 0.00^{c}

Significant differences between the substrates are indicated by different lower case letters (HSD-Test, $p < 0.05$, Mean ± Standard deviation, and $n = 3$).

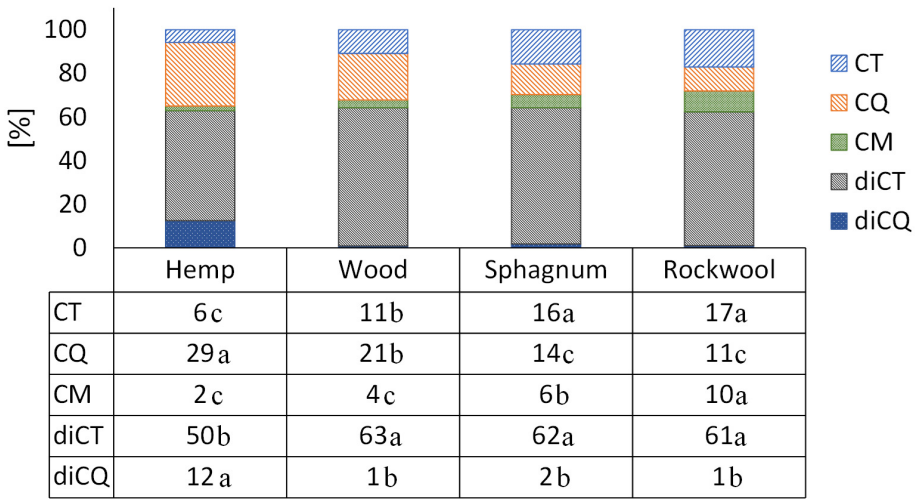

	Hemp	Wood	Sphagnum	Rockwool
CT	6c	11b	16a	17a
CQ	29a	21b	14c	11c
CM	2c	4c	6b	10a
diCT	50b	63a	62a	61a
diCQ	12a	1b	2b	1b

FIGURE 5 | The individual phenolic compounds as a proportion of the total amount of phenolic acids in the lettuce. Significant differences between the substrates are indicated by different lower case letters (HSD-Test, $p < 0.05$, Mean ± Standard deviation, and $n = 3$); CT: caffeoyltartaric acid, CQ: caffeoylquinic acid, CM: caffeoylmalic acid, diCT: dicaffeoyltartaric acid, and diCQ: dicaffeoylquinic acid.

with plants from rockwool or sphagnum (**Figure 5**). The phenolic acid profile in plants from wood showed a similar proportion of diCT and diCQ, but a shift from CT and CM toward CQ in comparison to rockwool and sphagnum. The proportions of the different phenolic acids were similar in plants of sphagnum and rockwool, except for CM which accounted for a lower proportion of phenolic acids in sphagnum.

DISCUSSION

Organic materials, to use as substitutes for the established rockwool in soilless cultivation, should enable the producer to achieve optimal yields and quality of the cultivated crops. In the ideal case, organic materials can be obtained as a waste product from other production processes, e.g., wood chips from the wood processing industry. If these would be amended on arable land after use as a substrate in hydroponic cultivation, this could help closing nutrient cycles and avoiding waste. In the present study, we tested hemp fiber, wood chips, and sphagnum moss as alternative substrates for rockwool. All substrates were examined for different physico-chemical properties and their effects on lettuce growth and quality.

Firstly, we checked physical properties like BD, TPS, AV, and EAW to see whether chosen organic materials might be suitable as substrates. The reference values for the evaluation of our results of water retention measurements were taken from the publication by Dannehl et al. (2015), which summarizes reference values from various sources. A comparison between the measured values and those recommended from other studies for BD, TPS, AV, and EAW showed that the substrates we investigated are almost all within the reference values, even if significant differences were found between the substrates (**Table 1**). Bulk densities ranged from 0.05 $g\ cm^{-3}$ (rockwool), 0.08 $g\ cm^{-3}$ (sphagnum) to 0.10 $g\ cm^{-3}$ (hemp and wood), which are similar to those found by Dannehl et al. (2015). The TPS in the current study was largest in rockwool (90 vol%) and sphagnum (87 vol%) followed by wood (81 vol%) and hemp (76 vol%). This contradicts the results published by

Dannehl et al. (2015), but is in a similar range, which is not true for the AV and EAW values. The air-filled pores have a proportion of 13 vol% in sphagnum, 14 vol% in hemp, 19 vol% in rockwool. The highest proportion of air-filled pores is 30 vol% in wood. Again, all substrates are within the reference range (10–30 vol%). The proportion of EAW in hemp (41 vol%) and rockwool (70 vol%) is well above the reference range of 20–30 vol% (De Boodt and Verdonck, 1972), whereas wood and sphagnum are within this range. In Gruda and Schnitzler (2004) described values for EAV and AV of wood chips were in a similar range in our study, but we measured a lower TPS. Nevertheless, these results indicate that the selected organic materials could be suitable as substrates. As an additional factor, the mineralization in which the organic materials differ from the stable rockwool was also examined in **Table 1**. Since hemp had decomposed already to 30% within the relatively short time of the experiment of 53 days, it should be considered whether this substrate could be used in hydroponic greenhouse cultivation, if the cultivation period for, e.g., tomatoes is significantly longer. In this case, wood and sphagnum substrates with a lower degradation of ∼11% in 53 days would be more suitable. It should be noted that the roots remained in the substrate at the end. This resulted in higher masses of organic material being detected than were actually present, which causes the mineralization to be somewhat underestimated. The mineral rockwool is not degraded, but shows a mass increase of 1.7% at the end of the experiment, which results from the ingrowing roots.

The differences shown in the degradability of the substrates can have an impact on the physico-chemical properties during the entire crop cycle as was shown for wood fiber and coconut fiber in Domeño et al. (2009). Different organic materials might influence the composition of mineralizing microorganisms and thus microclimatic conditions created and/or substances synthesized by the activity of microorganisms during mineralization. It was known for sphagnum to facilitate lower pH levels (Clymo, 1967) in surrounding water, so in our case within the substrate solution. Processes influenced by pH include nutrients solubility and availability as well as microorganism activity. The measured pH values in peat moss eluates were in the range of 4.5 to 5.5 which is lower than the pH proposed pH for lettuce cultivation (5.9; Knight and Mitchell, 1983), whereas the pH values of the other substrate eluates were higher than 7 and for rockwool almost 8, except for the last week (**Figure 1A**). In wood, hemp and rockwool substrates the pH measured was higher than recommended which opens up the possibility that nutrients are no longer as readily available as at lower pH levels and may have led to the poorer yields compared to sphagnum. The lower pH values in the substrate solution of sphagnum can be traced back to unesterified polyuronic acids, which can account for 10–25% of the dry weight of sphagnum, depending on the species (Clymo, 1964).

The EC was highest in rockwool at all time points, ranging from 1.9 mSi cm^{-1} to 2.8 mSi cm^{-1} and seems to reflect the fertilization regime during cultivation (**Figure 1B**). Increasing EC values over time in rockwool substrates resulted from evaporated water from the pots, leaving nutrient salts in the solution. Our measured EC values in rockwool eluates are in the recommended range of 2.0–3.0 mSi cm^{-1} according to Economakis (1991), who also showed in his study on two lettuce varieties that their fresh mass was hardly affected by changes in EC values within a range of 1.5–5.0 mSi cm^{-1}. The lower EC (1.3–1.9 mSi cm^{-1}) values of organic substrate eluates at all time points might indicate nutrients to have been bound to the substrate or to have been incorporated into microbial biomass.

It was initially assumed that the microbial biomass that developed during the test period consumed oxygen from the substrate solution and thus could lead to oxygen deficiency in the rhizosphere of the plants. The assumption was supported by an odor of decay, which was perceived rising from the hemp substrates, indicating anaerobic degradation processes. As shown in **Figure 1C**, a decrease in oxygen was detected in hemp substrate eluates, exclusively (**Figure 1C**), suggesting higher activity of microorganisms than in other substrates tested. These result fits well with the result of the substrate stability of hemp, which was lowest in our experiment (**Table 1**) and to data of nitrate contents in pots (**Figure 2A**). The amounts of nitrate in the eluate from rockwool substrates corresponded to the weekly nutrient doses added to the pots and prove that more than sufficient nitrate was available for yield formation. In the sphagnum variety nitrate might be incorporated into microbial biomass as well as in plant biomass, resulting in lower amounts of nitrate in the eluate when compared to rockwool. Nitrate in hemp solution was lowest, close to the lower detection limit, and at 44 and 51 DAS not detectable, although all substrate pots received equal amounts of nutrients. It is highly probable that nitrate was used to build up microbial biomass, thus reducing the availability of nitrate for plants, which led to strongly retarded growth in the hemp variant. Lettuce plants grown on wood exhibited better growth than lettuce plants from hemp. The reason for improved growth might be the higher mineralization stability of wood in comparison to hemp, resulting in lower microbial activity and thus in higher oxygen and nitrate levels within the root zone. Sphagnum was similarly susceptible to degradation as wood, contained similar amounts of oxygen and had similar EC values as wood, but supported plant growth best. Beside the afore mentioned higher nutrient availability due to the lower pH in Sphagnum, the high contents of ammonium in sphagnum pots (**Figure 2B**) might support a better growth of lettuce. The sphagnum variant was the only one to show significant contents of both N-forms in its substrate solution. A suitable balance of nitrate and ammonium nutrition compared to the use of either nitrate or ammonium sources alone has led to an increase in vegetable yield and nutritional quality in many vegetable crops, e.g., tomato (Claussen, 2002), spinach (Wang et al., 2009), endive (Santamaria and Elia, 1997), and lettuce (McCall and Willumsen, 1998). In rockwool substrates, ammonium was almost absent (**Figure 2B**) and nitrate was highest (**Figure 2B**) during cultivation, which, in combination with highest EC values detected, might be a reason for less yield compared to the yield from sphagnum substrates. Nutrition with different forms of nitrogen also has

an effect on the pH value of the nutrient solution. It is known that a nitrate nutrition leads to increased pH values due to OH^- or HCO_3^- released into nutrient solution to balance ion uptake by the plant roots, whereas ammonium nutrition leads to a lowering of the pH values because of H^+ excretion during NH_4^+ uptake and nitrification of NH_4^+-N to NO_3^--N within the solution which releases H^+ as well (Barker and Mills, 1980). Since we fertilized the plants with NO_3^--N and detected NH_4^+-N in sphagnum solution exclusively, this could contribute additionally to the observed differences in pH beside the mentioned unesterified polyuronic acids in sphagnum substrate. To what extent there is a connection between the low pH value in sphagnum substrate and the presence of ammonium is unclear. A shift in pH toward acidity can lead to a shift in the microbial decomposer community from bacteria to fungi (Rousk et al., 2009). Sphagnan present in sphagnum, also was shown to influence microorganisms. The pectin-like polysaccharide is considered for antibacterial and wound healing effects (Børsheim et al., 2001). Differences in the opacity of the eluates obtained from the substrates (hemp very opaque, other substrate eluates clear; data not shown) indicate different compositions and quantities of mineralizing organisms. To what extent this is responsible for the accumulation of ammonium in sphagnum solution remains the subject of further studies. Different compositions of the microbial population in the wood and sphagnum substrates could mean different nitrogen requirements for the formation of microbial biomass and its metabolites. This could also explain why, at similar mineralization stability, differences in the amount of nitrate were found in the eluates. The different contents of the two N-forms per pot influences the N-nutritional status of the plant. Nitrogen within the plant is needed for chlorophyll synthesis. Chlorophyll concentrations in leaves were measured indirectly by SPAD meter. The SPAD values obtained in turn allow conclusions to be drawn about the nitrogen supply status of the plant (Blackmer and Schepers, 1995). During growth period, clear differences in SPAD values were found 29 and 35 DAS with increasing values from hemp > wood > rockwool > sphagnum. No differences in SPAD between wood, sphagnum and rockwool were present in the last 3 weeks. Plants from hemp had the lowest SPAD values at all time points, reflecting low nitrate/ammonium contents in substrate solution (**Figure 2**). Nitrate was high in rockwool and sphagnum at 44 and 51 DAS, while ammonium was high just in sphagnum substrate solution at these time points. SPAD Values around these time points gave similar values not just for sphagnum and rockwool grown plants, but for wood grown plants as well. Substrate solution from wood contained much lower contents of any of the N-forms analyzed than from sphagnum or rockwool. It can be assumed that the lettuce on wood meets the lower supply of nitrogen with limited growth in order to keep the nitrogen concentration in the plant at a constant level or allocated more biomass to roots for enhanced nitrogen uptake what was shown for example for 27 herbaceous plants by (Müller et al., 2000).

The different growth is confirmed by the data for yield, leaf number and leaf area in **Table 2**. While the leaf number of lettuce plants from sphagnum and rockwool do not differ significantly, the leaf area is largest in plants grown on sphagnum and so is the yield. Yields and leaf areas decreased in the order sphagnum > rockwool > wood > hemp. Due to the different growth in the variants, water used per gram of biomass created differed significantly (**Table 2**). Most biomass per g water given was created on sphagnum and rockwool. Only one third of the biomass formed on sphagnum or rockwool was formed on wood and almost no biomass was formed on hemp.

As the focus is increasingly being placed on product quality in addition to yield, we have looked at the phenolic acid and flavonoid content of the leaves, as these are considered to be nutritionally valuable components due to their health-promoting properties (Birt et al., 2001; Nicolle et al., 2004). The production of phenolic compounds in plants is strongly influenced by nitrogen availability, whereby a reduction in nitrogen availability generally leads to an increase in phenolic acid concentrations. For lettuce this has already been shown in studies by Qadir et al. (2017) and Zhou et al. (2018), but is true for other species as well, e.g., artichoke and cardoon (Rouphael et al., 2012). This could also be shown in our results (**Table 3** and **Figure 2**). Nitrogen was found in pots of hemp and wood in the smallest amounts and led to twice as high total phenolic acid concentrations in the leaves as in the plants on rockwool and sphagnum. The concentration of the flavonoid Quercetin 3-*O*-(6″-malonylglucoside) in hemp and wood grown plants was even several times higher than the concentrations in leaves of rockwool or sphagnum varieties. The different substrates not only caused different concentrations in the phenolic acids and flavonoids, but also a shift in the proportions of the individual phenolic acids within the total phenolic acids. The phenolic acid pattern in lettuce heads of hemp substrates was shifted toward CQ derivatives at the expense of CT derivatives compared to the phenolic acid profiles of lettuce from rockwool (**Figure 5**). Also in the wood variant, the phenolic acids are shifted toward CQ at the expense of CT and CM. Cultivation on sphagnum led to no change in the phenolic acid pattern compared to cultivation on rockwool. A study by Zhou et al. (2019) showed an increase in the proportion of a CQ derivative in lettuce under nitrogen-limiting conditions as well and is therefore consistent with our results. In nutrient solution aeration experiments with hydroponically cultivated lettuce Encarnación et al. (2015) found higher phenolic acid levels in lettuce plants in non-aerated nutrient solutions than in lettuce from aerated nutrient solutions. Since similar higher phenolic acid concentrations in lettuce from hemp and wood were measured in our experiments, but the severe oxygen deficiency only occurred in hemp, the availability of nitrogen seems to have a greater effect on phenolic acid concentrations.

CONCLUSION

Even though the highest phenolic acid and flavonoid content in lettuce has been found on hemp substrates, the use of hemp as a substrate is not advisable due to the extremely low yield

and the high instability. Yields caused by wood substrates were higher, but did not reach the yields of rockwool and sphagnum. Nevertheless, wood could be a suitable alternative to rockwool if the nutrients in the nutrient solution, which are removed by immobilization, would be optimized. The extent to which yields on wood substrates can be increased by controlling pH and nutrient levels, while maintaining increased phenolic acid and flavonoid levels, needs to be investigated in more detail. In our study, sphagnum was found to provide optimal properties for lettuce growth and is a good substitute for rock wool.

DATA AVAILABILITY STATEMENT

The raw data supporting the conclusions of this article will be made available by the authors, without undue reservation.

AUTHOR CONTRIBUTIONS

AN and DD contribute equally to the study conception and design, acquisition, analysis and interpretation of data, and drafting of the manuscript. Both authors contributed to the article and approved the submitted version.

FUNDING

The project is supported by funds of the Federal Ministry of Food and Agriculture (BMEL) based on a decision of the Parliament of the Federal Republic of Germany via the Federal Office for Agriculture and Food (BLE) under the innovation support program (Funding Number: 28-1-B2.035-16). Furthermore, we acknowledge support by the German Research Foundation (DFG) and the Open Access Publication Fund of Humboldt-Universität zu Berlin.

REFERENCES

Allaire, S. E., Caron, J., Ménard, C., and Dorais, M. (2005). Potential replacements for rockwool as growing substrate for greenhouse tomato. *Can. J. Soil Sci.* 85, 67–74.

Ao, Y., Sun, M., and Li, Y. (2008). Effect of organic substrates on available elemental contents in nutrient solution. *Bioresour. Technol.* 99, 5006–5010. doi: 10.1016/j.biortech.2007.09.011

Barker, A. V., and Mills, H. A. (1980). "Ammonium and nitrate nutrition of horticultural crops," in *Horticultural Reviews*, ed. J. Janick (Hoboken, NJ: Wiley), 395–423.

Benoit, F., and Ceustermans, N. (1995). *A Decade of Research on Ecologically Sound Substrates*. Leuven: International Society for Horticultural Science (ISHS), 17–30.

Birt, D. F., Hendrich, S., and Wang, W. (2001). Dietary agents in cancer prevention: flavonoids and isoflavonoids. *Pharmacol. Ther.* 90, 157–177. doi: 10.1016/S0163-7258(01)00137-1

Blackmer, T. M., and Schepers, J. S. (1995). Use of a chlorophyll meter to monitor nitrogen status and schedule fertigation for corn. *J. Prod. Agric.* 8, 56–60. doi: 10.2134/jpa1995.0056

Blok, C., and Urrestarazu, M. (2010). Substrate growing developments in Europe 2010-2027. *Horticom Plataforma*. Available online at: https://edepot.wur.nl/137023 (accessed September 1, 2020).

Børsheim, K. Y., Christensen, B. E., and Painter, T. J. (2001). Preservation of fish by embedment in Sphagnum moss, peat or holocellulose: experimental proof of the oxopolysaccharidic nature of the preservative substance and of its antimicrobial and tanning action. *Innov. Food Sci. Emerg. Technol.* 2, 63–74. doi: 10.1016/S1466-8564(00)00029-1

Claussen, W. (2002). Growth, water use efficiency, and proline content of hydroponically grown tomato plants as affected by nitrogen source and nutrient concentration. *Plant Soil* 247, 199–209. doi: 10.1023/A:1021453432329

Clymo, R. (1967). "Control of cation concentrations, and in particular of pH, in Sphagnum dominated communities," in *Chemical Environment in the Aquatic Habitat*, eds H. L. Golterman and R. S. Clymo (Amsterdam: North Holland), 273–284.

Clymo, R. S. (1964). The origin of acidity in sphagnum bogs. *Bryologist* 67, 427–431. doi: 10.2307/3240768

R Core Team (2020). *R: A Language and Environment for Statistical Computing*. Vienna: R Foundation for Statistical Computing.

Dannehl, D., Suhl, J., Ulrichs, C., and Schmidt, U. (2015). Evaluation of substitutes for rock wool as growing substrate for hydroponic tomato production. *J. Appl. Bot. Food Q.* 88, 68–77. doi: 10.5073/JABFQ.2015.088.010

De Boodt, M., and Verdonck, O. (1972). "The physical properties of the substrates in horticulture," in *III Symposium on Peat in Horticulture 26*, ed. F. Penningsfeld (Leuven: International Society for Horticultural Science (ISHS)), 37–44.

de Mendiburu, F. (2020). *agricolae: Statistical Procedures for Agricultural Research. R package version 1.3-2*. Boston, MA: R Studio.

Domeño, I., Irigoyen, N., and Muro, J. (2009). Evolution of organic matter and drainages in wood fibre and coconut fibre substrates. *Sci. Hortic.* 122, 269–274. doi: 10.1016/j.scienta.2009.05.006

Economakis, C. D. (1991). *Effect of Solution Conductivity on Growth and Yield of Lettuce in Nutrient Film Culture*. Leuven: International Society for Horticultural Science (ISHS), 309–316.

Encarnación, C., Juan, A. F., Diana, N., and Catalina, E.-G. (2015). Nutrient solution aeration and growing cycles affect quality and yield of fresh-cut baby leaf red lettuce. *Agric. Food Sci.* 24, 313–322. doi: 10.23986/afsci.52792

Förster, N., Ulrichs, C., Schreiner, M., Arndt, N., Schmidt, R., and Mewis, I. (2015). Ecotype variability in growth and secondary metabolite profile in Moringa oleifera: impact of sulfur and water availability. *J. Agric. Food Chem.* 63, 2852–2861. doi: 10.1021/jf506174v

Gruda, N. (2009). Do soilless culture systems have an influence on product quality of vegetables? *J. Appl. Bot. Food Q.* 82, 141–147.

Gruda, N., and Schnitzler, W. H. (2004). Suitability of wood fiber substrate for production of vegetable transplants: I. Physical properties of wood fiber substrates. *Sci. Hortic.* 100, 309–322. doi: 10.1016/j.scienta.2003.10.001

Islam, S., Khan, S., Ito, T., Maruo, T., and Shinohara, Y. (2002). Characterization of the physico-chemical properties of environmentally friendly organic substrates in relation to rockwool. *J. Hortic. Sci. Biotechnol.* 77, 143–148. doi: 10.1080/14620316.2002.11511470

Jansson, S. L. (1958). Tracer studies on nitrogen transformations in soil with special attention to mineralization-immobilization relationships. *Ann. Roy. Agr. Coll. Sweden* 24, 101–361.

Kim, M. J., Moon, Y., Tou, J. C., Mou, B., and Waterland, N. L. (2016). Nutritional value, bioactive compounds and health benefits of lettuce (*Lactuca sativa* L.). *J. Food Compos. Anal.* 49, 19–34. doi: 10.1016/j.jfca.2016.03.004

Knight, S. L., and Mitchell, C. A. (1983). Enhancement of lettuce yield by manipulation of light and nitrogen nutrition. *HortScience* 108, 750–754.

Llorach, R., Martínez-Sánchez, A., Tomás-Barberán, F. A., Gil, M. I., and Ferreres, F. (2008). Characterisation of polyphenols and antioxidant properties of five lettuce varieties and escarole. *Food Chem.* 108, 1028–1038. doi: 10.1016/j.foodchem.2007.11.032

Massantini, F., Favilli, R., Magnani, G., and Oggiano, N. (1988). Soilless culture, biotechnology for high quality vegetables. *Soilless Culture* 4, 27–40.

McCall, D., and Willumsen, J. (1998). Effects of nitrate, ammonium and chloride application on the yield and nitrate content of soil-grown lettuce. *J. Hortic. Sci. Biotechnol.* 73, 698–703. doi: 10.1080/14620316.1998.11511036

Müller, I., Schmid, B., and Weiner, J. (2000). The effect of nutrient availability on biomass allocation patterns in 27 species of herbaceous plants. *Perspect. Plant Ecol. Evol. Syst.* 3, 115–127.

Nicolle, C., Cardinault, N., Gueux, E., Jaffrelo, L., Rock, E., Mazur, A., et al. (2004). Health effect of vegetable-based diet: lettuce consumption improves cholesterol

metabolism and antioxidant status in the rat. *Clin. Nutr.* 23, 605–614. doi: 10.1016/j.clnu.2003.10.009

Politycka, B., Wójcik-Wojtkowiak, D., and Pudelski, T. (1985). *Phenolic Compounds as A Cause of Phytotoxicity in Greenhouse Substrates Repeatedly used in Cucumber Growing*. Leuven: International Society for Horticultural Science (ISHS), 89–94.

Qadir, O., Siervo, M., Seal, C. J., and Brandt, K. (2017). Manipulation of contents of nitrate, phenolic acids, chlorophylls, and carotenoids in lettuce (*Lactuca sativa* L.) via contrasting responses to nitrogen fertilizer when grown in a controlled Environment. *J. Agric. Food Chem.* 65, 10003–10010. doi: 10.1021/acs.jafc.7b03675

Quantis (2012). *Comparative Life Cycle Assessment of Horticultural Growing Media Based on Peat and Other Growing Media Constituents. Report prepared for the European Peat and Growing Media Association*. Lausanne: Quantis.

Rouphael, Y., Cardarelli, M., Lucini, L., Rea, E., and Colla, G. (2012). Nutrient solution concentration affects growth, mineral composition, phenolic acids, and flavonoids in leaves of artichoke and cardoon. *HortSci. Horts* 47:1424. doi: 10.21273/hortsci.47.10.1424

Rousk, J., Brookes, P. C., and Bååth, E. (2009). Contrasting soil pH effects on fungal and bacterial growth suggest functional redundancy in carbon mineralization. *Appl. Environ. Microbiol.* 75, 1589–1596. doi: 10.1128/AEM.02775-08

Sahin, U., Anapali, O., and Ercisli, S. (2002). Physico-chemical and physical properties of some substrates used in horticulture. *Gartenbauwissenschaft* 67, 55–60.

Santamaria, P., and Elia, A. (1997). Producing nitrate-free endive heads: effect of nitrogen form on growth, yield, and ion composition of endive. *Am. Soc. Hortic. Sci.* 122, 140–145. doi: 10.21273/jashs.122.1.140

Shaw, N. L., Cantliffe, D. J., Funes, J., and Shine, C. (2004). Successful Beit Alpha cucumber production in the greenhouse using pine bark as an alternative soilless media. *Am. Soc. Hortic. Sci.* 14, 289–294. doi: 10.21273/horttech.14.2.0289

Sonneveld, C. (1991). "Rockwool as a substrate for greenhouse crops," in *High-Tech and Micropropagation I*, ed. Y. P. S. Bajaj (Berlin: Springer), 285–312.

Veihmeyer, F. J., and Hendrickson, A. H. (1931). The moisture equivalent as a measure of the field capacity of soils. *Soil Sci.* 32, 181–194.

Wang, J., Zhou, Y., Zhou, C., Shen, Q., and Putheti, R. (2009). Effects of NH_4^+-N/NO_3^--N ratios on growth, nitrate uptake and organic acid levels of spinach (Spinacia oleracea L.). *Afr. J. of Biotechnol.* 8, 3597–3602. doi: 10.5897/AJB2009.000-9356

Wilson, G. C. S. (1984). *Tomato Production in Bark Substrates*. Leuven: International Society for Horticultural Science (ISHS), 271–276.

Xiong, J., Tian, Y., Wang, J., Liu, W., and Chen, Q. (2017). Comparison of coconut coir, rockwool, and peat cultivations for tomato production: nutrient balance, plant growth and fruit quality. *Front. Plant Sci.* 8:1327. doi: 10.3389/fpls.2017.01327

Xu, H.-l, Gauthier, L., and Gosselin, A. (1995). Effects of fertigation management on growth and photosynthesis of tomato plants grown in peat, rockwool and NFT. *Sci. Hortic.* 63, 11–20. doi: 10.1016/0304-4238(95)00791-Q

Zhou, W., Chen, Y., Xu, H., Liang, X., Hu, Y., Jin, C., et al. (2018). Short-term nitrate limitation prior to harvest improves phenolic compound accumulation in hydroponic-cultivated lettuce (*Lactuca sativa* L.) without reducing shoot fresh weight. *J. Agric. Food Chem.* 66, 10353–10361. doi: 10.1021/acs.jafc.8b02157

Zhou, W., Liang, X., Dai, P., Chen, Y., Zhang, Y., Zhang, M., et al. (2019). Alteration of phenolic composition in lettuce (*Lactuca sativa* L.) by reducing nitrogen supply enhances its anti-proliferative effects on colorectal cancer cells. *Int. J. Mol. Sci.* 20:4205. doi: 10.3390/ijms20174205

Conflict of Interest: The authors declare that the research was conducted in the absence of any commercial or financial relationships that could be construed as a potential conflict of interest.

The handling editor declared a shared affiliation, with the authors, at the time of the review.

frontiers in Plant Science

ORIGINAL RESEARCH
published: 15 February 2021
doi: 10.3389/fpls.2021.638525

Current Situation and Key Parameters for Improving Wheat Quality in China

Mingming Ma[1], Yingchun Li[1], Cheng Xue[2]*, Wei Xiong[3], Zhengping Peng[2], Xue Han[1], Hui Ju[1] and Yong He[1]*

[1] Institute of Environment and Sustainable Development in Agriculture, Chinese Academy of Agricultural Sciences, Beijing, China, [2] College of Resources and Environmental Science, Agricultural University of Hebei, Baoding, China, [3] International Maize and Wheat Improvement Center (CIMMYT), Texcoco, Mexico

Processing quality of winter-wheat is affected by genotype, environmental conditions, and crop husbandry practices. In the present study, a data set of 17 quality-related traits for 211 main winter-wheat varieties in China during 2006 to 2018 was extracted from China Wheat Quality Report. Analysis was carried out to evaluate the quality status and variations, to reveal correlation between quality-related traits, as well as to identify key influencing factors. Results indicated that the quality indicators of medium-gluten or medium-strong-gluten wheat varieties were acceptable, whereas those of weak- and strong-gluten wheat varieties were far below national standard, especially hardness index (HI), crude protein content (CPC), wet gluten content (WG), and water absorption for weak-gluten wheat and sedimentation value (SV), stability time (ST), and stretch area (SA) for strong-gluten wheat, respectively. Correlation analysis showed that WA, WG, development time, HI, CPC, falling number, ST, and tractility directly affected the overall quality of winter-wheat. CPC, SV, and WG in medium-gluten wheat had no significant correlation with the processing quality of noodles score, whereas gluten index significantly correlated with noodle score ($P < 0.001$). This implied that protein quality might play a more important role than protein quantity in determining medium-gluten wheat quality. Furthermore, analysis of variance showed that genetic characteristics (cultivars) had significant influences on the restriction indexes (SV, ST, and SA) of strong-gluten wheat, whereas genetic characteristics, environment conditions, and crop growing practices (cultivars, locations, and years) significantly affected the restriction indexes (HI, CPC, WG, and WA) of weak-gluten wheat. The results suggest that improvement of Chinese strong-gluten wheat should mainly focus on cultivating new varieties. As to weak-gluten wheat, cultivation and husbandry practices should be paid more attention to limit undesired high grain protein content.

Keywords: wheat, quality traits, variation, correlation, cultivar, year, location

OPEN ACCESS

Edited by:
Christoph Martin Geilfus, Humboldt University of Berlin, Germany

Reviewed by:
Xingyu Hao, Shanxi Agricultural University, China
Yinghua Zhang, China Agricultural University, China

****Correspondence:***
Yingchun Li
liyingchun@caas.cn
Cheng Xue
xuechenghebau@hotmail.com

Specialty section:
This article was submitted to Plant Nutrition, a section of the journal Frontiers in Plant Science

Received: *07 December 2020*
Accepted: *06 January 2021*
Published: *15 February 2021*

Citation:
Ma M, Li Y, Xue C, Xiong W, Peng Z, Han X, Ju H and He Y (2021) Current Situation and Key Parameters for Improving Wheat Quality in China. Front. Plant Sci. 12:638525. doi: 10.3389/fpls.2021.638525

INTRODUCTION

As the second staple crop in the world, wheat (*Triticum aestivum* L.) provides approximately 20% of protein and 20–40% of minerals for human nutrition globally (Food and Agriculture Organization of the United Nations [FAO], 2019). Besides, wheat supplies 20% of the calories consumed worldwide (Reynolds et al., 2012) and occupies approximately 25% of the global cereal production

area (Punia et al., 2019). By 2018, cultivated area of winter-wheat accounts for 93.7% of the total area of wheat in China, and the production accounts for 95.1% (Ministry of Agriculture and Rural Affairs of PRC, 2020). In recent years, with the improvement of people's living standards, the focus of China's wheat production has gradually shifted from the pursuit of high grain yield to high processing quality. The quality of winter-wheat is classified into several categories (such as grain quality, flour quality, and dough quality), and they are determined by different quality indexes. For example, crude protein content (CPC), wet gluten content, gluten index (GI), development time (DT), and stretch area (SA) are some of the key factors in evaluating the quality of wheat-based food products. Noodles are one of the Chinese people's favorite foods and play an important role in three meals a day. Therefore, their impacting factors of quality traits are needed to be explored in order to improve wheat quality.

Quality of wheat grain is jointly affected by genotypes, environmental conditions, and husbandry practices (Hellemans et al., 2018; Zörb et al., 2018). Cultivation measures, genetics, and milling and processing conditions were major factors affecting the quality of flour and the corresponding products (Kweon et al., 2011). Wheat quality was affected to some extent by the climatic conditions during irrigation, and the correlation coefficient could be positive, negative, or close to zero, depending on the temperature and water input at this stage (Rharrabti et al., 2003a,b). The sedimentation value (SV) of wheat under drought stress was lower than that under normal irrigation conditions (Magallanes-López et al., 2017). Environmental conditions also affected grain ash content (AC), which was increased under high transpiration conditions (Araus et al., 1998). Protein quality was mainly affected by wheat genotypes, whereas no obvious differences were found across production years (Torbica et al., 2016). During dough development, gluten quantity was the main factor determining consistency of dough (Fu et al., 2017), and the genotype had a significant effect on the GI (Šekularac et al., 2018). Protein and gluten properties, in particular, significantly impacted dough strength measurements. Cultivars displaying stronger gluten strengths may result in dough with better dough-handling properties (Tozatti et al., 2020). Falling number (FN) and protein concentration were highly influenced by environment, whereas for SV, hardness, water absorption (WA), and loaf volume genotypes accounted for more than 60% of total variation. Strong relations exist among protein concentration, SV, and loaf volume (Laidig et al., 2017). Moreover, it can be observed that the quality of different wheat cultivars, or even the same wheat cultivar, might vary significantly across growing regions and years (Mohan and Gupta, 2011).

Consistent emphasis on high grain yield and the lack of germplasm resources had led China to its wheat varieties concentrated mainly on medium-gluten and medium-strong-gluten wheat (Hu et al., 2017). Although grain protein content of wheat in China was comparable to that in Europe and the United States, dissatisfactory protein quality (composition of protein components and their subunits) caused weak-gluten strength, poor rheological properties of dough, low SV, and inferior processing quality (especially for strong-gluten and weak-gluten wheat). In addition, most of the current research focused only on the analysis of wheat quality in a single region (Rozbicki et al., 2015; da Silveira et al., 2020). There has been no systematic analysis and comprehensive comparison study on wheat quality in China. Even for evaluations of wheat quality, they were predominately based on one or several limited indicators (especially wheat grain protein content as the core evaluation indicator) (Delcour et al., 2012).

Studies on independent as well as interacted effects of cultivars, growing locations, and years on winter-wheat quality in China were limited. Nevertheless, such information is essential for breeding, regional planting arrangement, and large-scale production of high-quality wheat. Quality properties that are predominantly determined by genotypes could be improved through crop breeding, and those significantly affected by external environmental conditions might be adjusted and optimized via husbandry management. In this study, data were extracted from the China Wheat Quality Report published by the Ministry of Agriculture of the People's Republic of China. A variety of statistical analysis methods were carried out to screen and analyze a total of 17 quality traits for the 211 winter-wheat cultivars during 2006–2018 in six growing regions in China. The main objectives of this study were (1) to evaluate current situation of winter-wheat quality in China, (2) to identify key parameters limiting the quality improvement, and (3) to analyze the impacts of different cultivars, locations, and years on quality traits.

MATERIALS AND METHODS

Data Source

We selected wheat cultivars data on four quality-related parameters from the 2006–2018 China Wheat Quality Report published by the Ministry of Agriculture of the People's Republic of China, and box chart method was performed to eliminate outliers. In total, a set of 1,055 winter-wheat quality data for 211 cultivars was collected. According to the classification guide of wheat quality regions in China (He et al., 2002), winter-wheat growing areas were divided into six regions (**Figure 1**), including North strong-gluten wheat region (1), North Huanghuai strong- and medium-strong-gluten wheat region (2), South Huanghuai medium-gluten wheat region (3), the medium-weak-gluten wheat region in the middle and lower Reaches of the Yangtze River (4), Sichuan Basin medium-weak-gluten wheat region (5), and Yungui Plateau wheat region (6).

Statistical Analysis

Standard-Reaching Rates and Variation Analysis

According to the China National Standard GB/T 17320-2013 (AQSIQ, 2013), eight quality parameters (**Table 1**), including hardness index (HI), CPC, SV, wet gluten content (WG), WA, stability time (ST), max resistance (MAXR), and SA were analyzed for the standard-reaching rates (SRs) of winter-wheat.

Descriptive statistics were applied to evaluate the variability of examined factors: the means, minimum, maximum, and standard deviations. Coefficients of variation (CVs) were also calculated (variation analysis).

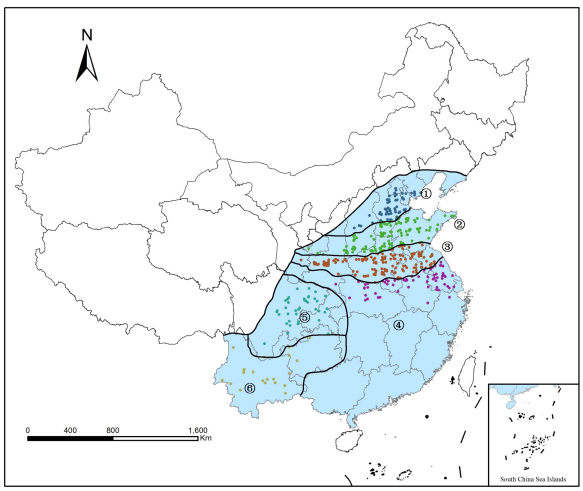

FIGURE 1 | Distributions of sampling areas and six growing regions of winter-wheat in China (MARA, 2016).

TABLE 1 | National standard for wheat quality in China.

Index	Strong-gluten	Medium-strong-gluten	Medium-gluten	Weak-gluten
Hardness index (HI)	≥60	≥60	≥50	<50
Crude protein content (CPC)	≥14	≥13	≥12.5	<12.5
Sedimentation value (SV)	≥40	≥35	≥30	<30
Wet gluten content (WG)	≥30	≥28	≥26	<26
Water absorption (WA)	≥60	≥58	≥56	<56
Stability time (ST)	≥8	≥6	≥3	<3.0
Max resistance (MAXR)	≥350	≥300	≥200	–
Stretch area (SA)	≥90	≥65	50	–

Correlation Analysis

Pearson correlation analysis was performed on 17 quality traits of winter-wheat using R 3.6.2 (R package corrplot).

Multifactor Analysis of Variance

Multifactor analysis of variance was conducted using R 3.6.2 to evaluate the effects of the examined factors and their interactions on grain, flour, and dough quality. In the homogeneity of variance and normal distribution using R 3.6.2 (R package car), the results show that the data are normally distributed, and the variance is homogeneous.

RESULTS

The Standard-Reaching Rates of Winter-Wheat Quality Traits

SRs of different grades of winter-wheat were analyzed according to the national standard GB/T 17320-2013 (**Table 2**). In terms of HI, the SRs of the medium-gluten wheat reached 91%, but that of weak-gluten wheat was only 9%. The SRs of CPC for medium-, medium- strong-, strong-, and weak-gluten wheat were 87, 79, 54, and 13%, respectively. In terms of the SV, the SRs of medium-, medium- strong-, weak-, and strong-gluten wheat were 54, 28, 46, and only 11%, respectively. For WG, 90% of the medium-gluten, 79% of the medium-strong-gluten, 61% of the strong-gluten and only 10% of the weak-gluten wheat samples met the corresponding standards. The SRs of the medium-, medium-strong-, strong-, and weak-gluten wheat for WA were 77, 60, 41, and 23%, respectively. When it came to the ST, the SRs of the medium-, medium- strong-, weak-, and strong-gluten wheat were 69, 33, 31, and 24%, respectively. The SRs of MAXR for medium-, medium- strong-, and strong-gluten wheat were 93, 82, and 67%, respectively. Finally, the SRs of SA for the medium-, medium- strong-, and strong-gluten wheat were 90, 68, and 27%. The results showed that the SRs of medium-gluten and medium-strong-gluten winter-wheat were relatively higher compared with those of strong-gluten and weak-gluten wheat in China. Analysis of quality traits showed that for weak-gluten wheat, the SRs of HI, WG, CPC, and WA were relatively low, whereas for strong-gluten wheat, the SRs of SV, ST, and SA were relatively low.

TABLE 2 | Analysis of quality traits reaching the national wheat quality standard.

Indexes	Strong-gluten	Medium-strong-gluten	Medium-gluten	Weak-gluten
Hardness index (HI)	78 (62–75)	78 (62–72)	91 (50–75)	9 (32–49)
Crude protein content (CPC) (%)	54 (14–18)	79 (14–18)	87 (13–19)	13 (9–12)
Sedimentation value (SV) (mL)	11 (40–52)	28 (35–44)	54 (30–66)	46 (5–25)
Wet gluten content (WG) (%)	61 (30–44)	79 (30–50)	90 (26–47)	10 (16–25)
Water absorption (WA) (%)	41 (60–70)	60 (58–71)	77 (56–71)	23 (51–54)
Stability time (ST) (min)	24 (8–20)	33 (6–35)	69 (3–54)	31 (1–3)
Max resistance (MAXR) (E.U)	67 (416–969)	82 (302–774)	93 (200–1,638)	–
Stretch area (SA) (cm^2)	27 (90–215)	68 (68–215)	90 (32–239)	–

Data outside the brackets indicate the percentages of the compliance rate, and data inside brackets represent the variation range of wheat samples that reached the national wheat quality standard. "–" represents data not included in the standard.

Analysis of Variation of Winter-Wheat Quality Traits

Based on the variation analysis of quality traits (**Table 3**), the CVs were listed as follows: ST > MAXR > SA > DT > GI > TRA > SV > FN > AC > WG> HI>CPC >WC> FER > WA > NS > TW. The CV of ST was the highest among all quality traits, reaching 79.3%. The CVs of MAXR, SA, DT, GI, TRA, and SV were 49.9, 48.4, 43.2, 28.4,

TABLE 3 | Variation of analysis wheat quality traits.

Categories	Indexes	Minimum	Maximum	Average	*SD*	CV (%)
Grain quality	Hardness index (HI)	32.0	75.0	63.7	6.0	9.5
	Test weight (TW) (g L^{-1})	703.0	854.0	795.8	22.9	2.9
	Water content (WC) (%)	7.9	14.3	10.8	0.9	8.2
	Crude protein content (CPC) (%)	9.0	18.8	14.0	1.2	8.9
	Falling number (FN) (s)	73.0	529.0	360.8	59.4	16.5
Flour quality	Flour extraction rate (FER) (%)	11.5	77.3	67.9	4.3	6.4
	Sedimentation value (SV) (mL)	5.0	66.2	30.6	6.8	22.2
	Ash content (AC) (%)	0.3	0.9	0.5	0.1	15.4
	Wet gluten content (WG) (%)	16.4	50.0	30.9	3.8	12.2
	Gluten index (GI) (%)	0.0	100.0	68.7	19.5	28.4
Dough quality	Water absorption (WA) (%)	51.0	71.0	58.9	3.6	6.1
	Development time (DT) (min)	0.7	11.2	3.3	1.4	43.2
	Stability time (ST) (min)	0.7	54.2	5.3	4.2	79.3
	Stretch area (SA) (cm^2)	4.0	239.0	87.4	42.3	48.4
	Tractility (TRA) (mm)	59.0	665.0	156.3	36.5	23.3
	Max resistance (MAXR) (E.U)	30.0	1,638.0	424.8	212.0	49.9
Processing quality	Noodles score (NS)	70.0	91.0	81.3	3.7	4.6

SD, standard deviation; CV, coefficient of variation.

23.3, and 22.2%, respectively. The CVs of FN, AC, and WG were 16.5, 15.4, and 12.2%, respectively. The CVs of HI, CPC, WC, FER, WA, and NS were relatively low at 9.5, 8.9, 8.2, 6.4, 6.1, and 4.6%, respectively. The CV of TW was the smallest at only 2.9%.

Correlation Analysis of Winter-Wheat Quality Traits

The correlations of winter-wheat quality-related parameters are summarized in **Figure 2**. On the whole, wheat quality indicators were closely correlated, especially WG and CPC, SA and SV, SA and GI, MAXR, and GI. In terms of grain quality, only FN was significantly correlated with HI, test weight (TW), water content (WC), and CPC. This indicated that FN could be the most important indicator for evaluating grain quality, followed by HI, TW, and WC. In terms of flour quality, WG was correlated with the other quality traits, which involved flour extraction rate (FER), SV, AC, and WG, and GI was correlated with the other five quality traits (FER, SV, AC, WG, and GI). This suggested that WG and GI were the most important indicators of flour quality. Moreover, with regard to dough quality, DT, ST, and tractility (TRA) were significantly correlated with other dough quality, indicating that DT and ST could be the core trait of dough quality.

On the whole, WA was significantly correlated with 13 other traits of winter-wheat quality. WG and DT were significantly correlated with 12 other traits of winter-wheat quality. HI, CPC, FN, ST, and TRA were significantly correlated with 11 other traits. These results indicated that WA, WG, DT, HI, CPC, FN, ST, and TRA directly affected the overall quality of winter-wheat.

The correlation analysis of wheat samples meeting the standard of medium-gluten and noodle scores is presented in **Figure 3**. There was a close correlation between indicators of wheat samples achieving medium-gluten SRs (GB/T 17320-2013), especially the relationship between WG and CPC, ST and DT, ST and GI, SA and GI, SA and ST, MAXR and GI, MAXR and DT, MAXR and ST, and MAXR and SA. Noodles score (NS) has a significant correlation with HI, TW, WC, AC, GI, DT, ST, SA, and MAXR.

Variance Analysis of Winter-Wheat Quality Traits

According to the analysis of variance, the effects of growing locations, cultivars, and years varied across different traits (**Table 4**). Although interaction effects existed, winter-wheat quality parameters were mainly affected by single factor effect (i.e., locations, cultivars, or years). Specifically, HI, TW and CPC, FER, and SV were significantly affected by location and cultivars, but were not influenced by years, because these index interactions between locations and years significantly affected HI and FER. WC, FN, GI, WA, and TRA were significantly affected by locations, years, and cultivars. SA and MAXR were only significantly affected by cultivars. AC was only significantly affected by growing locations. For ST and DT, no significant influences were detected between locations, cultivars, years, and their interactions.

DISCUSSION

Restricting Parameters for Strong-Gluten Wheat and Weak-Gluten Wheat

In recent years, China has made remarkable achievements in increasing wheat yield and total production. At the same time, with the increased income of residents, their demand for wheat quality is also upgrading. In general, the quality of medium- and medium-strong-gluten wheat in China is relatively high and can basically meet the market quality requirements. However, the strong-gluten wheat used for making bread and the weak-gluten

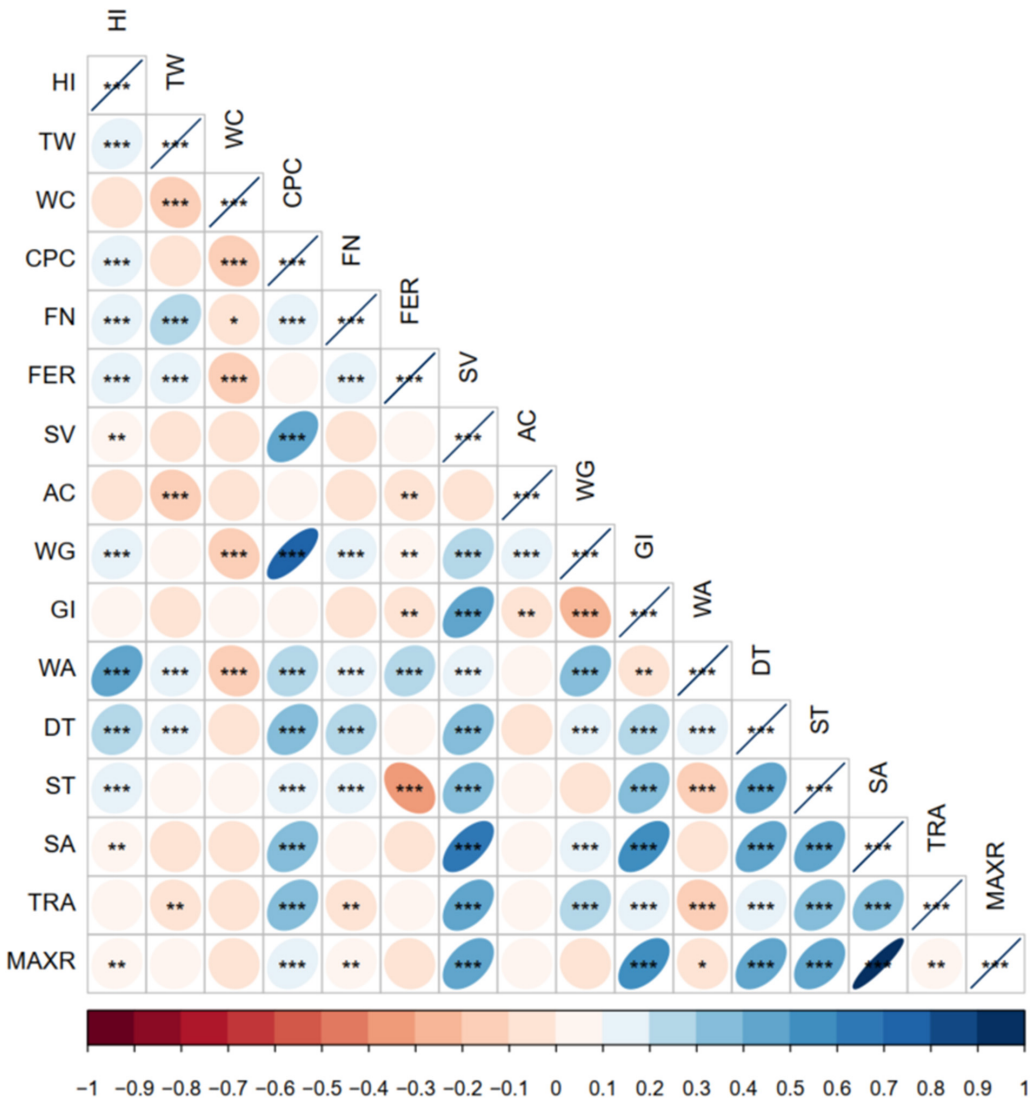

FIGURE 2 | Correlation analysis of all winter-wheat quality traits. Significant correlation at *0.05, **0.01, and ***0.001 levels (bilateral), respectively.

wheat for cake are far from meeting the market demand, making it less competitive compared with high-quality agricultural products from other countries (Deliberali et al., 2010). As a result, a significant quantity of high-quality strong- and weak-gluten wheat was imported each year.

Currently, many researches focus on identifying how the wheat quality could meet the strong-gluten or weak-gluten standard more quickly and accurately, so as to obtain optimal traits for wheat breeding. Compared with other testing techniques, rheometry is considered as a better technique to predict final product quality (Dobraszczyk and Morgenstern, 2003; Hrušková et al., 2006). Based on China National Standard (GB/T 17320-2013), the SRs of Chinese wheat quality indicators were different among strong-, medium-, medium-, and weak-gluten. SRs of HI, WG, MAXR, and WA were all greater than 90% (**Table 2**) in medium-gluten wheat, indicating that the quality of medium-gluten wheat was relatively high in China. These results suggested that HI, WG, MAXR, and WA were no longer limiting factors in quality improvement of medium-gluten wheat in China. However, the SRs of weak-gluten wheat were relatively low in China, especially for HI (9%), CPC (13%), WG (10%), and WA (23%) (**Table 2**). However, the rheological index is time-consuming and laborious, which is not conducive to quick grasp. Our results indicate that HI, CPC, WG, and WA had become major factors affecting the development of weak-gluten wheat in China. Therefore, it could be applied to determine whether the wheat meets the standard of weak-gluten wheat by determining the quality of HI, CPC, WG, and WA. The latest research also suggests that WA, CPC, and WG should be the main factors in the quality selection of weak-gluten wheat (Hu et al., 2020). For weak-gluten wheat in China, WG and CPC are not insufficient, but even high. Hu et al. (2020) think field management is difficult

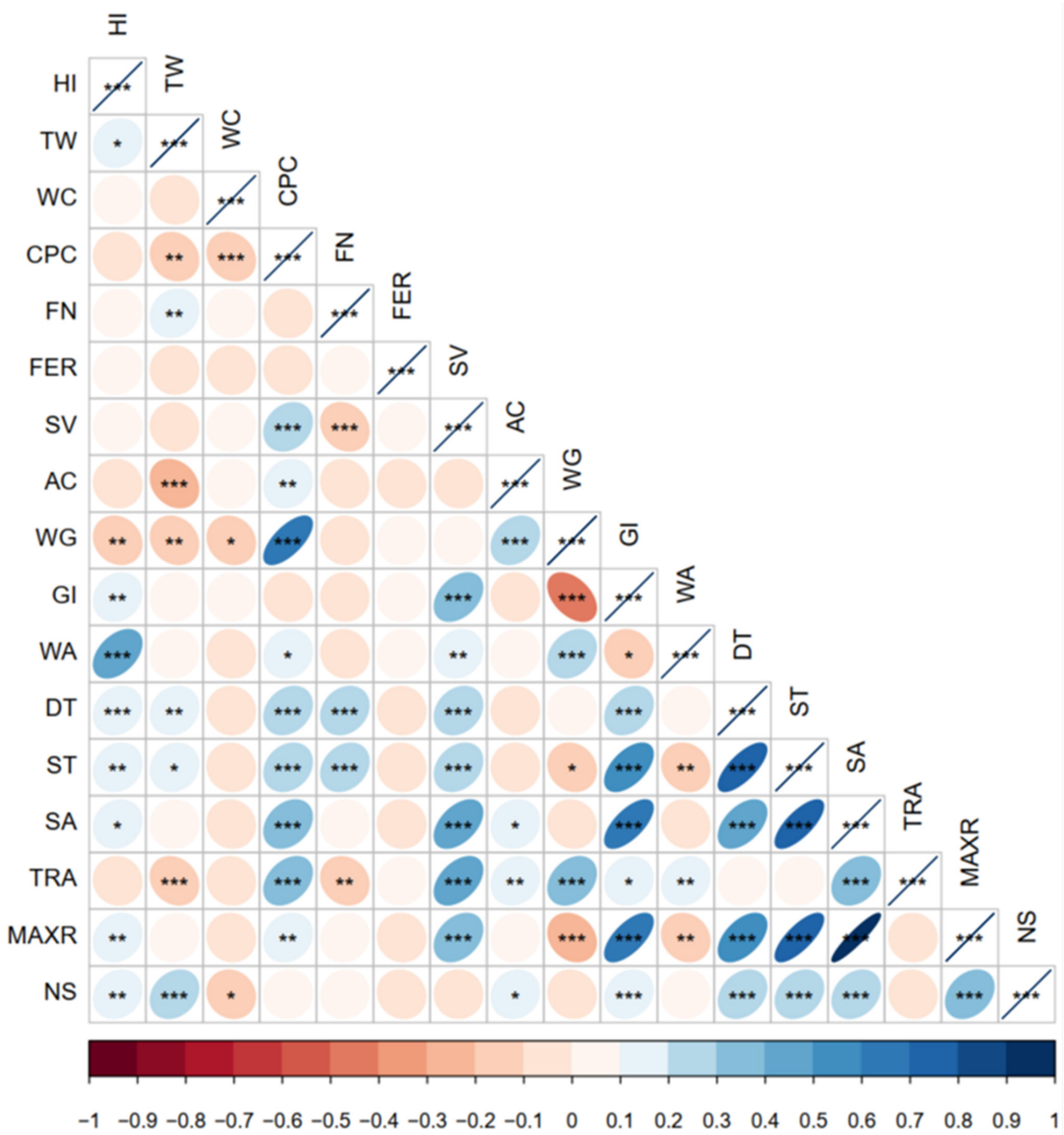

FIGURE 3 | Correlation analysis of wheat samples meeting the standard of medium-gluten and noodle scores. Significant correlation at *0.05, **0.01, and ***0.001 levels (bilateral), respectively.

to take into account the quality, leading to the high CPC and WG. Therefore, the extreme value in the national standard should be relaxed appropriately.

The overall compliance rate of strong-gluten wheat was higher than that of weak-gluten wheat, but strong-gluten wheat quality in China still needs to be improved. This study found that the improvement of strong-gluten wheat was limited by SV, ST, and SA (**Table 2**). Regarding ST and SA, the low SRs in association with extremely high CV (**Tables 2**, **3**) implied that the large variability of ST (Zhao et al., 2019) and SA should be a key reason responsible for the low SRs of strong-gluten wheat in China. Consequently, special attention should be paid to select strong-gluten wheat cultivars with long dough ST and strong tensile properties. Furthermore, providing a suitable growth environment is essential to ensure the quality stability.

Correlation Among Quality Indexes of Winter-Wheat

Multiple quality parameters for winter-wheat that are closely related to each other made it difficult to evaluate wheat quality. Based on the correlation analysis of 13 years' data of six major wheat regions in China, CPC and WG are significantly correlated (**Figure 2**), and this result is consistent with the that of Rozbicki et al. (2015). Previous study showed that gliadin and glutenin are the main components of wet gluten (Shewry et al., 2000),

TABLE 4 | Variance analysis of winter-wheat quality traits.

Categories	Traits	Location (L)	Cultivar (C)	Year (Y)	L*C	L*Y	C*Y	L*C*Y
Grain quality	Hardness index (HI)	**	**	ns	ns	*	*	ns
	Test weight (TW)	**	**	ns	ns	ns	ns	ns
	Water content (WC)	**	**	**	ns	**	*	ns
	Crude protein content (CPC)	**	**	ns	ns	ns	ns	ns
	Falling number (FN)	**	**	**	**	**	*	ns
Flour quality	Flour extraction rate (FER)	**	**	ns	ns	**	**	ns
	Sedimentation value (SV)	**	**	ns	ns	ns	ns	ns
	Ash content (AC)	**	ns	ns	ns	ns	ns	ns
	Wet gluten content (WG)	**	**	**	ns	ns	ns	ns
	Gluten index (GI)	**	**	**	**	ns	ns	ns
Dough quality	Water absorption (WA)	**	**	**	**	**	*	ns
	Development time (DT)	ns	ns	ns	ns	ns	ns	ns
	Stability time (ST)	ns	ns	ns	ns	ns	ns	ns
	Stretch area (SA)	ns	**	ns	ns	ns	ns	ns
	Tractility (TRA)	**	**	**	ns	**	**	ns
	Max resistance (MAXR)	ns	**	ns	ns	ns	ns	ns

*Significant at $P < 0.05$ level. **Significant at $P < 0.01$ level. ns, not significant.*

and gluten comprises some 75% protein on a dry weight basis, with most of the remainder being starch and lipids (Shewry et al., 2002). This may be the main reason for the significant correlation between CPC and WG. In addition, we found that GI, MAXR, and SA were all significantly correlated. On the one hand, the high GI value indicated that the quality of glutenin and gliadin was high, and high-quality glutenin provides the tensile resistance of the dough, whereas high-quality gliadin provides the adhesion required for dough fluidity and ductility. However, there was no significant correlation between WG and MAXR. This result indicates that the composition and structure of protein may have a more important effect on quality than protein quantity, which is similar to the result of Xue et al. (2016b). On the other hand, both SA and MAXR are extensibility indexes of dough. SA indicates dough strength: higher value of SA reflects greater strength of dough. There is a significant positive correlation between SA and MAXR.

The correlation between the quality indicators of medium-gluten wheat and NS showed that NS has no significant correlation with quantitative parameters of proteins (CPC, SV, and WG), but significant correlation ($P < 0.001$) with protein composition index (GI) (**Figure 3**). Previous research found that the ratio of gliadin to glutenin and their subunit composition, especially the composition and proportion of high-molecular-weight glutenin subunits, had a significant effect on the baking quality of wheat (Xue et al., 2016a). This may be one of the reasons that the correlation between noodle quality and protein content indexes of medium-gluten wheat was not significant, but highly correlated with protein composition index.

Influencing Factors of Winter-Wheat Quality in China

Genotype and environmental conditions are internal and external factors affecting the quality of winter-wheat. This study selected three influencing factors including growing locations, years, and cultivars. Growing locations represented husbandry practices and the spatial characteristics of soil and climatic conditions. Wheat cultivars represented genetic characteristics of the winter-wheat. Growing years mainly reflects the interannual climate conditions. Our results indicated that SV, ST, and SA were the main factors limiting the development of strong-gluten wheat (**Table 2**). The CV of ST (79.3%) was the largest (**Table 3**); the high CV of ST may be due to the fact that there was no effect of locations, cultivars, and years on ST, which was consistent with the study of Baric et al. (2004). However, cultivars had significant effects on SV and SA ($P < 0.01$), and especially SV had a high genetic stability (Moonen et al., 1982; Yong et al., 2004). Therefore, there is high potential for future development of strong-gluten wheat in China through breeding new varieties with excellent genes.

On the contrary, the quality of weak-gluten wheat was mainly restricted by HI, CPC, WG, and WA (**Table 2**). The results in **Table 4** showed that HI, CPC, WG, and WA were significantly affected by locations and cultivars ($P < 0.01$). However, Rozbicki et al. (2015) found that CPC and WG were more significantly affected by environment than genotypes (varieties). Therefore, the core influencing factors of CPC and WG in different countries are not consistent. The interaction among wheat locations, varieties, and years had little effect on wheat quality, which was consistent with the results of Peterson et al. (1998). In addition, an important portion of the observed variability in quality was determined by the environment, and the nitrogen supply was the principal factor determining protein content and composition (Xue et al., 2019). The total protein content increases with higher supplies of nitrogen, and as the grain protein increases, the gliadin and glutenin contents and their ratio also increased (Triboi et al., 2000). As a consequence, breeding of wheat cultivars with low protein content and WG should be placed at the first priority in improving weak-gluten winter-wheat quality in China. It is suggested to strictly control the topdressing of

wheat at the later stage and to ensure the irrigation amount before and after grain filling stage (Xue et al., 2016a).

CONCLUSION

The winter-wheat quality status in China and their impact factors were analyzed in the present study. In general, the quality of medium-gluten or medium-strong-gluten wheat in China was relatively high, which can basically meet quality requirements. However, SRs of quality traits in strong- and weak-gluten wheat were not high, especially for SV, ST, and SA in strong-gluten varieties, as well as for HI, CPC, WG, and WA in weak-gluten winter-wheat. As a result, China imported a proportion of high-quality strong- and weak-gluten each year to satisfy market demand.

Medium-gluten wheat in the quantitative parameters of proteins (CPC, SV, WG) had no significant correlation on the processing quality of NS, but the composition parameter of proteins (GI) was very significant for noodle score, which indicates that protein composition is more important than protein content on determining the processing quality. The analysis of variance showed that genetic characteristics had significant influence on the restriction indexes of strong-gluten wheat (SV, ST, and SA), and genetic characteristics, ecological environment, and management measures had significant influence on the restriction indexes of weak-gluten wheat quality (HI, CPC, WG, and WA). Analysis on the influencing factors of different winter-wheat quality indicators is useful to accelerate variety selection and strengthen their environmental adaptation and ultimately improve winter-wheat quality in China.

DATA AVAILABILITY STATEMENT

The raw data supporting the conclusions of this article will be made available by the authors, without undue reservation, to any qualified researcher.

AUTHOR CONTRIBUTIONS

MM: data curation and writing—original draft. YL: conceptualization and writing—review and editing. CX: visualization and investigation. WX: method. ZP and YH: investigation. XH: formal analysis. HJ: project administration and supervision. All authors discussed the results as well as read and approved the final manuscript for publication.

FUNDING

This work was supported by the National Key R&D Program of China (No. 2019YFA0607403), the National Natural Science Foundation of China (No. 31801931), Central Public-interest Scientific Institution Basal Research Fund (No. Y2020PT05), and the Agricultural Science and Technology Innovation Program (ASTIP).

ACKNOWLEDGMENTS

We thank Dr. Wen Wang for polishing the manuscript.

REFERENCES

AQSIQ (2013). *General Administration of Quality Supervision, Inspection and Quarantine of the People's Republic of China (AQSIQ). Standardization Administration of the People's Republic of China.* GB/T 17320-2013. Beijing: Standards Press of China.

Araus, J. L., Amaro, T., Casadesus, J., Asbati, A., and Nachit, M. M. (1998). Relationships between ash content, carbon isotope discrimination and yield in durum wheat. *Funct. Plant Biol.* 25, 835–842. doi: 10.1071/PP98071

Baric, M., Pecina, M., Sarcevic, H., and Keresa, S. (2004). Stability of four Croatian bread winter wheat (*Triticum aestivum* L.) cultivars for quality traits. *Plant Soil Environ.* 50, 402–408. doi: 10.17221/4051-PSE

da Silveira, M. M., Dittgen, C. L., de Souza Batista, C., Biduski, B., Gutkoski, L. C., and Vanier, N. L. (2020). Discrimination of the quality of Brazilian wheat genotypes and their use as whole-grains in human nutrition. *Food Chem.* 312:126074. doi: 10.1016/j.foodchem.2019.126074

Delcour, J. A., Joye, I. J., Pareyt, B., Wilderjans, E., Brijs, K., and Lagrain, B. (2012). Wheat gluten functionality as a quality determinant in cereal-based food products. *Annu. Rev. Food Sci. Technol.* 3, 469–492. doi: 10.1146/annurev-food-022811-101303

Deliberali, J., Oliveira, M., Durigon, A., Dias, A. R. G., Gutkoski, L. C., and Elias, M. C. (2010). Effects of drying process and storage time on technological quality of wheat. *Ciência e Agrotecnol.* 34, 1285–1292. doi: 10.1590/S1413-70542010000500029

Dobraszczyk, B. J., and Morgenstern, M. P. (2003). Rheology and the breadmaking process. *J. Cereal Sci.* 38, 229–245. doi: 10.1016/S0733-5210(03)00059-6

Food and Agriculture Organization of the United Nations [FAO] (2019). *E. coli.* Available online at: http://www.fao.org/faostat/en/#data/FS (accessed September 15, 2019)

Fu, B. X., Wang, K., and Dupuis, B. (2017). Predicting water absorption of wheat flour using high shear-based GlutoPeak test. *J. Cereal Sci.* 76, 116–121. doi: 10.1016/J.JCS.2017.05.017

He, Z. H., Lin, Z. Y., Wang, L. J., Xiao, Z. M., Wan, F. S., and Zhuang, Q. S. (2002). Classification on Chinese wheat regions based on quality. *Sci. Agric. Sin.* 35, 359–364. (in Chinese),

Hellemans, T., Landschoot, S., Dewitte, K., Van Bockstaele, F., Vermeir, P., Eeckhout, M., et al. (2018). Impact of crop husbandry practices and environmental conditions on wheat composition and quality: a review. *J. Agri. Food Chem.* 66, 2491–2509. doi: 10.1021/acs.jafc.7b05450

Hrušková, M., Švec, I., and Jirsa, O. (2006). Correlation between milling and baking parameters of wheat varieties. *J. Food Eng.* 77, 439–444. doi: 10.1016/J.JFOODENG.2005.07.011

Hu, X. X., Guo, L. L., Wang, L. K., Tian, J. C., and Wang, B. J. (2020). Discussion on quality classification standards of wheat varieties tested in national trials. *Qual. Saf. Agro Prod.* 2020, 16–20. (in Chinese),

Hu, X. X., Sun, L. J., Zhou, G. Y., Wu, L. N., Lu, W., and Li, W. X. (2017). Quality characteristics of winter wheat varieties tested in national trials in northern region and Yellow-huai River valley winter wheat zone from 2000 to 2015. *Acta Agronom. Sin.* 43, 501–509. (in Chinese),

Kweon, M., Slade, L., and Levine, H. (2011). Solvent retention capacity (SRC) testing of wheat flour: principles and value in predicting flour functionality in different wheat−based food processes and in wheat breeding—a review. *Cereal Chem.* 88, 537–552. doi: 10.1094/CCHEM-07-11-0092

Laidig, F., Piepho, H. P., Rentel, D., Drobek, T., Meyer, U., and Huesken, A. (2017). Breeding progress, environmental variation and correlation of winter wheat yield and quality traits in German official variety trials and on-farm during 1983–2014. *Theor. Appl. Genet.* 130, 223–245. doi: 10.1007/s00122-016-2810-3

Magallanes-López, A. M., Ammar, K., Morales-Dorantes, A., González-Santoyo, H., Crossa, J., and Guzmán, C. (2017). Grain quality traits of commercial durum wheat varieties and their relationships with drought stress and glutenins composition. *J. Cereal Sci.* 75, 1–9. doi: 10.1016/J.JCS.2017.03.005

MARA (2016). *Ministry of Agriculture and Rural Affairs of the People's Republic of China (MARA), Department of Planting Management, Ministry of Agriculture and Rural Affairs, 2016 China Wheat Quality Report*. Beijing: China agricultural science and technology press.

Ministry of Agriculture and Rural Affairs of PRC (2020). *E. coli*. Available online at: http://zdscxx.moa.gov.cn:8080/nyb/pc/index.jsp (accessed October 8, 2020)

Mohan, D., and Gupta, R. K. (2011). Harness value-addition in bread wheat (*Triticum aestivum*) through genotype and location specificity in highly productive North-Western Indo-Gangetic plains. *Indian J. Agric. Sci.* 81, 433–437.

Moonen, J. H., Scheepstra, A., and Graveland, A. (1982). Use of the SDS-sedimentation test and SDS-polyacrylamidegel electrophoresis for screening breeder's samples of wheat for bread-making quality. *Euphytica* 31, 677–690. doi: 10.1007/BF00039206

Peterson, C. J., Graybosch, R. A., Shelton, D. R., and Baenziger, P. S. (1998). Baking quality of hard winter wheat: response of cultivars to environment in the Great Plains. *Euphytica* 100, 223–228. doi: 10.1023/A:1018361502435

Punia, S., Sandhu, K. S., and Siroha, A. K. (2019). Difference in protein content of wheat (*Triticum aestivum* L.): effect on functional, pasting, color and antioxidant properties. *J. Saudi Soc. Agric. Sci.* 18, 378–384. doi: 10.1016/j.jssas.2017.12.005

Reynolds, M., Foulkes, J., Furbank, R., Griffiths, S., King, J., Murchie, E., et al. (2012). Achieving yield gains in wheat. *Plant Cell Environ.* 35, 1799–1823. doi: 10.1111/j.1365-3040.2012.02588.x

Rharrabti, Y., Royo, C., Villegas, D., Aparicio, N., and del Moral, L. G. (2003a). Durum wheat quality in Mediterranean environments: I. Quality expression under different zones. latitudes and water regimes across Spain. *Field Crops Res.* 80, 123–131. doi: 10.1016/S0378-4290(02)00176-4

Rharrabti, Y., Villegas, D., Royo, C., Martos-Núñez, V., and Del Moral, L. G. (2003b). Durum wheat quality in Mediterranean environments: II. Influence of climatic variables and relationships between quality parameters. *Field Crops Res.* 80, 133–140. doi: 10.1016/S0378-4290(02)00177-6

Rozbicki, J., Ceglińska, A., Gozdowski, D., Jakubczak, M., Cacak-Pietrzak, G., Mądry, W., et al. (2015). Influence of the cultivar, environment and management on the grain yield and bread-making quality in winter wheat. *J. Cereal Sci.* 61, 126–132. doi: 10.1016/j.jcs.2014.11.001

Šekularac, A., Torbica, A., Živančev, D., Tomić, J., and Knežević, D. (2018). The influence of wheat genotype and environmental factors on gluten index and the possibility of its use as bread quality predictor. *Genetika* 50, 85–93. doi: 10.2298/GENSR1801085S

Shewry, P. R., Halford, N. G., Belton, P. S., and Tatham, A. S. (2002). The structure and properties of gluten: an elastic protein from wheat grain. *Philos. Trans. R. Soc. B* 357, 133–142. doi: 10.1098/rstb.2001.1024

Shewry, P. R., Popineau, Y., Lafiandra, D., and Belton, P. (2000). Wheat glutenin subunits and dough elasticity: findings of the EUROWHEAT project. *Trends Food Sci. Technol.* 11, 433–441. doi: 10.1016/S0924-2244(01)00035-8

Torbica, A., Drašković, M., Tomić, J., Dodig, D., Bošković, J., and Zeěević, V. (2016). Utilization of mixolab for assessment of durum wheat quality dependent on climatic factors. *J. Cereal Sci.* 69, 344–350. doi: 10.1016/J.JCS.2016.04.012

Tozatti, P., Güldiken, B., Fleitas, M. C., Chibbar, R. N., Hucl, P., and Nickerson, M. T. (2020). The interrelationships between wheat quality, composition, and dough rheology for a range of Western Canadian wheat cultivars. *Cereal Chem.* 97, 1010–1025. doi: 10.1002/cche.10324

Triboi, E., Abad, A., Michelena, A., Lloveras, J., Ollier, J. L., and Daniel, C. (2000). Environmental effects on the quality of two wheat genotypes: 1. quantitative and qualitative variation of storage proteins. *Eur. J. Agronomy* 13, 47–64. doi: 10.1016/S1161-0301(00)00059-9

Xue, C., Erley, G. S., Rucker, S., Koehler, P., Obenauf, U., and Muhling, K. H. (2016a). Late nitrogen application increased protein concentration but not baking quality of wheat. *J. Plant Nutr. Soil Sci.* 179, 591–601. doi: 10.1002/jpln.201500569

Xue, C., Matros, A., Mock, H. P., and Mühling, K. H. (2019). Protein composition and baking quality of wheat flour as affected by split nitrogen application. *Front. Plant Sci.* 10:642. doi: 10.3389/fpls.2019.00642

Xue, C., Rossmann, A., Schuster, R., Koehler, P., and Mühling, K. H. (2016b). Split nitrogen application improves wheat baking quality by influencing protein composition rather than concentration. *Front. Plant Sci.* 7:738. doi: 10.3389/fpls.2016.00738

Yong, Z., Zhonghu, H., Ye, G., Aimin, Z., and Van Ginkel, M. (2004). Effect of environment and genotype on bread-making quality of spring-sown spring wheat cultivars in China. *Euphytica* 139, 75–83. doi: 10.1007/s10681-004-2131-5

Zhao, P. T., Zhao, W. G., Luo, H. L., Zhai, Z. P., Li, B. J., and Gou, S. X. (2019). The main quality traits of wheat: correlation analysis and principal components analysis. *Chn. Agric. Sci. Bull.* 35, 7–13. doi: 10.11924/j.issn.1000-6850.casb18070115 (in Chinese),

Zörb, C., Ludewig, U., and Hawkesford, M. J. (2018). Perspective on wheat yield and quality with reduced nitrogen supply. *Trends Plant Sci.* 23, 1029–1037. doi: 10.1016/j.tplants.2018.08.012

Conflict of Interest: The authors declare that the research was conducted in the absence of any commercial or financial relationships that could be construed as a potential conflict of interest.

frontiers in Plant Science

ORIGINAL RESEARCH
published: 20 May 2021
doi: 10.3389/fpls.2021.643116

Nitrate Increases Cadmium Accumulation in Sweet Sorghum for Improving Phytoextraction Efficiency Rather Than Ammonium

*Zhenqing Bai[1,2], Dan Li[2], Lin Zhu[2], Xiaoyu Tang[2], Yanfeng Wang[1,2], Renjun Mao[1,2] and Jiawen Wu[1,2]**

[1] Shaanxi Key Laboratory of Chinese Jujube, Yan'an University, Yan'an, China, [2] College of Life Sciences, Yan'an University, Yan'an, China

Sweet sorghum has potential for phytoextraction of cadmium (Cd) owning to its large biomass and relatively high Cd tolerance. Nitrogen affects both growth and Cd concentrations in plants. However, different forms of nitrogen effects on Cd accumulation in sweet sorghum to improve efficiency of Cd phytoremediation is still elusive. In this study, nitrate substantially promoted both dry weight and Cd concentrations in leaves, stems + sheaths and roots of sweet sorghum when compared with ammonium. As a result, Cd accumulation in nitrate-supplied sweet sorghum was around 3.7-fold of that in ammonium-supplied plants under unbuffered pH condition, while the fold was about 2.2 under buffered pH condition. We speculated pH values and Cd species in the growth medium to some extent contributed to increased Cd accumulation as affected by nitrate. Net photosynthesis rate and Fv/Fm of nitrate-treated plants under Cd stress were higher than that of ammonium-treated plants when the pH was unbuffered. Responses of antioxidant capacity in roots to Cd stress with nitrate application were stronger than that with ammonium supplementation. Taken together, nitrate is more suitable than ammonium for Cd phytoextraction by using sweet sorghum, which is able to enhance at least double efficiency of phytoextraction.

Keywords: biomass, Cd, nitrogen, pH value, phytoremediation

OPEN ACCESS

Edited by:
Christoph Martin Geilfus, Humboldt University of Berlin, Germany

Reviewed by:
Yongxing Zhu, Yangtze University, China
Mujahid Farid, University of Gujrat, Pakistan

***Correspondence:**
Jiawen Wu
wujiawende@126.com
orcid.org/0000-0001-8646-126X

Specialty section:
This article was submitted to Plant Nutrition, a section of the journal Frontiers in Plant Science

Received: *17 December 2020*
Accepted: *26 April 2021*
Published: *20 May 2021*

Citation:
Bai Z, Li D, Zhu L, Tang X, Wang Y, Mao R and Wu J (2021) Nitrate Increases Cadmium Accumulation in Sweet Sorghum for Improving Phytoextraction Efficiency Rather Than Ammonium. Front. Plant Sci. 12:643116. doi: 10.3389/fpls.2021.643116

INTRODUCTION

Cadmium (Cd) contamination in soils including arable land is increasingly concerned worldwide as foundry, mining, smelting, sewage sludge application, indiscriminate supply of pesticide and low-grade fertilizers inevitably introduce Cd into pedosphere (Nagajyoti et al., 2010; Wu et al., 2019). Cd pollution in arable land generally shows a low to moderate degree of Cd pollution with a vast of polluted areas (Clemens et al., 2013; Shi et al., 2019). In moderately Cd-polluted soils, the Cd concentration in pore water is normally less than 0.5 μM, while this level is below 0.1 μM if amendments are added in soils (Quintela-Sabarís et al., 2017; Cornu et al., 2020). By contrast, numerous published papers studied Cd toxicity in plants by using 50–100 μM Cd concentrations which are hundreds times higher than that in pore water of Cd-contaminated soils. Thus, it is necessary to study response of plants to Cd stress that is lower than the level of 0.5 μM. Additionally, in the most of cases, low concentration of Cd in soils is negligible since this level of pollutant shows almost no harmful symptoms for crops growth and yields (Yan B.F. et al., 2019; Viala et al., 2021).

However, if edible organs of crops harvested from Cd-polluted soils, even with a low amount of Cd, are consumed via food chain, human health will be damaged due to the enrichment of this heavy metal in bodies (Bernard, 2008). Therefore, strategies are required to decontaminate Cd in soils, while phytoremediation is the most suitable strategy to cope with Cd-polluted arable land.

Phytoextraction belongs to one of phytoremediation scenarios, which is a technique by using plants to remove Cd from soils and concentrate this pollutant into shoots of plants (Wu et al., 2018b; Mishra et al., 2019). Subsequently, the harvested shoots are buried, burned, composted or re-extracted for collecting heavy metal. Accordingly, plants used for Cd phytoextraction should deploy large biomass or tolerate high Cd concentration or both to improve the efficiency of remediation (de Sousa Leite and Monteiro, 2019). Although the well-known or newly discovered Cd hyperaccumulator plants such as *Sedum alfredii*, *Sedum plumbizincicola*, *Solanum nigrum* L., *Viola baoshanensis*, *Lantana camara* L., *Noccaea caerulescens*, etc. can endure high Cd concentrations without toxic symptoms, they normally have slow growth rate and small biomass (Li et al., 2018; Liu et al., 2019), thus limiting the efficiency of phytoremediation. By contrast, large biomass plants are able to accumulate high amounts of Cd although they are not Cd hyperaccumulators. In this regard, sorghum (*Sorghum bicolor* (L.) Moench.) is a C4 plant with high biomass and rapid growth rate, whilst sweet sorghum belongs to one variant of sorghum which has high sucrose content that is excellent feedstock for production of bioethanol (Mathur et al., 2017; Liu et al., 2020). By using sweet sorghum, a bioenergy plant, to remediate Cd-polluted agricultural soils, Cd will transfer from food chain to energy chain which could ensure efficacy of phytoextraction polluted-soils and economic incomes simultaneously (Grzegórska et al., 2020; Liu et al., 2020). Moreover, sweet sorghum performs better to tolerate Cd stress than maize (*Zea mays* L.) and wheat (*Triticum aestivum* L.) (Metwali et al., 2013). Zhuang et al. (2009) also found that sorghum accumulated more Cd in plants than sunflower (*Helianthus annuus* L.) another high biomass plant. Lyubun et al. (2020) indicated sorghum was a potential phytoremediation plant for not only Cd pollution but also oil sludge.

To further improve the efficiency of Cd phytoextraction, enlargement of plant biomass and/or enhancement of Cd concentrations in plants are beneficial. Nitrogen as the largest amount element after carbon required by plants has been well-known to be related to plant growth and Cd tolerance (Kovacik et al., 2011; Yang et al., 2020). However, the most two important forms of nitrogen taken up by roots, nitrate and ammonium distinctly regulate Cd accumulation in plants. For example, ammonium accelerates Cd accumulation in wheat (*T. aestivum* L.) (Yu et al., 2019), *Populus* clones (Bi et al., 2020), two Cd hyperaccumulators *Carpobrotus rossii* and *S. nigrum* (Cheng et al., 2016), whereas nitrate facilitates Cd accumulation in tomato (*Solanum lycopersicum*) (Luo et al., 2012), rice (*Oryza.sativa* L.) (Yang et al., 2016), Cd hyperaccumulators *N. caerulescens* and *S. plumbizincicola* (Hu et al., 2013). Wang et al. (2021) reported that absorption of ammonium with the root proton efflux decreased rhizosphere pH resulting in remobilized Cd in soils and increased Cd accumulation in amaranth (*Amaranthus mangostanus* L.). Zeng et al. (2020) indicated that ammonium increased Cd accumulation in *Brassica napus* as a result of decreased rhizosphere pH under a relatively low level of Cd treatment, whereas nitrate increased Cd accumulation in plants because of high biomass under a relatively high level of Cd treatment. Based on those findings, rhizosphere pH might play a crucial role in Cd accumulation in plants as affected by ammonium and nitrate. To elucidate effects of different nitrogen forms on plant growth and Cd concentrations in the large biomass plant sweet sorghum for enhancing the efficiency of phytoextraction, in the present study, buffered and unbuffered pH conditions were designed to investigate changes of Cd speciation in the growth medium, biomass, Cd accumulation, and physiochemical reactions such as antioxidant defense system and photosynthesis in ammonium or nitrate-suppled plants with or without Cd treatment.

MATERIALS AND METHODS

Plant Cultivation and Treatments

Seeds of sweet sorghum cv. Dalishi were surface sterilized and then soaked in 0.5 mM $CaCl_2$ with aeration for 8 h. Afterward, seeds with saturated water were germinated on three layers of moist filter papers. When the height of seedlings reached about 8 cm, uniform ones were transferred for hydroponics. To avoid osmotic stress, seedlings were cultivated in 1/4 strength nutrient solution for 3 days, and then 1/2 strength for 4 days. Subsequently, full-strength was used and Cd stress was started as well. Compositions of full-strength nutrient solution were macro-nutrient including K_2SO_4, 1.0 mM; KH_2PO_4, 0.2 mM; $MgSO_4$, 0.5 mM and micro-nutrient including Fe-EDTA, 200 μM; H_3BO_3, 5 μM; $MnSO_4$, 2 μM; $ZnSO_4$, 0.5 μM; $CuSO_4$, 0.3 μM; $(NH_4)_2Mo_7O_{24}$, 0.01 μM. Nitrogen source was supplied as 4 mM NO_3^-(N) in the form of $Ca(NO_3)_2$ or 4 mM NH_4^+ (A) in the form of NH_4Cl, and nitrogen concentration was selected according to our previous study in sweet sorghum (Bai et al., 2021). To compensate the extra Ca^{2+} introduced by $Ca(NO_3)_2$, $CaCl_2$ was added in the treatments without NO_3^- addition. To be in accordance with the level of Cd concentration in pore water of most moderately Cd-polluted soils as stated in introduction section, 0.5 μM Cd in the form of $CdCl_2$ was added in the present study, thus resulting in four treatments, N, N + Cd, A and A + Cd. Moreover, nutrient solution was divided into unbuffered and buffered pH two groups. Under buffered pH condition, at the beginning 10 days of Cd treatment, 2 mM 2-morpholinoethanesulfonic acid (MES) was added for keeping constant pH values among different treatments, and MES was increased to 5 mM between 11th and 20th day Cd addition. The concentration of MES was 10 mM after 20 days Cd treatment. In this study, Cd stress lasted 35 days and the changes of MES concentrations to buffer pH around 6.0 between nitrate and ammonium treatments were based on our preliminary experiment data. Four biological replicates were designed for each treatment, and one pot (two plants per pot) was regarded as one biological

replicate. The whole experiment was conducted in the growth chamber with 28°C in the daytime, 20°C in the night, 75% humidity, a 14 h photoperiod and 350 μmol photon m^{-2} s^{-1} light intensity.

Values of pH, Cd Speciation in the Growth Medium and Cd Accumulation Determination

Nutrient solution with unbuffered or buffered pH was changed every 5 days, and the renewed nutrient solution was always adjusted to 6.0 ± 0.1 with HCl and NaOH. The pH values in the unbuffered or buffered pH solution were determined at 10:00 in the morning every day until the end of 35 days Cd treatment.

Cd speciation in the growth medium with nitrate or ammonium supply was calculated by Visual MINTEQ 3.1 software. The concentrations of cations and anions individuals under 3.0, 4.0, 5.0, 6.0, and 7.0 pH were entered in the software for calculating proportions of different Cd species.

Cd accumulation was determined based on the result of dry weight multiplying Cd concentrations. In the present study, after 35 days Cd stress, sweet sorghum plants were divided into roots, stems + sheaths and leaves, dried at 75°C until constant weight, and then dry weight was measured. Afterward, the dried materials were milled into fine powder and then digested into ultra-pure HNO_3 by a microwave oven (ETHOS UP, Milestone, Italy). Subsequently, the digested solution was diluted with 2% (v/v) HNO_3 and then Cd concentrations were determined by inductively coupled plasma mass spectroscopy (ICP-MS, Agilent 7500, the United States) (Wu et al., 2016). It was worth mentioning that Cd concentrations in plants of non-Cd added treatments were not determined here since analytical grade chemicals and deionized water were used in the experiment. According to our preliminary study, Cd concentrations in those organs without Cd addition were below 0.05 μg g^{-1} dry weight which could be negligible when compared with high Cd concentrations in Cd-supplied plants (e.g., 30–120 μg g^{-1} dry weight in this experiment).

Photosynthesis

The net photosynthesis rate (A), transpiration rate (E), stomatal conductance (Gs), intercellular CO_2 concentration (Ci) and water use efficiency (WUE) of the third fully expanded leaves from bottom to top were determined by using a portable photosynthesis system (CIRAS-3, PP Systems, the United States). The parameters were measured between 9:00 and 11:00 in the morning.

Chlorophyll fluorescence parameters including the maximum efficiency of the PSII (Fv/Fm), photochemical quantum yield (QY), non-photochemical quenching (NPQ) and photochemical quenching (qP) of the third fully expanded leaves were measured by using a closed chlorophyll fluorescence imaging system (800MF, FluorCam, Czech Republic). Before measurement, the leaves were adapted in the darkness for at least 20 min, and then the plants avoiding light were transferred into the chamber of chlorophyll fluorescence imaging instrument for determining the chlorophyll fluorescence parameters (Singh et al., 2021).

H_2O_2 Content Determination and Antioxidant Defense System

After Cd treatment, roots and the third fully expanded leaves were washed with deionized water at least three times, gently dried by tissue paper, quickly frozen in liquid N_2 and then stored at −80°C for determining H_2O_2 contents, total antioxidants, superoxide dismutase (SOD), catalase (CAT), guaiacol peroxidase (POD) activities and reduced glutathione contents (GSH). The H_2O_2 contents and total antioxidants were determined according to our previous work (Wu et al., 2018a), in which the materials were homogenized in 0.1% (w/v) trichloroacetic acid (TCA) and then centrifuged at 12,000 g for 10 min at 4°C. The supernatant was incubated with 10 mM potassium phosphate buffer (pH 7.0) and 1 M potassium iodide (KI) for 15 min. Subsequently, OD values of incubated solution were determined at 390 nm by a spectrophotometer (F-4500, Hitachi, Japan), while H_2O_2 contents were calculated based on the standard curve of H_2O_2 contents. For measuring the total antioxidants, materials were homogenized in 50% (v/v) ethanol and then centrifuged at 12,000 g for 10 min at 4°C. Afterward, the supernatant was added with 99% (v/v) ethanol and 3 mM 1, 1-diphenyl-2-picrylhydrazyl radical (DPPH.) which should be freshly prepared in the darkness for 10 min. OD values of the reaction solution were determined at 515 nm. Positive control was the reaction with 99% (v/v) ethanol instead of supernatant from materials. The percentages of different absorbance between positive control and samples accounted for positive control were regarded as total antioxidants (Wu et al., 2018a).

Activities of SOD and CAT, and GSH contents were also determined according to our previous published paper (Wu et al., 2015). Briefly, SOD activity was determined based on nitroblue tetrazolium (NBT) method. CAT activity was determined based on enzyme kinetics of decomposing H_2O_2, while the absorbance was measured at 240 nm. GSH was determined based on dithiobis-2-nitrobenzoic acid (DTNB) method, in which cautions should take for finishing the determination at 412 nm in 5 min after the incubation. POD activity was determined by reagent kit (Solarbio) using guaiacol method, which was calculated based on enzyme kinetics of decomposing H_2O_2 at 470 nm.

Statistical Analysis

All the data presented in this study was four replicates ± standard deviation (SD). Significant differences between N, N + Cd, A and A + Cd treatments were analyzed according to One-Way ANOVA at the level of 0.05, while the differences between N + Cd and A + Cd treatments were analyzed according to student *t*-test by using SPSS (16.0) software.

RESULTS

Effects of Nitrogen Forms on Cd Species and pH Changes in the Growth Medium

As can been seen in **Figure 1A**, regardless of Cd addition, nitrate (N) remarkably alkalized the growth medium with

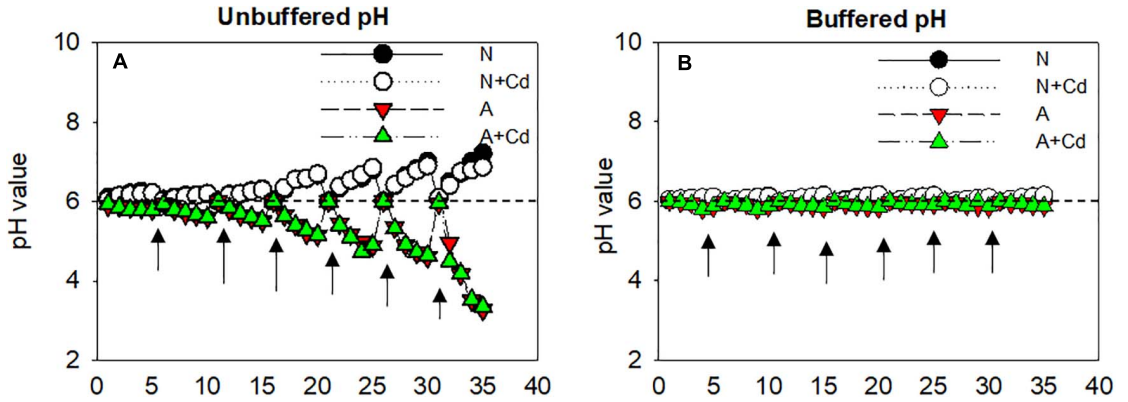

FIGURE 1 | Changes of pH values in the growth medium as affected by nitrate and ammonium in the presence or absence of Cd under unbuffered **(A)** or buffered **(B)** pH condition. N, nitrate; N + Cd, nitrate with Cd; A, ammonium; A + Cd, ammonium with Cd. Arrows represented time points of renewing nutrient solution which was changed every 5 days.

the gradually increased pH values, whereas ammonium (A) acidified the growth medium with the gradually decreased pH values. Although nutrient solution was renewed every 5 days and adjusted the pH to 6 ± 0.1, the pH values in the growth medium were changed as the uptake of NH_4^+ or NO_3^- by roots and the acidification or alkalization was sharper at the later growth stage. To distinguish whether pH in the root rhizosphere as affected by nitrate and ammonium played a pivotal role in Cd accumulation in sweet sorghum, MES was added in the nutrient solution to buffer constant pH values compared with unbuffered nutrient solution. In the buffered pH growth medium, pH values were 6 ± 0.1 during the whole cultivation period irrespective of nitrogen forms (**Figure 1B**).

In the present study, a chemical equilibrium model, Visual MINTEQ was used to estimate the proportions of different Cd speciation in the nutrient solution as affected by different nitrogen forms and pH values. According to **Figure 1**, changes of pH varied from about 3.0–7.0 influenced by nitrate and ammonium. Thus, Cd speciation in the growth medium was calculated from 3.0 to 7.0 under nitrate or ammonium with Cd treatment. When pH value in the nutrient solution was 7.0, Cd^{2+} and $CdHPO_4^0$ accounted for 76.96 and 12.56% under nitrate treatment, while the major species were Cd^{2+} and $CdCl^+$ with 50.74 and 34.78%, respectively, under ammonium treatment (**Table 1**). Nevertheless, under 6.0, 5.0, 4.0, and 3.0 pH values, the largest two percentages of Cd speciation were Cd^{2+} with 85.68, 87.86, 88.16, and 89.02%, and $CdSO_4^0$ with 10.70, 10.96, 10.89, and 10.06% under nitrate supplementation. In contrast, in ammonium-treated growth medium, under 6.0, 5.0, 4.0, and 3.0 pH values, Cd^{2+} was the most important speciation with 54.12, 54.91, 55.02, and 55.41, while the second important speciation $CdCl^+$ occupied 37.12, 37.66, 37.71, and 37.75%. Except aforementioned Cd speciation, $CdOH^+$, $CdCl_2^0$, $Cd(SO_4)_2^{2-}$, $CdNO_3^+$, and $CdNH_3^{2+}$ also existed in the growth medium, but they only contributed to minor proportions (**Table 1**).

Nitrogen Forms Affect Biomass and Cd Accumulation in Sweet Sorghum Under Unbuffered and Buffered pH Conditions

In this study, a low concentration of 0.5 μM Cd was conducted since Cd contamination in agricultural soils usually shows thus low concentration of pollution. Dry weight of leaves, stems + sheaths and roots in sweet sorghum was not significantly affected by Cd stress regardless of nitrogen forms or pH in the growth medium (**Figure 2**). However, under unbuffered pH condition, dry weight of leaves, stems + sheaths and roots in nitrate-treated plants was substantially higher than that in ammonium-treated plants (**Figure 2A**). Under buffered pH condition, dry weight of stems + sheaths and roots with nitrate supply was also higher than that with ammonium supply, whereas dry weight of leaves was similar between two different nitrogen forms treatments (**Figure 2B**). With regard to Cd concentrations, under both unbuffered and buffered pH conditions, Cd concentrations in leaves, stems + sheaths and roots with nitrate treatment were drastically increased when compared with ammonium-treated plants (**Figures 3A,B**). Based on the data of dry weight and Cd concentrations, under unbuffered pH condition, Cd accumulation amounts in leaves, stems + sheaths, roots and total plant per sweet sorghum with nitrate supply were about 2. 98-, 3. 62-, 4. 60-, and 3.73-fold of that in ammonium-treated plants (**Figure 3C**). Under buffered pH condition, Cd accumulation values in nitrate-treated plants were 1. 82-, 2. 46-, 2. 47-, and 2.25-fold in leaves, stems + sheaths, roots and total plant of that in ammonium-treated plants, respectively (**Figure 3D**).

Nitrogen Forms Affect Photosynthesis and Antioxidant Defense System in Sweet Sorghum Under Unbuffered and Buffered pH Conditions

Net photosynthesis rate (A), transpiration rate (E), stomatal conductance (Gs), intercellular CO_2 concentration (Ci), water

TABLE 1 | Distribution of Cd speciation as affected by nitrate and ammonium under different pH values in the growth medium.

pH	Treatments	Name of Cd speciation (% of total concentration)								
		Cd^{2+}	$CdOH^{+}$	$CdCl^{+}$	$CdCl_2^{0}$	$CdSO_4^{0}$	$Cd(SO_4)_2^{2-}$	$CdNO_3^{+}$	$CdNH_3^{2+}$	$CdHPO_4^{0}$
7.0	N + Cd	76.960	0.045	0.014	None	9.621	0.16	0.638	None	12.560
	A + Cd	50.748	0.028	34.788	1.338	5.317	0.089	None	0.360	7.330
6.0	N + Cd	85.688	None	0.016	None	10.703	0.178	0.711	None	2.698
	A + Cd	54.127	None	37.121	1.428	5.667	0.095	None	0.039	1.520
5.0	N + Cd	87.867	None	0.017	None	10.966	0.182	0.729	None	0.238
	A + Cd	54.910	None	37.662	1.449	5.745	0.096	None	None	0.133
4.0	N + Cd	88.162	None	0.017	None	10.896	0.180	0.730	None	0.014
	A + Cd	55.027	None	37.713	1.45	5.707	0.095	None	None	None
3.0	N + Cd	89.026	None	0.017	None	10.068	0.154	0.732	None	None
	A + Cd	55.414	None	37.753	1.447	5.302	0.082	None	None	None

The "None" represented this type of Cd speciation was not found. Proportions of different Cd speciation in this table were calculated based on a chemical equilibrium software, Visual MINTEQ 3.1.

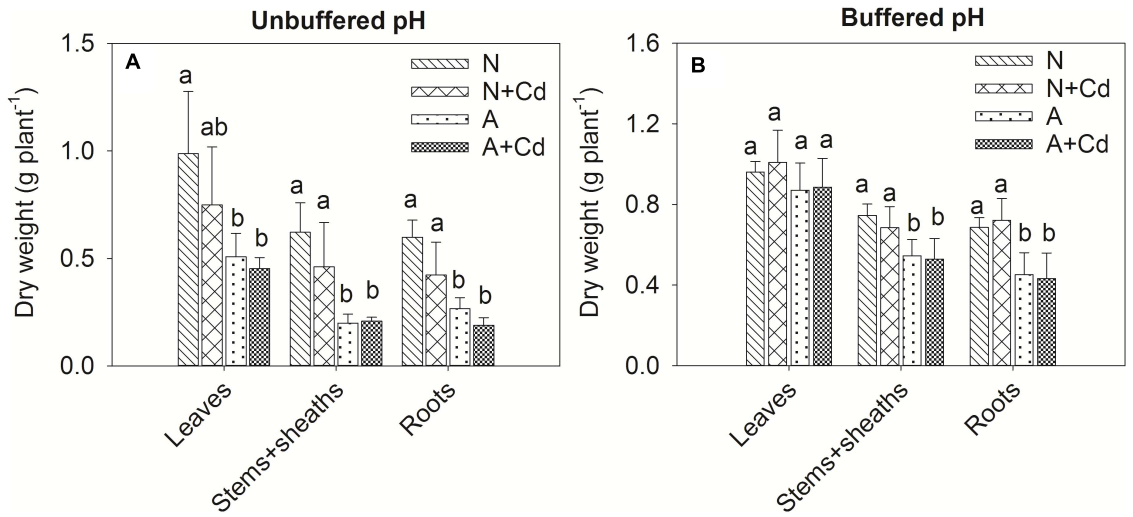

FIGURE 2 | Dry weight of leaves, stems + sheaths and roots in sweet sorghum as affected by nitrate and ammonium in the presence or absence of Cd under unbuffered **(A)** or buffered **(B)** pH condition. N, nitrate; N + Cd, nitrate with Cd; A, ammonium; A + Cd, ammonium with Cd. Different letters above the bars of one organ represented significant differences at the level of 0.05 based on One-Way ANOVA and Duncan's multiply analysis.

use efficiency (WUE), and parameters regarding fluorescence of photosynthesis such as Fv/Fm, QY, NPQ and qP were determined in this study. Under unbuffered pH condition, in accordance with the results of dry weight (**Figure 2A**), Cd stress had no effects on A, E, Gs, Ci and WUE when compared with their corresponding nitrogen treatments (**Figures 4A–E**), which indicated the same trends for Fv/Fm, QY, NPQ and qP (**Figure 5A**). Compared with ammonium supply under Cd addition, nitrate significantly increased A and decreased Ci in Cd-stressed sweet sorghum plants (**Figures 4A,D**). Under buffered pH condition, in nitrate-added plants, Cd stress had no significant effects on A, E, Gs and Ci except declined WUE compared with non-Cd treatment (**Figures 4F–J**), while Fv/Fm, QY, NPQ, and qP were not affected either (**Figure 5B**). Nevertheless, in ammonium-added plants, Cd stress remarkably elevated A, E and Gs with unchanged Ci and WUE when compared with non-Cd treatment (**Figures 4F–J**), whereas their fluorescence parameters of photosynthesis Fv/Fm, QY, NPQ, and qP were not changed (**Figure 5B**).

In regard to oxidative stress and antioxidant defense system, under unbuffered pH condition, ammonium significantly increased H_2O_2 contents in leaves of sweet sorghum compared with nitrate when no Cd was added, while total antioxidants, SOD, CAT, POD activities, and GSH contents were not changed between two nitrogen forms. Under Cd stress, the low level of Cd in the present study had no effects on H_2O_2 production and anti-oxidases activities in leaves with nitrate application, whereas Cd decreased CAT activity with ammonium application when other antioxidant enzymes were unaffected compared with non-Cd added treatment (**Table 2**). Interestingly, Cd stress drastically decreased H_2O_2 contents and SOD activity, but increased GSH contents in nitrate-treated roots of sweet sorghum. In contrast, Cd stress also elevated GSH contents,

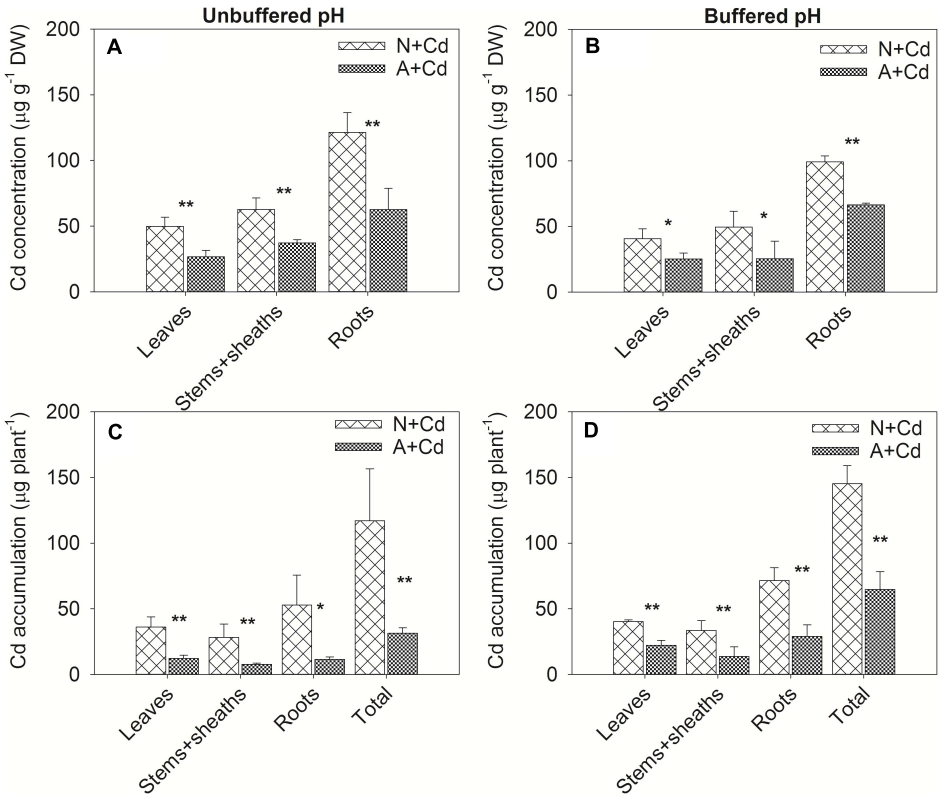

FIGURE 3 | Cd concentrations and accumulation in leaves, stems + sheaths and roots of sweet sorghum as affected by nitrate and ammonium in the presence or absence of Cd under unbuffered **(A,C)** or buffered **(B,D)** pH condition. N + Cd, nitrate with Cd; A + Cd, ammonium with Cd. One asterisk "*" indicated significant difference between the two treatments at the level of 0.05 based on student *t*-test, while two asterisks "**" represented at the level of 0.01.

while H_2O_2 contents, total antioxidants, SOD, CAT and POD activities were not affected in ammonium-treated roots of plants when compared with non-Cd addition (**Table 2**). Under buffered pH condition, Cd stress significantly increased CAT and POD activities in nitrate-supplied leaves of plants compared with non-Cd added treatment, while Cd exposure had no effects on all the determined antioxidant enzymes activities with ammonium supply (**Table 3**). In roots, nitrate application significantly decreased total antioxidants, SOD and POD activities under Cd stress when compared with non-Cd added treatment, whereas ammonium increased SOD activity under Cd stress with no changes on other antioxidant enzymes activities (**Table 3**).

DISCUSSION

Phytoextraction of Cd-polluted soils by high biomass crops such as sweet sorghum is increasingly concerned (Liu et al., 2020; Lyubun et al., 2020). Nitrogen management is not only one of important agronomic measures, but also a pivotal element determining biomass of plants (Hawkesford et al., 2012). Owing to effects of different nitrogen forms on Cd uptake, translocation and accumulation in different species of plants differently, how the two frequently used nitrogen forms, nitrate and ammonium functions on Cd accumulation in sweet sorghum are still unclear. Since nitrate and ammonium are physiologically alkaline and acidic fertilizers due to influx and efflux of protons in the growth medium separately (de Sousa Leite and Monteiro, 2019; Zeng et al., 2020), unbuffered and buffered conditions were conducted in the present study to exam pH effects on Cd accumulation in sweet sorghum treated with different forms of nitrogen. Empirically, when roots absorb one molecular NH_4^+, one molecular H^+ will be pumped from cytosol into rhizosphere leading to a decrease of rhizosphere pH (Hawkesford et al., 2012), thus increasing bioavailability of Cd and accumulation of this toxic element in plants. However, our results showed that nitrate-supplied plants accumulated much higher Cd than ammonium-supplied plants regardless of pH conditions (**Figure 3**), representing pH was not the main factor influencing Cd accumulation as affected by nitrate and ammonium. This conclusion was consistent with the finding in *N. caerulescens* that nitrate compared with ammonium facilitated Cd and Zn accumulation irrespectively of rhizosphere pH (Xie et al., 2009). Considering speciation forms also affect Cd uptake by roots, different Cd species between pH 3.0 and pH 7.0 based on unbuffered pH conditions as affected by nitrate and ammonium were determined (**Figure 1**). When pH values decreased from 7.0 to 3.0, percentages of Cd species including Cd^{2+} were only slightly elevated with the exception of a decreased $CdHPO_4^0$ in nitrate-added growth medium. Cd species in

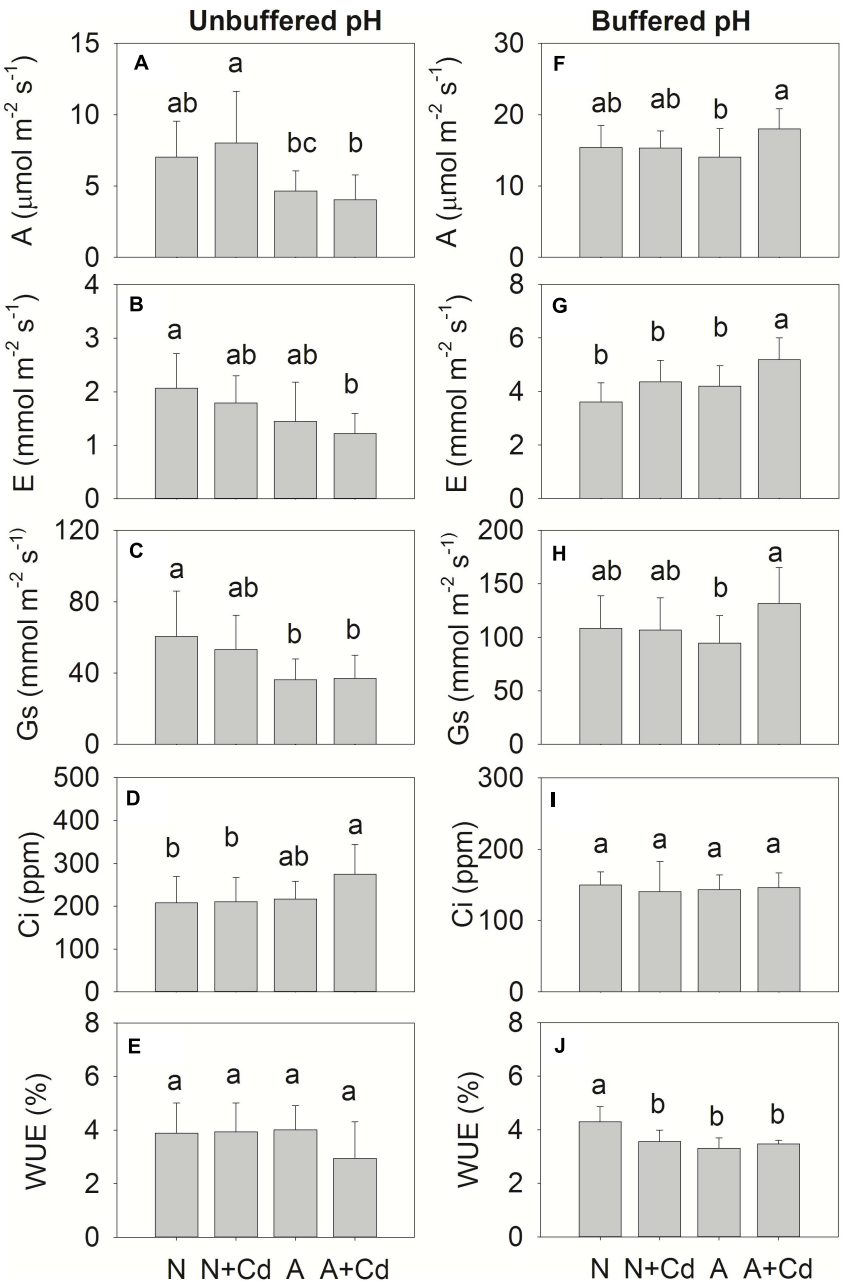

FIGURE 4 | Net photosynthesis rate (A), transpiration rate (E), stomatal conductance (Gs), intercellular CO_2 concentration (Ci) and water use efficiency (WUE) in leaves of sweet sorghum as affected by nitrate and ammonium in the presence or absence of Cd under unbuffered **(A–E)** or buffered **(F–J)** pH condition. N, nitrate; N + Cd, nitrate with Cd; A, ammonium; A + Cd, ammonium with Cd. Different letters above the bars represented significant differences at the level of 0.05 based on One-Way ANOVA and Duncan's multiply analysis.

ammonium-supplied growth medium were also slightly affected by different pH values. However, Cd^{2+} and $CdSO_4^0$ occupied the majority of Cd species ranging 76.9–89.0 and 9.6–10.1% in nitrate-treated growth medium, while Cd^{2+} and $CdCl^+$ accounted for 50.7–55.4 and 34.8–37.7% in ammonium-treated growth medium (**Table 1**). Our previous studies found that $CdSO_4^0$ was easier to be taken up by roots than Cd^{2+} because of faster diffusion (Wu et al., 2018b). Weggler et al. (2004) showed that excessive supply of Cl^- significantly increased mobilization and bioavailability of Cd in soils, whereas Geilfus (2019) indicated Cl immobilized Cd availability because of Cd and Cl^- complexes formation. In view of chemical theory, diffusion of $CdCl^+$ in roots should be faster than Cd^{2+} as binding ability of monovalent ions are weaker than divalent ions with functional groups such as carboxyl or hydroxyl in cell walls. Nevertheless, evaluating Cd bioavailability only by proportions of Cd species in the growth

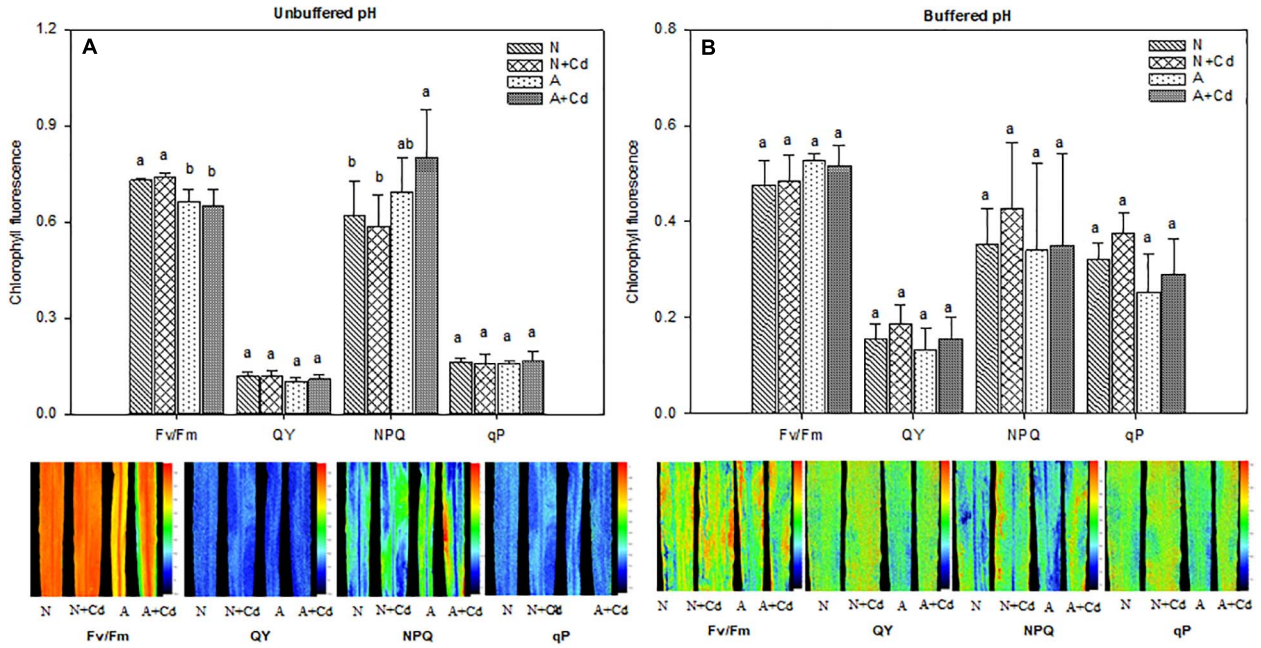

FIGURE 5 | Maximum efficiency of the PSII (Fv/Fm), photochemical quantum yield (QY), non-photochemical quenching (NPQ) and photochemical quenching (qP) in leaves of sweet sorghum as affected by nitrate and ammonium in the presence or absence of Cd under unbuffered **(A)** or buffered **(B)** pH condition. N, nitrate; N + Cd, nitrate with Cd; A, ammonium; A + Cd, ammonium with Cd. Different letters above the bars represented significant differences at the level of 0.05 based on One-Way ANOVA and Duncan's multiply analysis.

TABLE 2 | Effects of nitrate and ammonium on antioxidant defense systems in leaves and roots of sweet sorghum with or with Cd stress under unbuffered pH condition.

Organ	Treatment	H_2O_2 content (μ mol g^{-1} FW)	Total antioxidants (%)	SOD activityU g^{-1} FW)	CAT activity (Δ 240 μ g protein^{-1} min^{-1})	POD activity (Δ 470 μ g protein^{-1} min^{-1})	GSH content (μ g g^{-1} FW)
Leaves	N	128.1 ± 40.8^{b}	28.0 ± 5.9^{a}	197.4 ± 27.4^{a}	480.1 ± 246.8^{ab}	89.3 ± 19.2^{a}	92.2 ± 5.2^{a}
	N + Cd	141.7 ± 30.1^{b}	36.3 ± 6.3^{a}	192.9 ± 50.0^{a}	228.5 ± 130.2^{b}	71.9 ± 8.2^{ab}	133.2 ± 47.7^{a}
	A	248.5 ± 58.4^{a}	35.4 ± 7.8^{a}	208.4 ± 25.7^{a}	696.0 ± 131.0^{a}	68.8 ± 15.3^{ab}	126.5 ± 29.9^{a}
	A + Cd	183.2 ± 43.6^{ab}	33.2 ± 5.9^{a}	197.1 ± 34.5^{a}	289.1 ± 153.8^{b}	54.1 ± 12.1^{b}	125.4 ± 14.3^{a}
Roots	N	70.7 ± 30.7^{a}	16.7 ± 2.6^{ab}	218.1 ± 15.9^{a}	139.1 ± 30.7^{a}	538.4 ± 174.5^{a}	25.6 ± 8.9^{b}
	N + Cd	40.1 ± 9.0^{b}	21.9 ± 5.7^{a}	145.2 ± 11.4^{b}	106.5 ± 35.2^{ab}	533.7 ± 59.0^{a}	99.4 ± 10.8^{a}
	A	37.3 ± 11.6^{b}	15.7 ± 2.4^{b}	151.1 ± 45.3^{b}	77.9 ± 43.0^{b}	391.9 ± 80.6^{a}	36.6 ± 13.2^{b}
	A + Cd	38.3 ± 4.8^{b}	17.8 ± 1.8^{ab}	146.2 ± 28.5^{b}	81.8 ± 10.8^{b}	398.9 ± 82.6^{a}	87.3 ± 17.8^{a}

Values were means ± SD (n = 4). Different letters in the same column of leaves or roots represented significant differences at the level of 0.05 based on One-Way ANOVA and Duncan's multiply analysis. N, nitrate; N + Cd, nitrate with Cd; A, ammonium; A + Cd, ammonium with Cd.

medium is still difficult to judge how much Cd accumulation in plants. On account of transporters like IRT1, Nramp1, Nramp5, HMA2, HMA3, and HMA4 etc. correlated with Cd^{2+} uptake and transport are well-known, but transporters for taking up $CdCl^{+}$, $CdSO_4{}^{0}$ or other Cd-complex are unidentified in plants to date (Clemens et al., 2013). Cheng et al. (2016) reported neither ammonium nor nitrate had effects on existence of Cd speciation in *planta* of *C. rossii* and *S. nigrum*. Therefore, although Cd species in the growth medium are differently changed by nitrate and ammonium, their effects on Cd uptake and accumulation in plants are still limited.

Biomass and Cd concentration are two determinants of total Cd accumulation in plants that directly correlates with Cd phytoextraction efficiency. Vazquez et al. (2020) found ammonium supply increased plant biomass contributed to declined Cd concentrations in *Arabidopsis thaliana* because of "dilution effect," which was also reported in wheat (Yu et al., 2019). Yang et al. (2019) showed $(NH_4)_2SO_4$ and CH_4N_2O had no effect on Cd concentrations but increased plant biomass resulting in raised Cd accumulation in *S. nigrum*. Cheng et al. (2016) reported ammonium compared with nitrate increased Cd accumulation as the consequence of elevated Cd concentrations in *C. rossii* and *S. nigrum* although biomass was unchanged. Our results showed that nitrate compared with ammonium promoted both dry weight and Cd concentrations in sweet sorghum regardless of pH in

TABLE 3 | Effects of nitrate and ammonium on antioxidant defense systems in leaves and roots of sweet sorghum with or without Cd stress under buffered pH condition.

Organ	Treatment	H_2O_2 content (μ mol g^{-1} FW)	Total antioxidants (%)	SOD activity (U g^{-1} FW)	CAT activity (Δ 240 μ g $protein^{-1}$ min^{-1})	POD activity (Δ 470 μ g $protein^{-1}$ min^{-1})	GSH content (μ g g^{-1} FW)
Leaves	N	173.8 ± 83.9^{a}	20.9 ± 9.1^{a}	145.3 ± 41.5^{a}	84.9 ± 24.4^{b}	103.1 ± 13.9^{b}	82.6 ± 39.5^{a}
	N + Cd	122.1 ± 39.1^{a}	11.6 ± 4.5^{a}	183.6 ± 18.3^{a}	176.3 ± 74.5^{a}	176.4 ± 65.9^{a}	86.7 ± 14.8^{a}
	A	181.1 ± 43.1^{a}	19.9 ± 3.9^{a}	157.4 ± 15.7^{a}	100.2 ± 31.7^{ab}	73.5 ± 20.7^{b}	85.9 ± 20.6^{a}
	A + Cd	223.2 ± 77.9^{a}	19.0 ± 6.6^{a}	178.1 ± 13.3^{a}	134.4 ± 59.5^{ab}	112.7 ± 37.7^{b}	110.7 ± 7.22^{a}
Roots	N	55.9 ± 28.5^{a}	6.25 ± 2.09^{a}	131.2 ± 21.0^{a}	29.9 ± 9.1^{a}	500.9 ± 140.9^{a}	18.9 ± 17.7^{b}
	N + Cd	35.8 ± 10.7^{ab}	3.51 ± 1.18^{b}	23.2 ± 6.17^{c}	42.9 ± 8.6^{a}	203.1 ± 28.3^{b}	41.2 ± 22.9^{ab}
	A	28.4 ± 12.2^{ab}	4.17 ± 1.64^{ab}	37.4 ± 16.2^{c}	39.3 ± 12.0^{a}	437.1 ± 75.8^{a}	46.6 ± 11.9^{ab}
	A + Cd	27.6 ± 1.34^{b}	3.42 ± 0.23^{b}	63.1 ± 13.4^{b}	46.9 ± 14.9^{a}	409.4 ± 52.7^{a}	54.3 ± 26.7^{a}

Values were means ± SD (n = 4). Different letters in the same column of leaves or roots represented significant differences at the level of 0.05 based on One-Way ANOVA and Duncan's multiply analysis. N, nitrate; N + Cd, nitrate with Cd; A, ammonium; A + Cd, ammonium with Cd.

the growth medium (**Figures 2**, **3**). Accordingly, total Cd accumulation in nitrate-supplied plants were about 3.7- and 2.2-fold of that in ammonium-supplied plants under unbuffered and buffered pH, respectively, suggesting that nitrate enhances Cd phytoextraction efficiency when compared with ammonium.

Photosynthesis provides substrates for plant growth which is closely related to biomass (Alves et al., 2020). As a toxic element, Cd is able to damage photosynthesis apparatus leading to retarded plant growth (Nagajyoti et al., 2010). Based on majority of Cd concentration in pore water of Cd-contaminated soils (Quintela-Sabarís et al., 2017), 0.5 μM Cd was used in this study. Nonetheless, net photosynthesis rate and Fv/Fm were not decreased by Cd stress (**Figures 4**, **5**) which contributed to unchanged dry weight of shoots and roots of sweet sorghum as affected by Cd addition in this study (**Figure 2**). In contrast, Cornu et al. (2020) showed that a lower level of 0.1 μM Cd exposure significantly decreased dry weight of sunflower. It seems that sweet sorghum is more Cd tolerant than sunflower although both of them are high biomass plants, indicating better potential of sweet sorghum for Cd phytoextraction. Yan L. et al. (2019) found ammonium tended to enhance roots rather than shoots growth of terrestrial plants, while nitrate preferred to promote shoots growth by using a meta-analysis, which suggests nitrate-treated plants have higher biomass of shoots that is more suitable for Cd phytoremediation. In the present study, nitrate increased dry weight of both roots and shoots of sweet sorghum (**Figure 2**), which was the result of nitrate-enhanced net photosynthesis rate and Fv/Fm under Cd stress compared with ammonium (**Figures 4**, **5**). It was worth mentioning that Cd hormesis in the presence of ammonium deployed the ability of improving photosynthesis by increasing stomatal open and transpiration (**Figure 4**), and this kind of heavy metal hormesis was also reported in maize by Małkowski et al. (2020). Although Cd stimulated net photosynthesis rate under ammonium, the Fv/Fm was unchanged under buffered pH growth medium (**Figures 4**, **5**), which might be the reason that dry weight of leaves between nitrate and ammonium treatments were same (**Figure 2**). Overall, photosynthesis rates of nitrate-supplied sweet sorghum are higher than that of ammonium-supplied plants especially under unbuffered pH condition. Regarding Cd toxicity, oxidative stress is one of the toxic biomarkers although this element dose not directly involve in Fenton or Haber-Weiss reactions producing ROS (reactive oxygen species) (Nagajyoti et al., 2010). Correspondingly, plants evolve enzymatic antioxidants such as SOD, CAT, POD, GR (glutathione reductase) or APX (ascorbate peroxidase) and non-enzymatic antioxidants such as AsA (ascorbate), GSH or phenolics to scavenge the excessive ROS that maintains redox homeostasis (Wu et al., 2015). In this study, compared with non-Cd added treatments H_2O_2 contents were not increased by nitrate or ammonium with Cd added treatment (**Tables 2**, **3**), which indicated excessive ROS was not induced by Cd addition and further proved Cd tolerance of sweet sorghum. However, Lin et al. (2011) showed that high level of nitrogen compared with the low level significantly increased some antioxidant enzymes contributing to mitigation of Cd toxicity in rice. Jalloh et al. (2009) found rice plants supplied with ammonium had less oxidative stress than nitrate-supplied plants as induced by Cd stress, which was also confirmed by Wu et al. (2020) that ammonium enhanced antioxidant system and AsA-GSH cycle in rice. In contrast, Nogueirol et al. (2018) reported nitrate alleviated Cd-caused oxidative stress by improving CAT, APX, SOD, POD and GR activities in tomato. Bi et al. (2020) indicated nitrate significantly elevated POD, SOD and GR activities in leaves of Nanlin1388 *Populus* clone under Cd stress, while nitrate had no effects on those anti-oxidase enzymes activities in Nanlin 895. Thus, enzymatic and non-enzymatic antioxidants were differently regulated by nitrogen forms in different plant species under Cd stress. Our results showed that nitrate compared with ammonium significantly increased POD activity in leaves, but decreased SOD and POD activities in roots of sweet sorghum in the presence of Cd addition (**Table 3**). SOD could convert superoxide radicals (O_2^-) into H_2O_2, while POD is responsible for catalyzing H_2O_2 into water and oxygen (Wu et al., 2015). Increased POD activity in leaves as affected by nitrate under Cd stress in sweet sorghum indicated enhanced antioxidant capacity, and decreased SOD and POD activities in roots might be a consequence of low oxidative stress that antioxidant enzymes were not required for scavenging excessive

ROS. Therefore, we speculate that anti-oxidative responses of roots in nitrate-supplied sweet sorghum to Cd addition are stronger than that of ammonium-supplied plants.

CONCLUSION

Nitrate significantly increases Cd accumulation in roots, stems + sheaths and leaves of sweet sorghum when compared with ammonium as the consequence of enhanced both dry weight and Cd concentrations. Total Cd amounts in nitrate-treated sweet sorghum is about 3.7-fold of that in ammonium-treated plants under unbuffered pH condition, while it is 2.2-fold under buffered pH condition. We reason the pH and different proportions of Cd species in the growth medium to some extent contribute to improvement of Cd accumulation as affected by nitrate. In addition, nitrate elevates photosynthesis rate under Cd stress compared with ammonium especially under unbuffered pH condition, which might be the reason of promoted dry weight by nitrate. Anti-oxidative responses to Cd stress in nitrate-supplied roots are stronger than that in ammonium-supplied plants. Taken together, nitrate enhances Cd accumulation in sweet sorghum aiming at improvement of phytoextraction efficiency when compared with ammonium.

DATA AVAILABILITY STATEMENT

The original contributions presented in the study are included in the article/supplementary material, further inquiries can be directed to the corresponding author/s.

AUTHOR CONTRIBUTIONS

ZB, DL, LZ, and XT carried out the experiments. ZB and LZ wrote the manuscript with support from JW. DL analyzed data for this work and revised the manuscript with support from JW. YW and RM helped to supervise the project. JW conceived the original idea and supervised the project.

FUNDING

We thank the Research Foundation of Education Bureau of Shaanxi Province, China (No. 20JK0997), the Natural Science Basic Research Plan in Shaanxi Province of China (No. 2020JQ-794), the Start-up Funds for Excellent Talents of Yan'an University (No. YDBK2019-17), and the Natural Science Basic Research Program of Yan'an University (No. YDY2019-27) for financial support.

REFERENCES

Alves, L. R., Rossatto, D. R., Rossi, M. L., Martinelli, A. P., and Gratão, P. L. (2020). Selenium improves photosynthesis and induces ultrastructural changes but does not alleviate cadmium-stress damages in tomato plants. *Protoplasma* 257, 597–605. doi: 10.1007/s00709-019-01469-w

Bai, Z. Q., Zhu, L., Chang, H. X., and Wu, J. W. (2021). Enhancement of cadmium accumulation in sweet sorghum as affected by nitrate. *Plant Biol.* 23, 66–73. doi: 10.1111/plb.13186

Bernard, A. (2008). Cadmium & its adverse effects on human health. *Indian J. Med. Res.* 128, 557–564.

Bi, J., Liu, X., Liu, S., Wang, Y., and Liu, M. (2020). Microstructural and physiological responses to cadmium stress under different nitrogen forms in two contrasting Populus clones. *Environ. Exp. Bot.* 169:103897. doi: 10.1016/j.envexpbot.2019.103897

Cheng, M., Wang, P., Kopittke, P. M., Wang, A., Sale, P. W. G., and Tang, C. (2016). Cadmium accumulation is enhanced by ammonium compared to nitrate in two Hyperaccumulators, without affecting speciation. *J. Exp. Bot.* 67, 5041–5050. doi: 10.1093/jxb/erw270

Clemens, S., Aarts, M. G., Thomine, S., and Verbruggen, N. (2013). Plant science: the key to preventing slow cadmium poisoning. *Trends Plant Sci.* 18, 92–99. doi: 10.1016/j.tplants.2012.08.003

Cornu, J. Y., Bussière, S., Coriou, C., Robert, T., Maucourt, M., Deborde, C., et al. (2020). Changes in plant growth, Cd partitioning and xylem sap composition in two sunflower cultivars exposed to low Cd concentrations in hydroponics. *Ecotoxicol. Environ. Saf.* 205:111145. doi: 10.1016/j.ecoenv.2020.111145

de Sousa Leite, T., and Monteiro, F. A. (2019). Nitrogen form regulates cadmium uptake and accumulation in Tanzania guinea grass used for phytoextraction. *Chemosphere* 236:124324. doi: 10.1016/j.chemosphere.2019.07.055

Geilfus, C. M. (2019). Chloride in soil: from nutrient to soil pollutant. *Environ. Exp. Bot.* 157, 299–309. doi: 10.1016/j.envexpbot.2018.10.035

Grzegórska, A., Rybarczyk, P., Rogala, A., and Zabrocki, D. (2020). Phytoremediation—from environment cleaning to energy generation—current status and future perspectives. *Energies* 13:2905. doi: 10.3390/en13112905

Hawkesford, M., Horst, W., Kichey, T., Lambers, H., Schjoerring, J., Møller, I.S., et al. (2012). "Chapter 6 - functions of macronutrients," in *Marschner's Mineral Nutrition of Higher Plants*, Third Edition, ed. P. Marschner. (San Diego: Academic Press), 135–189.

Hu, P., Yin, Y. G., Ishikawa, S., Suzui, N., Kawachi, N., Fujimaki, S., et al. (2013). Nitrate facilitates cadmium uptake, transport and accumulation in the hyperaccumulator *Sedum plumbizincicola*. *Environ. Sci. Pollut. Res.* 20, 6306–6316. doi: 10.1007/s11356-013-1680-3

Jalloh, M. A., Chen, J., Zhen, F., and Zhang, G. (2009). Effect of different N fertilizer forms on antioxidant capacity and grain yield of rice growing under Cd stress. *J. Hazard. Mater.* 162, 1081–1085. doi: 10.1016/j.jhazmat.2008.05.146

Kovacik, J., Klejdus, B., Stork, F., and Hedbavny, J. (2011). Nitrate deficiency reduces cadmium and nickel accumulation in chamomile plants. *J. Agric. Food Chem.* 59, 5139–5149. doi: 10.1021/jf104793b

Li, J. T., Gurajala, H. K., Wu, L. H., Van Der Ent, A., Qiu, R. L., Baker, A. J. M., et al. (2018). Hyperaccumulator plants from China: a synthesis of the current state of knowledge. *Environ. Sci. Technol.* 52, 11980–11994. doi: 10.1021/acs.est.8b01060

Lin, Y. L., Chao, Y. Y., Huang, W. D., and Kao, C. H. (2011). Effect of nitrogen deficiency on antioxidant status and Cd toxicity in rice seedlings. *Plant Growth Regulation* 64, 263–273. doi: 10.1007/s10725-011-9567-0

Liu, S., Ali, S., Yang, R., Tao, J., and Ren, B. (2019). A newly discovered Cd-hyperaccumulator Lantana camara L. *J. Hazard. Mater.* 371, 233–242. doi: 10.1016/j.jhazmat.2019.03.016

Liu, Z. Q., Li, H. L., Zeng, X. J., Lu, C., Fu, J. -Y., Guo, L. J., et al. (2020). Coupling phytoremediation of cadmium-contaminated soil with safe crop production based on a sorghum farming system. *J. Clean. Prod.* 275:123002. doi: 10.1016/j.jclepro.2020.123002

Luo, B. F., Du, S. T., Lu, K. X., Liu, W. J., Lin, X. Y., and Jin, C. W. (2012). Iron uptake system mediates nitrate-facilitated cadmium accumulation in tomato (*Solanum lycopersicum*) plants. *J. Exp. Bot.* 63, 3127–3136. doi: 10.1093/jxb/ers036

Lyubun, Y., Muratova, A., Dubrovskaya, E., Sungurtseva, I., and Turkovskaya, O. (2020). Combined effects of cadmium and oil sludge on sorghum: growth, physiology, and contaminant removal. *Environ. Sci. Pollut. Res.* 27, 22720–22734. doi: 10.1007/s11356-020-08789-y

Małkowski, E., Sitko, K., Szopiński, M., Gieroń, Ż., Pogrzeba, M., Kalaji, H. M., et al. (2020). Hormesis in plants: the role of oxidative stress, auxins and

photosynthesis in corn treated with Cd or Pb. *Int. J. Mol. Sci.* 21:2099. doi: 10.3390/ijms21062099

Mathur, S., Umakanth, A. V., Tonapi, V. A., Sharma, R., and Sharma, M. K. (2017). Sweet sorghum as biofuel feedstock: recent advances and available resources. *Biotechnol. Biofuels* 10:146.

Metwali, E. M. R., Gowayed, S. M. H., Al-Maghrabi, O. A., and Mosleh, Y. Y. (2013). Evaluation of toxic effect of copper and cadmium on growth, physiological traits and protein profile of wheat (*Triticum aestivium* L.), maize (*Zea mays* L.) and sorghum (*Sorghum bicolor* L.). *World Appl. Sci. J.* 21, 301–314.

Mishra, R., Datta, S. P., Annapurna, K., Meena, M. C., Dwivedi, B. S., Golui, D., et al. (2019). Enhancing the effectiveness of zinc, cadmium, and lead phytoextraction in polluted soils by using amendments and microorganisms. *Environ. Sci. Pollut. Res.* 26, 17224–17235. doi: 10.1007/s11356-019-05143-9

Nagajyoti, P. C., Lee, K. D., and Sreekanth, T. V. M. (2010). Heavy metals, occurrence and toxicity for plants: a review. *Environ. Chem. Lett.* 8, 199–216. doi: 10.1007/s10311-010-0297-8

Nogueirol, R. C., Monteiro, F. A., De Souza Junior, J. C., and Azevedo, R. A. (2018). NO3–/NH4+ proportions affect cadmium bioaccumulation and tolerance of tomato. *Environ. Sci. Pollut. Res.* 25, 13916–13928. doi: 10.1007/s11356-018-1588-z

Quintela-Sabarís, C., Marchand, L., Kidd, P. S., Friesl-Hanl, W., Puschenreiter, M., Kumpiene, J., et al. (2017). Assessing phytotoxicity of trace element-contaminated soils phytomanaged with gentle remediation options at ten European field trials. *Sci. Total Environ.* 599-600, 1388–1398. doi: 10.1016/j.scitotenv.2017.04.187

Shi, T., Zhang, Y., Gong, Y., Ma, J., Wei, H., Wu, X., et al. (2019). Status of cadmium accumulation in agricultural soils across China (1975-2016): from temporal and spatial variations to risk assessment. *Chemosphere* 230, 136–143. doi: 10.1016/j.chemosphere.2019.04.208

Singh, S., Prasad, S. M., Sharma, S., Dubey, N. K., Ramawat, N., Prasad, R., et al. (2021). Silicon and nitric oxide-mediated mechanisms of cadmium toxicity alleviation in wheat seedlings. *Physiol. Plant.* doi: 10.1111/ppl.13065

Vazquez, A., Recalde, L., Cabrera, A., Groppa, M. D., and Benavides, M. P. (2020). Does nitrogen source influence cadmium distribution in Arabidopsis plants? *Ecotoxicol. Environ. Saf.* 191:110163. doi: 10.1016/j.ecoenv.2020.110163

Viala, Y., Sappin-Didier, V., Bussière, S., Coriou, C., and Nguyen, C. (2021). Simple models efficiently predict free cadmium Cd2+ in the solutions of low-contaminated agricultural soils. *Sci. Total Environ.* 778:146428. doi: 10.1016/j.scitotenv.2021.146428

Wang, J. F., Li, W. L., Li, Q. S., Wang, L. L., He, T., Wang, F. P., et al. (2021). Nitrogen fertilizer management affects remobilization of the immobilized cadmium in soil and its accumulation in crop tissues. *Environ. Sci. Pollut. Res.* doi: 10.1007/s11356-021-12868-z

Weggler, K., Mclaughlin, M. J., and Graham, R. D. (2004). Effect of chloride in soil solution on the plant availability of biosolid-borne cadmium. *J. Environ. Qual.* 33, 496–504. doi: 10.2134/jeq2004.0496

Wu, J. W, Mock, H. P., Giehl, R. F. H., Pitann, B., and Muhling, K. H. (2019). Silicon decreases cadmium concentrations by modulating root endodermal suberin development in wheat plants. *J. Hazard. Mater.* 364, 581–590. doi: 10.1016/j.jhazmat.2018.10.052

Wu, J. W., Geilfus, C. M., Pitann, B., and Mühling, K. H. (2016). Silicon-enhanced oxalate exudation contributes to alleviation of cadmium toxicity in wheat. *Environ. Exp. Bot.* 131, 10–18. doi: 10.1016/j.envexpbot.2016.06.012

Wu, J. W., Guo, J., Hu, Y. H., and Gong, H. J. (2015). Distinct physiological responses of tomato and cucumber plants in silicon-mediated alleviation of cadmium stress. *Front. Plant Sci.* 6:453.

Wu, J. W., Mock, H. P., and Mühling, K. H. (2018a). Sulfate supply enhances cadmium tolerance in *Vicia faba* L. plants. *Environ. Sci. Pollut. Res.* 25, 33794–33805. doi: 10.1007/s11356-018-3266-6

Wu, J. W., Sagervanshi, A., and Mühling, K. H. (2018b). Sulfate facilitates cadmium accumulation in leaves of *Vicia faba* L. at flowering stage. *Ecotoxicol. Environ. Saf.* 156, 375–382. doi: 10.1016/j.ecoenv.2018.03.042

Wu, Z., Jiang, Q., Yan, T., Zhang, X., Xu, S., Shi, H., et al. (2020). Ammonium nutrition mitigates cadmium toxicity in rice (*Oryza sativa* L.) through improving antioxidase system and the glutathione-ascorbate cycle efficiency. *Ecotoxicol. Environ. Saf.* 189:110010. doi: 10.1016/j.ecoenv.2019.110010

Xie, H. L., Jiang, R. F., Zhang, F. S., Mcgrath, S. P., and Zhao, F. J. (2009). Effect of nitrogen form on the rhizosphere dynamics and uptake of cadmium and zinc by the hyperaccumulator *Thlaspi caerulescens*. *Plant Soil* 318, 205–215. doi: 10.1007/s11104-008-9830-y

Yan, B. F., Nguyen, C., Pokrovsky, O. S., Candaudap, F., Coriou, C., Bussière, S., et al. (2019). Cadmium allocation to grains in durum wheat exposed to low Cd concentrations in hydroponics. *Ecotoxicol. Environ. Saf.* 184:109592. doi: 10.1016/j.ecoenv.2019.109592

Yan, L., Xu, X., and Xia, J. (2019). Different impacts of external ammonium and nitrate addition on plant growth in terrestrial ecosystems: a meta-analysis. *Sci. Total Environ.* 686, 1010–1018. doi: 10.1016/j.scitotenv.2019.05.448

Yang, W., Dai, H., Skuza, L., and Wei, S. (2019). Strengthening role and the mechanism of optimum nitrogen addition in relation to *Solanum nigrum* L. Cd hyperaccumulation in soil. *Ecotoxicol. Environ. Saf.* 182:109444. doi: 10.1016/j.ecoenv.2019.109444

Yang, Y., Xiong, J., Chen, R., Fu, G., Chen, T., and Tao, L. (2016). Excessive nitrate enhances cadmium (Cd) uptake by up-regulating the expression of OsIRT1 in rice (*Oryza sativa*). *Environ. Exp. Bot.* 122, 141–149. doi: 10.1016/j.envexpbot.2015.10.001

Yang, Y., Xiong, J., Tao, L., Cao, Z., Tang, W., Zhang, J., et al. (2020). Regulatory mechanisms of nitrogen (N) on cadmium (Cd) uptake and accumulation in plants: a review. *Sci. Total Environ.* 708:135186. doi: 10.1016/j.scitotenv.2019.135186

Yu, L., Wang, X., Li, X., Wang, Y., Kang, H., Chen, G., et al. (2019). Protective effect of different forms of nitrogen application on cadmium-induced toxicity in wheat seedlings. *Environ. Sci. Pollut. Res.* 26, 13085–13094. doi: 10.1007/s11356-019-04747-5

Zeng, X., Zou, D., Wang, A., Zhou, Y., Liu, Y., Li, Z., et al. (2020). Remediation of cadmium-contaminated soils using *Brassica napus*: effect of nitrogen fertilizers. *J. Environ. Manag.* 255:109885. doi: 10.1016/j.jenvman.2019.109885

Zhuang, P., Shu, W., Li, Z., Liao, B., Li, J., and Shao, J. (2009). Removal of metals by sorghum plants from contaminated land. *J. Environ. Sci.* 10, 1432–1437.

Conflict of Interest: The authors declare that the research was conducted in the absence of any commercial or financial relationships that could be construed as a potential conflict of interest.

frontiers in Plant Science

MINI REVIEW
published: 20 May 2021
doi: 10.3389/fpls.2021.643047

Opening the Treasure Chest: The Current Status of Research on *Brassica oleracea* and *B. rapa* Vegetables From *ex situ* Germplasm Collections

Katja Witzel[1]*, *Anastasia B. Kurina*[2] *and Anna M. Artemyeva*[2]*

[1] Leibniz Institute of Vegetable and Ornamental Crops, Großbeeren, Germany, [2] Federal Research Center the N.I. Vavilov All-Russian Institute of Plant Genetic Resources (VIR), St. Petersburg, Russia

OPEN ACCESS

Edited by:
Carla S. Santos,
Catholic University of Portugal, Portugal

Reviewed by:
Karl Schmid,
University of Hohenheim, Germany
Nian Wang,
Huazhong Agricultural University, China
Zhansheng Li,
Insititute of Vegetables and Flowers, Chinese Academy of Agricultural Sciences, China

***Correspondence:**
Katja Witzel
witzel@igzev.de
Anna M. Artemyeva
akme11@yandex.ru

Specialty section:
This article was submitted to Plant Nutrition, a section of the journal Frontiers in Plant Science

Received: 17 December 2020
Accepted: 26 April 2021
Published: 20 May 2021

Citation:
Witzel K, Kurina AB and Artemyeva AM (2021) Opening the Treasure Chest: The Current Status of Research on Brassica oleracea and B. rapa Vegetables From ex situ Germplasm Collections. Front. Plant Sci. 12:643047. doi: 10.3389/fpls.2021.643047

Germplasm collections reflect the genetic variability in crops and their wild relatives. Hence, those genetic resources are tremendously valuable for breeders and researchers, especially in light of climatic change and stagnant crop production rates. In order to achieve improvements in crop production and end-use quality, favorable traits and donor alleles present in germplasm collections need to be identified and utilized. This review covers recent reports on the utilization of germplasm material to isolate genotypes of *Brassica oleracea* and *B. rapa* vegetables, focusing on high nutrient use efficiency, accumulation of biologically active metabolites, pest resistance, and favorable phenotypic appearance. We discuss the current state of *Brassica* vegetable collections in genebanks and summarize studies directed to the molecular characterization of those collections.

Keywords: *Brassica*, genebank, glucosinolate, phenotyping, vegetables

INTRODUCTION

National and international botanical genebanks collect, conserve, investigate, and provide genetic resources of plant species. It is crucial to preserve plant materials, such as landraces, old and advanced cultivars, inbred and double haploid lines, and hybrid populations, and to identify their characteristics. *Ex situ* conservation is most efficient in terms of ease for users to access the plant material and because of its cost efficiency. Genebanks have the task of providing precisely classified living plant material for basic research and various applied research areas, such as plant breeding (Halewood et al., 2020). By integrating morphological and anatomical analysis with molecular fingerprinting approaches, important questions about the evolution of plant diversity, species boundaries and intra-species variability are addressed and form an essential basis for reliable classification and identification of plants. More recently, high-throughput genotyping, coupled with phenotype characterization, has been introduced as a next step for efficiently mining germplasm material (Nguyen and Norton, 2020). Ideally, quality traits should also be provided for each accession, such as productivity, earliness, stress resistance, and biochemical composition (Davies and Allender, 2017), in addition to epiphenotype, the characterization of the plant-environment relationship. Hammer et al. (2018) highlight the importance of both *ex situ* and *in situ* local biodiversity conservation for a range of vegetable species, and describe the evolution of broccoli (*Brassica oleracea* var. *italica*) cultivars from a landrace. Genebanks are a valuable resource for

providing plant accessions with a high level of resistance to biotic and abiotic stresses, valuable biochemical profiles or preferable sensory traits in an era of large climate changes (Pignone and Hammer, 2013; Anglin et al., 2018).

Cultivars of *Brassica* species are horticulture and field crops worldwide. They are vegetable, oil, fodder, green manure or spice plants. Brassicaceous vegetables belong to the taxa *B. oleracea* (cabbage, broccoli, cauliflower, kale, Brussels sprouts, collard greens, savoy, kohlrabi, and Chinese kale), *B. rapa* (turnip, mizuna, napa cabbage, cime di rapa, turnip rape), *B. napus* (swede), and *B. juncea* (Indian mustard), etc. These plants are grown for their root (turnip, rutabaga/swede), their swollen stem base (kohlrabi), their leaves (cabbage, kale, pak choi) or their inflorescence (cauliflower, broccoli). The importance of this class of vegetables to human health lies not only in their contribution to the vitamin and mineral components of the human diet, but also in the beneficial effects of their numerous classes of plant secondary metabolites. Just as for crops generally, maintaining their productivity in the light of increasing climate change and the dynamically evolving pest and pathogen communities represents major challenges requiring the genetic diversity in genebank accessions (**Table 1**).

After briefly outlining the importance of *Brassica* vegetables in human nutrition, the current state of international efforts in *Brassica* vegetable collections will be discussed. Subsequently, we will summarize different quality traits that represent possible breeding targets for crop improvement and were the focus of recent research efforts, and pinpoint strategies to overcome current shortcomings in applying genebank material for crop improvement. This review focuses on developments and achievements between 2009 and 2021 in four areas where genebank accessions have been employed: to analyze nutrient use efficiency, to gain insight into the accumulation of special metabolites, to isolate sources of pest resistance and for phenotype studies.

TABLE 1 | Coverage of *Brassica* germplasm in genebanks.

Species name	Number of accessions
B. oleracea	14,700
B. napus	8,378
B. rapa	7,486
B. juncea	4,649
B. carinata	732
B. nigra	726
B. campestris	455
B. tournefortii	185
B. cretica	121
B. incana	78
B. fruticulosa	72
B. villosa	49
B. insularis	47
B. repanda	40
B. rupestris	35

The 15 most abundant Brassica species were retrieved from Genesys database (www.genesys-pgr.org, April 2021).

NUTRITIONAL AND BIOLOGICALLY ACTIVE COMPOUNDS IN *BRASSICA* VEGETABLE CROPS

In developed societies, the dietary and medicinal properties of food has become the most important factors when choosing food. *Brassica* crops have a high content of water and low fat, and consequently a low caloric content. They are characterized by a relatively high level of carbohydrates, proteins that include essential amino acids, and many mineral elements. The high value of *Brassica* crops for human nutrition is primarily determined by their wide variety of biologically active compounds – enzymes, pigments, vitamins, and secondary metabolites (Manchali et al., 2012). Breeding for biologically active compounds has been considered a priority (Prange and Hewett, 2003). Fresh *Brassica* vegetables contain antioxidants, such as vitamins C and E, carotenoids and antioxidant enzymes such as catalase, superoxide dismutase and peroxidase (Singh et al., 2010). Furthermore, they are also rich in beneficial plant metabolites, including glucosinolates, anthocyanins, flavonoids, terpenes, S-methylcysteine sulfoxide, coumarins, and other minor compounds (Manchali et al., 2012; Neugart et al., 2018).

The beneficial effects of *Brassica* vegetables on human health have been partially linked to these phytochemicals, which may act at different and complementary levels. They prevent oxidative stress, induce detoxification enzymes, stimulate the immune system, inhibit malignant transformation and carcinogenic mutations, and reduce proliferation of cancer cells (Boivin et al., 2009; Herr and Buchler, 2010; Kestwal et al., 2011). Consumption of cruciferous vegetables appears to lower the risk for some kinds of cancers, including renal, prostate and possibly colorectal cancers. Consumption of vegetables, including *Brassica* species, has been strongly associated with a reduced risk of chronic conditions such as cardiovascular disease, diabetes, Alzheimer's disease, cataracts and age-related functional decline (Cohen et al., 2000; Knekt et al., 2002; Higdon et al., 2007; Sergentanis et al., 2018).

Greater fundamental knowledge of the accumulation of nutrients and biologically active substances by plants is required to permit the development of a strategy for creating new varieties of Brassicaceae family vegetables with improved consumer properties. Genebank germplasm represents a valuable natural genetic resource that can be exploited for the improvement of traits related to plant growth, pest resistance, and nutrient use efficiency.

CURRENT STATUS OF *B. OLERACEA* AND *B. RAPA* VEGETABLE COLLECTIONS

Wheat, rice, barley and maize account for a total of about 1,656,000 genebank accessions (retrieved from http://www.fao.org/wiews/en/on October 15th 2020). In Europe, around 31% of agricultural production value is represented by less than 20 crops. These include the four main European staple crops (wheat,

potato, maize, and barley), several vegetable crops (tomato, sugar beet, cucumbers, melons/watermelons, *Brassicas*, and onion) and fruits (apples, citrus). Around one million accessions of these crops, held in worldwide genebanks, are listed in the Genesys online catalog, among them 31,653 accessions of *Brassica* vegetables[1]. For example, germplasm of broccoli (*B. oleracea* var. *italica*) is hold in genebank in the United Kingdom (448 accessions), Taiwan (316 accessions), Russia (172 accessions), United States (165 accessions), Germany (136 accessions), Italy (105 accessions), India (94 accessions), Australia (60 accessions), and Spain (56 accession), among others (see text footnote 1, April 2021). Most biological diversity of *Brassica* crops is now conserved *ex situ* in genebanks and breeders' materials. The largest national collections of *B. oleracea* are located at the Russian N.I.Vavilov Institute of Plant Genetic Resources (VIR) and the German Leibniz Institute of Plant Genetics and Crop Plant Research (IPK), while the largest *B. rapa* collections are maintained at the Australian Grains Genebank (AGG) and VIR. The history of the 97-years old Russian *Brassica* collection, and results and perspectives of its study were summarized recently (Artemyeva et al., 2019). Botanical and morphological descriptions of four *Brassica* species from the German national collection were presented by Gladis and Hammer (1992).

The formation of Russian state worldwide Brassicaceae collection kept at VIR had begun in 1923 after N. I. Vavilov's visit of West-European countries, United States, and Canada (1921-1922). After that, collecting missions had continued in Russia and all centers of plant origin and diversity worldwide. 1,500 accessions of vegetable *Brassicas* and 450 oilseed accessions were collected by N. I. Vavilov himself and his colleagues until 1940. As a result of the complex evaluation in the different ecologo-geographical zones of Russia and the phylogenetic studies of subspecies, varieties, forms, cultivar groups using many biological traits, descriptors were developed for *B. oleracea*, *B. rapa*, *B. napus*, *Raphanus sativus*, *B. juncea*, *Sinapis alba, S. nigra*, *S. arvensis*, among others (Sinskaya, 1928; Lizgunova, 1984). On this basis, Lizgunova divided the white cabbages into 7 eco-geographical groups and 33 cultivar types, cauliflower and broccoli into 7 groups and 21 cultivar types, savoy into 5 groups and 16 types, etc. Later, Artemyeva divided the Chinese cabbages (*B. rapa* ssp. *pekinensis*) into 14 cultivar types (Artemyeva, 2004). Nowadays the VIR Brassicaceae collection consists of 10,997 accessions from 11 genera and 32 species: vegetable, fodder, oilseed, spicy, ornamental crops from 98 countries. The collection includes the accessions of different status: wild species, landraces (30%), old and advanced breeding cultivars (58%), inbred and double haploid lines, hybrid populations, and mapping populations (12%).

The genetic diversity of local and traditional *Brassica* cultivars can be used to genetically improve plants, expand their base and create new cultivars adapted to growing in less favorable environmental conditions. Currently, the international movement of genetic resources takes place for a variety of purposes and in different forms: exchange of *ex situ* germplasm accessions, sales of varietal seeds, exchange through seed companies, and management of *in situ* storage. Within the framework of the international exchange of genebank accessions, several tens of thousands of transactions are carried out annually; such exchange plays an important role in the conservation, research and development of genetic resources. Continuous availability for research and development is a prerequisite for improving crops, including *Brassica* crops. The genetic resources of *Brassica* plants have the potential to create a variety of traits that can help address potential future challenges, such as the need for crops to adapt to changing climatic conditions or disease and insects resistance. Therefore, continued access to them is necessary to meet the growing demand for food, as well as access to neglected and underutilized crops, given their important role in nutrition. Until now, several domesticated and wild Brassica species have been subjected to genome analysis for the identification of beneficial alleles (Saad et al., 2021). Merging available genome information, reverse genetics resources and genome editing tools with the diversity in germplasm pools is the most promising strategy for crop improvement.

Most conserved accessions are labeled with basic descriptors of morphological traits and information on the origin of collected material. For example, the VIR passport database is based on 28 characteristics and includes all accessions from the collections; the characterization and evaluation databases include 60–90% accessions depending of crops, while also a separate trait database is operated for characteristics of genetic and breeding interest. Hence, a proportion of material consists of unwanted duplications that need to be identified and minimized within and between collections (Solberg et al., 2018; Palme et al., 2020). A further issue is the taxonomic misclassification of accessions. Molecular characterization of plant material has become a valuable tool to increase the efficiency of genebank management and to identify duplicated or misclassified accessions (Mason et al., 2015; Pelc et al., 2015; Koh et al., 2017; Stansell et al., 2018; Yousef et al., 2018). The genetic molecular resources represented by Brassicaceae seed collections have been reviewed (Knee et al., 2011). In order to assess the genetic diversity present in *Brassica* collections, amplified fragment length polymorphisms have been studied in 50 accessions of *B. oleracea* (van Hintum et al., 2007), 17 accessions of *B. oleracea* convar. *acephala* (Christensen et al., 2011) and 20 accessions of *B. oleracea* var. *capitata* (Faltusova et al., 2011). Sequence-specific amplification polymorphism has been shown to be useful for phylogenetic analysis of the *B. rapa* core collection of VIR, encompassing 96 accessions (Budahn et al., 2013). Others have used single-sequence repeat markers to investigate genebank germplasms, such as 25 accessions of different *B. oleracea* subspecies (El-Esawi et al., 2016) and 239 accessions of *B. rapa* divided into the main morphotypes (Zhao et al., 2010), as well as several core collections from the VIR *B. oleracea* and *B. rapa* accessions: 18 Russian local white cabbage accessions by SSRs were divided into Northern and Central Russian, Dutch and Central European, Southern European cultivars, when the level of single-sequence repeat DNA polymorphism within the Russian gene pool was higher than within the European gene pool (Artemyeva et al., 2006), 96 accessions of *B. rapa* (Artemyeva et al., 2008), 50 accessions from different *B. oleracea* varieties – cabbages, cauliflower, kales

[1] www.genesys-pgr.org

(Artemyeva et al., 2009) and 40 broccoli accessions were divided into four clusters according to vegetation period length, curd size and sprout development (Fateev and Artemyeva, 2020).

In order to determine genotype-phenotype correlations in germplasm collections, association mapping using mostly SSR markers have been performed in *B. rapa, B. oleracea* and *R. sativus* accessions with respect to agronomic traits and morphological characteristics: bolting time, growth related traits, morphological characters connected with quality and productivity (Artemyeva et al., 2013) as well as biochemical traits: content of dry matter, sugars, protein, ascorbic acid, carotenoids, chlorophylls (Artemyeva et al., 2016, 2017). For instance, in *B. rapa* the most important loci are located on the top of chromosome A02, on the bottom of A03, in the higher region of A10 that correspond to *BrFLC2, BrFLC5, BrFLC1* positions, supporting the importance of flowering time for the development of many morphological and biochemical traits in *Brassica* crops.

RESEARCH FOCUS OF THE LAST YEARS IN UTILIZING GERMPLASM MATERIAL

The large potential of germplasm material, sometimes referred to as "diamond in the rough," needs extensive work to make use of accessions more feasible. To establish the true value of genetic resources, broad evaluation is required by curators with respect to desired plant characteristics, e.g., agronomic, nutritional or resistance traits. For example, more than 500 vegetable *Brassica* accessions per year have been trialed at five VIR experimental stations.

Most genebanks have applied trait analyses. For example, systematic study of its worldwide collection of cultivated plants has been conducted at the VIR Department of Biochemistry since 1922, as summarized by Ivanov et al. (1938), Ermakov et al. (1972), Ermakov and Arasimovich (1961), and many others. Study of the biochemical composition of the Brassicaceae collection at VIR began in 1933. Accessions of cole crops were assessed by dry matter, sugars, protein, ascorbic acid, carotenoids, and chlorophylls. In 1951, studies on varieties of cabbage were performed to assess ascorbic acid, dry matter, sugars, fiber, mineral elements, carotene, and proteins, and the dynamics of accumulation and consumption of nutrients. Later, the genetic and geographical variabilities of the accumulation of biochemical compounds were established including vitamins, pigments, mustard oils, in cabbage (Lukovnikova, 1959; Lukovnikova and Lizgunova, 1965), turnips and rutabagas (Solovyeva et al., 2013), and radishes (Shebalina and Sazonova, 1985). In the 1970s, studies of the biochemical composition and varietal diversity of the *Brassica* collection were deepened (Lizgunova et al., 1978). In recent years, the focus of attention has been on accumulation of the major biochemical components and biologically active substances (Artemyeva et al., 2006; Solovyova et al., 2014).

Nutrient Use Efficiency

The optimal use of essential nutrients is very important for plant production in terms of productivity and sustainability. Increasing nutrient use efficiency is critical to improve crop yield, reduce fertilizer demand and alleviate environmental pollution. In order to determine the natural variation for shoot zinc content, 376 accessions of *B. oleracea* and 74 commercial cultivars were investigated, revealing high variation and also an interaction with soil phosphorus availability (Broadley et al., 2010). The same set of lines was tested for potassium use efficiency in the field and in the greenhouse, and a twofold variation in shoot potassium content was found, encouraging further breeding approaches (White et al., 2010).

Another aspect of plant nutrition is the use of organic farming production systems. Here, cultivars with high nutrient use efficiency are in demand due to the reduced input of fertilizers. Yousef et al. (2015) monitored the growth of 178 *B. oleracea* var. *botrytis* accessions under organic and conventional farming conditions, and identified genotypes that are suitable as parental lines for breeding under organic farming conditions.

Accumulation of Metabolites

As outlined above, *Brassica* vegetables are rich in biologically active metabolites that account for their health-promoting effects. Hence, there is a special interest in increasing the accumulation of these value-adding compounds in vegetables. Glucosinolates have been a focus of research activity for many years and numerous studies have evaluated germplasm material genotypes of diverse geographical origin.

In a field trail, a total of 146 cabbage (*B. oleracea* var. *capitata*) genotypes were analyzed and accessions identified with increased concentrations of glucosinolates (Bhandari et al., 2020). A collection of 70 Turkish white head cabbages (*B. oleracea* var. *capitata* sub. var. *alba*) grown in the field in two harvesting seasons revealed a large variation in glucosinolate composition and concentration, leading to the identification of promising genotypes for further breeding activities (Sarikamis et al., 2009).

Lee et al. (2013) profiled 48 *B. rapa* turnips for glucosinolate accumulation and found a grouping of genotypes. Similarly, the glucosinolate patterns and antioxidant activities of 62 varieties of Chinese cabbage (*B. rapa* ssp. *pekinensis*) were determined and several genotypes for further breeding were identified (Lee et al., 2014). Leaves and tubers of 16 *B. rapa* turnip accessions were assayed in parallel for their accumulation of glucosinolates and glucosinolate hydrolysis products (Klopsch et al., 2017). Besides a tissue-specific accumulation of glucosinolates and their breakdown products, the study revealed that clustering patterns of accessions based on their glucosinolate pattern differed from those based on the hydrolysis products, indicating the importance of profiling the latter bioactive compounds. The same observation was made when profiling 91 leafy *B. rapa* accessions from different subspecies (Klopsch et al., 2018). Correlations in abundance of specific glucosinolates and of their breakdown products were identified, with implications for future breeding activities.

Fifty-one accessions from 5 genera of family Brassicaceae from the VIR collection (*Sinapis alba*, *Lepidium sativum*, *Eruca sativa*, *Diplotaxis muralis*, *B. juncea*, *B. rapa*) were profiled for 21 glucosinolates. The highest content (more than 40 μM/g) was found in all accessions of white mustard (sinalbin) and

in six accessions of Indian mustard (sinigrin), hence, these species should be useful for biofumigation approaches. Seventeen glucosinolates components have been determined in *B. rapa*, among them were indol glucosinolates, which are more useful for human, and three local accessions of Chinese cabbage had threefold higher levels of indole glucosinolates as compared to the remaining tested cultivars (Solovyeva et al., 2013).

A set of 19 Italian kale (*B. oleracea* var. *acephala*) was profiled for the accumulation of phenols, flavonoids, and anthocyanins, representing the basis for further nutritional use of locally adapted accessions (Lotti et al., 2018). A set of 70 white cabbage and 30 cauliflower accessions were characterized for variability of biochemical compounds at VIR; the accumulation by different genotypes of protein, sugars, ascorbic acid, carotenoids, chlorophylls, amino acids, organic acids, fatty acids, and phenolic compounds was determined. The sources of high levels of nutritive and biologically active substances were found, mostly within central Russian and Dutch white cabbage accessions, and within German and French cauliflower accessions (Solovyova et al., 2014). The connection between primary and secondary metabolism in different colored cauliflower curds was investigated and revealed closely related metabolic networks (Park et al., 2013). The complex of morphological and biochemical traits of an Italian broccoli and cauliflower landraces collection compared with F1 was studied by Branca et al. (2018) who detected a large diversity of glucosinolate, anthocyanin, carotenoids, polyphenols and ascorbic acid contents. Single sequence repeat analysis divided the collection into five clusters; all Sicilian accessions were distinct. A core collection of 168 *B. rapa* accessions of different morphotypes and origins was explored to find genetic association between markers and tocopherols, carotenoids, chlorophylls and folate (Del Carpio et al., 2011).

Pest Resistance

Crop production is severely threatened by herbivores feeding on *Brassica* vegetables and the distribution of pests has increased in the recent years due to the expansion of rapeseed. Hence, the role of genetic sources of resistance, including landraces with high adaptability, is increasing in breeding programs. At the same time, the specificity of the human's consumption of these crops as food requires a maximum degree of ecological safety of products, and modern ecological thinking in plant protection requires minimizing the anthropogenic impact on the components of agrobiocenosis, including useful entomofauna.

The most common pests of Brassicaceae family crops are thrips (*Thrips tabaci*), cabbage root fly (*Delia radicum*), cabbage moth (*Mamestra brassicae*), cabbage aphid (*Brevicoryne brassicae*) and diamond back moth (*Plutella xylostella*). A screen of 27 cabbage (*B. oleracea* var. *capitata*) cultivars revealed a range of preference of cabbage aphid toward the tested accessions (de Melo et al., 2013). Plant resistance tests of eight genotypes of collard greens (*B. oleraceae* var. *acephala*) against cabbage aphid revealed an interactive effect of biochemical and morphological resistance mechanisms (Canassa et al., 2020). Sources of resistance against cabbage moth were detected in a screen of 21 local and commercial cabbage varieties and interactive effects of leaf traits, head compactness, and leaf glucosinolate content were identified (Cartea et al., 2010). A set of 56 turnip (*B. rapa* ssp. *rapa*) accessions were screened for resistance against cabbage root fly under controlled conditions and in the field, leading to the isolation of resistant cultivars and resistance plant traits (Santolamazza-Carbone et al., 2017). Resistance against cabbage whitefly (*Aleyrodes proletella*) was tested in a collection of 432 accessions of *B. oleracea* and its wild relatives. It was shown that the wild relatives exhibited an earlier resistance than the breeding cultivars, which is probably due to the earlier formation of trichomes (Pelgrom et al., 2015). The effect of epicuticular waxes on plant resistance against the green peach aphid (*Myzus persicae*) was minor in twelve kale genotypes (Costa et al., 2014).

Phenotypic Appearance

Besides health and welfare benefits, an important marketing goal of *Brassica* producers is the attractive appearance, size and shape of crops. Hence, genebank accessions are screened for phenotypic traits. Thirty kale genotypes were investigated for 44 morphological traits, revealing a limited extent of phenotypical variation albeit from a wide extent of genetical divergence (Azevedo et al., 2014). Thorwarth et al. (2018) selected 174 cauliflower accessions to gain insight into six curd-related traits. Further, they identified associations between these traits and genetic markers by genome-wide association mapping.

At VIR, a complete phenotyping of all accessions in the different eco-geographical zones of Russia is performed according to the same methodic during three years. The VIR evaluation databases include 47–55 morphological and phenological characters for vegetable crops, 18–23 characters for oilseeds, as well as separate immunological, physiological, and biochemical databases. Since pathogenic organisms spoil the phenotypic appearance of crops, trait collections have been established based on resistance/susceptibility to black rot, clubroot, downy mildew, and leaf spot disease. The range of responses was dependent on the crop, the pathogen race and geographical origin of the accessions. For instance, maximum frequency of *B. rapa* resistance to black rot originates from accessions from Central-Asian subpopulation, which is considered as the most genetically variable part of the species genepool, and to a subpopulation from Japan (Ignatov et al., 2011).

The variability of ten accessions of Chinese broccoli was investigated for morphological, biochemical, genetic properties and a large diversity was noted in this set, generally on plant habit, stem diameter and chlorophyll content (Fotev et al., 2018). Morphological and biochemical traits linked to consumer value of 96 *B. rapa* accessions from different morphotypes from the VIR core collection were screened in the field and under greenhouse conditions in the North-West Russia and in the field in South China. The study revealed correlations between characteristics, and sources for breeding and genetic markers for traits investigated (Artemyeva et al., 2017). A study of the morphological traits of the plant, leaf lamina and root of 16 local Scandinavian turnip accessions from the VIR collection allowed determination of typical (cvs. Petrovskaya, Karelskaya,

Tankard yellow) and rare types (cv. Kostenevskaya), and mixed populations, as well as valuable stock for breeding projects (Kornyukhin and Artemyeva, 2017).

CONCLUSION

Genebanks have many tasks and challenges (Fu, 2017; Diez et al., 2018). At present, the high-throughput use of omic tools for extensive germplasm collections is challenging due to the laborious sample preparation (nucleic acids, proteins, and metabolites), as well as suboptimal handling and analysis approaches of large-scale datasets. Further, unharmonized laboratory-specific analytical techniques hinder the exchange of results between labs. However, assimilating large amounts of genome, expression and metabolite data, in conjunction with phenotype information, will truly accelerate breeding processes and increase our understanding of the molecular background of trait formation. These enormous efforts need to be supported by increased public funding. Although the public awareness on safeguarding the agricultural and horticultural heritage has increased in recent years, funding of germplasm banks did not catch up with the demands, currently covering basically permanent activities (collect, inventory, and propagate, etc.), but insufficiently financing genome and phenome investigations. The utilization of *Brassica* vegetable germplasm collections to isolate promising genotypes for breeding activities has been achieved successfully. However, there is still underutilization of germplasms, and the link between conservation and use of collections must be strengthened further. Recent activities aimed at developing user-friendly databases to aid the access to germplasm collections, ultimately centralizing database management. Currently, besides international platforms, such as Genesys, Crop Wild Relatives Global Portal, EURISCO, New World Fruits Database, and ECPGR, also numerous national databases, such as GRIN, GBIS/I, and SeedStor are available. Centralized and detailed information about genotype, phenotype, stress resistance and metabolite accumulation of accessions would increase use of collections. Applying high-throughput molecular and phenotypic screening methods will allow the deep characterization of collections and yield valuable trait information for genebank curators as well as for researchers and breeders.

AUTHOR CONTRIBUTIONS

KW, AK, and AA wrote the manuscript. All authors contributed to the article and approved the submitted version.

ACKNOWLEDGMENTS

This work was prepared in accordance with the state assignment of Russian Federation No. 0662-2019-0003 "Genetic resources of vegetable and cucurbit crops of the VIR worldwide collection: effective ways to expand diversity, disclose the patterns of hereditary variability, use the adaptive potential," state registration number of R&D (RK), according to the plan of scientific research work of VIR AAAA-A19-11-9013090157-1.

REFERENCES

Anglin, N. L., Amri, A., Kehel, Z., and Ellis, D. (2018). A case of need: linking traits to genebank accessions. *Biopreserv. Biobank.* 16, 337–349. doi: 10.1089/bio.2018.0033

Artemyeva, A. (2004). "Donors and sources for a breeding of Brassica rapa *L. leafy* vegetables," in *Catalogue of VIR Worldwide Collection* (St. Petersburg: VIR Press).

Artemyeva, A. M., Chesnokov, Y. V., and Klocke, E. (2008). Genetic diversity and intraspecific phylogenetic relationships of *Brassica rapa* L. species crops based on microsatellite analysis. *Newsletter Vavilov Soc. Genet. Breed.* 12, 608–619.

Artemyeva, A. M., Chesnokov, Y. V., and Klocke, E. (2009). Analysis of phylogenetic relationships of *Brassica oleracea* L. *Newsletter Vavilov Soc. Genet. Breed.* 13, 759–771.

Artemyeva, A. M., Chesnokov, Y. V., Budahn, H., and Bonnema, G. (2013). "Association mapping of agronomically important traits in *Brassica rapa* L," in: Branca F, Tribulato A, eds *Acta Horticulturae*. Belgium: International Society for Horticultural Science doi: 10.17660/ActaHortic.2013.1005.17

Artemyeva, A. M., Solovjova, A. E., Kocherina, N. V., Berensen, F. A., Rudneva, E. N., and Chesnokov, Y. V. (2016). Mapping of chromosome loci determined manifestation of morphological and biochemical traits of quality in *Brassica rapa* L. crops. *Russ. J. Plant Physiol.* 63, 259–272. doi: 10.1134/S1021443716020047

Artemyeva, A. M., Solovyeva, A. E., Berensen, F. A., Kocherina, N. V., and Chesnokov, Y. V. (2017). Ecologo-genetic evaluation of morphological and biochemical traits in VIR *Brassica rapa* L. collection. *Agric. Biol.* 52, 129–142.

Artemyeva, A., Dubovskaya, A., and Kon'kova, N. (2019). The Russian brassicaceae collection - from NI Vavilov and EN sinskaya till nowadays. *Newsletter Vavilov Soc. Genet. Breed.* 23, 157–164. doi: 10.18699/VJ19.553

Artemyeva, A., Solovyeva, A. E., and Chesnokov, Y. V. (2006). Genetic properties of Russian white cabbage cultivars. *Agric. Biol.* 5, 53–61.

Azevedo, A. M., Junior, V. C. A., and Fernandes, J. S. C. (2014). Genetic divergence and importance of morphological characters in genotypes of kale. *Hortic. Bras.* 32, 48–54. doi: 10.1590/S0102-05362014000100008

Bhandari, S. R., Rhee, J., Choi, C. S., Jo, J. S., Shin, Y. K., and Lee, J. G. (2020). Profiling of individual desulfo-glucosinolate content in cabbage head (*Brassica oleracea* var. capitata) germplasm. *Molecules* 25:1860 doi: 10.3390/molecules25081860

Boivin, D., Lamy, S., Lord-Dufour, S., Jackson, J., Beaulieu, E., and Cote, M. (2009). Antiproliferative and antioxidant activities of common vegetables: a comparative study. *Food Chem.* 112, 374–380. doi: 10.1016/j.foodchem.2008.05.084

Branca, F., Chiarenza, G. L., Cavallaro, C., Gu, H., Zhao, Z., and Tribulato, A. (2018). Diversity of Sicilian broccoli (*Brassica oleracea* var. italica) and cauliflower (*Brassica oleracea* var. botrytis) landraces and their distinctive bio-morphological, antioxidant, and genetic traits. *Genet. Resour. Crop Evol.* 65, 485–502. doi: 10.1007/s10722-017-0547-8

Broadley, M. R., Lochlainn, S. O., Hammond, J. P., Cakmak, I., Eker, S., and Erdem, H. (2010). Shoot zinc (Zn) concentration varies widely within *Brassica oleracea* L. and is affected by soil Zn and phosphorus (P) levels. *J. Horticult. Sci. Biotechnol.* 85, 375–380. doi: 10.1080/14620316.2010.11512683

Budahn, H., Artemyeva, A. M., and Chesnokov, Y. V. (2013). S-SAP markers - a valuable tool for genetic distance analysis in *Brassica rapa* L. *Acta Hortic.* 1005, 133–139. doi: 10.17660/ActaHortic.2013.1005.12

Canassa, V. F., Baldin, E. L. L., Lourencao, A. L., Barros, D. R. P., Lopes, N. P., and Sartori, M. M. P. (2020). Feeding behavior of *Brevicoryne brassicae* in resistant and susceptible collard greens genotypes: interactions among morphological and chemical factors. *Entomol. Exp. Appl.* 168, 228–239. doi: 10.1111/eea.12897

Cartea, M. E., Francisco, M., Lema, M., Soengas, P., and Velasco, P. (2010). Resistance of cabbage (*Brassica oleracea* capitata group) crops to *Mamestra brassicae*. *J. Econ. Entomol.* 103, 1866–1874. doi: 10.1603/EC09375

Christensen, S., Von Bothmer, R., Poulsen, G., Maggioni, L., Phillip, M., and Andersen, R. A. (2011). AFLP analysis of genetic diversity in leafy kale (*Brassica oleracea* L. convar. acephala (DC.) Alef.) landraces, cultivars and wild populations in Europe. *Genet. Resour. Crop Evol.* 58, 657–666. doi: 10.1007/s10722-010-9607-z

Cohen, J. H., Kristal, A. R., and Stanford, J. L. (2000). Fruit and vegetable intakes and prostate cancer risk. *J. Natl. Cancer Inst.* 92, 61–68. doi: 10.1093/jnci/92.1.61

Costa, E. M. R., Marchese, A., Maluf, W. R., and Silva, A. A. (2014). Resistance of kale genotypes to the green peach aphid and its relation to leaf wax. *Rev. Cienc. Agron.* 45, 146–154. doi: 10.1590/S1806-66902014000100018

Davies, L. R., and Allender, C. J. (2017). Who is sowing our seeds? A systematic review of the use of plant genetic resources in research. *Genet. Res. Crop Evol.* 64, 1999–2008. doi: 10.1007/s10722-017-0491-7

de Melo, B. D. C., Bleicher, E., Bertini, C., and Da Silva, J. F. (2013). Genetic divergence between cabbage commercial cultivars as to cabbage aphid preference. *Pesqui. Agropecu. Bras.* 48, 459–465. doi: 10.1590/S0100-204X2013000500001

Del Carpio, D. P., Basnet, R. K., De Vos, R. C. H., Maliepaard, C., Paulo, M. J., and Bonnema, G. (2011). Comparative methods for association studies: a case study on metabolite variation in a *Brassica rapa* core collection. *PLoS One* 6:e19624 doi: 10.1371/journal.pone.0019624

Diez, M. J., De La Rosa, L., Martin, I., Guasch, L., Cartea, M. E., and Mallor, C. (2018). Plant genebanks: present situation and proposals for their improvement. the case of the Spanish network. *Front. Plant Sci.* 9:1794. doi: 10.3389/fpls.2018.01794

El-Esawi, M. A., Germaine, K., Bourke, P., and Malone, R. (2016). Genetic diversity and population structure of *Brassica oleracea* germplasm in Ireland using SSR markers. *C. R. Biol.* 339, 133–140. doi: 10.1016/j.crvi.2016.02.002

Ermakov, A. I., and Arasimovich, V. V. (1961). *Biochemistry of Vegetable Crops*. Leningrad: John Wiley & Sons Ltd

Ermakov, A. I., Arasimovich, V. V., Smirnova-Ikonnikova, M. I., Yarosh, N. P., and Lukovnikova, G. A. (1972). *Methods for the Biochemical Analysis of Plants*. Springer: Leningrad.

Faltusova, Z., Kucera, L., and Ovesna, J. (2011). Genetic diversity of Brassica oleracea var. capitata gene bank accessions assessed by AFLP. *Electron. J. Biotechnol.* 14:10. doi: 10.2225/vol14-issue3-fulltext-4

Fateev, D. A., and Artemyeva, A. M. (2020). Molecular genetic characterisatics of broccoli (*Brassica oleracea* L. var. italica Plenck) from the VIR collection. *Proc. Appl. Bot. Genet. Breed.* 181, 91–99. doi: 10.30901/2227-8834-2020-3-91-99

Fotev, Y. V., Artemyeva, A. M., Fateev, D. A., Bugrovskaya, G. A., Belousova, V. P., and Kukushkina, T. A. (2018). Results of SSR analysis, properties of plant morphology and biochemical composition of Chinese broccoli – a new vegetable crop for Russia. *Veg. Crops Russia* 1, 12–19. doi: 10.18619/2072-9146-2018-1-12-19

Fu, Y. B. (2017). The vulnerability of plant genetic resources conserved ex situ. *Crop Sci.* 57, 2314–2328. doi: 10.2135/cropsci2017.01.0014

Gladis, T., and Hammer, K. (1992). Die gaterslebener brassica-kollektion: *Brassica juncea*, B. napus, B. nigra und B. rapa. *Feddes Repert.* 103, 469–507. doi: 10.1002/fedr.19921030704

Halewood, M., Jamora, N., Noriega, I. L., Anglin, N. L., Wenzl, P., and Payne, T. (2020). Germplasm acquisition and distribution by CGIAR genebanks. *Plants Basel* 9:1296 doi: 10.3390/plants9101296

Hammer, K., Montesano, V., Direnzo, P., and Laghetti, G. (2018). Conservation of crop genetic resources in Italy with a focus on vegetables and a case study of a neglected race of *Brassica oleracea*. *Agric. Basel* 8:105. doi: 10.3390/agriculture8070105

Herr, I., and Buchler, M. W. (2010). Dietary constituents of broccoli and other cruciferous vegetables: implications for prevention and therapy of cancer. *Cancer Treat. Rev.* 36, 377–383. doi: 10.1016/j.ctrv.2010.01.002

Higdon, J. V., Delage, B., Williams, D. E., and Dashwood, R. H. (2007). Cruciferous vegetables and human cancer risk: epidemiologic evidence and mechanistic basis. *Pharmacol. Res.* 55, 224–236. doi: 10.1016/j.phrs.2007.01.009

Ignatov, A., Artemyeva, A., Chesnokov, Y. V., Polityko, V. A., Matveeva, E. V., and Oraevskiy, A. A. (2011). Resistance of *Brassica rapa* L. and B. napus L. to black rot and leaf spot pathogens. *Agric. Biol.* 1, 85–92.

Ivanov, N., Knjaginicev, M., and Smirnova, M. (1938). *Biochemistry of cultivated plants*. Leningrad: Institute of Plant Industry.

Kestwal, R. M., Lin, J. C., Bagal-Kestwal, D., and Chiang, B. H. (2011). Glucosinolates fortification of cruciferous sprouts by sulphur supplementation during cultivation to enhance anti-cancer activity. *Food Chem.* 126, 1164–1171. doi: 10.1016/j.foodchem.2010.11.152

Klopsch, R., Witzel, K., Artemyeva, A. M., Ruppel, S., and Hanschen, F. S. (2018). Genotypic variation of glucosinolates and their breakdown products in leaves of *Brassica rapa*. *J. Agric. Food Chem.* 66, 5481–5490. doi: 10.1021/acs.jafc.8b01038

Klopsch, R., Witzel, K., Börner, A., Schreiner, M., Hanschen, F. S. (2017). Metabolic profiling of glucosinolates and their hydrolysis products in a germplasm collection of *Brassica rapa* turnips. *Food Res. Int.* 100, 392–403. doi: 10.1016/j.foodres.2017.04.016

Knee, E. M., Rivero, L., Crist, D., Grotewold, E., and Scholl, R. (2011). "Germplasm and molecular resources," in. *Genetics and Genomics of the Brassicaceae*, eds R. Schmidt. and I. Bancroft. Berlin: Springer doi: 10.1007/978-1-4419-7118-0_16

Knekt, P., Kumpulainen, J., Jarvinen, R., Rissanen, H., Heliövaara, M., and Reunanen, A. (2002). Flavonoid intake and risk of chronic diseases. *Am. J. Clin. Nutr.* 76, 560–568. doi: 10.1093/ajcn/76.3.560

Koh, J. C. O., Barbulescu, D. M., Norton, S., Redden, B., Salisbury, P. A., Kaur, S. (2017). A multiplex PCR for rapid identification of Brassica species in the triangle of U. *Plant Methods* 13:49. doi: 10.1186/s13007-017-0200-8

Kornyukhin, D. L., and Artemyeva, A. M. (2017). Scandinavian table and stubble turnips: variability and value for breeding. *Veg. Crops Russia* 4, 58–61. doi: 10.18619/2072-9146-2017-4-58-61

Lee, J. G., Bonnema, G., Zhang, N. W., Kwak, J. H., De Vos, R. C. H., and Beekwilder, J. (2013). Evaluation of glucosinolate variation in a collection of turnip (*Brassica rapa*) germplasm by the analysis of intact and desulfo glucosinolates. *J. Agric. Food Chem.* 61, 3984–3993. doi: 10.1021/jf400890p

Lee, M. K., Chun, J. H., Byeon, D. H., Chung, S. O., Park, S. U., and Park, S. (2014). Variation of glucosinolates in 62 varieties of Chinese cabbage (*Brassica rapa* L. ssp pekinensis) and their antioxidant activity. *LWT-Food Sci. Technol.* 58, 93–101. doi: 10.1016/j.lwt.2014.03.001

Lizgunova, T. V. (1984). *Cultural Flora of the USSR. XI: Cabbage (Brassica oleracea L.).* Leningrad: Kolos Press.

Lizgunova, T. V., Boos, G. V., and Dzhokhadze, T. I. (1978). *Formation, results of study and use of VIR cabbage collection. VIR Bulletin* 85, 33–56.

Lotti, C., Iovieno, P., Centomani, I., Marcotrigiano, A. R., Fanelli, V., and Mimiola, G. (2018). Genetic, bio-agronomic, and nutritional characterization of kale (*Brassica oleracea* L. var. acephala) diversity in Apulia, Southern Italy. *Divers. Basel* 10:11. doi: 10.3390/d10020025

Lukovnikova, G. A. (1959). Variability of the amount and quality of the nitrogenous substances in cabbage species and varieties. *Proc. Appl. Bot. Genet. Breed.* 32, 149–158.

Lukovnikova, G. A., and Lizgunova, T. V. (1965). Comparative biochemical characteristic of cabbage organs. *Proc. Appl. Bot. Genet. Breed.* 37, 17–25.

Manchali, S., Murthy, K. N. C., and Patil, B. S. (2012). Crucial facts about health benefits of popular cruciferous vegetables. *J. Funct. Foods* 4, 94–106. doi: 10.1016/j.jff.2011.08.004

Mason, A. S., Zhang, J., Tollenaere, R., Vasquez Teuber, P., Dalton-Morgan, J., Hu, L. (2015). High-throughput genotyping for species identification and diversity assessment in germplasm collections. *Mol. Ecol. Resour.* 15, 1091–1101. doi: 10.1111/1755-0998.12379

Neugart, S., Baldermann, S., Hanschen, F. S., Klopsch, R., Wiesner-Reinhold, M., and Schreiner, M. (2018). The intrinsic quality of brassicaceous vegetables: how secondary plant metabolites are affected by genetic, environmental, and agronomic factors. *Sci. Hortic.* 233, 460–478. doi: 10.1016/j.scienta.2017.12.038

Nguyen, G. N., and Norton, S. L. (2020). Genebank phenomics: a strategic approach to enhance value and utilization of crop germplasm. *Plants Basel* 9:817. doi: 10.3390/plants9070817

Palme, A. E., Hagenblad, J., Solberg, S. O., Aloisi, K., and Artemyeva, A. (2020). SNP markers and evaluation of duplicate holdings of Brassica oleracea in two European genebanks. *Plants Basel* 9:925. doi: 10.3390/plants9080925

Park, S. Y., Lim, S. H., Ha, S. H., Yeo, Y., Park, W. T., Kwon, D. Y. (2013). Metabolite profiling approach reveals the interface of primary and secondary metabolism in colored cauliflowers (*Brassica oleracea* L. ssp botrytis). *J. Agric. Food Chem.* 61, 6999–7007. doi: 10.1021/jf401330e

Pelc, S. E., Couillard, D. M., Stansell, Z. J., Farnham, M. W. (2015). Genetic diversity and population structure of collard landraces and their relationship to other *Brassica oleracea* crops. *Plant Genome* 8:eplantgenome2015.04.0023 doi: 10.3835/plantgenome2015.04.0023

Pelgrom, K. T. B., Broekgaarden, C., Voorrips, R. E., Bas, N., Visser, R. G. F., and Vosman, B. (2015). Host plant resistance towards the cabbage whitefly in *Brassica oleracea* and its wild relatives. *Euphytica* 202, 297–306. doi: 10.1007/s10681-014-1306-y

Pignone, D., and Hammer, K. (2013). "Conservation, evaluation, and utilization of biodiversity," in: Kole C, ed. *Genomics and Breeding for Climate-Resilient Crops*: Vol. 1 *Concepts and Strategies*. Berlin: Springer doi: 10.1007/978-3-642-37045-8_2

Prange, P. K., and Hewett, E. W. (2003). *A proceedings of the XXVI International Horticultural Congress, Toronto, Canada, 11-17 August, 2002: Issues and Advances in Postharvest Horticulture*. Leuven: International Society for Horticultural Science Press.

Saad, N. S. M., Severn-Ellis, A. A., Pradhan, A., Edwards, D., and Batley, J. (2021). Genomics armed with diversity leads the way in Brassica improvement in a changing global environment. *Front. Genet.* 12:28. doi: 10.3389/fgene.2021.600789

Santolamazza-Carbone, S., Velasco, P., and Cartea, M. E. (2017). Resistance to the cabbage root fly, Delia radicum (Diptera, Anthomyiidae), of turnip varieties (*Brassica rapa* subsp rapa). *Euphytica* 213:274 doi: 10.1007/s10681-017-2069-z

Sarikamis, G., Balkaya, A., and Yanmaz, R. (2009). Glucosinolates within a collection of white head cabbages (*Brassica oleracea* var. capitata sub.var. alba) from Turkey. *Afr. J. Biotechnol.* 8, 5046–5052.

Sergentanis, T. N., Psaltopoulou, T., Ntanasis-Stathopoulos, I., Liaskas, A., Tzanninis, I. G., and Dimopoulos, M. A. (2018). Consumption of fruits, vegetables, and risk of hematological malignancies: a systematic review and meta-analysis of prospective studies. *Leuk. Lymphoma* 59, 434–447. doi: 10.1080/10428194.2017.1339873

Shebalina, M., and Sazonova, L. (1985). *Cultural Flora of the USSR. XVIII: Root crops (Brassica – Turnip, Rutabaga, Radish, Small Radish)*. Leningrad: Ahropromyzdat Press. 324.

Singh, B. K., Sharma, S. R., and Singh, B. (2010). Antioxidant enzymes in cabbage: variability and inheritance of superoxide dismutase, peroxidase and catalase. *Sci. Hortic.* 124, 9–13. doi: 10.1016/j.scienta.2009.12.011

Sinskaya, E. N. (1928). The oleiferous plants and root crops of the family Cruciferae. *Proc. Appl. Bot. Genet. Breed.* 19:656.

Solberg, S. O., Artemyeva, A., Yndgaard, F., Dorre, M., Niss, J., and Burleigh, S. (2018). Duplication assessments in Brassica vegetable accessions. *Plant Genet. Resour.* 16, 201–208. doi: 10.1017/S1479262117000156

Solovyeva, A. E., Artemyeva, A. M., and Schütze, W. (2013). Peculiar properties of glucosinolate accumulation in the Brassicaceae family. *Russian Agric. Sci.* 4, 12–14. doi: 10.3103/S1068367413050169

Solovyova, A. E., Sokolova, D. V., Piskunova, T. M., and Artemyeva, A. M. (2014). Nutrients and biologically active substances in vegetable crops and their role in improving nutrition. *Proc. Appl. Bot. Genet. Breed.* 175, 5–19.

Stansell, Z., Hyma, K., Fresnedo-Ramirez, J., Sun, Q., Mitchell, S., and Bjorkman, T. (2018). Genotyping-by-sequencing of Brassica oleracea vegetables reveals unique phylogenetic patterns, population structure and domestication footprints. *Hortic. Res.* 5:38. doi: 10.1038/s41438-018-0040-3

Thorwarth, P., Yousef, E. A. A., and Schmid, K. J. (2018). Genomic prediction and association mapping of curd-related traits in gene bank accessions of cauliflower. *G3* 8, 707–718. doi: 10.1534/g3.117.300199

van Hintum, T. J. L., De Wiel, C., Visser, D. L., Van Treuren, R., and Vosman, B. (2007). The distribution of genetic diversity in a Brassica oleracea gene bank collection related to the effects on diversity of regeneration, as measured with AFLPs. *Theor. Appl. Genet.* 114, 777–786. doi: 10.1007/s00122-006-0456-2

White, P. J., Hammond, J. P., King, G. J., Bowen, H. C., Hayden, R. M., and Meacham, M. C. (2010). Genetic analysis of potassium use efficiency in *Brassica oleracea*. *Ann. Bot.* 105, 1199–1210. doi: 10.1093/aob/mcp253

Yousef, E. A. A., Muller, T., Borner, A., and Schmid, K. J. (2018). Comparative analysis of genetic diversity and differentiation of cauliflower (*Brassica oleracea* var. botrytis) accessions from two ex situ genebanks. *PLoS One* 13:e0192062. doi: 10.1371/journal.pone.0192062

Yousef, E., Lampei, C., and Schmid, K. (2015). Evaluation of cauliflower genebank accessions under organic and conventional cultivation in Southern Germany. *Euphytica* 201, 389–400. doi: 10.1007/s10681-014-1225-y

Zhao, J. J., Artemyeva, A., Del Carpio, D. P., Basnet, R. K., Zhang, N., and Gao, J. (2010). Design of a Brassica rapa core collection for association mapping studies. *Genome* 53, 884–898. doi: 10.1139/G10-082

Conflict of Interest: The authors declare that the research was conducted in the absence of any commercial or financial relationships that could be construed as a potential conflict of interest.

frontiers in Plant Science

ORIGINAL RESEARCH
published: 07 June 2021
doi: 10.3389/fpls.2021.665168

Groundwater Depths Affect Phosphorus and Potassium Resorption but Not Their Utilization in a Desert Phreatophyte in Its Hyper-Arid Environment

Bo Zhang[1,2,3], Gangliang Tang[1,3], Hui Yin[1,3], Shenglong Zhao[4], Muhammad Shareef[1,3], Bo Liu[5], Xiaopeng Gao[6] and Fanjiang Zeng[1,3,7]**

[1] Xinjiang Key Laboratory of Desert Plant Roots Ecology and Vegetation Restoration, Xinjiang Institute of Ecology and Geography, Chinese Academy of Sciences, Urumqi, China, [2] National Engineering Technology Research Center for Desert-Oasis Ecological Construction, Xinjiang Institute of Ecology and Geography, Chinese Academy of Sciences, Urumqi, China, [3] Cele National Station of Observation and Research for Desert-Grassland Ecosystems, Cele, Xinjiang, China, [4] Northwest Institute of Eco-Environment and Resources, Academy of Science, Lanzhou, China, [5] College of Resources and Environment, Linyi University, Linyi, China, [6] Department of Soil Science, University of Manitoba, Winnipeg, MB, Canada, [7] State Key Laboratory of Desert and Oasis Ecology, Xinjiang Institute of Ecology and Geography, Chinese Academy of Sciences, Urumqi, China

OPEN ACCESS

Edited by:
Christian Roger Marc Hermans, Université Libre de Bruxelles, Belgium

Reviewed by:
Amitava Rakshit, Banaras Hindu University, India
Jianting Zhu, University of Wyoming, United States
Shankar Lal Jat, Indian Council of Agricultural Research (ICAR), India

***Correspondence:**
Bo Zhang
zhangbo@ms.xjb.ac.cn
Fanjiang Zeng
zengfj@ms.xjb.ac.cn

Specialty section:
This article was submitted to Plant Nutrition, a section of the journal Frontiers in Plant Science

Received: 07 February 2021
Accepted: 06 May 2021
Published: 07 June 2021

Citation:
Zhang B, Tang G, Yin H, Zhao S, Shareef M, Liu B, Gao X and Zeng F (2021) Groundwater Depths Affect Phosphorus and Potassium Resorption but Not Their Utilization in a Desert Phreatophyte in Its Hyper-Arid Environment. Front. Plant Sci. 12:665168. doi: 10.3389/fpls.2021.665168

Nutrients are vital for plant subsistence and growth in nutrient-poor and arid ecosystems. The deep roots of phreatophytic plants are necessary to access groundwater, which is the major source of nutrients for phreatophytes in an arid desert ecosystem. However, the mechanisms through which changes in groundwater depth affect nutrient cycles of phreatophytic plants are still poorly understood. This study was performed to reveal the adaptive strategies involving the nutrient use efficiency (NUE) and nutrient resorption efficiency (NRE) of desert phreatophytes as affected by different groundwater depths. This work investigated the nitrogen (N), phosphorus (P), and potassium (K) concentrations in leaf, stem, and assimilating branch, as well as the NUE and NRE of the phreatophytic *Alhagi sparsifolia.* The plant was grown at groundwater depths of 2.5, 4.5, and 11.0 m during 2015 and 2016 in a desert-oasis transition ecotone at the southern rim of the Taklimakan Desert in northwestern China. Results show that the leaf, stem, and assimilating branch P concentrations of *A. sparsifolia* at 4.5 m groundwater depth were significantly lower than those at 2.5 and 11.0 m groundwater depths. The K concentrations in different tissues of *A. sparsifolia* at 4.5 m groundwater depth were significantly higher than those at 2.5 and 11.0 m groundwater depths. Conversely, the NRE of P in *A. sparsifolia* was the highest among the three groundwater depths, while that of K in *A. sparsifolia* was the lowest among the three groundwater depths in 2015 and 2016. The N concentration and NUE of N, P, and K in *A. sparsifolia*, however, were not influenced by groundwater depth. Further analyses using structural equation models showed that groundwater depth had significant effects on the P and K resorption of *A. sparsifolia* by changing soil P and senescent leaf K concentrations. Overall, our results suggest groundwater

depths affect P and K concentrations and resorption but not their utilization in a desert phreatophyte in its hyper-arid environment. This study provides a new insight into the phreatophytic plant nutrient cycle strategy under a changing external environment in a hyper-arid ecosystem.

Keywords: nutrient resorption, *Alhagi sparsifolia*, groundwater table, internal nutrient cycling, desert ecosystem

INTRODUCTION

Nutrient utilization and resorption are vital for plant growth and ecosystem processes in various ecosystems (Aubrey et al., 2012; Zhao et al., 2017; Wang et al., 2020). First, the total net primary production per unit nutrient absorption is described as nutrient use efficiency (NUE) (Vitousek, 1982). NUE is defined as the product of the mean residence time (MRT) of nutrients in plants and nutrient productivity (NP), which is the rate of biomass increase per unit nutrient in plants (Berendse and Aerts, 1987); a functional interpretation of NUE is considered in accordance with different nutrient use strategies: high NP is strongly associated with low MRT and NP is not related to MRT (Eckstein and Karlsson, 2001; Yuan et al., 2008). Previous studies showed that NUE is affected by nutrient availability and species. For example, NUE decreases as nutrient availability increases (Vitousek, 1982). The effect of species on NUE remains unclear, with one report suggesting that the NUE of C4 grass (*Chloris virgata*) is higher than that of the C3 grass (*Leymus chinensis*) despite nitrogen treatments in the temperate grasslands in northern China (Yuan et al., 2007), and the NUE of tree species is influenced by species but not by N availability (Aubrey et al., 2012). Other suggested that the NUE of woody shrubs and perennial herbs are similar among species and different habitats (high and low water supply) in a typical agropastoral ecotone in the central part of Inner Mongolia Autonomous Region, China (Yuan et al., 2007). Thus, knowledge gap on the roles of species type and nutrient availability in affecting NUE still exists in various ecosystems.

Nutrient resorption from senescing tissues to green tissues has important consequences for plants that live in nutrient-limited habitats. Nutrient resorption helps plants re-use nutrients directly to become less dependent on external nutrient concentrations (Aerts and Chapin, 2000; Wang et al., 2014, 2020; Zhao et al., 2017; Huang et al., 2018). Hence, nutrient resorption is an important mechanism of nutrient conservation in plants. Nutrient resorption efficiency (NRE) is a crucial indicator of internal nutrient recycling in plants (Aerts, 1996; Killingbeck, 1996). The NRE of plants is the percentage of nitrogen (N, P, and K) removed from senescing tissues. On a global scale, the mean N and P resorption efficiencies from senescent to young leaves of terrestrial plants are approximately 62 and 65%, respectively (Vergutz et al., 2012). NRE is usually higher in nutrient-limited habitats than in nutrient-rich ones (Killingbeck, 1996; Yuan and Chen, 2009). Recently, evidence has suggested that NRE is affected by climate, soil/leaf nutrient and stoichiometry, plant functional group, plant age, spatial pattern, and land utilization (Brant and Chen, 2015; Netzer et al., 2017; Xu et al., 2017; Zhao et al., 2017; Wang et al., 2020). Previous studies have shown that increasing water condition decreases the NRE of N, but increases that of P of three graminoid species, *Agropyron cristatum*, *Achnatherum sibiricum,* and *Stipa grandis*, and one forb species, *Potentilla bifurca* in Inner Mongolia, China (Lü and Han, 2010). Huang et al. (2018) reported that the NRE of N and P of three life-form plants (five spring annuals, two summer annuals and two shrubs) are not influenced by increasing water condition in a temperate desert in China. Hence, it is unclear if changing water condition affects NRE of plants in natural environment.

Phreatophytes are largely distributed worldwide except in Antarctica. The deep roots of phreatophytic plants depend on access to groundwater as a major source of nutrients and water (Arndt et al., 2004; Zeng et al., 2006; Thomas, 2014). However, with intensive human intervention, increasing anthropogenic water use intensifies groundwater limitation (Antunes et al., 2018). Groundwater table is gradually lowered in desert oasis transition ecotones, indicating the increasing shortage of water resources (Liu, 2007). Thus, limited plant access to groundwater caused by groundwater lowering is expected to have a major impact on plant nutrient utilization and absorption. Therefore, nutrient utilization and absorption of phreatophytes in nutrient-deficient deserts in response to the declining groundwater depth should be investigated to restore sparse phreatophytes and enhance protection for fragile arid desert ecosystems.

The Taklimakan Desert is the second largest shifting desert in the world and the largest desert in China. As a dominant perennial phreatophyte grown in arid and semi-arid regions between oasis and deserts, *Alhagi sparsifolia* Shap. can stabilize sand dunes, prevent land erosion, and thus support fragile desert ecosystems (Zeng and Liu, 2012; Li et al., 2015; Zhang et al., 2018a,b). *A. sparsifolia* is a leguminous plant that can fix atmospheric N_2 (Arndt et al., 2004). It is also an economically important species, which can be used as a livestock source by local farmers in winter (Li et al., 2013; Zhang et al., 2018b). The deep root system of *A. sparsifolia* can reach groundwater, which is the major source of water and nutrients (Arndt et al., 2004; Zeng et al., 2006). Our previous study found that the declining water table affects the biomass, leaf physiological parameters, leaf nutrient, root characteristics, clonal growth, and propagation traits of *A. sparsifolia* (Gui et al., 2013; Zeng et al., 2013; Li et al., 2015; Zhang et al., 2018a).

Although changes in the NP, MRT, and NUE of nitrogen (N) have been widely explored, variations in the NUE of phosphorus (P) and potassium (K) in plants have been seldom investigated. Most studies have assessed nutrient resorption in woody, deciduous, and evergreen plants in response to environmental factors. However, only a few ones have investigated N, P, and K

utilization and resorption in desert phreatophytes with a deep root system in a reduced groundwater depth in a hyper-arid region. In the present study, we hypothesize that varying groundwater depth can affect variations of NUE and NRE of N, P, and K in *A. sparsifolia* because of the changes in N, P, and K concentrations in *A. sparsifolia* in a hyper-arid desert ecosystem. Desert phreatophytes, such as *A. sparsifolia,* can adjust NUE and NRE to adapt to declining groundwater depth in a hyper-arid desert ecosystem.

MATERIALS AND METHODS

Study Area

The study site is located at the Cele National Station of Observation and Research for Desert and Grassland Ecosystem (37°00.77″N, 80°43.45″E, **Supplementary Figure 1**) at the southern edge of the Taklimakan Desert in the Xinjiang Uyghur Autonomous Region of China. Cele Station located in the desert-oasis transition ecotone is characterized by a 5–10 km belt of sparse phreatophytic species dominated by *A. sparsifolia* (Zeng et al., 2013). The groundwater depth ranges from 2.5 to 15.0 m in this area. The study site has an elevation of 1366 m (asl), a mean annual temperature of 11.9°C, a mean annual potential evaporation of 2600 mm, and a mean annual precipitation of 35 mm (Gui et al., 2013; Liu et al., 2016). The climate is hyper-arid, with hot and dry summers and cold and dry winters. Extreme temperatures can reach 41.9°C in summer and −31°C in winter. Soils are sandy, and their bulk density is 1.35 g/cm^3 (Liu et al., 2013, 2016). Soil C, N, and P concentrations at 2.5 m groundwater depth are similar to those at 4.5 m groundwater depth, while soil C, N, and P concentrations at 2.5 and 4.5 m groundwater depths are significantly lower than those at 11.0 groundwater depth (Zhang et al., 2018a).

Three sites with varying groundwater depths were selected: 2.5 m (37°01′18″N, 80°42′29″E), 4.5 m (37°00′40″N, 80°42′13″E), and 11.0 m (37°00′33″N, 80°42′25″E, **Supplementary Figure 2**). In each research area, the groundwater depth in a well was measured every month. The fluctuation in groundwater depth was minor from April to October in 2015 and 2016. Each site has a large area of approximately 2 ha. At each sampling stage, three plots with an area of 9 m^2 were randomly selected at each site.

Field Sampling and Chemical Analysis

At each groundwater depth, three *A. sparsifolia* plants in different plots with similar canopy sizes, heights, and numbers of stems were selected each month from June to October 2015 and 2016. In the experimental period, nine plots were sampled nine times per month. Thus, 45 samplings in 2015 and 2016 were performed. During sampling, plant above-ground was collected by chipping at the ground level and further separating into different tissues, including leaf, stem, and assimilating branch. The samples were oven-dried at 105°C for 15 min and at 70°C to a constant weight. The dry biomass of leaf, stem, and the assimilating branches of *A. sparsifolia* were weighed. All samples were subsequently ground using a miller and sieved through a 1 mm mesh screen for chemical element analysis. Plant tissues were digested using 0.02 M sulfuric acid, and N concentrations were determined by the Kjeldahl acid-digestion method (Sparks et al., 1996). The P and K concentrations were determined using the colorimetric analysis and a flame analyzer (2655–00, Chicago, United States), respectively, after digestion with sulfuric acid (Thomas et al., 1967).

Definition and Calculations

NUE (g g^{-1}) is calculated as the product of NP (g g^{-1} year^{-1}) and MRT (year) of nutrients (Berendse and Aerts, 1987; Garnier and Aronson, 1998; Yasumura et al., 2002; Yuan et al., 2004, 2006, 2007; Norby and Iversen, 2006). NP was calculated for short intervals (Eckstein and Karlsson, 2001; Yuan et al., 2004, 2007) in accordance with the following equation:

$$\mathrm{NP} = \frac{M_2 - M_1}{t_2 - t_1} \cdot \frac{lnN_2 - lnN_1}{N_2 - N_1}$$

where M is biomass of *A. sparsifolia* and N is the average leaf, stem, and assimilating branch N concentration, respectively, in two consecutive harvests conducted at times t_1 and t_2. The mean annual nutrient concentration was estimated as a weighted average in the entire year of 2015 and 2016. Besides, MRT was calculated as the ratio between the average nutrient concentration of leaf, stem, and assimilating branch of *A. sparsifolia* and the annual nutrient losses of *A. sparsifolia* (Eckstein and Karlsson, 2001; Norby and Iversen, 2006). Nutrient losses were determined on the nutrient concentration of the aboveground dead *A. sparsifolia* harvested in October 2015 and 2016.

Nutrient concentrations in green and senescing tissues of *A. sparsifolia* were used to calculate N-resorption efficiency (NRE, %) = [(Ng–Ns)/Ng]·100, where Ng and Ns are the nutrient concentrations in green and senescing tissues of *A. sparsifolia*, respectively. Nutrient concentration in senescing tissues of *A. sparsifolia* (October 2015 and 2016) was used as a direct indicator of nutrient resorption proficiency (NRP), that is, the extent to which nutrient concentration is reduced in senescent tissues. A high resorption proficiency usually indicates low nutrient concentration in senesced tissues (Killingbeck, 1996; Richardson et al., 2005; Yuan et al., 2007; Wang et al., 2014).

Data Analysis

One-way ANOVA with Tukey's test was carried out for the multiple comparisons of N, P, and K concentrations, NP, MRT, NUE, NRE, and NRP at different groundwater depths to test statistical significance ($p < 0.05$). Analyses were performed using SPSS 19.0. Piecewise structural equation modeling (piecewise SEM) was used to statistically tease apart and quantify direct and indirect effects of groundwater depth on plant leaf nutrient, nutrient utilization and resorption using R software (version 4.0.3) with the package "piecewiseSEM" (Lefcheck, 2016). D-separation test of Piecewise SEM was used to evaluate whether the causal model misses important links and $p > 0.05$ indicates that the model is acceptable (Shipley, 2002).

RESULTS

N, P, and K Concentrations of *A. sparsifolia* as Affected by Groundwater Depth

The P and K concentrations in the leaf, stem, and assimilating branch of *A. sparsifolia* were significantly affected by groundwater depth (**Figures 1**, **2**). The P concentration in different tissues of *A. sparsifolia* at 4.5 m groundwater were significantly lower than those at 2.5 and 11.0 m groundwater depths (**Figure 1**). The K concentration in all three parts of *A. sparsifolia* at 4.5 m groundwater depth were the highest among the three groundwater depths. The K concentration in all parts of *A. sparsifolia* at 2.5 m groundwater depth were greater than those at 11.0 m groundwater depth (**Figure 2**). However, the N concentration in leaf, stem, and assimilating branch of *A. sparsifolia* were not influenced by groundwater depth in both years (**Figure 3**).

N, P, and K Use and Resorption Strategies as Affected by Groundwater Depth

Groundwater depth significantly influenced the P resorption parameters, such as NRE and NRP of P but not the P utilization parameters, such as NP, MRT, and NUE of P (**Table 1**). The NRE of P was significantly greater at 4.5 m groundwater depth

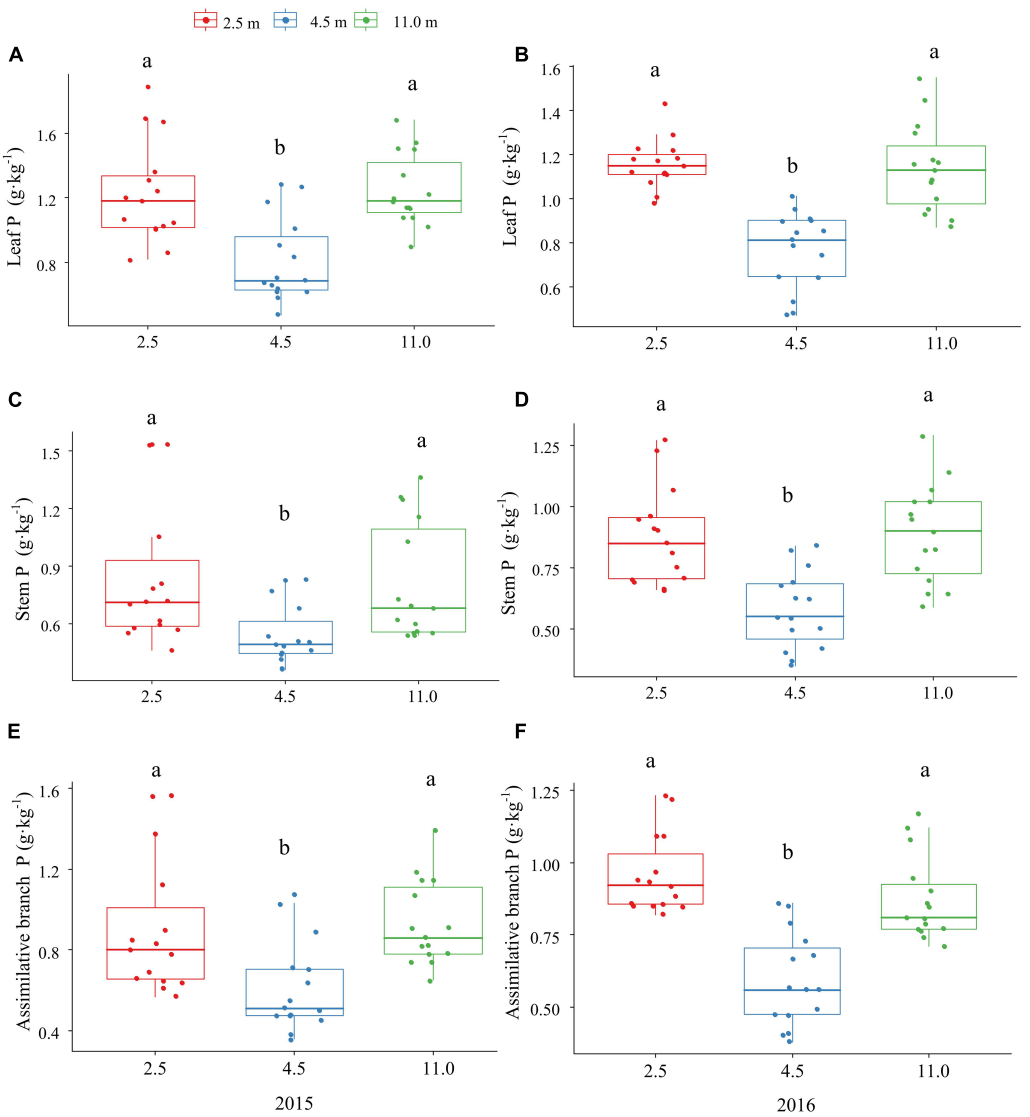

FIGURE 1 | Changes in the P concentrations in leaf, stem, and assimilating branch of *A. sparsifolia* at 2.5, 4.5, and 11.0 m groundwater depths in the growing season in 2015 and 2016. The vertical bars denote standard deviations and letters indicate significant differences among the different groundwater depths ($p < 0.05$). **(A,C,E)** represent variations of leaf P, stem P, and assimilative branch P under different groundwater depths in 2015. **(B,D,F)** represent variations of leaf P, stem P, and assimilative branch P under different groundwater depths in 2016.

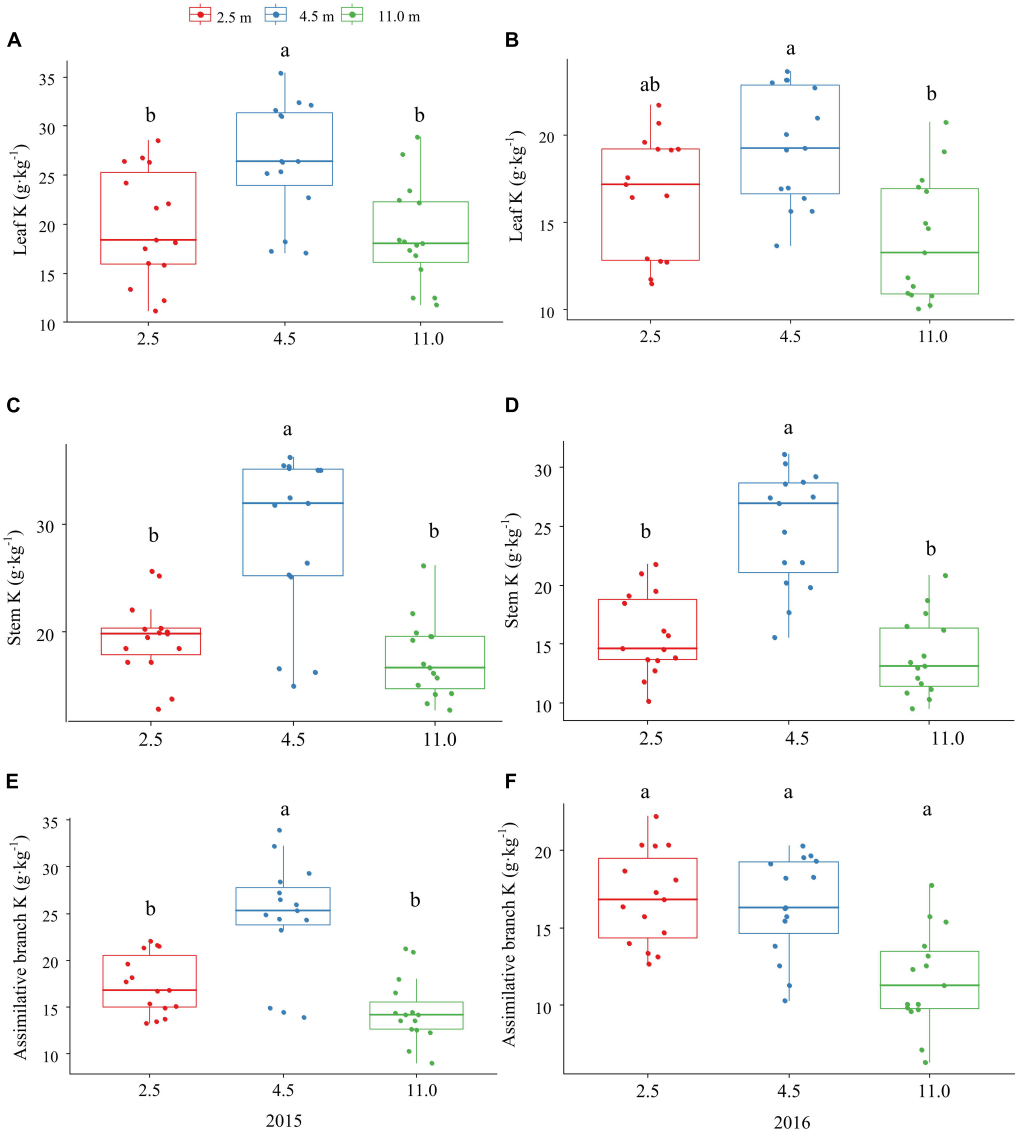

FIGURE 2 | Changes in the *K* concentrations in leaf, stem, and assimilating branch of *A. sparsifolia* at 2.5, 4.5, and 11.0 m groundwater depths in the growing season in 2015 and 2016. The vertical bars denote standard deviations and letters indicate significant differences among the different groundwater depths ($p < 0.05$). **(A,C,E)** represent variations of leaf K, stem K, and assimilative branch K under different groundwater depths in 2015. **(B,D,F)** represent variations of leaf K, stem K, and assimilative branch K under different groundwater depths in 2016.

than at 2.5 and 11.0 m groundwater depths in 2015 and 2016, corresponding to the lower NRP of P at 4.5 m groundwater depth than at 2.5 and 11.0 m groundwater depths in 2015 and 2016, respectively. Groundwater depth did not affect the N utilization and resorption parameters, such as NP, MRT, NUE, NRE, and NRP of N in *A. sparsifolia* in both years (**Table 2**).

Similarly, groundwater depth significantly affected the K resorption parameters, such as NRE and NRP of K, but not the K utilization parameters, such as NP, MRT, and NUE (**Table 3**). The NRE of K at 11.0 m groundwater depth was the greatest among the three groundwater depths, and the NRP at 11.0 m groundwater depth was the lowest in 2015. The NRE of K at 4.5 m groundwater depth was the lower than that at 2.5 and 11.0 m groundwater depth, corresponding to the highest NRP at 4.5 m groundwater depth in 2015.

Factors Affecting Variation in N, P, and K Resorption

The factors affecting variation in N, P, and K resorption were explored using structural equation models (SEM) (**Figure 4**). The model explained 57, 66, and 40% of the variance in NRE of N, P, and K (**Figures 4A–C**). Groundwater depth had no direct and indirect effects on the NRE of N (**Figure 4A**). The NRE of N was directly affected by green leaf and senesced leaf N concentrations. In addition, groundwater depth had indirect effect on the NRE of

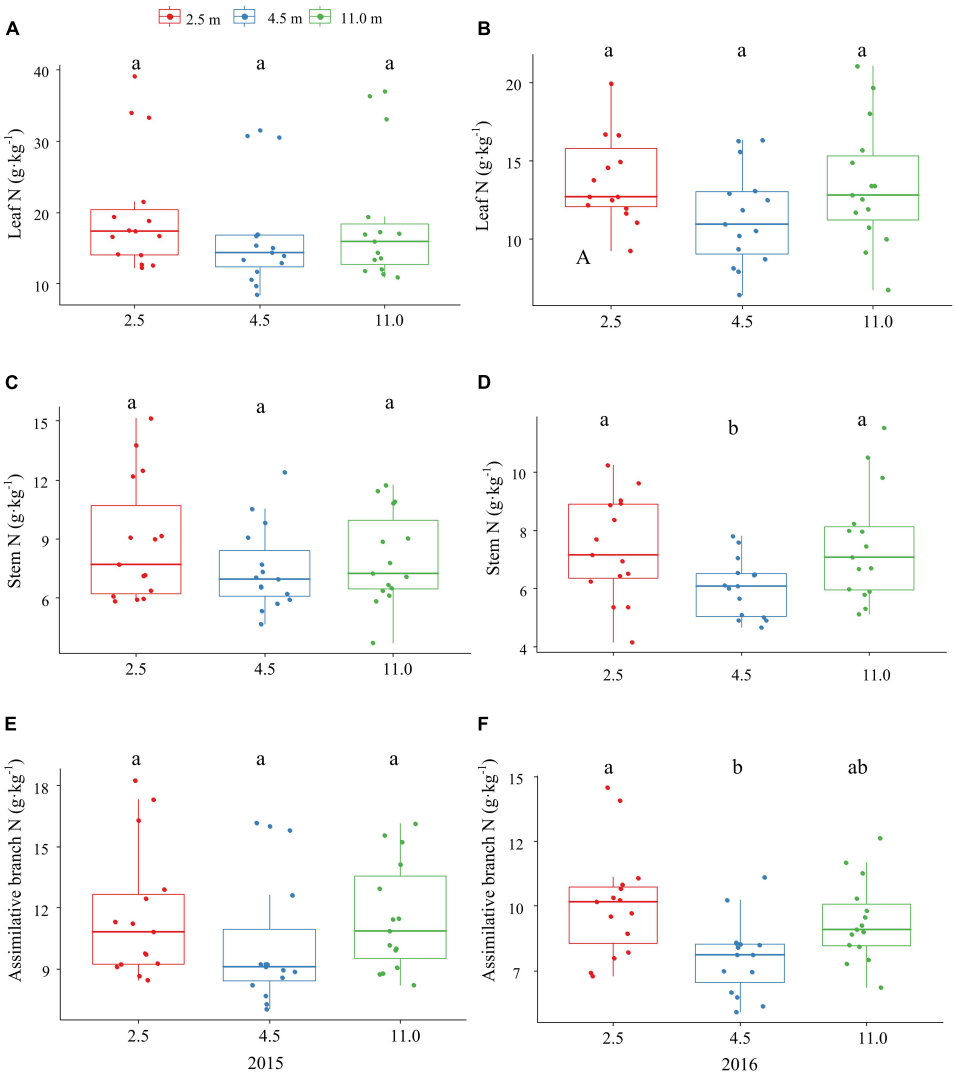

FIGURE 3 | Changes in the N concentrations in leaf, stem, and assimilating branch of *A. sparsifolia* at 2.5, 4.5, and 11.0 m groundwater depths in the growing season in 2015 and 2016. The vertical bars denote standard deviations and letters indicate significant differences among the different groundwater depths ($p < 0.05$). **(A,C,E)** represent variations of leaf N, stem N, and assimilative branch N under different groundwater depths in 2015. **(B,D,F)** represent variations of leaf N, stem N, and assimilative branch N under different groundwater depths in 2016.

P (**Figure 4B**). The NRE of P was directly affected by green leaf P concentrations and soil P concentration. Soil P concentration was most positively related to groundwater depth. Moreover, groundwater depth had an indirect effect on the NRE of K (**Figure 4C**). The NRE of K was directly affected by senesced leaf K concentration. Besides, senesced leaf K concentration was negatively related to groundwater depth.

DISCUSSION

Effect of Groundwater Depth on N, P, and K Concentrations of *A. sparsifolia*

Our results showed that groundwater depth had a significant effect on P concentrations in different tissues of phreatophytic *A. sparsifolia*. This result is consistent with that of previous studies that leaf P concentration of *A. sparsifolia* was significantly affected by groundwater depth. This is consistent with the observation that leaf P concentration of *A. sparsifolia* at 4.5 m is lower than those at 2.5 and 11.0 m groundwater depths in 2015 and 2016 because biomass of *A. sparsifolia* at 4.5 m is geater than those at 2.5 and 11.0 m groundwater depths. Hence, a biomass dilution effect existed in leaf P concentration of *A. sparsifolia* at 4.5 m groundwater depths (Zhang et al., 2018a). Moreover, the effect of groundwater depth on leaf P concentration is likely caused by direct effect of groundwater on soil P concentration (**Figure 4B**), which is strongly related to the plant P concentration of *A. sparsifolia* (Zhang et al., 2018a). These results are in accordance with previous experiments that soil P concentration

TABLE 1 | Phosphorus use strategies of *A. sparsifolia* affected by 2.5, 4.5, and 11.0 m groundwater depths in 2015 and 2016.

2015	NP (g g^{-1} $year^{-1}$)	MRT (year)	NUE (g g^{-1})	NRE (%)	NRP (mg g^{-1})
2.5 m	8.77 ± 3.10^{a}	1.36 ± 0.40^{a}	12.68 ± 6.79^{a}	49.08 ± 9.76^{ab}	0.83 ± 0.15^{a}
4.5 m	4.55 ± 2.72^{a}	0.97 ± 0.05^{a}	4.46 ± 2.81^{a}	50.15 ± 10.37^{a}	0.49 ± 0.08^{b}
11.0 m	3.86 ± 3.26^{a}	0.95 ± 0.08^{a}	3.83 ± 2.81^{a}	29.15 ± 2.71^{b}	0.87 ± 0.08^{a}
2016	NP (g g^{-1} $year^{-1}$)	MRT (year)	NUE (g g^{-1})	NRE (%)	NRP (mg g^{-1})
2.5 m	4.38 ± 1.14^{a}	1.51 ± 0.19^{a}	6.48 ± 1.23^{a}	69.74 ± 4.75^{b}	0.83 ± 0.11^{a}
4.5 m	4.58 ± 2.46^{a}	1.74 ± 0.54^{a}	7.46 ± 3.37^{a}	81.07 ± 4.32^{a}	0.42 ± 0.01^{b}
11.0 m	2.73 ± 0.59^{a}	2.19 ± 0.40^{a}	5.91 ± 1.36^{a}	71.81 ± 2.78^{ab}	0.84 ± 0.07^{a}

Means followed by different letters are significantly different at $p < 0.05$.
NP, nutrient productivity; MRT, mean residence time; NUE, nutrient-use efficiency; NRE, nutrient-resorption efficiency; NRP, nutrient-resorption proficiency.
"ab" means that there are no significant differences among a, ab, and b at $p < 0.05$.

TABLE 2 | Nitrogen use strategies of *A. sparsifolia* affected by 2.5, 4.5, and 11.0 m groundwater depths in 2015 and 2016.

2015	NP (g g^{-1} $year^{-1}$)	MRT (year)	NUE (g g^{-1})	NRE (%)	NRP (mg g^{-1})
2.5 m	0.62 ± 0.20^{a}	1.33 ± 0.32^{a}	0.86 ± 0.40^{a}	46.25 ± 6.20^{a}	11.76 ± 1.35^{a}
4.5 m	0.26 ± 0.16^{a}	0.94 ± 0.05^{a}	0.24 ± 0.16^{a}	55.14 ± 4.11^{a}	8.43 ± 0.56^{a}
11.0 m	0.40 ± 0.05^{a}	0.95 ± 0.07^{a}	0.38 ± 0.07^{a}	46.16 ± 8.29^{a}	11.08 ± 2.03^{a}
2016	NP (g g^{-1} $year^{-1}$)	MRT (year)	NUE (g g^{-1})	NRE (%)	NRP (mg g^{-1})
2.5 m	0.52 ± 0.16^{a}	1.14 ± 0.05^{a}	0.59 ± 0.17^{a}	47.34 ± 7.44^{a}	9.37 ± 1.49^{a}
4.5 m	0.42 ± 0.22^{a}	1.04 ± 0.15^{a}	0.43 ± 0.18^{a}	52.90 ± 8.69^{a}	7.29 ± 0.30^{a}
11.0 m	0.34 ± 0.09^{a}	1.74 ± 0.59^{a}	0.60 ± 0.31^{a}	50.58 ± 5.31^{a}	9.23 ± 1.37^{a}

Means followed by different letters are significantly different at $p < 0.05$.
NP, nutrient productivity; MRT, mean residence time; NUE, nutrient-use efficiency; NRE, nutrient-resorption efficiency; NRP, nutrient-resorption proficiency.
"a" means that there is no significant difference in the three groundwater depths.

TABLE 3 | Potassium use strategies of *A. sparsifolia* affected by 2.5, 4.5, and 11.0 m groundwater depths in 2015 and 2016.

2015	NP (g g^{-1} $year^{-1}$)	MRT (year)	NUE (g g^{-1})	NRE (%)	NRP (mg g^{-1})
2.5 m	7.30 ± 4.17^{a}	0.98 ± 0.29^{a}	7.93 ± 5.47^{a}	17.92 ± 2.14^{ab}	16.78 ± 1.12^{b}
4.5 m	4.21 ± 2.91^{a}	0.76 ± 0.11^{a}	3.15 ± 2.36^{a}	7.21 ± 4.95^{b}	31.62 ± 1.29^{a}
11.0 m	4.04 ± 2.44^{a}	0.65 ± 0.08^{a}	2.67 ± 1.38^{a}	25.49 ± 5.91^{a}	12.11 ± 0.42^{c}
2016	NP (g g^{-1} $year^{-1}$)	MRT (year)	NUE (g g^{-1})	NRE (%)	NRP (mg g^{-1})
2.5 m	0.95 ± 0.47^{a}	0.85 ± 0.15^{a}	0.76 ± 0.31^{a}	13.66 ± 6.33^{a}	17.62 ± 0.72^{a}
4.5 m	1.01 ± 0.52^{a}	0.70 ± 0.04^{a}	0.71 ± 0.38^{a}	19.96 ± 1.07^{a}	20.33 ± 3.09^{a}
11.0 m	0.41 ± 0.27^{a}	1.30 ± 0.51^{a}	0.47 ± 0.28^{a}	17.41 ± 9.12^{a}	14.64 ± 4.58^{a}

Means followed by different letters are significantly different at $p < 0.05$.
NP, nutrient productivity; MRT, mean residence time; NUE, nutrient-use efficiency; NRE, nutrient-resorption efficiency; NRP, nutrient-resorption proficiency.

is the key factor affecting the growth and salt Tolerance of *A. sparsifolia* in different habitat in Northwest China (Zhang et al., 2018b).

In addition, K concentration in phreatophytic *A. sparsifolia* was significantly affected by groundwater depth. The leaf, stem, and assimilating branch K concentrations of *A. sparsifolia* at 4.5 m groundwater depth were significantly higher than those at 2.5 and 11.0 m groundwater depths and is mainly due to the direct negative effect of groundwater depth on senesced leaf K concentration (**Figure 4C**) and leaf K concentration is affected by soil K concentration (Zeng et al., 2001) and water stress (Saneoka et al., 2004). Moreover, N concentration in the phreatophytic *A. sparsifolia* was unaffected by various groundwater depth because this plant is a leguminous plant, and more than 80% of its total leaf N is fixed by the atmosphere (Arndt et al., 2004).

Effect of Groundwater Depth on the Nutrient Resorption of *A. sparsifolia*

Herein, our data partly supported the hypothesis that groundwater depth had a significant influence on the nutrient resorption (NRE of P and K) of the phreatophytic *A. sparsifolia,* but its effect on nutrient utilization (NUE of N, P, and K) was minimal. Groundwater depth significantly affected the NRE of P in *A. sparsifolia*. Although groundwater depth had no direct effect of the NRE of P, it had an indirect effect on the NRE of P via soil P concentration that is mostly determined by groundwater depth (**Figure 4**). This result is similar to that of our previous experiments that leaf P concentration in *A. sparsifolia* is positively linked to soil P concentration under different groundwater depths (Zhang et al., 2018a). Similar reports have noted that the NRE of P in herbaceous species decreases with

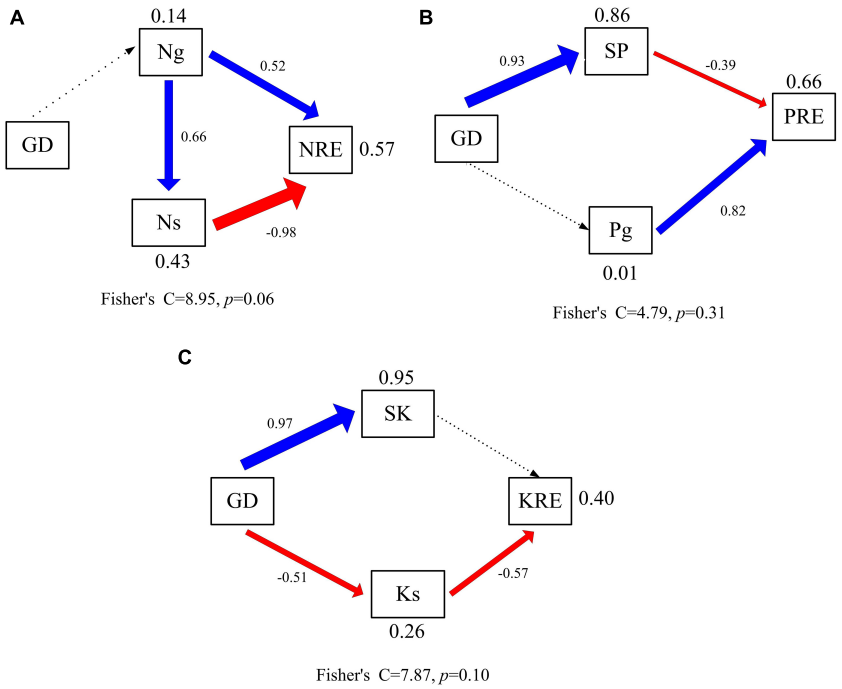

FIGURE 4 | Controlling factors analysis of leaf resorption efficiency using the structural equation model. Significant regressions are indicated by solid lines ($p < 0.05$) and nonsignificant regressions by dashed lines. The thickness of the significant paths has been scaled based on the magnitude of the standardized regression coefficient. Black arrows denote positive relationships, and red arrows negatives ones. GD, groundwater depth; Ng, nitrogen concentrations of green leaves; Ns, nitrogen concentrations of senesced leaves; NRE, nitrogen resorption efficiency; SP, soil available phosphorus concentration; Pg, phosphorus concentrations of green leaves; PRE, phosphorus resorption efficiency; SP, soil available potassium concentration; Ks, potassium concentrations of senesced leaves; KRE, potassium resorption efficiency. **(A)** Controlling factors analysis of leaf nitrogen resorption efficiency. **(B)** Controlling factors analysis of leaf phosphorus resorption efficiency. **(C)** Controlling factors analysis of leaf potassium resorption efficiency.

increasing soil P concentration as indicated by global data analysis (Wang et al., 2018).

The NRE of P in *Cleistogenes squarrosa* (Trin. ex Ledeb.) Keng is significantly affected by green and senesced leaf P concentrations in overgrazing treatments (Wang et al., 2020). Herein, the NRE of P in *A. sparsifolia* at 4.5 m groundwater depth was significantly higher than that at 2.5 m (**Table 1**), suggesting that *A. sparsifolia* at 4.5 m groundwater depth could have translocated more P from the senescing tissues to the green tissues to support plant growth as indicated in our previous report that the soil P concentrations between 4.5 and 2.5 m groundwater depths in the same area were not significantly different (Zhang et al., 2018a). This funding is also supported by the lower P concentration in senescent tissues (NRP of P) at 4.5 m groundwater depth than that at 2.5 m (**Table 1** and **Figure 1**). The NRE of P in *A. sparsifolia* at 4.5 m groundwater depth was significantly greater than that at 11.0 m groundwater depth because soil available P concentration at 4.5 m groundwater depth is significantly lower than those at 11.0 m groundwater depth (Zhang et al., 2018a). The results suggested that *A. sparsifolia* in the P-limited habitat adopt better nutrient conservation mechanisms to reduce nutrient loss through internal nutrient cycling. This result is also consistent with the observation that desert plants in nutrient-poor environments usually rely on high NRE to alleviate nutrient limitation (Drenovsky and Richards, 2006; Vergutz et al., 2012; Brant and Chen, 2015).

In the present study, the observed NRE of P in *A. sparsifolia* under different groundwater depths ranges from 29.2 to 81.1% and it similar to that of a legume (*Oxytropis* sp.) that grows on the Tibetan Changtang Plateau (Zhao et al., 2017). The P resorption efficiency in 2015 was 29.15–50.15%, which was lower than the global value of 64.9%; the P resorption efficiency values in 2016 was 69.74–81.07% and greater than the global P resorption efficiency (Vergutz et al., 2012). There are significant difference between NRE of P in *A. sparsifolia* in 2015 and 2016 and interactive effects of groundwater depth and year were found on NRE of P in *A. sparsifolia* in 2015 and 2016 (**Supplementary Table 2**). It is important to note that leaf P resorption enhances with increasing mean annual precipitation (Brant and Chen, 2015). Leaf P resorption efficiencies of woody plants increase with mean annual precipitation at the global scale (Yuan and Chen, 2009), and P resorption efficiencies of a legume (*Oxytropis* sp.), grass (*S. purpurea*), and forb (*Potentilla bifurca* L) are enhanced with increasing precipitation on the Tibetan Changtang Plateau (Zhao et al., 2017). Therefore, the significant difference between NRE of P in *A. sparsifolia* in 2015 and 2016 was likely due to the limited precipitation in 2015 (34.2 mm), which was 26.9% less than that in 2016 (43.4 mm, **Supplementary Table 1**). These results are in accordance with previous findings

of Ren et al. (2018) who reported that the nutrient resorption of two perennial grasses, *Cleistogenes songorica*, and *Stipa breviflora*, and one perennial semi-shrub, *Artemisia frigida*, to warming and nitrogen fertilization could be regulated by natural precipitation variations in a desert grassland in Inner Mongolia, northern China. These results are also consistent with the observation that leaf P resorption in Lucerne enhances with increasing water conditions in the greenhouse (Lu et al., 2019).

Similarly, groundwater depth had no direct effect on the NRE of K, had an indirect effect on the NRE of K via the senesced leaf K concentration (**Figure 4**). The NRE of K in *A. sparsifolia* at 11.0 m groundwater depth was the higher than 2.5 and 4.5 m groundwater depths, while the NRP of K in *A. sparsifolia* at 11.0 m groundwater depth was the lower than the 2.5 and 4.5 m groundwater depths in 2015 (**Table 3**). As such, *A. sparsifolia* at 11.0 m groundwater depth had a greater NRE of K than others, resulting in the lowest K concentration in senescent tissues (NRP of K) to adapt to the largest groundwater depth at the southern rim of the Taklimakan Desert (**Figure 2**). The NRE of K in *A. sparsifolia* under different groundwater depths ranged from 7.2 to 25.5% in 2015 and 13.7 to 20.0% in 2016, respectiely, which was significantly lower than the highest global K resorption efficiency of 70.1% (Vergutz et al., 2012) and in lucerne that varies from 21.0 to 49.8 % with an average of 36.9 % (Wang et al., 2014). Besides, no significant difference between NRE of K was observed in *A. sparsifolia* in 2015 and 2016 (**Supplementary Table 2**). These results may because sand soil in the desert had higher K concentration and lower soil N and P concentrations (Liu et al., 2013), and the NRE in nutrient-rich habitats is lower than that in nutrient-poor habitats, compared with other soil types (Killingbeck, 1996; Yuan and Chen, 2009). Hence, the low NRE of K in *A. sparsifolia* was attributed to the high K availability in soil and the high K availability in soil results in no significant difference between NRE of K in *A. sparsifolia* in 2015 and 2016. In the present study, groundwater depth had no effect on the NRE of N (**Figure 4**). The NRE of N in *A. sparsifolia* under different groundwater depths was 46.1–55.1% and significantly lower than the highest global N resorption efficiency (62.1%) (Vergutz et al., 2012) and the NRE in grass (*Stipa purpurea*; 74.4%), sedge (*Carex moorcroftii*; 73.7%), and forb (*Potentilla bifurca* L; 73.5%) (Zhao et al., 2017). However, the observed values were similar to that of a legume (*Oxytropis* sp.) on the Tibetan Changtang Plateau (47.2%) (Zhao et al., 2017) and higher than that of lucerne (a perennial legume) with an average of 16.2% (Wang et al., 2014). These results suggested that *A. sparsifolia* can fix atmospheric N_2, resulting in a relatively lower resorption efficiency of N in *A. sparsifolia* than in non-legume plants.

Effect of Groundwater Depth on Nutrient Utilization in *A. sparsifolia*

In the present study, the NUE of P and K were decreased with increasing groundwater depth, while the NUE of P and K among 2.5, 4.5, and 11.0 m groundwater depth had no significant differences (**Tables 1–3**). This result is mainly due to *A. sparsifolia* that adapt to the changes only by adjusting the nutrient resorption process rather than the nutrient utilization process. This result is similar to those of previous studies that the NUE of six species were similar at high and low water supply treatments in a typical agropastoral ecotone in China (Yuan et al., 2008), and the NUE of tree species depended on the species but not on nutrient availability (Aubrey et al., 2012). The NUE of N at 4.5 m groundwater depth was lower than that of 2.5 and 11.0 m groundwater depths because *A. sparsifolia* is a leguminous plant that can fix N in air, its biomass at 4.5 m groundwater depth is higher than that at 2.5 and 11.0 m groundwater depths (Zhang et al., 2018a). Future research should focus on the effects of nutrient and salinity in groundwater combined with groundwater depth on the nutrient resorption of phreatophytes. Long-term data on plant and soil in control and field experiments are also needed to measure and understand the responses of phreatophytes to groundwater drawdown combined with global change, such as variations in precipitation, temperature, and nitrogen deposition. In addition, only one phreatophyte chooses in this study, so if other phreatophytes have similar nutrient cycling strategies will need more research work in the future.

CONCLUSION

Groundwater depth significantly affected P and K concentrations in leaf, stem, and assimilating branch of *A. sparsifolia*, but did not influence N concentrations in different tissues of *A. sparsifolia* in the southern rim of the Taklimakan Desert. *A. sparsifolia* under different groundwater depths drastically altered the nutrient resorption parameters, such as NRP and NRE of P and K, but not the nutrient uptake parameters, such as NP, MRT, and NUE. Besides, groundwater depth had significant indirect effects on the P and K resorption of *A. sparsifolia* by changing soil P concentration and senescent leaf K concentration. Hence, the variations in P and K concentrations in *A. sparsifolia* under different groundwater depths were highly associated with their resorption rather than their utilization by plants. Our results presented a new internal nutrient cycling strategy for nutrient conservation of a desert phreatophyte grown under poor soil fertility at different groundwater depths in a desert-oasis ecotone. This study may contribute to protecting and restoring phreatophytes in a hyper-arid desert ecosystem.

DATA AVAILABILITY STATEMENT

The original contributions presented in the study are included in the article/**Supplementary Material**, further inquiries can be directed to the corresponding author/s.

AUTHOR CONTRIBUTIONS

BZ, XG, and FZ designed the study. BZ and SZ performed the experiments and collected the data. BZ analyzed the data. BZ, GT, HY, MS, BL, XG, and FZ interpreted the data and wrote the manuscript. All authors contributed to the article and approved the submitted version.

FUNDING

This study was supported by the Western Young Scholar Program-B of the Chinese Academy of Sciences (2018-XBQNXZ-B-018), the National Natural Science Foundation of China (31500367), the Program of Joint Funds of the National Natural Science Foundation of China and the Government of Xinjiang Uygur Autonomous Region of China (U1903102), the Youth Innovation Promotion Association Foundation of the Chinese Academy of Sciences (2020435), The Third Batch of Tianshan Talents Program of Xinjiang Uygur Autonomous Region (2021-2023) and the Project for Cultivating High-level talent of Xinjiang Institute of Ecology and Geography (E0502101).

ACKNOWLEDGMENTS

We thank Hanlin Luo, Shiming Li, Bo Wang, and Jinfeng Pang for assistance in field work at the Cele Station, and Mingfang Hu for assistance in soil and plant elemental analysis. We are also grateful to the referees for their reviewing of this manuscript.

SUPPLEMENTARY MATERIAL

The Supplementary Material for this article can be found online at: https://www.frontiersin.org/articles/10.3389/fpls.2021.665168/full#supplementary-material

REFERENCES

Aerts, R. (1996). Nutrient resorption from senescing leaves of perennials: are there general patterns? *J. Ecology* 84, 597–608. doi: 10.2307/2261481

Aerts, R., and Chapin, F. S. I. I. I. (2000). The mineral nutrition of wild plants revisited: a re-evaluation of processes and patterns. *Adv. Ecol. Res.* 30, 1–67. doi: 10.1016/s0065-2504(08)60016-1

Antunes, C., Chozas, S., West, J., Zunzunegui, M., Cruz, M., Barradas, D., et al. (2018). Groundwater drawdown drives ecophysiological adjustments of woody vegetation in a semi-arid coastal ecosystem. *Global Change Biol.* 24, 4894–4908. doi: 10.1111/gcb.14403

Arndt, S. K., Kahmen, A., Arampatsis, C., Popp, M., and Adams, M. (2004). Nitrogen fixation and metabolism by groundwater-dependent perennial plants in a hyperarid desert. *Oecologia* 141, 385–394. doi: 10.1007/s00442-004-1655-7

Aubrey, D. P., Coyle, D. R., and Coleman, M. D. (2012). Functional groups show distinct differences in nitrogen cycling during early stand development: implications for forest management. *Plant soil* 351, 219–236. doi: 10.1007/s11104-011-0946-0

Berendse, F., and Aerts, R. (1987). Nitrogen use efficiency: a biologically meaningful definition? *Funct. Ecol.* 1, 293–296.

Brant, A. N., and Chen, H. Y. H. (2015). Patterns and mechanisms of nutrient resorption in plants. *Crit. Rev. Plant Sci.* 34, 471–486. doi: 10.1080/07352689.2015.1078611

Drenovsky, R. E., and Richards, J. H. (2006). Low leaf N and P resorption contributes to nutrient limitation in two desert shrubs. *Plant Ecol.* 183, 305–314. doi: 10.1007/s11258-005-9041-z

Eckstein, R. L., and Karlsson, P. S. (2001). Variation in nitrogen-use efficiency among and within subarctic graminoids and herbs. *New Phytol.* 150, 641–651. doi: 10.1046/j.1469-8137.2001.00130.x

Garnier, E., and Aronson, J. (1998). "Nitrogen-use efficiency from leaf to stand level: clarifying the concept," in *Inherent Variation in Plant Growth. Physiological Mechanisms and Ecological Consequences*, eds H. Lambers, H. Poorter, and M. M. I. Van Vuuren (Leyden: Backhuys), 515–538.

Gui, D. W., Zeng, F. J., Liu, Z., and Zhang, B. (2013). Characteristics of the clonal propagation of Alhagi sparsifolia Shap. (Fabaceae) under different groundwater depths in Xinjiang, China. *Rangeland J.* 35, 355–362. doi: 10.1071/rj13004

Huang, G., Su, Y. G., Mu, X. H., and Li, Y. (2018). Foliar nutrient resorption responses of three life-form plants to water and nitrogen additions in a temperate desert. *Plant Soil.* 424, 479–489. doi: 10.1007/s11104-017-3551-z

Killingbeck, K. T. (1996). Nutrients in senesced leaves: keys to the search for potential resorption and resorption proficiency. *Ecology* 77, 1716–1727. doi: 10.2307/2265777

Lefcheck, J. S. (2016). PiecewiseSEM: piecewise structural equation modeling in R for ecology, evolution, and systematics. *Methods Ecol. Evol.* 7, 573–579. doi: 10.1111/2041-210x.12512

Li, C. J., Zeng, F. J., Zhang, B., Liu, B., Guo, Z. C., Gao, H. H., et al. (2015). Optimal root system strategies for desert phreatophytic seedlings in the search for groundwater. *J. Arid Land* 7, 462–474. doi: 10.1007/s40333-015-0006-3

Li, H. F., Zeng, F. J., Gui, D. W., Zhang, L. G., Song, C., Luo, W. C., et al. (2013). Effects of cutting and burning on regeneration of Alhagi sparsifolia Shap. on the southern fringe of the Taklamakan Desert, North-west China. *Rangeland J.* 34, 389–397. doi: 10.1071/rj12020

Liu, B., He, J. X., Zeng, F. J., Lei, J. Q., and Arndt, S. K. (2016). Life span and structure of ephemeral root modules of different functional groups from a desert system. *New Phytol.* 211, 103–112. doi: 10.1111/nph.13880

Liu, B., Zeng, F. J., Arndt, S. K., and He, J. X. (2013). Patterns of root architecture adaptation of a phreatophytic perennial desert plant in a hyperarid desert. *S. Afr. J. Bot.* 86, 56–62. doi: 10.1016/j.sajb.2013.02.003

Liu, M. (2007). *Study on Groundwater Spatiotemporal Distribution Law and Its Environmental Effects in Hotan Oasis. Ph, D, Thesis*. China: Xi'an University of Technology.

Lu, J. Y., Yang, M., Liu, M. G., Wang, Y. Y., and Yang, H. M. (2019). Leaf stoichiometry and resorption of N and P in lucerne at different growth stages under different water supplies. *J. Plant Nutr.* 42, 501–511. doi: 10.1080/01904167.2019.1567776

Lü, X. T., and Han, X. G. (2010). Nutrient resorption responses to water and nitrogen amendment in semi-arid grassland of inner mongolia, china. *Plant Soil* 327, 481–491. doi: 10.1007/s11104-009-0078-y

Netzer, F., Schmid, C., Herschbach, C., and Rennenberg, H. (2017). Phosphorus-nutrition of European beech (*Fagus sylvatica* L.) during annual growth depends on tree age and P-availability in the soil. *Environ. Exp. Bot.* 137, 194–207. doi: 10.1016/j.envexpbot.2017.02.009

Norby, R. J., and Iversen, C. M. (2006). Nitrogen uptake, distribution, turnover, and efficiency of use in a CO2-enriched sweetgum forest. *Ecology* 87, 5–14. doi: 10.1890/04-1950

Ren, H. Y., Kang, J., Yuan, Z. Y., Xu, Z. W., and Han, G. D. (2018). Responses of nutrient resorption to warming and nitrogen fertilization in contrasting wet and dry years in a desert grassland. *Plant Soil* 432, 65–73. doi: 10.1007/s11104-018-3775-6

Richardson, S. J., Peltzer, D. A., Allen, R. B., and McGlone, M. S. (2005). Resorption proficiency across a chronosequence: responses among communities and within species. *Ecology* 86, 20–25. doi: 10.1890/04-0524

Saneoka, H., Moghaieb, R. E., Premachandra, G. S., and Fujita, K. (2004). Nitrogen nutrition and water stress effects on cell membrane stability and leaf water relations in agrostis palustris huds. *Environ. Exp. Bot.* 52, 131–138. doi: 10.1016/j.envexpbot.2004.01.011

Shipley, B. (2002). *Cause and Correlation in Biology: a User's Guide to Path Analysis, Structural Equations and Causal Inference*. Cambridge: Cambridge University Press.

Sparks, D. L., Page, A., Helmke, P., Loeppert, R., Soltanpour, P., Tabatabai, M., et al. (1996). *Methods of Soil Analysis. Part 3-Chemical Methods*. Madison, WI: Soil Science Society of America Inc.

Thomas, F. M. (2014). *Ecology of Phreatophytes. Progress in Botany*. Berlin: Springer.

Thomas, R., Sheard, R., and Moyer, J. (1967). Comparison of conventional and automated procedures for nitrogen, phosphorus, and potassium analysis of plant material using a single digestion. *Agron. J.* 59, 240–243. doi: 10.2134/agronj1967.00021962005900030010x

Vergutz, L., Manzoni, S., Porporato, A., Novais, R. F., and Jackson, R. B. (2012). Global resorption efficiencies and concentrations of carbon and nutrients

in leaves of terrestrial plants. *Ecol. Monogr.* 82, 205–220. doi: 10.1890/11-0416.1

Vitousek, P. M. (1982). Nutrient cycling and nutrient use efficiency. *Am. Nat.* 119, 553–572. doi: 10.1086/283931

Wang, Z., Fan, Z., Zhao, Q., Wang, M., Ran, J., Huang, H., et al. (2018). Global data analysis shows that soil nutrient levels dominate foliar nutrient resorption efficiency in herbaceous species. *Front. Plant Sci.* 9:1431.

Wang, Z., Jimoh, S. O., Li, X., Ji, B., Struik, P. C., Sun, S., et al. (2020). Different responses of plant N and P resorption to overgrazing in three dominant species in a typical steppe of Inner Mongolia. *China. Peer J.* 8:e9915. doi: 10.7717/peerj.9915

Wang, Z. N., Lu, J. Y., Yang, H. M., Zhang, X., Luo, C. L., and Zhao, Y. X. (2014). Resorption of nitrogen, phosphorus and potassium from leaves of lucerne stands of different ages. *Plant Soil* 383, 301–312. doi: 10.1007/s11104-014-2166-x

Xu, S., Zhou, G. Y., Tang, X. L., Wang, W. T., Wang, G. X., Ma, K. P., et al. (2017). Diferent spatial patterns of nitrogen and phosphorus resorption efciencies in China's forests. *Sci Rep-UK* 7, 10584. doi: 10.1038/s41598-017-11163-7

Yasumura, Y., Hikosaka, K., Matsui, K., and Hirose, T. (2002). Leaf-level nitrogen-use efficiencyof canopy andunderstoreyspecies in a beechforest. *Funct. Ecol.* 16, 826–834. doi: 10.1046/j.1365-2435.2002.00691.x

Yuan, Z. Y., and Chen, H. Y. H. (2009). Global-scale patterns of nutrient resorption associated with latitude, temperature and precipitation. *Global Ecol .Biogeogr.* 18, 11–18. doi: 10.1111/j.1466-8238.2008.00425.x

Yuan, Z. Y., Chen, H. Y. H., and Li, L. H. (2008). Nitrogen use efficiency: does a trade-off exist between the N productivity and the mean residence time within species? *Aust. J. Bot.* 56, 272–277. doi: 10.1071/bt07139

Yuan, Z. Y., Li, L. H., Han, X. G., Chen, S. P., Wang, Z. W., Chen, Q. S., et al. (2006). Nitrogen response efficiency increased monotonically with decreasing soil resource availability: a case study from a semiarid grassland in northern China. *Oecologia* 148, 564–572. doi: 10.1007/s00442-006-0409-0

Yuan, Z. Y., Li, L. H., Han, X. G., Jiang, F. H., Zhao, M. X., and Lin, G. H. (2004). Effects of plant sizes on the nitrogen use strategy in an annual herb, Helianthus annuus (Sunflower). *Acta Botanica Sinica* 46, 889–895.

Yuan, Z. Y., Liu, W. X., Niu, S. L., and Wan, S. Q. (2007). Plant nitrogen dynamics and nitrogen-use strategies under altered nitrogen seasonality and competition. *Ann Bot -LONDON* 100, 821–830. doi: 10.1093/aob/mcm178

Zeng, F. J., Bleby, T. M., Landman, P. A., Adams, M. A., and Arndt, S. K. (2006). Water and nutrient dynamics in surface roots and soils are not modified by short-term flooding of phreatophytic plants in a hyperarid desert. *Plant Soil* 279, 129–139. doi: 10.1007/s11104-005-0498-2

Zeng, F. J., and Liu, B. (2012). *Root Ecology of Alhagi Sparsifolia*. Beijing: Science Press.

Zeng, F. J., Song, C., Guo, H. F., Liu, B., Luo, W. C., Gui, D. W., et al. (2013). Responses of root growth of Alhagi sparsifolia Shap. (Fabaceae) to different simulated groundwater depths in the southern fringe of the Taklimakan Desert. *China. J. Arid Land* 5, 220–232. doi: 10.1007/s40333-013-0154-2

Zeng, Q. P., Brown, P. H., and Holtz, B. A. (2001). Potassium fertilization affects soil k, leaf k concentration, and nut yield and quality of mature pistachio trees. *Hortscience* 36, 85–89. doi: 10.21273/hortsci.36.1.85

Zhang, B., Gao, X. P., Li, L., Lu, Y., Shareef, M., Huang, C. B., et al. (2018a). Groundwater depth affects phosphorus but not carbon and nitrogen concentrations of a desert phreatophyte in northwest China. *Front. Plant Sci.* 9:338. doi: 10.3389/fpls.2018.00338

Zhang, B., Gui, D. W., Gao, X. P., Shareef, M., Li, L., and Zeng, F. J. (2018b). Controlling soil factor in plant growth and salt tolerance of leguminous plant Alhagi sparsifolia Shap. in saline deserts, northwest China. *Contemp. Probl. Ecol* 11, 111–121. doi: 10.1134/s199542551801002x

Zhao, G. S., Shi, P. L., Wu, J. H., Xiong, D. P., Zong, N., and Zhang, X. Z. (2017). Foliar nutrient resorption patterns of four functional plants along a precipitation gradient on the Tibetan Changtang Plateau. *Ecol. Evol.* 7, 7201–7212. doi: 10.1002/ece3.3283

Conflict of Interest: The authors declare that the research was conducted in the absence of any commercial or financial relationships that could be construed as a potential conflict of interest.

Advantages of publishing in Frontiers

OPEN ACCESS
Articles are free to read for greatest visibility and readership

FAST PUBLICATION
Around 90 days from submission to decision

HIGH QUALITY PEER-REVIEW
Rigorous, collaborative, and constructive peer-review

TRANSPARENT PEER-REVIEW
Editors and reviewers acknowledged by name on published articles

Frontiers
Avenue du Tribunal-Fédéral 34
1005 Lausanne | Switzerland

Visit us: www.frontiersin.org
Contact us: frontiersin.org/about/contact

REPRODUCIBILITY OF RESEARCH
Support open data and methods to enhance research reproducibility

DIGITAL PUBLISHING
Articles designed for optimal readership across devices

FOLLOW US
@frontiersin

IMPACT METRICS
Advanced article metrics track visibility across digital media

EXTENSIVE PROMOTION
Marketing and promotion of impactful research

LOOP RESEARCH NETWORK
Our network increases your article's readership